The Carpathian-Balkans During the Holocene: Reconstructing Human Influences and Climatic Changes

Jack Longman

PhD

2018

Northumbria University at Newcastle

The Carpathian-Balkans During the Holocene: Reconstructing Human Influences and Climatic Changes

Jack Longman

A thesis submitted in partial fulfilment of the requirements of the University of Northumbria for the award of the degree Doctor of Philosophy

Research undertaken in the Faculty of Engineering and Environment

January 2018

Abstract

The Carpathian-Balkan region in south-eastern Europe is one of the longest inhabited regions in Europe, with evidence of some of the earliest examples of European agriculture, farming and metallurgy. Despite its importance for understanding past human activity and climate change, high-resolution reconstructions of Holocene hydroclimate variability and human impact are rare. This thesis provides a series of new high-resolution Holocene (the past 11,700 years) palaeoenvironmental records derived from peat bogs in the Carpathian Mountains of Romania, and the Dinaric Alps of Serbia, to investigate climate variation and human impact.

Two peat-derived archives of environmental change in Romania are presented. First, a 7500-year record of minerogenic deposition from the Southern Carpathians linked to heavy rainfall events provides the first record of extreme precipitation for the Carpathians. Such minerogenic depositional events began 4000 calibrated years before present (yr BP, where present is 1950 CE), with increased depositional rates during the Medieval Warm Period (1150 – 850yr BP), the Little Ice Age (350 – 100 yr BP) and during periods of societal upheaval (e.g. the Roman conquest of Dacia). The timing of minerogenic events appears to indicate a teleconnection between the North Atlantic Oscillation (NAO) and hydroclimate variability in south-eastern Europe, which persists throughout the mid-to-late Holocene. Secondly, a 10,800-year record of geochemically-derived dust deposition and testate amoeba-derived local wetness from the Eastern Romanian Carpathians highlights several discrepancies between eastern and western European dust depositional records and the impact of highly complex hydrological regimes in the Carpathian region. Specifically, the record outlines the increased impact of Saharan dust after 6100 yr BP which is associated with the end of the African Humid Period.

A lead (Pb) record from a peat bog in Western Serbia provides an unprecedented view on past pollution related to metal exploitation in the Balkans. Environmental Pb pollution is first observed in the very earliest Bronze Age, the oldest environmental Pb pollution in Europe. After 600 CE an almost linearly increasing Pb trend until the Medieval period is observed. Comparison with western European records suggests an alternative history of European metallurgy, one in which metal-related pollution does not cease with the fall of the Roman Empire, and which displays major Medieval pollution.

Pb isotopes provide a valuable insight into the sources of Pb observed within a sample, allowing for the fingerprinting of their metal's geological source, or production site. Presented here is the application of a state of the art Bayesian mixing model to such a purpose, outlining a 'best practice' and testing of the approach via a number of real-world examples.

List of Contents

List of Figures

List of Tables

List of Abbreviations

AHP – African Humid Period

AMS – Accelerator Mass Spectrometry

AP – Arboreal Pollen

BCE – Before Common Era

CAAPb – Cumulative, Atmospheric, Anthropogenic Pb

CE – Common Era

CRM – Certified Reference Material

DWT – Depth to Water Table

EA – East Atlantic

EA-WR – East Asia-West Russia

EF – Enrichment Factor

HCO – Holocene Climatic Optimum

ICP-OES/AES – Inductively Coupled Plasma-Optical Emission Spectrometry/Atomic Emission Spectrometrry

ITCZ – Intertropical Convergence Zone

LIA – Little Ice Age

LOI – Loss on Ignition

LPAZ – Local Pollen Assemblage Zone

MCA – Medieval Climate Anomaly

MCMC – Markov Chain Monte Carlo

MM – Minerogenic Matter

MWP – Medieval Warm Period

NAO – North Atlantic Oscillation

NAP – Non-Arboreal Pollen

OM – Organic Matter

PAR – Peat Accumulation Rate

POL – Polar-Eurasia Teleconnection

PPA – Pre-pollution Aerosol

RCC – Rapid Climate Change

RWP – Roman Warm Period

SLP – Sea Level Pressure

TA – Testate Amoeba

UCC – Upper Continental Crust

XRF – X-Ray Fluorescence

yr BP – Calibrated years Before Present, where 1950 CE is considered 'present'

Acknowledgements

First and foremost, I would like to thank Dr. Vasile Ersek, my principal supervisor, and principal guide through the rigours and challenges inherent to a PhD. Alongside Vasile, I have received tremendous support from my two other supervisors. Firstly, at the Romanian Academy, Dr. Daniel Veres has been a constant source of knowledge, advice, ideas and help, all of which have been profoundly beneficial to me. Secondly, Prof. Ulrich Salzmann, thank you for your advice, our lengthy discussions about pollen, and your tremendous attention to detail.

Others at Northumbria University have helped me immensely, with Lesley Dunlop, Dave Thomas and Will Thomas in particular having provided lab support and technical advice, and possibly most importantly; storage space! I am also indebted to Dr. Patrick Amaibi and Prof. John Dean for their support and help with dealing with the vagaries of the ICP, and Gordon Forrest for his endless energy to replace gas bottles. Outside of Northumbria, I must thank my other co-authors for their various acts of support with field work, sample preparation, some analyses and manuscript preparation; at the University of Cologne Marc Bormann, Dr. Volker Wennrich and Prof. Frank Schabitz and in Hungary, Dr. Katalin Hubay. Special thanks must also be made to Prof. Catherine Chauvel, Dr. Walter Finsinger and Dr. Don Philips, for their help with chapters 3 and 4.

I am indebted to the QRA for their award of 6 radiocarbon dates through the 14C Chrono Award, and to INQUA and PAGES for their financial support to allow me to attend conferences.

To those who I have shared an office with through this time, I am also grateful, for their encouragement, companionship and support. So, thanks Drs Rupert Bainbridge, Tom Shaw, Clare Webster, Stephanie Strother, Kate Winter and Mark Allan, and soon-to-be Drs Sam Cottingham, Adam Jenson, Bradley Sparkes, Flavia Burger and Mike Cullum, for everything.

And of course, my most profound gratitude is reserved for Dr. Sina Panitz. We started this process as simply office-mates but have ended it as soulmates. Thank you for everything you've given me, and everything you've put up with darling. Finally, thank you to my parents, who have provided me with all the belief and support necessary to allow me to pursue an academic career.

Declaration

I declare that the work contained in this thesis has not been submitted for any other award and that it is all my own work. I also conform that this work fully acknowledges opinions, ideas and contributions from the work of others. The work was conducted in collaboration with the Romanian Academy in Cluj-Napoca, contributing to the project "Millennial-scale geochemical records of anthropogenic impact and natural climate change in the Romanian Carpathians" and with the Universities of Cologne, Bonn and Aachen contributing to the project "Our way to Europe".

Any ethical clearance for the research presented in this thesis has been approved. Approval has been sought and granted by the University Ethics Committee on the 16th of February 2016.

I declare that the Word Count of this Thesis is 45,298.

Name: Jack Longman

Signature:

Date: 25/01/2017

Publications from this Thesis

Chapter 3 of this thesis has been published as: **Longman, J**., Ersek, V., Veres, D. and Salzmann, U.: Detrital events and hydroclimate variability in the Romanian Carpathians during the mid-to-late Holocene, Quaternary Science Reviews, 167, 78-95, https://doi.org/10.1016/j.quascirev.2017.04.029, 2017

Chapter 4 of this thesis has been published as: **Longman, J.,** Veres, D., Ersek, V., Salzmann, U., Hubay, K., Bormann, M., Wennrich, V., and Schäbitz, F.: Periodic input of dust over the Eastern Carpathians during the Holocene linked with Saharan desertification and human impact, Climate of the Past, 13, 897-917, https://doi.org/10.5194/cp-13-897-2017, 2017.

Chapter 1. Introduction

1.1. Project Overview

1.1.1. Rationale

The changing environment is one of the most prominent issues facing the world at the moment, with some changes reflecting natural causes, while others are directly as a result of humans. Our impact has reached a point, today, where the designation of a new geological period, the Anthropocene, appears necessary (Waters et al., 2016).

To place anthropogenic environmental impact into a framework of natural climate fluctuations, understanding the palaeoclimatic conditions is a necessary step. The reconstruction of past moisture conditions and water availability is crucial when considering the impact of water availability on the environment and human socio-economic development alike. Of particular interest are periods of extreme hydrological conditions, with climate predictions indicating such extreme periods are to become more common in the future worldwide (IPCC, 2013), understanding their cause, and the overall impact, is imperative. Considerable progress has been made in recent years in producing high-resolution and high-quality datasets outlining the history of extreme climate events within Europe. Several such studies have outlined periods of high precipitation (e.g. Swierczynski et al. 2013; Magny 2004) and of drought-related dust depositional events (e.g. Allan et al., 2013a; Sharifi et al., 2015), but as yet, few have been performed in the Carpathian-Balkan region (Feurdean et al., 2015; Haliuc et al., 2017; Magyari et al., 2014). In recent decades, research using proxy-climate indicators from bogs has widened in scope, and a range of proxies for past hydrological change have been developed (see Chambers et al., 2012 for a review). For this research, only a small number of potential proxies, focussed on two main themes (hydroclimate and palaeopollution) have been utilised.

Of the ways humans have impacted the environment, mining and smelting of metal through our history of economic development are amongst the most damaging (Eggert, 1994; Norgate and Haque, 2010; Pokhrel and Dubey, 2013). Either through direct scarring of the earth in the mining process, or the less obvious particulate and heavy metal pollution, it is clear humanity's desire for mineral resources has led to major environmental changes. To allow for comprehension of the scale of the problem, and to advise remediation attempts, long-term monitoring of the impact of such pollution and understanding of pre-human baselines is necessary, rather than approaching the matter in a reactive way. This is succinctly summarized by Blais et al., 2015:

"Much like arriving at the scene of an accident after-the-fact, environmental studies are usually initiated only *after* an environmental problem has been recognized."

To approach more proactively, natural archives (including ice cores, peat bogs and lake sediments) of historical pollution and environmental change may be used. Such approaches allow for the disentanglement of natural and anthropogenic forcings in the complex and constantly changing environment we live in, over a long period of anthropogenic influence. Heavy metals associated with mining and smelting have long been observed within such natural archives (Hong et al., 1996; Nriagu, 1996; Rosman, 2000; Rosman et al., 1997; Shotyk et al., 1998), not just from the recent industrial revolution, but back to the Bronze Age, so it is imperative to understand the scale and impact of this long mining history in Europe.

1.1.2. Why do we need palaeohydrological records in the Carpathian-Balkan region?

The Carpathian Mountains and bordering lowlands are one of the most rapidly reacting regions of Europe to climate change, and with the predicted increase in frequency of floods and droughts in the region (IPCC, 2013; Micu et al., 2015), understanding the mechanisms behind them is vital. Superimposed on the natural climatic fluctuations is the imprint of a long history of human habitation, with evidence for Neolithic cultures domesticating animals as far back as 9000 yr BP (Larson et al., 2007), and some of Europe's first farming communities from 7000–7500 yr BP (Price, 2000; van Andel and Runnels, 1995). Additionally, the earliest known examples of extractive metallurgy may be found in the region dating from 7000 yr BP (Radivojević et al., 2010), further evidence for a long history of significant anthropogenic impact (see Schumacher et al., 2016, for a review).

Climatically, the Romanian Carpathians are located at the confluence of three major atmospheric sea level pressure (SLP) systems: the North Atlantic, the Mediterranean and Siberian (Obreht et al., 2016). As a result, the region should be very sensitive in recording changes in climate resulting from periodic shifts in the dominant SLP pattern. The North Atlantic Oscillation (NAO) in particular, has been identified as a major control on climate in western and central Europe throughout the Holocene (Hurrell, 2005; van der Schrier et al., 2006; Wirth et al., 2013). It has been suggested that Eastern Europe should display similar climatic fluctuations forced by NAO variability, but few reconstructions extend before instrumental records began in the 1960s (Haliuc et al., 2017; Magyari et al., 2009). Such instrumental records have proven a correlation between the NAO and precipitation

(Bojariu and Giorgi, 2005; Tomozeiu et al., 2005), droughts (Stefan et al., 2004) and temperature (Bojariu and Giorgi, 2005) changes in the region.

Even with some improvements in the last few years, high-resolution, multi-proxy records of palaeohydrological changes in the Carpathian-Balkans are rare (see reviews from Buczko et al., 2009; Veres and Mîndrescu, 2013). Previous research has been focussed on pollen reconstructions (e.g. Fârcaş et al., 2013; Feurdean et al., 2008; Schumacher et al., 2016), which provide valuable indications of the reaction of vegetation to climatic fluctuations, but no record of the fluctuations themselves. A number of speleothem records (Constantin et al., 2007; Drăguşin et al., 2014; Onac et al., 2002), and other palaeohydrological proxy records (Brückner et al., 2010; Feurdean et al., 2015; Haliuc et al., 2017; Magyari et al., 2013; Schnitchen et al., 2006; Tóth et al., 2015) have attempted to address this dearth of palaeohydrological records. However, they are generally limited by resolution and strong inter-site variability.

In terms of past temperature variability, a tree ring reconstruction of summer temperatures from the region (Popa and Kern, 2009) indicates an intriguing lack of correlation to those in Central Europe (e.g. Büntgen et al., 2011), indicative of strong local forcing of climate in the Carpathian-Balkan region. This is further evidenced by pollen reconstructions which indicate strong north-south (Davis et al., 2003; Magny et al., 2013; Mauri et al., 2015) and east-west (Roberts et al., 2012, 2011) gradients in palaeoclimate and palaeohydrology in Europe over the Holocene. Understanding these apparent discrepancies is important, with connection, or lack thereof, with the NAO, and other SLPs, including the East Asia-West Russia (EA-WR) system, potentially being a control factor (Krichak et al., 2002).

To understand the linkages with major SLPs, and the mechanisms behind the palaeohydrological gradients, both North-South and East-West, two long-term peat records have been investigated in this respect. The first is a 7500-year record of periods of high precipitation as identified via geochemical indicators and vegetation changes linked to flooding events within a high-altitude bog in the Sureanu Mountains. The second is an 11000-year archive of bog wetness/drought, and dust deposition as indicated by trends in Ti, K, Si and Zr in a mid-altitude bog in the Eastern Carpathians. In both records, particular attention has been paid to the impact humans may have had on the regional environment, and vice versa.

1.1.3. Why do we need palaeopollution records in the Carpathian-Balkan region?

Most research into historical heavy metal pollution during the Holocene has focussed on Pb and Hg in ice cores (e.g. Hong et al. 1996) , lake sediments (e.g. Bränvall et al., 2001; Renberg et al., 2002, 2001) and peats (e.g. Shotyk et al. 1998). Subsequent efforts have built on these pioneering works, but almost all are focused on sites in the west of Europe: the UK (Le Roux et al. 2004; Kylander et al. 2009; Weiss et al. 2002; Mighall et al. 2009; 2014), Belgium (Allan et al., 2013b), France (Monna et al., 2004a), Spain (Martínez Cortizas et al. 2002; 2012; 2016; Kylander et al. 2005; Pontevedra-Pombal et al. 2013; García-Alix et al. 2013) and Switzerland (Shotyk et al., 1998; Weiss et al., 1997). Others may be found in areas outside the Roman Empire reach such as Sweden (e.g. Bränvall et al. 2001) and central Europe (Novák et al., 2003; Tudya et al., 2017; Veron et al., 2014). It is clear there is a major lack in our knowledge regarding long-term dynamics in multi-element records worldwide. This is especially clear when Eastern Europe is considered, where data are limited to archaeological finds (e.g. Constantinescu et al. 2008; Bugoi et al. 2013; Antonovic 2009; Pernicka et al. 2016), or short limnological records (covering the past 300 years at most) (e.g. Rose et al. 2009; Akinyemi et al. 2013; Hutchinson et al. 2016)

This dearth of research is more surprising when the history of the Carpathian-Balkan region is considered. The region hosts some of the oldest sites of extractive metallurgy (Radivojević et al. 2010; 2013; Boric 2009), dating back to 8000 yr BP (see O'Brien, 2014 for a review), possibly the oldest on Earth. Further evidence suggests even earlier evidence for salt mining, a precursor to metal extraction (Weller and Dumitroaia, 2005).This metalworking culture bloomed in the Bronze Age, when Transylvania was a key area in the development of new techniques for both mining and smelting (Kienlin, 2014). A culture of metalworking persisted throughout the Iron Age and the Roman period, through the Middle Ages and into the Industrial Revolution (Borcoş and Udubaşa, 2012). This rich history of mining was facilitated by the rich mineral ore endowment of the region. For example, Rosia Montana mine in the Apuseni Mountains (western Romania) comprises Europe's largest Au-Ag deposit (Manske et al., 2006; Xun, 2015), with various other sites in the nearby Metaliferi Mountains rich in both precious (Ag, Ag) and base (Cu, Pb, Zn) metal deposits of both Mesozoic and Neogene age (Alderton and Fallick, 2000; Borcoş and Udubaşa, 2012; Marcoux et al., 2002). Additional metal-rich mining fields exist in north-western Romania (Baia Mare and Baia Borsa regions), the Southern Carpathians (e.g. Banat) and eastern Romania (e.g. Dobrogea) (Xun, 2015). In addition to sites in Romania,

surrounding countries have other metal-rich sections of the 1500km-long Banatitic Magmatic and Metallogenic Belt, which runs from Romania, through Serbia and into Bulgaria, and is the most important ore-bearing (Cu-Au; polymetallic ores) igneous belt of the Alpine-Balkan-Carpathian-Dinaride realm (Ciobanu et al., 2002; von Quadt et al., 2005).

To fill this knowledge gap on past pollution, a high-resolution peat sediment record located close to the main mining fields of Serbia has been investigated. Multi-element (Cd, Co, Cu, Ni, Pb, Zn) concentrations are used to indirectly assess the impact of mining and smelting over much of the Carpathian-Balkan region. A model-based approach encompassing isotopic fingerprinting is presented to determine exact sources of the Pb seen within a selection of previously published studies. The sites mentioned cover the Southern Carpathians (Sureanu peat bog), Eastern Carpathians (Mohos peat bog) and western Serbia (Crveni Potok peat bog), whilst the modelled examples are from a site in the north of Spain (Kylander et al., 2005) and the Apuseni Mountains in Romania (Baron et al., 2011).

1.2. Project Overview

By utilising various proxies in a number of peat bog cores from the Carpathian-Balkan region in Eastern Europe, this thesis assembles a thorough chronology of the impacts both human and natural changes had on the region's environment over the Holocene. Special focus is placed on the palaeohydrological history, applying varied research methods on sites from the Romanian Carpathians. These multi-proxy approaches on two contrasting bog localities allow the reconstruction of Holocene variations in hydrology and land use. Additional focus is placed on the history of metal smelting in the region, with geochemical analysis of metals used to produce the first record of palaeopollution in the Carpathian-Balkan region. In addition, Pb isotopic analysis and modelling allows for provenance and source apportionment to determine the origin of the observed pollution. Here an innovative approach to source apportionment utilising a novel Bayesian mixing model is outlined.

1.3. Aims & Objectives

The focus of this project is on the Holocene (the last 11,700 years), a period of significant environmental changes, both because of natural climatic variations, and the impact of developing human society. This period encompasses the postglacial warming, and various millennial or centennial climate variations - both warm (mid-Holocene optimum, the

Roman period and the Medieval anomaly) and cold (the 9.5; 8.2; 6.6; 3.4kyr (thousand years) events and the Little Ice Age), and associated hydrological regime changes.

These natural climatic oscillations have been closely linked to the development, both societally and technologically, of humans. This period of study covers the shift from hunter-gatherers to farming/deforestation, through the beginnings of metal production and the related technological and cultural changes associated with the Copper, Bronze and Iron Ages, and onto the socioeconomic collapse of the Middle Ages, the industrial revolution and large-scale industrialisation resulting in the anthropogenically-altered condition we see today.

To successfully investigate these topics the focus is on:

1. Producing high-resolution, multi-proxy records of the history of extreme climate events (droughts and floods) in the Carpathian-Balkan region.
2. Determining the impact such events played in the development of civilisations in the region.
3. Investigating the extent to which humans have impacted the environment, via reconstructions of metal production-related pollution.
4. Identifying emission sources based on geochemical fingerprinting and radiogenic isotope tracing of pollution events using a model-based approach.

1.4. Thesis Structure

This thesis has been divided into eight chapters. Chapter one provides an overview of the research project, the main aims, objectives, and reasons for carrying out this work, followed by two sections outlining the background to the project. The first of these sections summarises the palaeoenvironmental history of Europe in general, and the Carpathian-Balkans specifically. The second section has a similar focus, but for the history of human metal work, and related pollution. Chapter two outlines the sites studied, and the methods used in this work. Chapter three presents the outcome of a study into periods of high rainfall in the Southern Carpathians over the past 7500 years. Chapter four displays results of an 11000-year record of dust depositional events in the Eastern Carpathians. Chapter five shows results of a first study into Balkan palaeopollution, reconstructed from a peatbog in Eastern Serbia, and focusing on downcore trends in heavy metal concentrations. Chapter six presents an original approach to Pb isotope modelling, utilising Bayesian mixing models. Finally, chapter seven brings together all main results

into one coherent summary section. Additionally, suggestions of avenues for further research are outlined.

1.5. Peatlands as Palaeoenvironmental Archives

Continental climate changes and the imprints from human activities in the environmental record throughout the Holocene have generally been identified using various archives such as marine and lake sediments, ice or speleothem records.

Peatlands are environments in which fossil plant material is accumulated (Fig.1.1). They are typically characterised by the presence of water at or near the surface, low oxygen levels under the surface, with anoxic conditions prevailing and a specific vegetation assemblage adapted to this environment (Chambers et al., 2012; Charman, 2002). To allow for peat development, near-constant saturation, and the presence of plant remains is needed. As outlined by Charman, (2002), the slow decay of vegetation in these waterlogged and oxygen-poor sites leads to a gradual accumulation of peat and acidic conditions are established (with a pH generally between 3–6).

Peat normally accumulates in two sorts of environments: minerotrophic and ombrotrophic, which are divided by their formation, vegetation and hydrological functioning (Charman, 2002). Minerotrophic bogs are those which are supplied by both precipitation and groundwater and are influenced by the mineral input from the surrounding catchment area. Their vegetation is typically diverse, with sedges such as *Carex* spp, *Manyanthes* spp, *Molinia* spp and *Equisetum* spp appearing alongside *Sphagnum*. In contrast, ombrotrophic bogs exclusively derive their nutrient input from the atmosphere, and rainfall, with a domination of *Sphagnum*, with some *Carex* spp and *Eriophorum* spp present. As a result, their nutrients, and crucially for this work, atmospheric particulates such as heavy metals, are solely derived via deposition of direct atmospheric fallout (Chambers et al., 2012; De Vleeschouwer et al., 2010; Shotyk et al., 1998).

Peat bogs have long been used as an archive for environmental and climatic imprints, with a Scandinavian peat bog providing the first chronostratigraphic divisions of the Holocene (Blytt, 1876; Sernander, 1908). However, a major misconception about the formation of bogs prevailed until the 1970s, delaying their potential use as climatic archives. The previous hypothesis of internal (autogenic) cyclic regeneration was eventually refuted, first by the indication of cyclic, sub-Milankovitch climate changes in the late Holocene from a Danish peat record (Aaby, 1976; Aaby and Tauber, 1975), and then by further work on the

Figure 1.1: *Examples of peat bogs from Romania. A: Semenic blanket bog, Banat region south-western Romania B & E: Sureanu bog, Southern Carpathians, formed in a glacially scoured cirque C & D: Pesteana bog, South-western Romania, a peat infilling of a deep lake basin, with a floating peat layer above a water pocket F: Close up of Sureanu peat core, between 1-2m in depth below surface.*

Bolton Fell Moss - with a demonstration of the 'directly coupled' nature of the atmosphere-bog record (Barber, 1981).

1.6. Palaeoenvironmental Reconstructions from Europe

Quantitative climate reconstructions, both of temperature and hydroclimate in Europe are generally based on syntheses of pollen datasets, aided by chironomid-based studies, and other syntheses using tree-ring widths and isotopic data. Quantitative Europe-wide pollen reconstructions are either performed at discreet points in time, e.g. 6000 yr BP (Bartlein et al., 2011), or via gridded climate reconstructions (Davis et al., 2003; Mauri et al., 2015; Wu et al., 2007). A similar approach has been used to produce a chironomid-based synthesis for the late glacial period (Heiri et al., 2014). Tree rings have been used to produce comparable records covering the past 2500 years, (Büntgen et al., 2011; Luterbacher et al., 2012) and for the past 1500 years (Mann et al., 2009) at very high temporal resolution.

Trends from these syntheses are generally in agreement, but highlight the difficulty in applying continent-wide reconstructions to individual locations. Using pollen-based summer temperature anomaly reconstructions, the early Holocene (11700–9000 yr BP) is characterised by continent-wide cooling, with temperatures generally 1–3°C below pre-industrial average, except in Lapland and the Alps, where warming is observed (Mauri et al., 2015). This pattern persists until around 7000 yr BP, with the appearance of a north-west/south-east divide in climate trends. South-eastern Europe remained cooler than present, with particular cooling around the Mediterranean and the Balkans (Bartlein et al., 2011; Mauri et al., 2015). North-western Europe, however, recorded a divergent pattern, with evidence for warming, between 2-5°C above pre-industrial temperatures particularly evident in the British Isles, Germany and Scandinavia (Mauri et al., 2015), with the warmest periods observed 7000 and 2000 yr BP. Iberia meanwhile appears to move in and out of cold periods independently (Mauri et al., 2015). Winter temperatures as reconstructed by the same method (Davis et al., 2003; Mauri et al., 2015) display a Europe-wide cooling at the start of the Holocene, prior to generally warmer conditions in the Northern half of the continent thereafter. From 10,000 yr BP onward, northern Europe, and Fennoscandia in particular, are characterised by warming, with peak temperatures reached by 7000 yr BP. Southern Europe, in contrast, displays fairly stable winter temperatures 2°C below preindustrial levels until the most recent two millennia, where temperatures slowly increased to present conditions.

In terms of palaeoprecipitation as derived from pollen records, summers during the Holocene were generally drier in Northern Europe, and wetter in Southern Europe (Magny et al., 2013; Mauri et al., 2015), with wettest conditions reached in the south between 8000-6000 yr BP, when rainfall was ~20mm/month greater than present. Winter precipitation is characterised by a NW-SE boundary, dividing wet northern and eastern Europe from dry south-western. Excessively dry conditions (~30mm/month less than present) Europe-wide are typical of the early Holocene (11700-9000 yr BP), with the wettest period again being around 7000 yr BP. In addition to general palaeohydrological records, those which document extremely high, or low periods of precipitation are also available. Flooding records are common from central Europe, with periods of flooding events reconstructed from lake sediments (e.g. Czymzik et al., 2016, 2013; Pierre et al., 2017; Swierczynski et al., 2013).

For the most recent two millennia, tree rings and other high-resolution proxies may be used to reconstruct temperature and precipitation changes on a much finer scale than those

which are pollen-based. Using such methods, data suggest the recent warming is unprecedented, but the evidence also suggests warm and wet conditions persisted through the Roman Warm Period (RWP; 1100-850 yr BP) and Medieval Warm Period (MWP; 1100-700 yr BP), whilst the influence of the Little Ice Age (LIA) is varied across Europe (Büntgen et al., 2011; Luterbacher et al., 2012; PAGES 2k Consortium, 2017, 2013).

1.6.1. The Palaeoenvironment of the Carpathian-Balkan region during the Holocene

In the Carpathian-Balkan region, high-resolution, multi-proxy studies of palaeoenvironment are rare (see Buczko et al., 2009 and Veres and Mîndrescu, 2013 for summaries) (Table 1.1), but considerable effort is being made to address this. However, many studies exploiting either one proxy at high resolution, or multi-proxy but poor resolution/short term studies do exist (Fig.1.2, Table 1.1).

Due to the location of the Carpathian-Balkans at the confluence of three major SLP systems, the North Atlantic, Siberian and Mediterranean (Obreht et al., 2017, 2016), the area is thought to be very sensitive to shifts in SLP system intensities or positions (Perșoiu et al., 2017).

Europe-wide Holocene climate reconstructions highlight the extent to which this region behaves separately from much of the rest of Europe, with south-eastern Europe characterised by cooler-than-present average annual mean conditions throughout the Holocene, whereas north-western Europe displays warming. Furthermore, east-west palaeoclimatic gradients have been observed for the last 1100 years across the Mediterranean (Roberts et al., 2012, 2011), and a strong north-south gradient is clear in palaeohydrology from Mediterranean sites (Magny et al., 2013). This is evident in southern (northern) Mediterranean sites indicating lake level maxima (minima) during the early to mid-Holocene. Additionally, tree ring records from the region (e.g. Popa and Kern, 2009), display a different pattern compared to central European conditions (e.g. Büntgen et al., 2011) during the last 1000 years, particularly during periods of reasonably rapid climate change (e.g. MWP, LIA), indicating the strong local forcing of climate in this region.

1.6.2. Controls on Palaeoenvironment of the Carpathian-Balkan Region

The variability mentioned above appears to have been caused by a combination of orbital, oceanic, solar, and local forcing factors. Magny et al. (2013) link the north-south gradient to the behaviour of the NAO, and the remnants of northern ice sheets discharging meltwater into the North Atlantic. Likewise, Roberts et al. (2012) ascribe to the NAO a major role in the forcing of Mediterranean climate (as also seen by Trouet et al., 2009), but

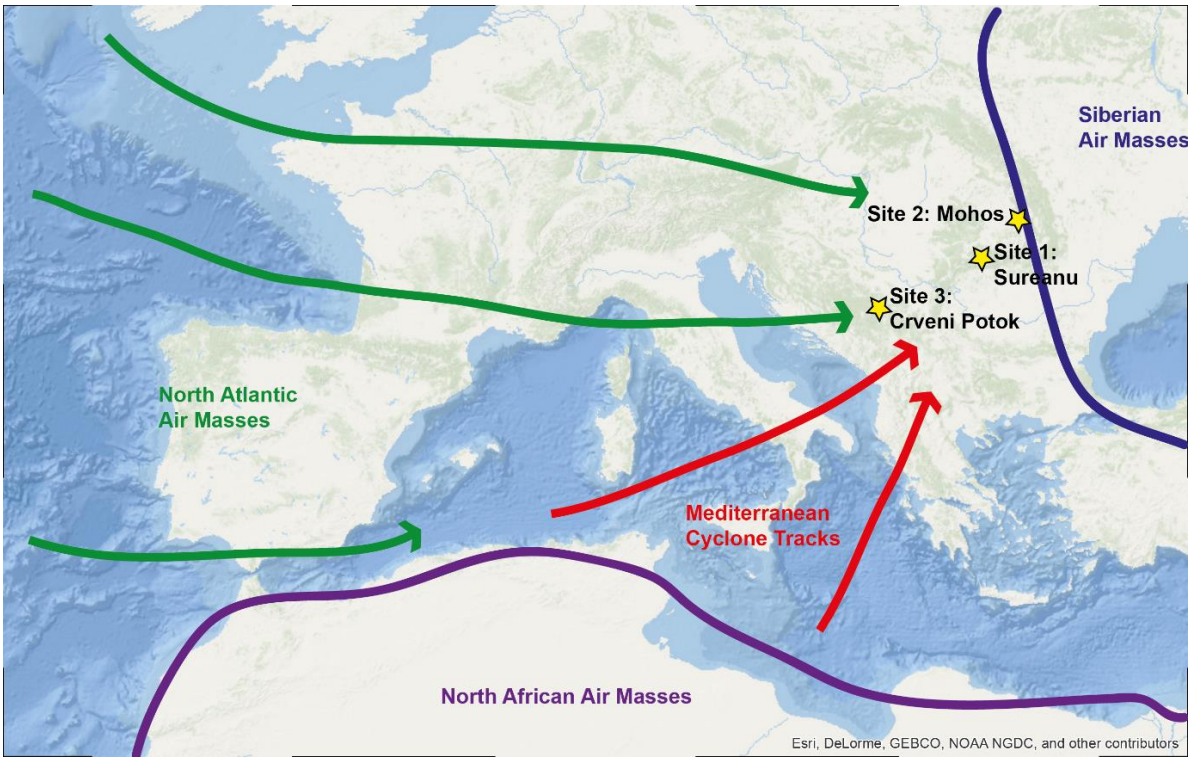

***Figure 1.2**: Map of Europe and North Africa indicating location of the three sites mentioned in this study. Green arrows indicate the direction of North Atlantic weather systems as they move into Eastern Europe. Red arrows indicate the direction of Mediterranean cyclone tracks. Also indicated are the location of two other atmospheric systems discussed Siberian air masses, including the Siberian High, and North African air masses.*

introduce the importance of further atmospheric systems, to the east (EA-WR, and the Polar/Eurasia Teleconnection (POL)) and west (including the EA (East Atlantic)). More recent studies introduce the importance of the Siberian High (Obreht et al., 2017, 2016) and periodic incursions of Mediterranean air masses (Garaba and Sfică, 2015; Haliuc et al., 2017; Obreht et al., 2016), and ascribe the erraticism to the region's location at the confluence of these systems. Theoretically, this results in small fluctuations, teleconnections and synergies between these systems being detectable in palaeoenvironmental records.

In Romania and the Carpathian-Balkan region, recent instrumental data indicates the most important of the aforementioned SLPs is the NAO. Changes in temperature (Bojariu and Giorgi, 2005; Roxana Bojariu and Paliu, 2001; Rimbu et al., 2015; Tomozeiu et al., 2002), precipitation (Bojariu and Giorgi, 2005; Tomozeiu et al., 2005) and drought periods (Stefan et al, 2004) have been linked to the NAO, with low NAO index values resulting in high precipitation and high temperatures.

The NAO plays such a major role as it dictates the direction of North Atlantic winter storm tracks as they move across the continent (Barnston and Livezey, 1987; Hurrell, 2005). When in a positive mode (i.e. the Icelandic low and Azores high are strengthened), there is an increased pressure gradient over the North Atlantic, resulting in stronger westerlies, and a strong north-eastern orientation to storm tracks, meaning the majority of low pressure systems move into north-west Europe. During weakened NAO periods, storm tracks shift to more of an east-west orientation (Fig. 1.2), moving depressions into Mediterranean Europe (Hurrell, 2005; Olsen et al., 2012; Trouet et al., 2009). This simultaneously allows the Siberian High to have more influence, bringing cold, dry air into the Mediterranean from the east. In Romania and the Carpathian-Balkan region, recent instrumental data indicates the importance of these NAO variations in forcing climate patterns. Changes in temperature (Bojariu and Giorgi, 2005; Roxana Bojariu and Paliu, 2001; Rimbu et al., 2015; Tomozeiu et al., 2002), precipitation (Bojariu and Giorgi, 2005; Tomozeiu et al., 2005) and drought periods (Stefan et al, 2004) have been linked to the NAO, with low NAO index values resulting in high precipitation and high temperatures.

Other work has proven the link between the EA-WR and temperature (Croitoru et al., 2012) and precipitation (Krichak et al., 2002) in Eastern Europe, and has indicated the ability of one SLP to impact others (Andrei and Roman, 2012; Rimbu et al., 2015), with the blocking nature of the Siberian system apparently a major control on extreme weather in Romania. Extension of these correlations beyond the instrumental records has proven difficult, but initial work indicates that the relationship between NAO and precipitation has persisted for much of the late Holocene (Haliuc et al., 2017; Magyari et al., 2013).

In addition to the interplay between the NAO and the Siberian High (Fig. 1.2), regular incursions of air masses from the Mediterranean, and their underlying controls appear to play a role on Carpathian-Balkan climate (Apostol, 2008; Garaba and Sfică, 2015). Mediterranean cyclones are formed in the central and western Mediterranean sea, primarily from the regeneration of weak North Atlantic systems (Apostol, 2008) and consist of warm and wet low pressure systems. Variations in the movement, or 'tracks' of cyclones as they move from west to east across the Mediterranean mean periodically they push further north and enter the Carpathian-Balkan region (Garaba and Sfică, 2015; Nissen et al., 2014). Such incursions bring with them both Mediterranean moisture, playing a major role in controlling precipitation (Garaba and Sfică, 2015), but also regularly entrain Saharan dust, resulting in frequent deposition of such material in the region (Varga et al., 2016, 2013). Furthermore, variations in the position of the Intertropical Convergence Zone (ITCZ) may

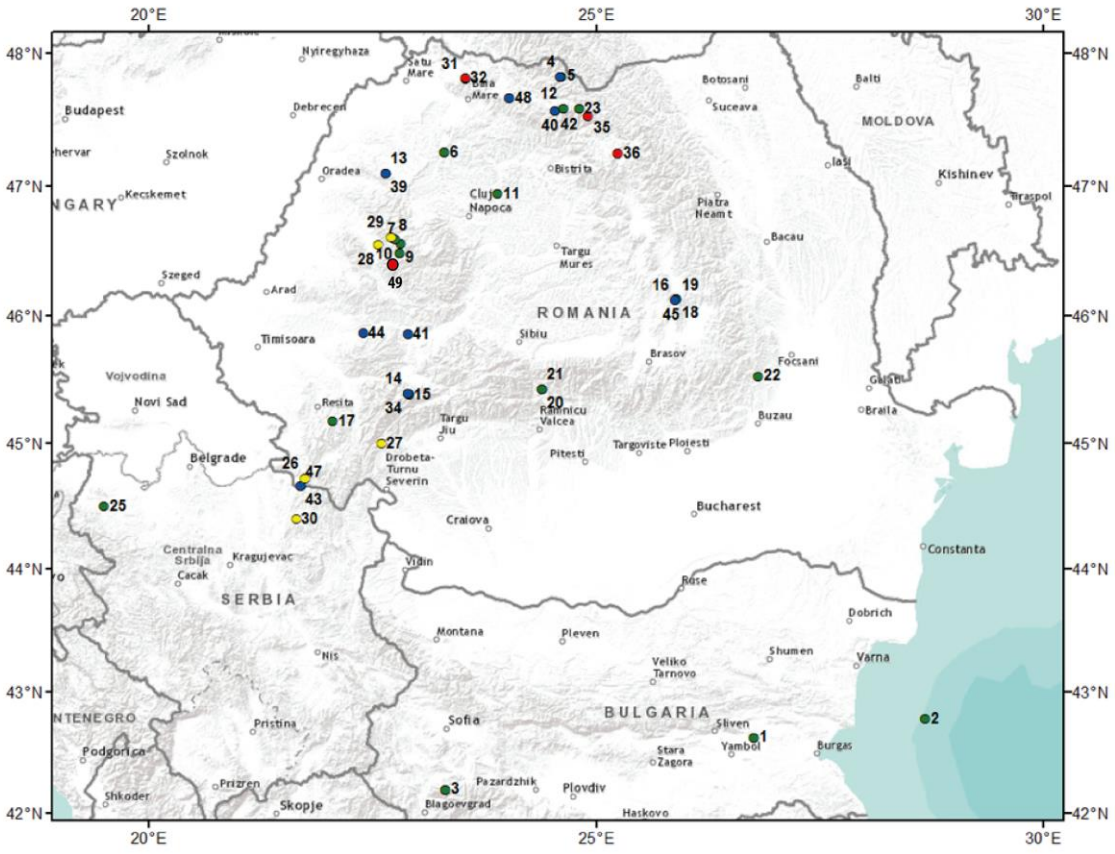

Figure 1.3: *Location map of all palaeoenvironmental sites mentioned in text, and outlined in Table 1.1. Blue circles indicate records of hydrological variability, green are vegetation studies, yellow are speleothem-based archives and red are either multi-proxy studies, or tree ring records.*

impinge on Mediterranean climate, therefore also having an impact on the Carpathian-Balkan region (Finné et al., 2011; Magny, 2004).

In addition to the atmospheric regimes, orography is another controller of local climate, as the region is home to several mountain ranges (e.g. Carpathians, Dinaric Alps, Balkans, Rila Mountains). Precipitation (Rîmbu et al., 2002; Tomozeiu et al., 2005) and temperature (Rimbu et al., 2015), in particular appear modulated by the presence of these mountain ranges. These may act as a buffer to the movement of air masses, and cause rain-out on their windward, and aridity on their leeward sides (Rîmbu et al., 2002).

Finally, local controls, and inter-site variability regularly impact the palaeoclimatic signal in the region, with an example being from Feurdean et al., (2008), where two similar sites in the same region display varying pollen records, a function of local pollen production, sedimentation rate, topography and other local controls.

Table 1.1: *Details regarding sites mentioned in text and indicated on Figure 1.2.*

ID	Longitude	Latitude	Site	Temporal Coverage (yr BP)	Archive Type	Altitude (m)	Dating type	Number of dates	Variable	Proxy/Proxies	Reference
1	26.77	42.63028	Straldzha	37000-4000	Drained Bog	138	^{14}C	13	Vegetation	Pollen	(Connor et al., 2013)
2	28.6847	42.78222	Coastal shelf	12000-Present	Ocean Sediment	-971	^{14}C	18	Vegetation	Pollen & Dinoflagellates	(Filipova-Marinova et al., 2013)
3	23.3155	42.2002	Trilistnika	15000-Present	Lake	2216	^{14}C	13	Vegetation	Pollen	(Tonkov et al., 2008)
4	24.6	47.8333	Tăul Mare-Bărdau	7000-Present	Peat bog	1615	^{14}C	6	Vegetation	Pollen	(Fărcaş et al., 2013)
5	24.6166	47.8333	Cristina	8000-2270	Peat bog	1573	^{14}C	4	Vegetation	Pollen	(Fărcaş et al., 2013)
6	23.3123	47.2564	Turbuta	13000-5000	Peat bog	275	^{14}C and U/Th	4 & 5	Vegetation	Pollen, charcoal & Sedimentology	(Feurdean et al., 2007)
7	22.8167	46.5632	Călineasa	6500-present	Infilled doline	1360	^{14}C and ^{210}Pb	5 & 5	Vegetation	Pollen, charcoal & Sedimentology	(Feurdean et al., 2009)
8	22.7323	46.5983	Padis Sondori	6500-present	Infilled doline	1290	C^{14} and ^{210}Pb	4 & 4	Vegetation	Pollen, charcoal & Sedimentology	(Feurdean et al., 2009)
9	22.8107	46.4894	Scărişoara Ice Cave	1000-100	Ice Core	1165	^{14}C	8	Vegetation	Pollen & Charcoal	(Feurdean et al., 2011a)
10	22.7641	46.5899	Molhasul Mare	5700-Present	Peat bog	1224	^{14}C	8	Vegetation	Pollen & Charcoal	(Feurdean and Willis, 2008)
11	23.9029	46.9467	Stiucii	12000-Present	Lake	239	^{14}C and ^{210}Pb	15 & 13	Vegetation and fire	Pollen & Charcoal	(Feurdean et al., 2013)
12	24.6431	47.5884	Buhăiescu Mare	11000-9800 and 4000-300	Lake	1918	C^{14} and ^{210}Pb	8 & 4	Vegetation	Pollen, macrofossils & charcoal	(Geantă et al., 2014)
13	22.65	47.1	Iaz	7000-Present	Peat bog	300	^{14}C	7	Vegetation	Pollen	(Grindean et al., 2014)
14	22.90167	45.39639	Lake Brazi	15750-10000	Lake	1740	^{14}C	8	Vegetation	Pollen, macrofossils & charcoal	(Magyari et al., 2012)
15	22.9091	45.385	Lake Gales	15200-10000	Lake	2040	^{14}C	5	Lake	Pollen, macrofossils & charcoal	(Magyari et al., 2012)
16	25.8881	46.1263	Lake sf Ana	26500-8000	Lake	946	^{14}C	10	Vegetation	Pollen, macrofossils & charcoal	(Magyari et al., 2014)
17	22.0594	45.18	Semenic	7665-present	Peat bog	1445	^{14}C	4	Vegetation	Pollen and charcoal	(Rösch et al., 2000)

18	25.9046	46.1337	Mohos 1	9200-Present	Peat bog	1050	^{14}C	20	Vegetation	Pollen	(Tanţău et al., 2003)
19	25.9046	46.1337	Mohos 2	9800-Present	Peat bog	1050	^{14}C	6	Vegetation	Pollen	(Tanţău et al., 2003
20	24.3947	45.43	Avrig 1	17600-Present	Peat/Lake	400	^{14}C	13	Vegetation	Pollen	(Tanţău et al., 2006)
21	24.3947	45.43	Avrig 2	4800-Present	Peat/Lake	400	^{14}C	4	Vegetation	Pollen	(Tanţău et al., 2006)
22	26.8166	45.5333	Bisoca	11400-Present	Peat bog	850	^{14}C	12	Vegetation	Pollen	(Tantău et al., 2009)
23	24.8165	47.5856	Poiana Ştiol	11000-Present	Peat bog	1540	^{14}C	9	Vegetation	Pollen, macrofossils & charcoal	(Feurdean et al., 2016; Tanţău et al., 2011)
24	25.7375	56.2969	Luci	16000-Present	Peat bog	1080	^{14}C & Pollen Markers	11 & 2	Vegetation	Pollen	(Tanţău et al., 2014)
25	19.505	44.5038	Donja Sipulja	450-Present	Sinkhole	250	^{14}C	8	Vegetation & land use change	Pollen, charcoal & Geochemistry	(Kulkarni et al., 2016)
26	21.75	44.72	Poleva cave	7500-2000	Speleothem	Underground (cave is 390)	U/Th	8	Temperature & Precipitation	Calcite $\delta^{18}O$ and $\delta^{13}C$	(Constantin et al., 2007)
27	22.6	45	Ascunsa cave	8200-Present	Speleothem	1050	U/Th	15	Temperature & Precipitation	Calcite $\delta^{18}O$ and $\delta^{13}C$	(Drăgușin et al., 2014)
28	22.5695	46.5538	Ursilor cave	7100-Present	Speleothem	482	U/Th	5	Temperature & Precipitation	Calcite $\delta^{18}O$ and $\delta^{13}C$	(Onac et al., 2002)
29	22.7083	46.6074	V11 Cave	14800-5600	Speleothem	1284	U/Th	22	Temperature & Precipitation	Calcite $\delta^{18}O$ and $\delta^{13}C$	(Tămaş et al., 2005)
30	21.65	44.4	Ceremošnja cave		Speleothem	530	^{14}C	6	Temperature	Calcite $\delta^{18}O$ and $\delta^{13}C$	(Kacanski et al., 2006)
31	23.5419	47.8133	Steregoiu	14700-Present	Lake/Peat	790	^{14}C	17	Temperature, Precipitation and Vegetation	Pollen	(Björkman et al., 2003; Feurdean et al., 2008)
32	23.5419	47.823	Preluca Tiganului	11500-Present	Peat bog	790	^{14}C	6	Temperature, Precipitation and Vegetation	Pollen	(Feurdean, 2005; Feurdean et al., 2008)
33	22.90167	45.39639	Lake Brazi	14500-11600	Lake	1740	^{14}C	14	Temperature & Productivity	Cladocera	(Korponai et al., 2011)
34	22.90167	45.39639	Lake Brazi	11500-Present	Lake	1740	^{14}C	14	Temperature	Chironomids	(Tóth et al., 2012)
35	24.9166	47.5333	Rodna Mountains	550-Present	Trees	1700-1800	Ring counting	n/a	Summer temperature	Tree rings	(Popa and Bouriaud, 2014)

36	25.25	47.25	Calimani Mountains	1000-Present	Trees	1780-1860	Ring counting	n/a	Temperature	Tree rings	(Popa and Kern, 2009)
37	22.90167	45.39639	Lake Brazi	15750-Present	Lake	1740	^{14}C	14	Lake levels and pH	Diatoms	(Buczkó et al., 2013)
38	24.6	47.8333	Tăul Mare-Bărdau	7000-Present	Peat bog	1615	^{14}C	6	Precipitation	Carbon isotopes	(Cristea et al., 2013)
39	22.65	47.1	Iaz	3000-Present	Peat bog	300	^{14}C & Pollen Markers	7 & 4	Hydroclimate	Testate Amoeba	(Diaconu et al., 2016)
40	24.545	47.5738	Tăul Muced	1150-Present	Peat bog	1360	^{14}C and 210Pb	12 & 11	Hydroclimate	Testate Amoeba, Macrofossils, Pollen	(Feurdean et al., 2015)
41	22.8988	45.8649	Zidită Cave	900-Present	Bat guano	Underground	^{14}C	12	Hydroclimate and vegetation	Isotopes, pollen & Charcoal	(Forray et al., 2015)
42	24.545	47.5738	Tăul Muced	9000-Present	Peat bog	1360	^{14}C and 210Pb	12 & 11	Precipitation	Macrofossils & Pollen	(Gałka et al., 2016)
43	21.6991	44.6647	Gaura cu Muscă Cave	800-Present	Bat guano	Underground	^{14}C	5	Hydroclimate	Multi-Proxy	(Geantă et al., 2012; Onac et al., 2014)
44	22.4	45.8666	Domogled National Park	323-Present	Trees	800-1100	Ring counting	n/a	Drought	Tree rings	(Levanič et al., 2013)
45	25.881	46.1263	Lake sf Ana	9500-Present	Lake	946	^{14}C	15	Lake Level & Productivity	Multi Proxy Diatoms	(Magyari et al., 2009)
46	22.90167	45.39639	Lake Brazi	14500-1370	Lake	1740	^{14}C	14	Precipitation	Diatom $\delta^{18}O$	(Magyari et al., 2013)
47	21.6991	44.6647	Gaura cu Muscă Cave	2500-Present	Bat guano	Underground	^{14}C	5	Vegetation and hydrology	Multi-Proxy	(Onac et al., 2015)
48	24.0333	47.6666	Fenyves-teto	9500-Present	Peat bog	1340	^{14}C	5	Hydroclimate	Testate Amoeba	(Schnitchen et al., 2006)
49	22.81047	46.4899	Scărișoara Ice Cave	10,000-Present	Ice Core	Underground	^{14}C	35	Temperature & Hydroclimate	$\delta^{18}O$	(Perșoiu et al., 2017)

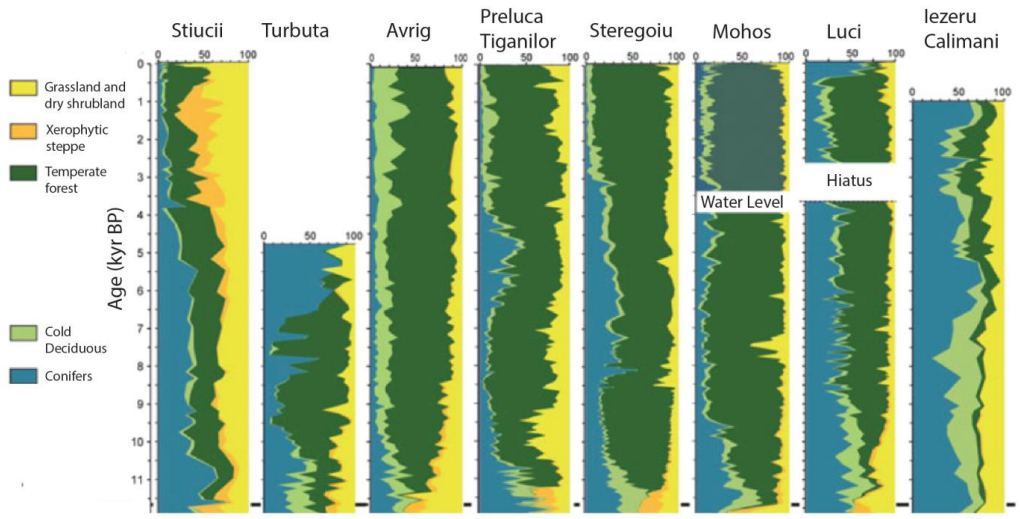

Figure 1.4: *Vegetation evolution of Romania through the Holocene as indicated by previously published data. Figure from Feurdean & Tantau, (2017).*

1.6.3. Vegetation reconstructions

Pollen-based vegetation reconstructions are the most common paleoenvironmental studies in the region. This summary mostly discusses well-dated and long-term (greater than 6000 years of coverage) studies relevant for this work, although all vegetation reconstructions are included in Figure 1.2 and Table 1.1. To allow for simple interpretation, and clearer visualisation of vegetation changes throughout the Holocene, a summary diagram from Feurdean and Tantau (2017) is presented (Fig. 1.3). Using the methodology outlined in Feurdean et al., (2014) the authors have grouped taxa according to Table 1.2.

1.6.3.1. Trees

As the cold and dry conditions of the Younger Dryas made way for the warmer and wetter Holocene, there was a concurrent decrease in steppe vegetation and Pine (*Pinus*), and increase in deciduous tree cover, particularly of cold adapted taxa. This was led by the spread of elm (*Ulmus*), due to its local survival in glacial refugia (Feurdean et al., 2012) followed by maple (*Acer*), hazel (*Corylus*), ash (*Fraxinus*), oak (*Quercus*) and lime (*Tilia*) after 10,300 yr BP. Alongside this, Spruce (*Picea*), another species with widespread glacial refugia in the Carpathian region, spread and has maintained its abundance throughout the entire Holocene, with a second expansion at ~8000 yr BP. Altitudinally, it is the dominant taxa between 1200–1800m asl. Even today, *Picea* makes up the majority of forest in mountain regions, with concentrations enhanced more recently via woodland management and plantations (Feurdean et al., 2009). Unlike *Picea*, *Ulmus*, along with *Acer*, *Fraxinus* and *Tilia* all declined after the early Holocene, with decreases noted from 8500 yr BP onwards, particularly in low-altitude sites (Feurdean et al., 2009, 2010; Tanţău et al, 2003;

Table 1.2: *Taxa groupings of typical vegetation found in Romania throughout the Holocene. From Feurdean et al., 2014.*

Coniferous taxa	*Picea abies, Pinus, Abies alba, Larix decidua, Juniperus*
Cold deciduous trees/shrubs	*Alnus, Betula, Salix, Populus*
Temperate deciduous taxa	*Ulmus, Quercus, Tilia, Corylus avellana, Acer, Fraxinus, Carpinus betulus, Hedera, Ilex, Fagus sylvatica, Viscum, Sambucas, Viburnum, Cornus, Frangula, Myrica, Prunus, Sorbus*
Warm and dry steppe	Ericaceae, *Calluna, Hippophäe,* Poaceae, Cyperaceae
Grasses and dry shrubs	*Artemesia*, Chenopodiaceae/Amaranthaceae

2006, 2009, 2014, Fârcaş et al, 2013). This initial decline continued throughout the mid-Holocene and their concentrations have never recovered. The decline of *Pinus* has reversed slightly in recent times, in a comparable manner to *Picea*, via plantations.

For the remainder of the Holocene, Romanian forests underwent a succession of changing co-dominant taxa (Fig. 1.4), reflecting both climatic shifts and human influence. *Picea* and *Quercus*, due to human cultivation appear to have persisted throughout (Feurdean and Tantau, 2017, Feurdean et al., 2009). Following the decline of *Fraxinus*, *Tilia* and *Ulmus*, *Corylus* flourished (Fig.1.4), spreading across Romanian forests from 10300 yr BP onwards (e.g. Fârcaş et al., 2013; Feurdean et al., 2010, 2009, 2007, Tanţău et al., 2011, 2006, 2003). This period of *Corylus-Picea* co-dominance reflects a biome configuration which is not observed today, and persisted until around 5500 yr BP, when hornbeam (*Carpinus)* largely replaced *Corylus* vegetation, an impact of increased human pressure (Feurdean and Tantau, 2017) (Fig. 1.4).

Between 5500–3500 yr BP, *Carpinus* was a major component of the forests, alongside *Fraxinus*, *Quercus* and *Tilia* at low-altitudes, and beech (*Fagus)* at higher (e.g (Fărcaş et al., 2013; Magyari et al., 2012; Rösch and Fischer, 2000). The late succession of *Fagus* appears to have replaced the *Carpinus* element in most forest areas since roughly 5000 yr BP (Fig. 1.4.) (see Feurdean and Tantau, 2017 for references). Its ability to grow in shade allowed out-competing of *Carpinus* and *Picea* under climatic and human-related stresses, and spreading widely (Feurdean et al., 2011b, 2010). Modern-day forests in mid-altitudes are dominated by *Fagus*, whilst in higher altitudes *Fagus* is generally co-dominant with

Picea (Toader and Dumitru, 2004), before the shift to *Pinus* (Toader and Dumitru, 2004). The treeline in Romania today is roughly at 1800–1900m (Feurdean et al., 2012), and above it species of shrub, grass and dwarf pine (*Pinus mugo*) dominate (e.g. Geantă et al., 2014).

1.6.3.2. Other Plant Taxa and Human Impact

Since the natural vegetation of the Carpathian-Balkan region consists of dense forest (Feurdean and Tantau, 2017), evidence, in the form of generally decreasing forest densities (see Fig. 1.3 and Kaplan et al., 2009), for humans having a major role in the distribution of vegetation is clear. This deforestation, caused either by logging activity, or pasture opening (Schumacher et al., 2016), may be directly attributed to human activity. More specifically, humans played a role in the downfall of *Carpinus* and rise of *Fagus*, whilst artificially increasing *Pinus* and *Picea* proportions in recent years (Feurdean, 2010; Schumacher et al., 2016). Alongside the observable indirect impact, a major increase in both primary anthropic indicator taxa (e.g. *Secale*, *Hordeum*, *Triticum*, *Zea* and other cereals) and secondary indicators (those of pastures and meadows, e.g. Poaceae, Cyperaceae, *Plantago* etc.) are present throughout much of the Holocene (Feurdean and Tantau, 2017). In many cases, such taxa have now made up a substantial percentage of the pollen record, particularly in lowland sites (e.g. Feurdean et al., 2015) but also in much higher altitudes (e.g. Fârcaş et al., 2013). The decrease in tree taxa in most locations is offset by the increase in these herbs, grasses and cereals.

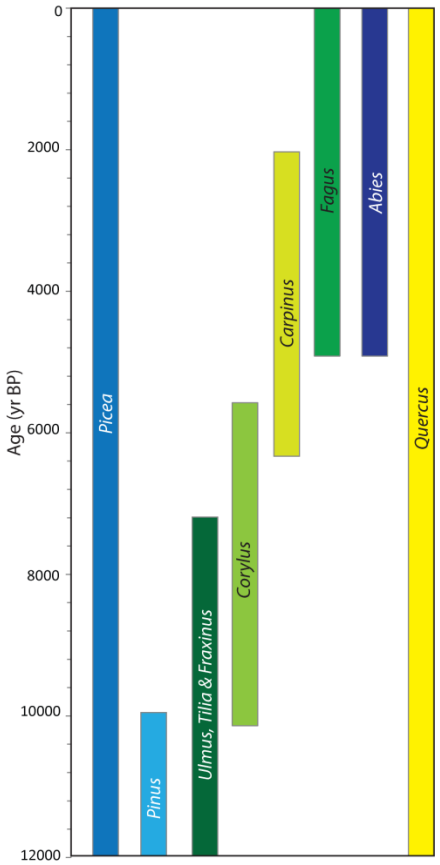

Figure 1.5: *General vegetation evolution through the Holocene as indicated by palaeoecological studies.*

The earliest evidence of human alteration may be seen in isolated examples of cultivated plants in lowland sites roughly 7500 yr BP, along with widespread charcoal-inferred forest burning to make room for livestock pastures at this time (Feurdean et al., 2015, 2013). Since roughly 4000 yr BP, continuous and abundant secondary anthropogenic indicators (especially *Plantago* and *Rumex*) may be seen across the region, indicative of the increased

human impact over the Bronze and Iron ages (Geantă et al., 2014), even in high mountain areas. During the Roman period, a major increase in all indicators may be observed, indicative of the increasing agriculture, and demand for wood for construction. From the Middle Ages onwards, cultivated plants become ubiquitous in records, regardless of altitude, but with increased concentrations in lowland sites (Feurdean and Tantau, 2017).

1.6.4. Hydrological Reconstructions

The availability of long and well-dated hydrological reconstructions in the Carpathian-Balkan region is poor (Haliuc et al., 2017; Magyari et al., 2014) (See Table 1.1). Diatoms have been exploited for their lake-level related assemblage changes (Buczkó et al., 2013; Magyari et al., 2009) and their ability to record changing $\delta^{18}O$ (Magyari et al., 2013). Macrofossils (Gałka et al., 2016), testate amoeba (Diaconu et al., 2016; Schnitchen et al., 2006), geochemistry (Haliuc et al., 2017) and pollen have also been used. Multi-proxy approaches are limited to more short-term records (e.g. Feurdean et al., 2015; Forray et al., 2015; Onac et al., 2015), with a recent exception being a multi-proxy approach to reconstructing carbon accumulation (Panait et al., 2017).

The early Holocene (10,700–8000 yr BP) period is characterised by low moisture availability (in summer), across the region, with evidence from both north-western and eastern Romanian sites (Buczkó et al., 2013; Feurdean et al., 2013; Magyari et al., 2013). This dry period follows the Younger Dryas cooling, with slowly increasing moisture availability until roughly 8000 yr BP. Further evidence of aridity may be seen in the high charcoal values throughout this period (Connor et al., 2013; Feurdean et al., 2013), and low lake levels in both the Eastern (Magyari et al., 2009) and Southern (Buczkó et al., 2013) Carpathians. Furthermore, dry conditions are indicated in eastern Hungary (Jakab and Sumegi, 2004) and southern Poland (Starkel et al., 2006), indicating the extent of drying across Eastern Europe. Within this period, the 8200 yr BP event is characterised by a short term increase in moisture, clear in multiple proxies (Buczkó et al., 2013; Magyari et al., 2013; Pal et al., 2016) from high-altitude sites in the Carpathians.

For much of the Mid-Late Holocene, alternating wet-dry phases are observed. These vary in timing and intensity dependant on location, but with some correlation. Dry periods as observed through changes in peat deposition (Gałka et al., 2016; Schnitchen et al., 2006) occur in line with periods of low fire activity (Feurdean et al., 2013) and low lake levels (Buczkó et al., 2013). The clearest of these, between 6300–5800, 5500–5000 and 3100–3000 yr BP may be seen in all such records (see Fig. 1.5). A major dry period is observed region-wide between 6000 and 5000 yr BP (Buczkó et al., 2013; Feurdean et al., 2013;

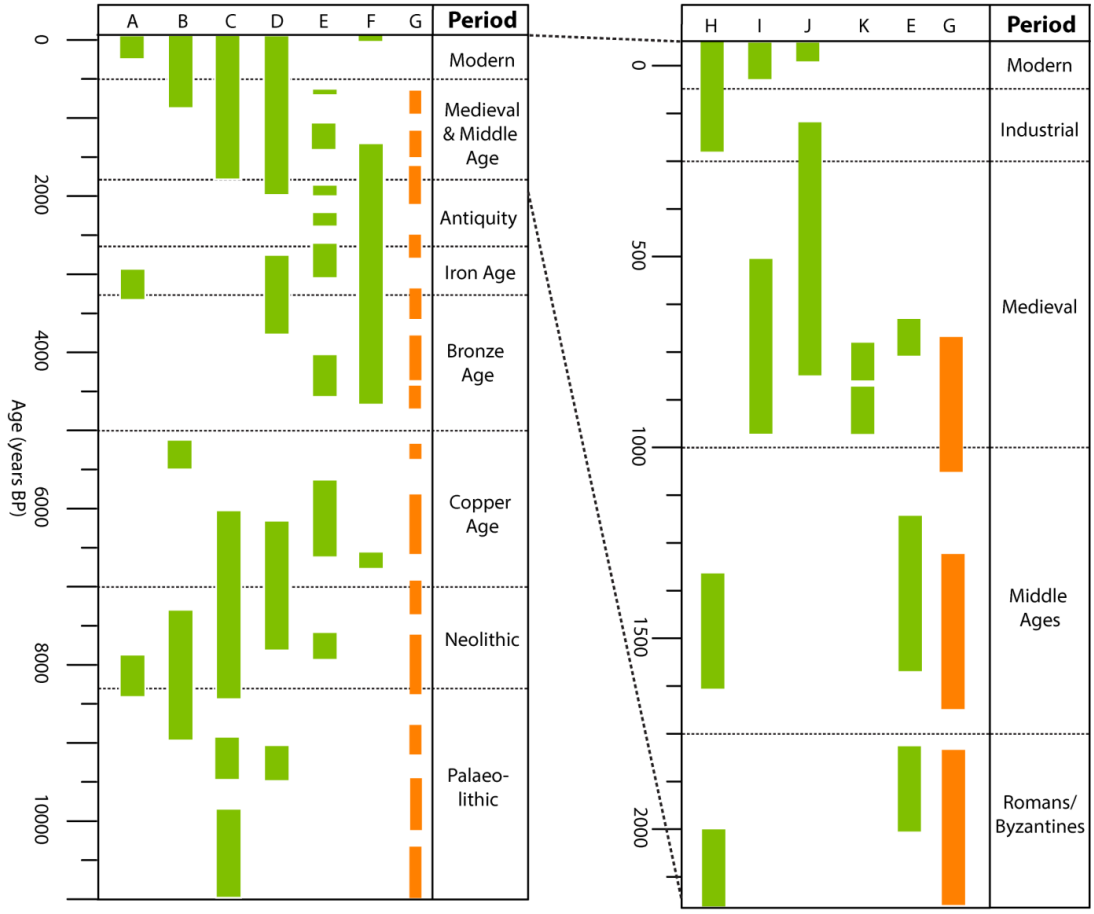

Figure 1.6: *Hydrological reconstructions from Romania. Orange bars are periods of low lake levels in central Europe as indicated by Magny, 2004. Data presented via green bars is drought/dry/low lake periods from the following publications in the Carpathian region. A: Schnitchen et al. (2006), B: Magyari et al. (2009), C: Buczkó et al. (2013), D: Magyari et al. (2013), E: Gałka et al. (2016), F: Cristea et al. (2013), G: Magny, (2004), H: Diaconu et al. (2016), I: Forray et al. (2015), J: Feurdean et al. (2015) and K: Onac et al. (2015).*

Gałka et al., 2016; Tămaş et al., 2005), possibly linked to a reorganisation of Eastern European climate teleconnections (Perșoiu et al., 2017).

It must be noted, however, that not all records are in agreement, with the climatic conditions surrounding the apparent 4200 yr BP event (see Gałka et al., 2016), and around 2800 yr BP displaying contrasting trends. For example, conditions around 2800 yr BP may be extremely wet (Feurdean et al., 2013; Magyari et al., 2009; Schnitchen et al., 2006), or dry (Feurdean et al., 2008; Onac et al., 2002), likely reflective of local site variability. As such, when considering reconstructions, the impact of local shifts must not be discounted. Another short period of dry conditions correlating to the Roman Warm Period (RWP, roughly 2250–1900 yr BP) is observed (Feurdean et al., 2013; Gałka et al., 2016; Magyari

et al., 2013) prior to wetter conditions prevailing through the Dark Ages (1900–1600 yr BP, Büntgen et al., 2011; Gałka et al., 2016).

Feurdean et al., (2015) have put together a valuable high-resolution, multi-proxy record of hydroclimate for the past 1300 years. From this, and other reconstructions, it appears hydroclimate has fluctuated in line with continental controls. This is manifested in a wet MWP (1200–700 yr BP, Cristea et al., 2013; Feurdean et al., 2015) and a dry LIA (550-150 yr BP; Feurdean et al., 2015, 2008; Schnitchen et al., 2006). All records display a clear drying in the past 100 years (Buczkó et al., 2013; Diaconu et al., 2016; Magyari et al., 2009, 2013; Morellón et al., 2016; Schnitchen et al., 2006) (Fig.1.5).

1.6.5. Dust

As a key component of the biogeochemical system, mineral dust as released by erosion of soil, rock and deserts is of great importance to our understanding of palaeoenvironment (Albani et al., 2015; Mahowald et al., 2014, 2010). Studies in western Europe have specified the impact of changing dust sources throughout the Holocene using peat cores (e.g. Allan et al., 2013b), with special focus having been placed on the dust-forming impact of desertification, and in particular the development of the Sahara (deMenocal et al., 2000; Jiménez-Espejo et al., 2014; Le Roux et al., 2012). Despite its role in such biogeochemical cycles, its involvement in moderation of incoming solar radiation (Mahowald et al., 2010; Yoshioka et al., 2007), as a nutrient supplier (Jickells, 2005), and the apparent linkage between dust emission and loess (which is extremely prevalent in the Balkans) formation (Ben Israel et al., 2015; Marković et al., 2015; Smalley et al., 2011), research in the Carpathian-Balkans is limited to modern observation-based studies (Ujvári et al., 2012; Varga et al., 2016, 2013). From such work, it is clear periodic Mediterranean (containing Saharan desert dust) incursions effect the region many times each year, and that dust flux into Eastern Europe is substantial (Varga et al., 2016).

1.7. Human History in the Carpathian-Balkans during the Holocene

1.7.1. Prehistory

The Carpathian-Balkan region is one of the longest continually-inhabited regions on Earth, with evidence for anatomically modern human occupation of south-western Romanian caves as far back as ~40,000 yr BP (Fu et al., 2015). It appears south-western Romania harboured a major human population long into the Holocene, and allowed for the transition from Palaeolithic hunter-gatherers to the eventually sedentary farmers of the Mesolithic

and Neolithic (Bonsall et al., 2015; Willis et al., 1994). During the Mesolithic the Danubian Iron Gates region appears to have become a centre of occupation, with various spectacular Mesolithic occupation-related finds, including at Lepenski Vir (Boric, 2002; Srejović, 1969), Climente (Bonsall et al., 2012) and Schela Cladovei (Boroneanț et al., 1999), all attributable to the local Starcevo-Cris-Koros culture.

The early Holocene was a period of great technological advances, with the region home to a number of advanced civilisations, including the Vinca and Cucuteni (Bailey, 2000). These, along with the Starcevo-Cris-Koros belong to the so-called "First Temperate Neolithic" (Chapman, 2000), the first cultures to practice agriculture in temperate Europe, facilitating the spread of these practices northwards from their origins in modern-day Greece (Budja, 2001; Chapman, 2000; Rossi and Toynbee, 1971). In addition to farming, the Vinca were potentially the first culture in the world to develop written text (Lazarovici and Merlini, 2005), the first to employ crude metallurgy (Radivojević et al., 2010), and the first to create anthropomorphic figurines in Europe (Chapman, 1981), whilst the Starcevo-Cris-Koros were the first to exploit salt as a resource (Weller and Dumitroaia, 2005). These cultures, and those which followed them in the Carpathian-Balkans make up what has been termed "Old Europe" (Anthony and Chi, 2009; Gimbutas, 1982); a stable, possibly matriarchal and advanced (particularly with regards to metallurgy, see Boroffka et al., 2015) group of prehistoric cultures, who developed in the region prior to the city states of the Bronze Age (Anthony and Chi, 2009) (Fig. 1.6).

1.7.2. Metal Ages

A number of hypotheses have been postulated regarding the decline of Old Europe, with climatic deterioration (Anthony, 2010; Todorova, 1995), and conquest from the east (Gimbutas, 1974) common explanations. Whatever the cause, the Carpathian-Balkans transitioned into the Bronze Age at around 5500 yr BP, approximately 1000 years before Western Europe (Anthony and Chi, 2009; Jovanović, 2009; Nikolova et al., 1999)

The Early Bronze Age was a cultural mosaic within the region (see Gogâltan, 2015 for a review). Remainders of Old Europe slowly disappeared, to be replaced by the chieftain-led, tumulus-building, bronze forging Cotofeni and Baden cultures (Coles and Harding, 2014; Gogâltan, 2015, 1998, 1995; Hansen, 2013). Development continued throughout the Middle and Late Bronze Ages, and with local cultures (e.g. Cotofeni, Wietenberg, Otomani and Nuoa) leading the region to the forefront of European metallurgy, as high-quality local ores were exploited. During this time metal production became a major facet of the economy (Gogâltan, 1998), alongside traditional animal breeding and agriculture. This was

particularly in the late Bronze Age, when non-ferrous mineral sources were discovered, and technology arrived from the east via the Noua culture (Wittenberger, 2008). With further innovations from the south (via the Otomani culture), and as a result of high-quality local metal deposits, Transylvania and the Carpathian Basin, by the end of the Bronze Age, had become a centre of European metal production (Hansen, 2013). Mobility during this period was high, with evidence of far-reaching trade networks including as far north as Scandinavia (Ling et al., 2014) and south to the Mycenaeans (Kristiansen and Larsson, 2005).

Much changed with the Late Bronze Age collapse (roughly 3200–3100 yr BP), as various Eastern Mediterranean civilisations (including the Hittites and Mycenaeans) disappeared (Kaniewski et al., 2013). Such a collapse was not limited to the southern Balkans, with archaeological finds attesting to the cessation of a number of Carpathian cultures, including the advanced, salt-mining Gava (Ciugudean, 2012) and the aforementioned Wietenberg (Makkay, 1995). Furthermore, DNA evidence indicates this shift was accompanied by an influx of migrants from the east, indicating the transitional nature of this period (Hervella et al., 2015).

Following the upheaval of the end of the Bronze Age, the Iron Age (3100 yr BP onward) was ushered into Romania and surrounding locations by the Basarabi and associated Hallstatt cultures (e.g. Bosut in Serbia) (Bozhinova, 2012). These cultures occupied what was later named Thrace by the ancient Greeks, who upon their first contact with the descendants of these early Iron Age cultures within modern-day Romania and Bulgaria, designated them the Getae, whilst Roman scholars used the term Dacians (Taylor, 1994). Whatever the nomenclature, the local population appear to have been various indo-European tribes, who excelled in metalworking (most famously the Dacian gold bracelets; see Constantinescu et al., 2009), whilst there is evidence they had knowledge of botany and other scientific pursuits, including astronomy (Oprea and Oprea, 2015). From 82 BCE under King Burebista, these tribes united briefly, forming the Kingdom of Dacia which comprised much of modern-day Romania. For a while they resisted Roman invasions, until their final conquest in 106 CE by Trajan (Rossi and Toynbee, 1971; Schmitz, 2005). It must be noted that Dacia's rich metallurgical resources, exploiting the local Apuseni Mountains ores was one of the primary drivers behind the Roman Empire's goal to conquer the area (Luttwak, 1976).

Throughout the metal ages, the territory of modern-day Serbia, underwent invasion by many peoples after the decline of the fairly stable Vinca culture (Bailey, 2000). By the Iron

Age, parts were under Greek control, whilst the majority was dominated by Thracian, Illyrian and Celtic tribes, the most famous of which were the Scordisci (Papazoglu, 1978).

1.7.3. Roman Dacia and Byzantium

The Scordisci were Romanised after receiving Roman citizenship from Emperor Trajan, and the area was incorporated into the Roman province of Moesia after roughly 100 A.D (Buzon, 2009). In Dacia, however, the aforementioned factors, coupled with the Dacian king Burebista's expansionist policies, resulted in the a series of wars, including the final Dacian wars (101–106 CE), a sequence of attempted Roman conquests, prior to successful assimilation after 106 CE (Gudea, 1979; Rossi and Toynbee, 1971) as Roman Dacia (MacKendrick, 2000; Taylor, 1994).

The Romans began a major reorganisation of Dacia. Particular attention was paid to the mining of the region (Borcoș and Udubașa, 2012), exploiting existing deposits, especially in the Apuseni Mountains (Baron et al., 2011; Ciugudean, 2012), and exploring others. As a result, the Apuseni area became one of Rome's main sources of metal (Baron et al., 2011; Pundt, 2012). In addition to mining, the Romans also greatly improved agricultural and commercial practices, including the creation of agricultural terraces on mountainsides (Cioacă and Dinu, 2010). Roman Dacia suffered from internal, and external resistance to the Roman rulers (Oltean, 2007; Schmitz, 2005). Mass invasion of Roman Dacia and Moesia by surrounding tribes, including the Quadi, Roxolani and previously Dacian Cotoboci was commonplace throughout the occupation (Sarnowski, 2015; Wilkes, 2005), whilst the Dacians rebelled a number of times (Pop, 1999; Sarnowski, 2015). Unsurprisingly, therefore, it was amidst a climate of tribal invasions (this time by Goths and Dacian Carpi) the Romans abandoned Dacia by 271 CE (MacKendrick, 2000), moving the north-eastern frontier of the empire to the Danube.

1.7.4. Middle Ages and the Medieval Period

An element of Daco-Roman heritage persisted into the Middle Ages, prior to a period of tumult and migration (Cioacă and Dinu, 2010). The first new arrivals, the Gepids and Goths (Poulter, 2007; Sarnowski, 2015), were transitory and their appearance marked the end of town life for the region until the Medieval period. Following them, various other tribal invaders came and went, including the Avars, Slavs and Bulgars (Curta, 2008; Engel, 2005), before the integration of some of Romania (Transylvania) and Serbia into the Kingdom of Hungary by 1100 CE. This occurred prior to Mongol invasions, which destroyed much of the Kingdom, including the major Transylvanian settlements at Alba Iulia and Cetatea de Balta in 1241 and 1242 CE (Sălăgean, 2005).

The later Middle Ages and Early Medieval periods in the Carpathian-Balkans were typically characterised by small principalities (voivodeships, districts and counties), ruled by noblemen, counts and kings (Nagler, 2005). Wallachia, Moldavia and Transylvania were established as independent Romanian states (Treptow, 1997), with Vojvodina the Serbian equivalent (Fodor and Dávid, 2000). Under Hungarian influence, Catholicism spread and technology gradually improved, with the re-opening of mines in the Apuseni Mountains in the 15th century indicative of this (Pop, 2005). In Serbia, the early Medieval period was one of great economic growth, built upon its mineral wealth. Mining in the area flourished with the arrival of Saxon miners between after 1141 CE, who aided development of silver mines in the Dinaric Alps, and the Danube valley (Stojkovic, 2010; Stojković, 2013).

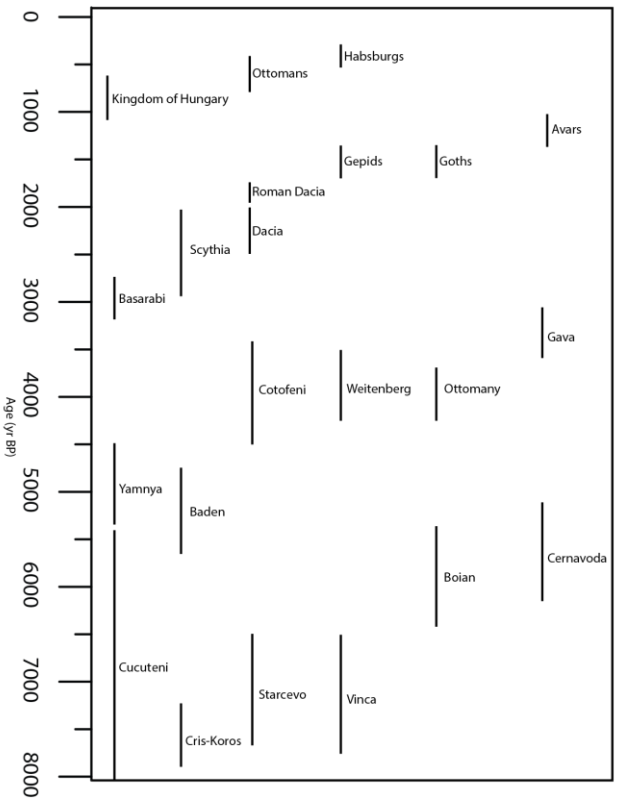

Figure 1.7: *Simplified diagram indicating appearance and disappearance of the major controlling cultures in what is modern-day Romania and Serbia.*

This configuration persisted until the downfall of the Kingdom of Hungary following the battle of Mohacs in 1526 CE, where the Ottomans delivered a crushing defeat (Engel, 2005; Fine, 1994). Much of the Carpathian-Balkans was subjected to Ottoman rule, with principalities paying tributes to Ottoman sultans, but preserving internal autonomy (Barta and Köpeczi, 1994). Under the Ottomans, mining and metallurgy continued, but with progressively tighter controls, resulting in excessive bureaucracy (Stojkovic, 2010) and reduced production in the 17th Century.

From the late 17th Century onwards, Christian forces began the slow process of forcing the Ottomans from the Balkans, with Serbia and Transylvania falling under Habsburg influence from 1688 CE onwards (Bachman, 1989; Barta and Köpeczi, 1994; Pop, 1999). Bessarabia, the eastern part of Moldavia, meanwhile, fell under Russian rule from the mid-

18th Century. Serbia, meanwhile, with the assistance of the Austrians, gained independence after two uprisings in the early 19th Century (Bachman, 1989; Pop, 1999).

The first attempts to unify modern-day Romania, still under Ottoman rule, were made with the support of the Russian Empire. Failed revolutions were attempted in Wallachia in 1821 and 1848 CE (Stavrianos, 1958) prior to independence for the semi-unified Kingdom of Romania (including Wallachia and Moldova) following the Russo-Turkish war of 1877–1878, when Romania fought with the Russians against the ruling Turks (Barta and Köpeczi, 1994; Kellogg, 1995). However, Romania as it exists today was not truly united until after the First World War, when Transylvania, Bessarabia and Bukovina joined the Kingdom of Romania resulting in a 'Greater Romania' (Constantinescu, 1971; Livezeanu, 1995).

1.7.5. Industrial to Modern

The nascent Kingdom of Romania underwent a period of stability and growth in the years just prior and after its independence was achieved. Industrially, the country grew fast, with abundant oil and natural resources. Indeed, one of the first oil refineries was built at Ploiesti in 1857 (Buzatu, 2002), prior to sugar and brick factories, and a railway network. Agriculture was still the dominant occupation for Romanians at this time (Barta and Köpeczi, 1994), but the Industrial Revolution certainly had a major impact during the mid-late 19th Century (Bachman, 1989; Borcoş and Udubaşa, 2012), with the opening of a large number of mines exploiting the rich local resources.

This stability persisted until two major conflicts, first the Second Balkan War between Bulgaria and much of the rest of the Balkans, and the First World War. Romania remained neutral until 1916, when it entered on the side of the Allies, with Russian support (Stevenson, 2011). This involvement was disastrous, and the Axis powers, following Russia's descent into civil war, forced the nation to sign an armistice in 1917 (Barrett, 2013), prior to the unification of Greater Romania in 1918 (Bachman, 1989; Livezeanu, 1995).

Authoritarian rule began shortly before the Second World War, in which Romania fought alongside the Nazis after 1941 (Bachman, 1989) until King Michael's coup d'état in August 1944. After the war, full communist rule prevailed, with the Kingdom of Romania replaced by the Socialist Republic of Romania, most famously, under Nicolae Ceaușescu (after 1965) (Behr, 1991). With the help of foreign credits he oversaw rapid economic growth and industrialisation, with very few concerns regarding its environmental impact (Judt, 2005). Mines and industrial works were opened across the country, exploiting rich

oil, gas and ore deposits (Borcoş and Udubaşa, 2012), including a number of uranium mines in the Bihor and Banat regions (Aurelian et al., 2007). This development, however, gradually gave way to austerity and political repression, a climate within which his totalitarian government fell in December 1989 (Sebestyen, 2010). Most recently, Romania has joined both NATO (in 2004) and the EU (in 2007), part of a concerted effort to realign its politics with Brussels and not Moscow.

1.8. Archaeometallurgy

Of all of humanity's innovations, the discovery and use of metals have had arguably the largest impact on the development of modern society (Table 1.3). As such, it is vital to understand the history and development of such key components of human existence. Archaeometallurgy is the study of the history of metals, both their use and production. The production and accumulation of metals has played a key role in human development and since large amounts of valued metals rarely occur near to regions of demand, the chase of sources has led much of the world's exploration, colonization and trade. The impact of metallurgy on human history cannot be underestimated.

1.8.1. Origins of Metallurgy

The earliest evidence of metal in the archaeological record is of copper, since it appears (albeit rarely) in its native form, or associated with carbonates or silicates of copper such as azurite malachite, and dioptase minerals (Killick and Fenn, 2012; Patterson, 1971). Due to their lustre, colour and tonality it is likely they were selected to produce objects of distinction. The first evidence of such use of metallic minerals appears in the archaeological record in the Near East and Iraq roughly 12000–10000 yr BP (Solecki, 1969), before the slow spread westward into Europe (Roberts et al., 2009; Wertime, 1973). Another metal which occurs frequently in its native form is gold, though large nuggets are incredibly rare, and so no similarly ancient golden artefacts have been discovered (Table 1.3).

The use of metal in its native form may be considered premetallurgical, with hammering and annealing the limit of such metalwork. As such, the development of extractive (smelting, or heating of rock or ore, to recover the metal) methods may be considered the true inception of metallurgy. Due to the high melting points of both copper (1085°C) and gold (1064 °C), specialised methods must have been developed. These required 1) the burning of charcoal to produce a reducing agent (carbon monoxide) 2) bellows or blowpipes to force air into the system and burn the charcoal faster, yielding higher

Table 1.3: *Earliest appearance of selected metals in the archaeological record presented alongside Average Crustal Abundance (ACA). Table from Killick and Fenn, (2012).*

Metal	ACA (ppm)	Earliest appearance/regular usage
Copper (native)	55	Late ninth millenium BCE
Lead	13	Late sixth millenium BCE
Copper (smelted)	55	Late sixth millenium BCE
Silver (native/smelted)	0.07	Mid-sixth ninth millenium BCE/ early fouth millenium BCE
Gold (native)	<0.01	Fifth millenium BCE
Arsenic (as Cu-As alloy)	1.8	Fifth millenium BCE
Antimony (as Cu-Sb alloy)	0.2	Fifth millenium BCE
Tin (as Cu-Sn alloy)	2	Fourth millenium BCE/late third millenium BCE
Zinc (as Cu-Zn alloy)	70	Third millenium BCE/late first millenium BCE
Iron	50000	Early second millenium BCE/late second millenium BC
Aluminium	81300	Late nineteenth century CE
Titanium	4400	Late nineteenth century CE

temperatures, and 3) crucibles to contain the reaction (Killick and Fenn, 2012). As a result of the demanding procedure of extractive metallurgy, it is no surprise there exists a gap of more than 3000 years from the appearance of worked native metals, and proper smelting.

The first evidence for such extractive metallurgy (of copper) is in the Carpathian-Balkan region, attributed to Vinca culture extending from central Romania into what is modern-day Serbia roughly 5000 BCE (Radivojević et al., 2013, 2010). Similarly-dated finds have also been made in Iran (Frame, 2004; Oudbashi et al., 2012). Alongside evidence of early copper metalworking, the Balkans (specifically the Varna horde from Bulgaria) also preserve evidence of the earliest gold smelting, between 4560-4450 B.C (Chernyk, 1992; Higham et al., 2007).

1.8.2. Development of Metals

1.8.2.1. Bronze

The development of metallurgy worldwide follows a simple pathway, from native copper, through smelted copper to bronze (Wertime, 1973). The smelting of copper alongside tin (or arsenic) was found to produce an alloy far stronger than either in isolation; bronze. Again, the first evidence of such activity is from the Balkans, with the Vinca appearing to have mastered the art of tin-alloy Bronze around 4500 BCE (Radivojević et al., 2013). Other early examples exist from c.4000 BCE in Egypt (Nicholson and Shaw, 2000) and the

near east roughly 3300 yr BP (Helwing, 2008). Due to the scarcity of tin, and the value of bronze, a large trading network developed during the Bronze Age, linking copper sources (particularly the Balkans and Cyprus) with tin sources (as far away as Britain and Scandinavia) (Ling et al., 2014), or in the Balkans (Huska et al., 2014; Mason et al., 2016).

1.8.2.2. Iron

The use of iron required a separate innovation to allow for its separation due to the strong bonds of iron to oxygen. As such, an iron smelter needs very low partial pressure of oxygen, technology which was not invented until the 2nd millennium BCE, with evidence of smelting iron from Egypt and the Near East (Photos, 1989), and Sub-Saharan Africa (Miller and Van Der Merwe, 1994). Iron production at this time utilised a bloomery, which produced porous iron, which subsequently had to be hammered to harden it. By the end of the Iron Age, it had been discovered that heating iron with charcoal caused some of the carbon to be fused into the iron, to form steel. This was found to greatly increase the hardness of the metal, particularly when rapidly cooled, via water quenching. Steel was first developed in Anatolia, but made famous by specialists in South India, producing the Wootz steel (Bronson, 1986; Srinavasan, 1994), and subsequently by Persian specialists, producing Damascus steel (Verhoeven et al., 1998). The emergence of cast iron in the 5th Century BCE in China (Wagner, 1993), and the continued production of other steels meant ferrous metallurgy has remained the dominant form of metal production throughout the past 2000 years.

Metal production reached a peak during the Roman period, when large amounts of steel for weapons, lead for pipes, and silver and gold for coins and jewellery were produced and traded. Roman technology was far more advanced than before, and allowed for the production of such metals on a scale previously unseen (Hillman et al., 2017; Nriagu, 1996; Settle and Patterson, 1980). Indeed, even the development observed at the end of the Medieval period (e.g. Baron et al., 2006; Brännvall et al., 1999) did not reach Roman levels, and production of many metals was unmatched until the Industrial Revolution (Nriagu, 1996). As may be seen in Table 1.3, natively-common metals (Cu, Pb, Au and Ag) and their associated alloying metals (As, Sb, Sn, Zn and Pb), alongside Fe, were the only metals exploited in any quantity until the late 19th Century, and the industrial revolution (Killick and Fenn, 2012).

1.8.3. Environmental Impact of Mining and Metallurgy

Whatever the metal being exploited, and whichever way, metallurgy causes a whole host of environmental impacts. In the first instance, mining releases large amounts of particulates and aggregates, much of which is contaminated by metals and metalloids (Csavina et al., 2012). Alongside direct dust produced, mine wastes and tailings, rich in metals, may be easily leached or remobilised (Salomons, 1995), inputting further dust into the atmosphere and surface waters.

Further to the direct erosion and emission of metal-rich dust, smelting processes release even greater quantities of metal-based atmospheric pollution (Dudka and Adriano, 1997; Nriagu and Pacyna, 1988). Although most mines are specific to one or a few metal commodities, they may produce large quantities of other elements as by-products. This is because ores, and especially Pb ores, are generally polymetallic, and so a wide range of metals are released when they are smelted, including Cu, Ni, Cd and As (Nriagu, 1996). In the modern world, Pb is a key component of batteries, dyes, weaponry, solders, radiation shields and many other products, and so Pb-specific mines and smelters are commonplace (Patil et al., 2006; Zhang et al., 2015). These are far from the only Pb-polluting sites, however. Zn, another important metal in today's society, is generally found in polymetallic ores alongside Pb, and so any Zn extraction is invariably linked to Pb pollution (Zhang et al., 2012). The Carpathian-Balkan Region and Metallurgy

1.8.4. The Carpathian-Balkan region and Metallurgy

The history of metallurgy in the Carpathian-Balkans is based almost exclusively on archaeological work. The Carpathian-Balkan region hosts a number of the earliest known sites of metallurgy (see O'Brien, (2014), for a summary), with mines at Rudna Glava (Jovanović, 2009), Plocnik and Belovode in Serbia (Radivojević et al., 2013, 2010) and Ai Bunar (Chernyk, 1992) in Bulgaria dating back to the 6th millennium BCE. These sites, associated with the local Vinca culture, have yielded copper slag, refined copper droplets (at Belovode), and tin bronze foil (at Plocnik), some of the earliest evidence of extractive metallurgy, with the Bolovode site, in particular, purported to be the earliest such example in the world (Radivojević et al., 2010), although the exact timing of these activities are subject to some controversy (Sljivar and Borić, 2014). Such chronological uncertainties, and the lack of knowledge about the extent of such ancient activities are some of the issues this study attempts to address.

The existing archaeological evidence indicate the beginnings of a rich history of metalworking, which bloomed in the Bronze Age, when metallic artefacts from the region

explode in number (Bugoi et al., 2013; Chernyk, 1992) after 3000/2800BCE (Kienlin, 2014). Evidence for a well-established mining community, with strong trade links with other civilisations, including the Myceneans (Wells, 2016), and even possibly as far as Scandinavia (Ling et al., 2014) hint at the region being a major centre for metallurgical activities throughout the Bronze Age (Makkay, 1995). However, the lack of Pb isotope tracing on artefacts, particularly in the Romanian Carpathians, and of long-term palaeopollution records prior to this study mean confirmation of this hypothesis has been difficult.

Further evidence for exploitation of Carpathian ores is clear from the Roman period. After the conquering of the local Dacian people, the Romans set about modernising and organising the metallic assets of their new province. From numerous stone inscriptions, and wax tablets, evidence for major mining and smelting activity, particularly around the Rosia Montana in the Apuseni Mountains is clear (Baron et al., 2011). Recent studies have indicated the existence of large mining works underground, linked by mining galleries, and equipped with drainage mechanisms and wooden lifting wheels (Baron et al., 2011; Manske et al., 2006; Tamas et al., 2009). Further indications hint at exploration to the northern Romanian Baia Mare region (Borcoş and Udubaşa, 2012) by Roman scouts as well.

After the decline of the Roman Empire, direct evidence for mining in the Carpathian-Balkans is rare. Intermittent written records document activity only after around 1500 CE (Radulescu, 2004) but little clear evidence is available until the industrial revolution. The influx of Saxon miners to the central Balkans, however, in the 12th Century CE (Stojković, 2013) suggest some mining was occurring, and suggestions of Hungarian exploitation of the silver-rich lead ores have been made (Bálint, 2010; Paulinyi, 1981), but as yet there is little to no hard evidence of this medieval exploitation. Most recently, the industrial revolution in the 19th Century, and unchecked industrialisation under socialist control in the late 20th Century greatly exploited local ores and mines, with little regard for controlling pollution (Borcoş and Udubaşa, 2012).

To understand why this region apparently played host to such a large number of ancient to modern mining sites, the economic geology of the region must be considered.

The Apuseni mountains are home to the Rosia Montana mining field, Europe's largest Au-Ag deposit (Baron et al, 2011), and the so-called Metaliferi Mountains, rich in both precious (Ag, Ag) and base (Cu, Pb, Zn) metal deposits of both Neogene and Mesozoic age (Fig. 1.7). In addition to the Apuseni area, many other mining areas have been, and still are

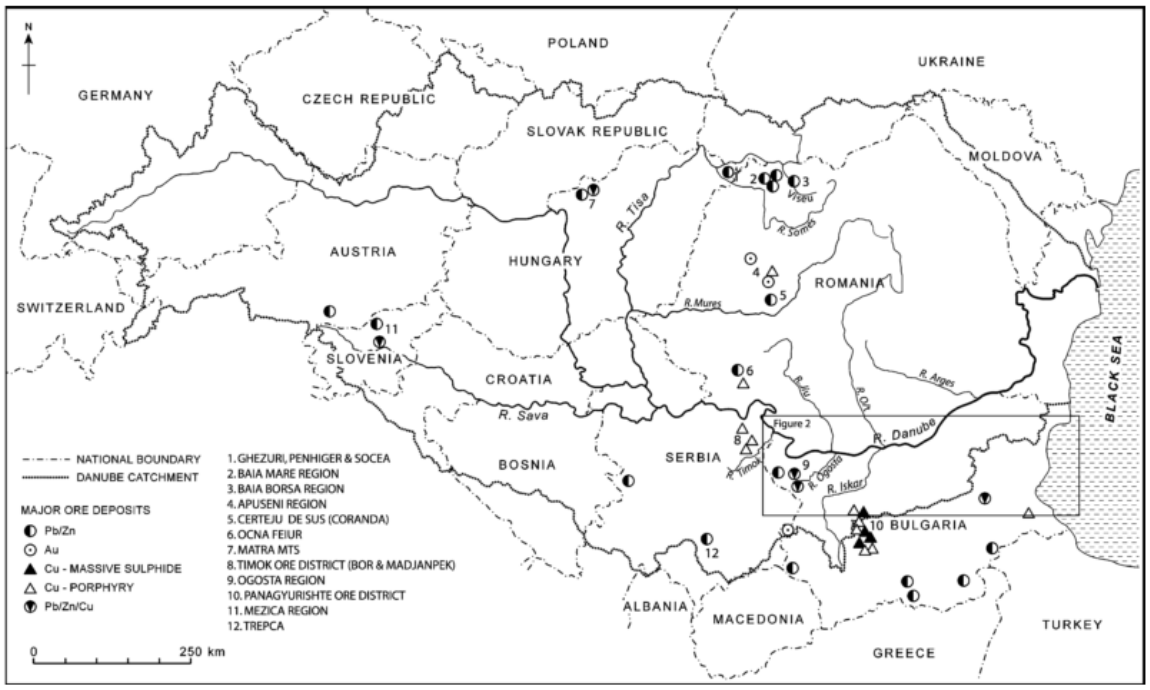

***Figure 1.8**: Map of the Carpathian-Balkan region indicating locations of major metallic ore deposits, from Bird et al. (2010a).*

being exploited on the 1500km-long Banatitic magmatic and metallogenic belt, which runs from Romania through Serbia, and into Bulgaria, and is the most important ore-bearing (Cu-Au) belt of the Alpine-Balkan-Carpathian realm (Ciobanu et al., 2002; Heinrich and Neubauer, 2002; Neubauer et al., 1995). It contains numerous important mining centres, including the Southern Apuseni, Poiana Rusca and Banat (Romania), Timok and Madjanpek (Serbia), and the Srednogorie mining district (Bulgaria). Little knowledge exists on the past use of ores from north-western Romania (eg., Baia Mare and Baia Borsa ore fields; Bird et al., 2010a) or southern Serbia (e.g. Trepca) (Fig. 1.7).

1.9. Peatlands as Archives for Archaeometallurgy

To understand the history of the Carpathian-Balkans and the interactions between natural and human forces, long-term, high resolution archives are needed. As already outlined, peatlands may provide valuable records of climatic shifts, but they are not limited to recording of just natural shifts. They have long been used, via pollen analysis, to distinguish changes relating to human activities, especially deforestation, and agriculture (see Schumacher et al., 2016 for a review in the Carpathian region).

Due to the atmospheric derivation of all nutrients within ombrotrophic bog systems, it is clear any polluting metals recorded in such environments must be derived from the atmosphere. As a result, heavy metal geochemical records from peat cores have been used

to determine background deposition from the anthropogenic record (e.g. Lantzy and Mackenzie, 1979).

1.9.1. Lead

Building on previous work which had clearly established the importance, and sheer scale of pre-industrial metallurgy (Patterson, 1971; Settle and Patterson, 1980), initial studies indicated the dimensions of the historical lead record. First, from a selection of 19 Swedish lakes (Renberg et al., 1994), and then from the Greenland ice core record (Hong et al., 1994), the impact of anthropogenic smelting on the Pb record was outlined. From these early studies, a clear peak in the lead record was resolved to be 2000 years ago, during the zenith of the Roman Empire, with a decline during the so called Dark Ages, and a renewed increase in lead during the Medieval Period with continued increases to a peak in the 1970s, as a result of the prevalence of leaded gasoline (see Fig. 1.8). Although attempts to explain these concentration changes as natural (Rasmussen, 1998) have been made, advances in isotopic methods have supported the pollution origin of trends in lead concentrations throughout the Late Holocene (Rosman et al., 1997).

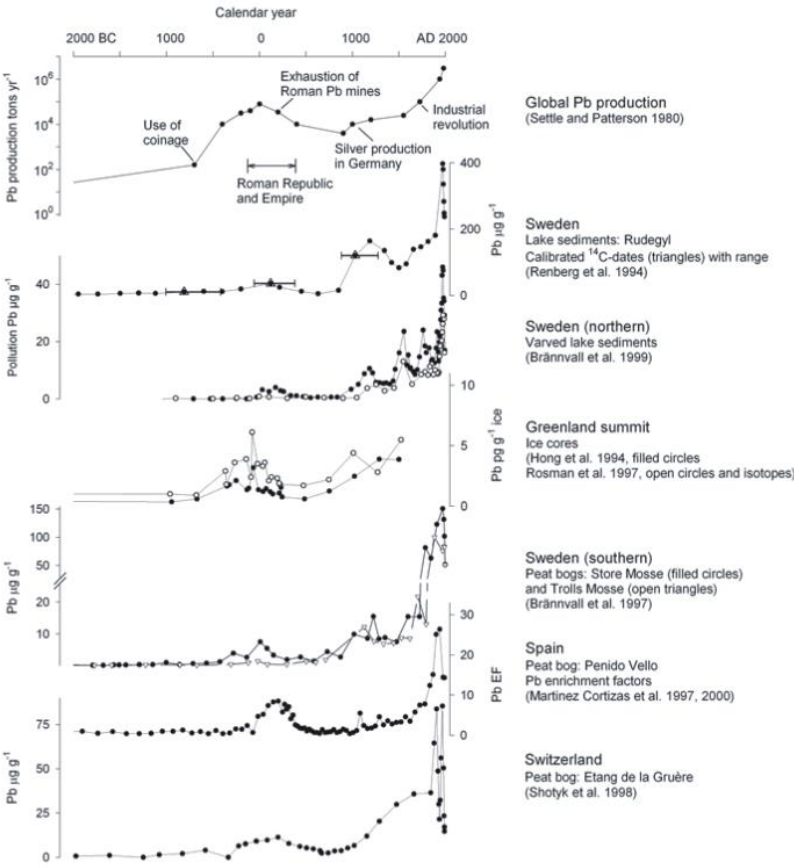

Figure 1.9: *Comparison of global Pb production as estimated by Settle and Patterson, (1980) with various sediment- and ice-based records of Pb pollution, from Hansson et al. (2015)*

Following on from these initial investigations, and the acceptance of the value of peat bogs as reliable archives, a number of long-term peat records have been published, notably from Spain (Martinez-Cortizas et al., 1997; Martínez Cortizas et al., 2002), Sweden (Klaminder

et al., 2003), Switzerland (Shotyk et al., 1998; Weiss et al., 1999, 1997), China (Ferrat et al., 2012) and the UK (e.g. Kylander et al., 2009; Le Roux et al., 2004), among others (Fig.1.8). In all cases the lead record has been coherent and reliable, to the point where it has been suggested there is potential for use as a general chronological marker (Renberg et al., 2001).

1.9.1.1. Lead Isotopes

In addition to Pb concentration variations through time, much work has been performed to analyse isotopes (^{204}Pb, ^{206}Pb, ^{207}Pb and ^{208}Pb) of the Pb deposited within a bog. Because the isotopic composition of most Pb sources are distinct (see Sangster et al., 2000 for a review of modern lead deposits and their isotopic makeup), Pb concentration and isotope ratios may be used as a fingerprint to trace the source of Pb.

In the natural environment, Pb is mainly present as four stable isotopes: ^{208}Pb (52%), ^{206}Pb (24%), ^{207}Pb (23%) and ^{204}Pb (1%) (Komárek et al., 2008). Isotope ^{204}Pb is the only primordial stable isotope, whilst ^{206}Pb, ^{207}Pb and ^{208}Pb are the products of the decay chains of ^{238}U, ^{235}U and ^{232}Th, respectively (Gulson, 2008; Komárek et al., 2008). Thus, the abundance of different Pb isotopes depends on the concentrations of primordial U, Th and Pb, and the length of the half-lives of the parent isotopes (Haynes, 2014). Pb isotopic data is commonly presented as ratios, with ^{206}Pb/^{204}Pb, ^{206}Pb/^{207}Pb, ^{208}Pb/^{206}Pb typically used (Baron et al., 2014). Analysis of ore bodies has indicated the variability of Pb isotope ratios dependent on the type of ore, age, and style of mineralization (Komárek et al., 2008). A simple example is the difference observable between the ^{206}Pb/^{207}Pb ratio of very old ores (e.g. the Broken Hill ore, which was formed 1700–1800 million years ago and used in European leaded petrol; ^{206}Pb/^{207}Pb = 1.05–1.1, Grousset et al. 1994; Weiss et al. 1999) when compared to younger ones (most Jurassic to Miocene age, or 'young', ores fall within the range ^{206}Pb/^{207}Pb= 1.18–1.25, Hansmann and Köppel 2000). Old ores (e.g. Proterozoic age) were formed, and the Pb isotope ratios were set, during a very early stage of the Earth's evolution, and so the decay of Th and U contributed little to the Pb budget. Conversely, younger ores contain variable amounts of radiogenic lead, since time has allowed for more decay of parent isotopes (^{238}U, ^{235}U and ^{232}Th, respectively) to occur (Bacon, 2002; Farmer et al., 2000) prior to their incorporation into the ore.

Crucially for archaeometallurgical inferences, the Pb isotopic ratios are not severely altered by physical or chemical fractionation processes during ore processing, smelting, and casting, although some minor variations may occur (Baron et al., 2009). Therefore it can be assumed the lead isotope values of the pollution-related Pb are very similar to those of the

parent ore body (Bollhöfer and Rosman, 2002). As such, precise isotopic ratios may be used to 'link' lead deposited in a substrate (bogs, lakes, ice) to a certain ore (Bollhöfer and Rosman, 2002; Komárek et al., 2008) (Fig. 1.9). It has been demonstrated that records of Pb concentration from sedimentary archives such as peat bogs, lake sediments and ice cores may retain the isotopic signature of the original source of Pb, since once deposited within such environments, Pb is largely immobile (Hansson et al., 2015; Marx et al., 2016). Such work has clearly indicated the impact of metal pollution from local sources (e.g. Shotyk et al., 2016), and long range atmospheric transport (e.g. Rosman et al., 1997; Le Roux et al., 2004; Shotyk et al., 1998) through time. However, the signal recorded within a bog or lake represents a mixture of many local, regional and extraregional inputs, including contribution from natural sources (dust, biomass burning, volcanoes, etc) and disentangling these has proven challenging (Cheng and Hu, 2010).

1.9.1.2. Sources of Lead

It is importnant to note that the final isotopic composition of Pb deposited on a bog results from the mixing of a large number of sources (Fig. 1.9) (see Komarek et al., 2008 for a review). Despite this, much work has been done successfully providing provenance for pollution signals. In recent records (especially deposited between 1940–1990 CE), one of the major sources of Pb has been the use of leaded petrol, with the impact of such activity on the isotopic signal of recent sediment outlined above.

Prior to leaded petrol, Pb pollution may be tied to the burning of coal and smelting of metallic ores. Unlike other resources, the isotopic signature of coal is not age-dependent, with $^{206}Pb/^{207}Pb$ ranging from 1.16–1.21 (Novak et al., 2003; Komarek et al., 2008). Through smelting of metals, tiny particles of Pb, either the focus of the smelting, or contaminants within the ore, are released, reflective of the isotopic composition of the material being smelted. Due to the variety of polymetallic ores, and ore bodies now exploited, metal production may utilise a wide isotopic range of sources.

In the Carpathian-Balkan region and especially prior to the Industrial Revolution, lead resulting from metallurgy is likely to be the major source of any pollution observed. This is due to the great history of metallurgical activity in the region, dating back to the Bronze Age. After the Industrial Revolution, coal mining, particularly in the Jiu Valley and subsequently leaded gasoline, may also have had an influence of the Pb isotope mixtures.

1.9.1.3. Lead Isotopes in Peat

Many studies have utilised peatlands as archives of lead pollution, with an increasing number of studies now coupling the concentration-related time series with provenance-providing Pb isotopes. Most early studies only provided isotopic data on $^{206}Pb/^{207}Pb$, as ^{204}Pb is much harder to analyse, due to its rarity. Such studies utilised both ombrotrophic (e.g. Kylander et al., 2009; Martínez Cortizas et al., 2002; Shotyk et al., 1998; Weiss et al., 2002) and minerotrophic (Monna et al., 2004a; Shotyk, 2002; Shotyk et al., 2016) bogs, and indicated the impact mining and smelting had on the $^{206}Pb/^{207}Pb$ ratio, with anthropogenic lead perturbing the recent values in all cases. Such studies often focussed on the Industrial Revolution and modern period (Novák et al., 2003; Weiss et al., 1999) but longer cores have been investigated, covering the late Holocene (e.g. Shotyk et al., 2005; Le Roux et al., 2004) and even the whole Holocene (e.g. Shotyk et al., 1998). These long-term studies are extremely useful in determining not just the extent of ancient pollution, but the sources.

1.9.1.4. Lead Isotopes in Lake Sediments

Prior to the widespread utilisation of peat records, lead isotope studies largely focused on lake sediments. Due to the nature of lacustrine sediment, very high-resolution studies are common, but the majority are limited to coverage of the past 500 years (e.g. Bindler et al., 2001; Chen et al., 2016; Grayson and Plater, 2008). Exceptions to this are becoming more common, with longer cores initially investigated in Sweden and Switzerland, with coverage of much of the Holocene possible. Most recently, such studies have focussed on sites worldwide, with examples from Canada (Aebischer et al., 2015; Gallon et al., 2006), France (Garçon et al., 2012) and South America (Cooke et al., 2007; De Vleeschouwer et al., 2014).

1.9.1.5. Lead Isotopes in Other Archives

Other than the two terrestrial archives outlined above, attempts have been made to apply lead isotopic analysis to ice cores (e.g. Vallelonga et al., 2010, 2003), snow (e.g. Van de Velde et al., 2005), marine sediments (e.g. Abouchami and Zabel, 2003; Pichat et al., 2014; Véron et al., 2013), soils (e.g. Hansmann and Köppel, 2000; Reimann et al., 2012), speleothems (e.g. Allan et al., 2015) and tree rings (e.g. Bindler et al., 2004; Steinhilber et al., 2012).

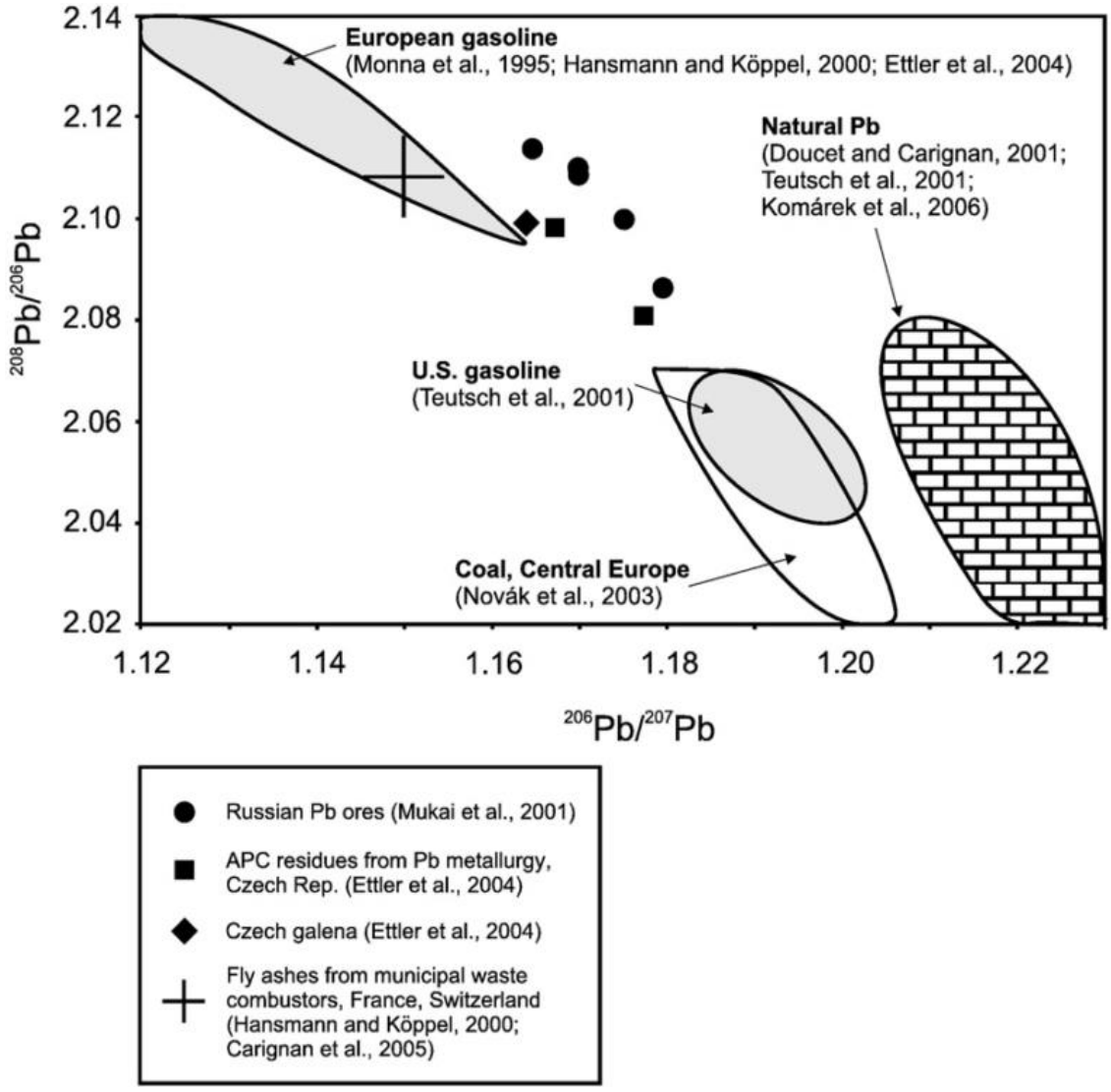

***Figure 10**: Example 3-isotope ($^{206}Pb/^{207}Pb$ vs. $^{208}Pb/^{206}Pb$) plot outlining typical signatures of various modern Pb sources, from Komárek et al. (2008).*

1.9.2. Utilisation of Pb Isotope Mixing Models for Provenance Studies

Since the Pb isotopic mixture deposited within the substrate records the source(s) from which it was derived, investigating this signal allows for the investigation of source contribution. The final isotope signal is formed from a mixture of many possible inputs. Understanding the proportion of contribution of each potential source to this mixture is vital when using Pb isotopes to trace anthropogenic pollution (e.g. Álvarez-Iglesias et al., 2012) or natural lead sources (Grousset and Biscaye, 2005).

Conventionally, interpretation of Pb isotopic ratios is performed via a 3-isotope plot (see Fig. 1.9, and Kylander et al. 2005), and comparing the location of the sink mixture data (the isotope signal recorded within the archive) to the isotopic signatures of known ores. More recent studies attempted modelling of the sink mixture (the isotopic signature of the substrate) as a way of quantitatively assessing the relationships between sinks, and sources.

Until now, Pb isotope mixing models have generally been limited to considering either two (e.g. Bird et al., 2010b; Monna et al., 2000; Brugam et al., 2011) or three (Álvarez-Iglesias et al., 2012) potential sources. This approach is adequate in a very well determined system, where only a few possible sources may be considered, or only a couple of broad sources are of interest (e.g. Monna et al., 2000; Brugam et al., 2011). This approach allows the user to identify very general source inputs, such as anthropogenic vs lithogenic Pb, but the lack of further source consideration precludes definition of the source to an ore body, or mining region (Brugam et al., 2011). This is due to the limitations related to the models and the Pb isotope systems themselves, where generally only three isotope ratios (n) are interpreted, and such models are limited to n+1 sources. Such models, therefore, may be useful, but the complexity of potential Pb inputs, particularly in an anthropogenically polluted world, mean such approaches are likely oversimplifications, with only simple conclusions possible (Brugam et al., 2011).

In the field of biology, mixing models have long been used to apportion large numbers of sources within a predator's diet (e.g Inger et al. 2006; Layman et al. 2012; Benstead et al. 2006), from stable isotope composition using mixing models such as IsoSource (Phillips and Gregg, 2003) and MixSIAR (Parnell et al., 2010; Stock and Semmens, 2013). When IsoSource was developed, an initial attempt to apply it to pollution sourcing via Pb isotopes was made (Phillips and Gregg, 2003). However, very little further work to apply this method to the field has been done (Soto-Jiménez and Flegal, 2009). Other approaches to Pb isotope modelling have been applied, with simple Euclidean distance calculation used to determine potential source(s) for archaeological artefacts (Ling et al., 2014; Stos, 2009). This method, however, is unable to apportion proportions of source input, simply indicating the most likely ores (or mines) within the database.

1.9.3. Other Metals

Although much less attention has been paid to the quantification and understanding of the long-term record of other metals, there are still a number of studies for most of those which may be smelting- related. Copper has been studied in various locations, initially via ice cores (Hong et al., 1996) but more recently via bogs (Mighall et al., 2014; Mighall et al., 2009; Monna et al., 2004a, 2004b). In many of these studies cadmium and zinc have been analysed concurrently, alongside other metals, like antimony, tin, bismuth and silver (Cooke et al., 2007; Forel et al., 2010; Garçon et al., 2012). The finest and most complete record of peat geochemistry comes from the Etang de la Gruyere, in Switzerland, where work has produced records of over 30 elements, using a variety of analytical methods. In

addition to individual records, a multi-proxy approach allows co-variance of elements to be investigated (Le Roux et al., 2012; Shotyk, 2002, 1996; Shotyk et al., 1998; Weiss et al., 1997). Most recently, the geochemical approach has been coupled with pollen analysis (De Vleeschouwer et al., 2009a; Veron et al., 2014), providing a valuable comparison between the direct metallic input, and the implied vegetation and climatic changes as recorded via pollen.

1.10. Summary

The climate of the Carpathian-Balkan region during the Holocene was stable when compared to much of Western Europe, with temperature and precipitation changes generally less pronounced. Nevertheless, transitions did occur, with the early Holocene characterised by dry and warm conditions, prior to a shift at roughly 5000 yr BP. At the same time, evidence suggests an enhanced Mediterranean influence on the regional climate. However, the lack of long-term well-dated and multi-proxy records in the region precludes detailed investigation of these trends until the most recent 1000 years. During the last millennium, the climate was dry and warm until 700 yr BP, prior to the early onset of a prolonged and erratic (rapid shifts in both temperature and precipitation) LIA, which persisted until roughly 50 yr BP. Further studies indicate the impact anthropogenic warming is having on the local climate.

With regards to pollution, so far estimates of long-term impacts of mining and smelting are restricted to central-western Europe and the British Isles. This has led to difficulties in resolving regional differences in Eastern Europe, particularly when combined with insufficient knowledge on past emission sources, and on the isotopic signatures of various ores (both exhausted and still in use).

As a result of these knowledge gaps, the causal relationship between humans and the environment, and the human impact versus natural causes of environmental change are insufficiently explored, particularly within the Carpathian-Balkan region. These limitations suggest strongly that for a better understanding of pollution load, variability and change, more sites must be studied especially in regions of mineral wealth and long term human impact on the environment - this area being a fine example.

In addition to the elevated levels of environmental pollution, and long history of metallurgy in the region, modelling suggests this area is one of the most vulnerable to human-driven climate changes and as such the Carpathian region provides an exceptional

area for a comparative analysis of the anthropogenic activities, and their relation to natural changes in climate.

Utilising a series of peat bogs from the region, presented here are two new climatic records from Romania, and the first long-term record of heavy metal pollution from Serbia. These records provide new data, firstly on the magnitude and regularity of heavy rainfall events and their linkage to the North Atlantic Oscillation, and secondly on the occurrence of major dust deposition and its connection with Saharan desertification. Finally, the first application of a Bayesian mixing model to provenance studies of Pb within sediment via their isotopic signature is outlined.

Chapter 2. Site Locations, Materials and Methods.

2.1. Site Locations

2.1.1. Site 1: Sureanu

Sureanu peat bog (45°34'51"N, 23°30'28"E), is a small bog located adjacent to a tarn (Iezerul Sureanu) in the Sureanu Mountains, Southern Carpathians (Romania) at an elevation of 1840 m above sea level (a.s.l, Fig. 2.1). Iezerul Sureanu is roughly 100m long, and 90m wide, with a maximum depth of 7.5m. It is frozen for around 6 months a year, and is separated from the bog basin by a morphological rise, likely a small moraine (see Fig. 2.1). Further upslope is another palaeomoraine, with exposed rock and possible avalanche channels. Other mass-wasting related features may be masked by the dense vegetation (Fig. 2.1D). The bog is roughly 200m long and 100m wide, and is surrounded on three sides by the steep slopes of the Sureanu palaeoglacier cirque, with a slope gradient in excess of 1 in 2 (Fig. 2.1). The bog is domed, with occasional streams at its extremities that periodically drain the Iezerul Sureanu Lake during high water stands.

The bog vegetation is dominated by *Sphagnum*, with patches of *Lycopodium*, and various species of Poaceae and Cyperaceae. The peatbog is still uncovered, with peripheral forests consisting primarily of *Picea abies* and *Alnus glutinosa*. At lower altitudes, *Fagus sylvatica* occurs, a vegetation assemblage typical of the *Picea* belt of the Carpathian Mountains. The location of the bog, at the uppermost extent of the spruce forest in this area (circa 1800m, as defined by Cristea, 1993), and just below the transition into the subalpine belt (dominated by *Pinus mugo* and *Juniperus*) means the bog should be well placed to capture shifts in the local treeline and related palaeoecological changes. Due to its location, the bog is likely to preserve a record of periods of high precipitation through the associated land erosion and minerogenic deposition. This is because it sits at the base of steep slopes, and is hydrologically coupled to the neighbouring Iezerul Sureanu Lake, and so should receive input of sediment from mass wasting of the slopes, or flooding of the lake, although parts of the runoff will be deposited in the lake (when it is not frozen).

The basement geology is dominated by Late Proterozoic – Early Paleozoic gneisses of the Getic-Supragetic nappe (Iancu et al., 2005). Recent human impact can be seen in the form of ski slopes constructed on the far side of Sureanu peak and recent deforestation to allow for building of hotels in the area, as well as long-term (centuries if not millennia old) high-altitude pasturing and hay harvesting on the high plateau of Sureanu Mountains.

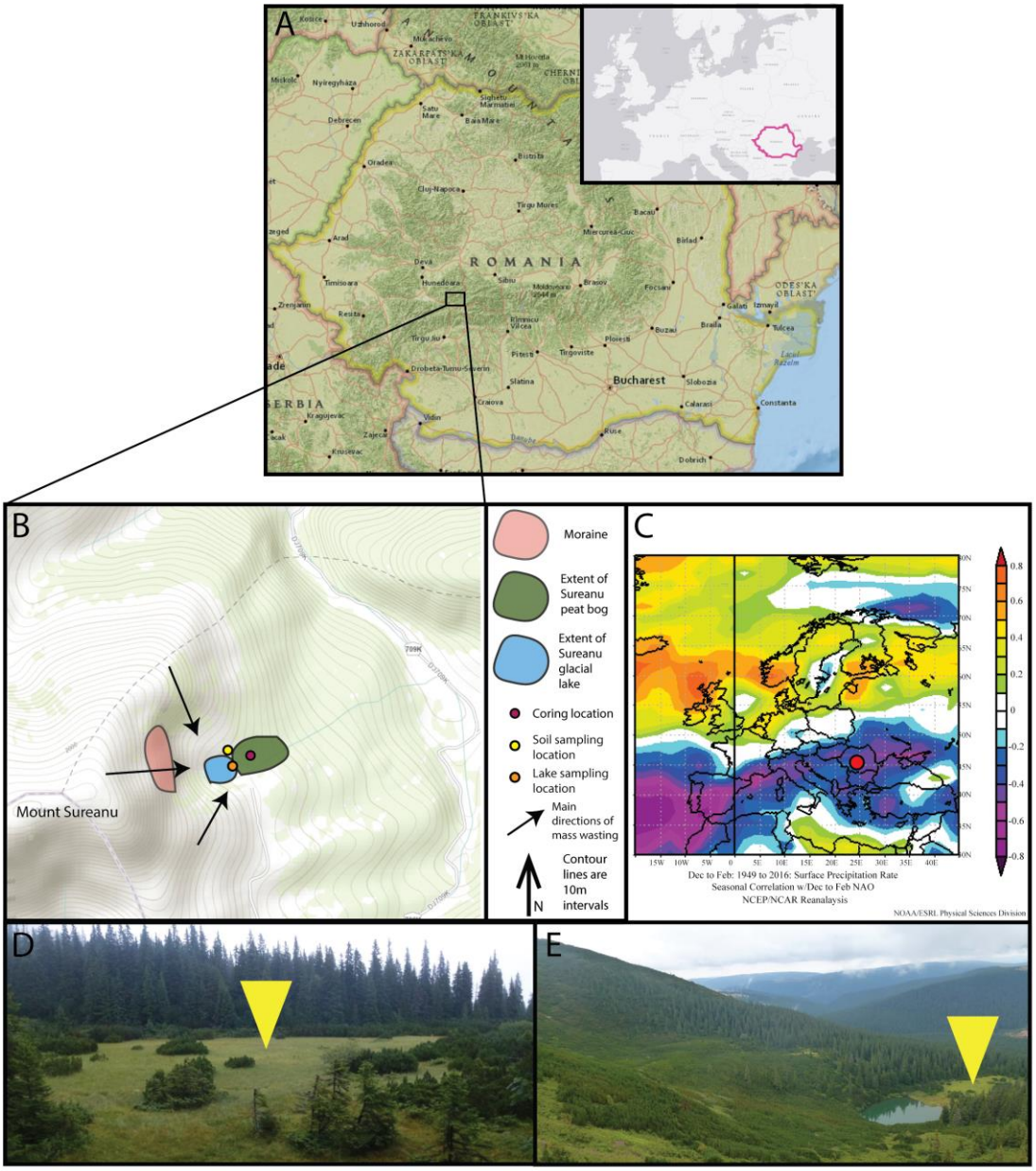

Figure 2.1. *A: Location of Sureanu bog. B: Topographical map indicating location of bog, lake (Iezerul Sureanu), moraine, all sampling sites and flow directions of mass wasting. C: Correlation of high North Atlantic Oscillation (NAO) index to winter precipitation, indicating reduced precipitation at times of intense NAO in Eastern Europe. Location in the southern Carpathians denoted by red circle. D: Closer view of bog, indicating location of coring site (yellow arrow). E: View looking down onto site, with coring site indicated by yellow arrow.*

A 603cm-long core was taken in October 2014 in the central part of the bog (Fig. 2.1). Additional samples were taken from local rocks, lake sediment and soil, to allow for characterisation of debris found within the bog. One sediment sample consisting of fine gravel and sand was taken from the lake-shore, and a soil sample from the surrounding

vegetated slopes between lake and bog. Both were sampled by hand trowel, down to a depth of 5cm. The cores were wrapped in cling film before transportation to Northumbria University. The core was documented and described prior to being photographed in the lab. It was then cut into 1cm slices prior to selection of samples for future analysis.

The climate of the area is considered as temperate continental (Fărcaş and Sorocovschi, 1992) with average winter temperatures ranging from -2°C below and -7°C above 1900m a.s.l., and corresponding average summer temperatures of 19°C and 8°C respectively at the same elevations.

Due to the interplay of Mediterranean and Atlantic air masses, temperature inversions are common, with resultant fluctuations especially prevalent in the winter and spring (Trufas, 1986). Rainfall amounts are between 900 and 1800 mm per year, with extensive snow cover common throughout the winter (around 100 days a year at low altitudes and over 200 days above 2000 m a.s.l.). In common to other regions in the Southern Carpathians, it is believed the area receives precipitation mainly of Atlantic origin, but with periodic incursions of south-easterly air masses from the Mediterranean Sea (Fărcaş and Sorocovschi, 1992).

2.1.2. Site 2: Mohos

The Mohos peat bog (25°54'13.26E; 46°08'0.52N; 1050 m altitude, Fig.2.2) is in the Eastern Carpathians, Romania, in the Ciomadul volcanic massif (Fig. 2.2). The *Sphagnum*-dominated bog covers some 80 hectares, and occupies an infilled volcanic crater. There is no riverine inflow, which means that inorganic material deposited within the bog is almost exclusively derived via direct atmospheric transport. Surrounding vegetation is typical of this altitude in the Carpathians (Cristea, 1993), the bog being located at the upper limit of the beech forest, with spruce also found on surrounding slopes. Vegetation on the bog itself is diverse, with common occurrences of *Pinus sylvestris*, *Alnus glutinosa,* and *Betula pubescens*, alongside various *Salix* species (Pop, 1960; Tanţău et al., 2003).

The Mohos crater is related to volcanic activity from the Ciomadul volcano, which last erupted roughly 29.6 kyr BP in the neighbouring younger crater currently occupied by the Lake St Ana (Harangi et al., 2010; Karátson et al., 2016; Magyari et al., 2014; Wulf et al., 2016). The surrounding geology is dominated by andesites and dacites, occasionally capped by pyroclastic deposits and a thick soil cover.

A Russian peat corer was used to recover a 950cm-long peat sequence from the middle part of Mohos bog. The material consists mainly of *Sphagnum* peat and lacustrine

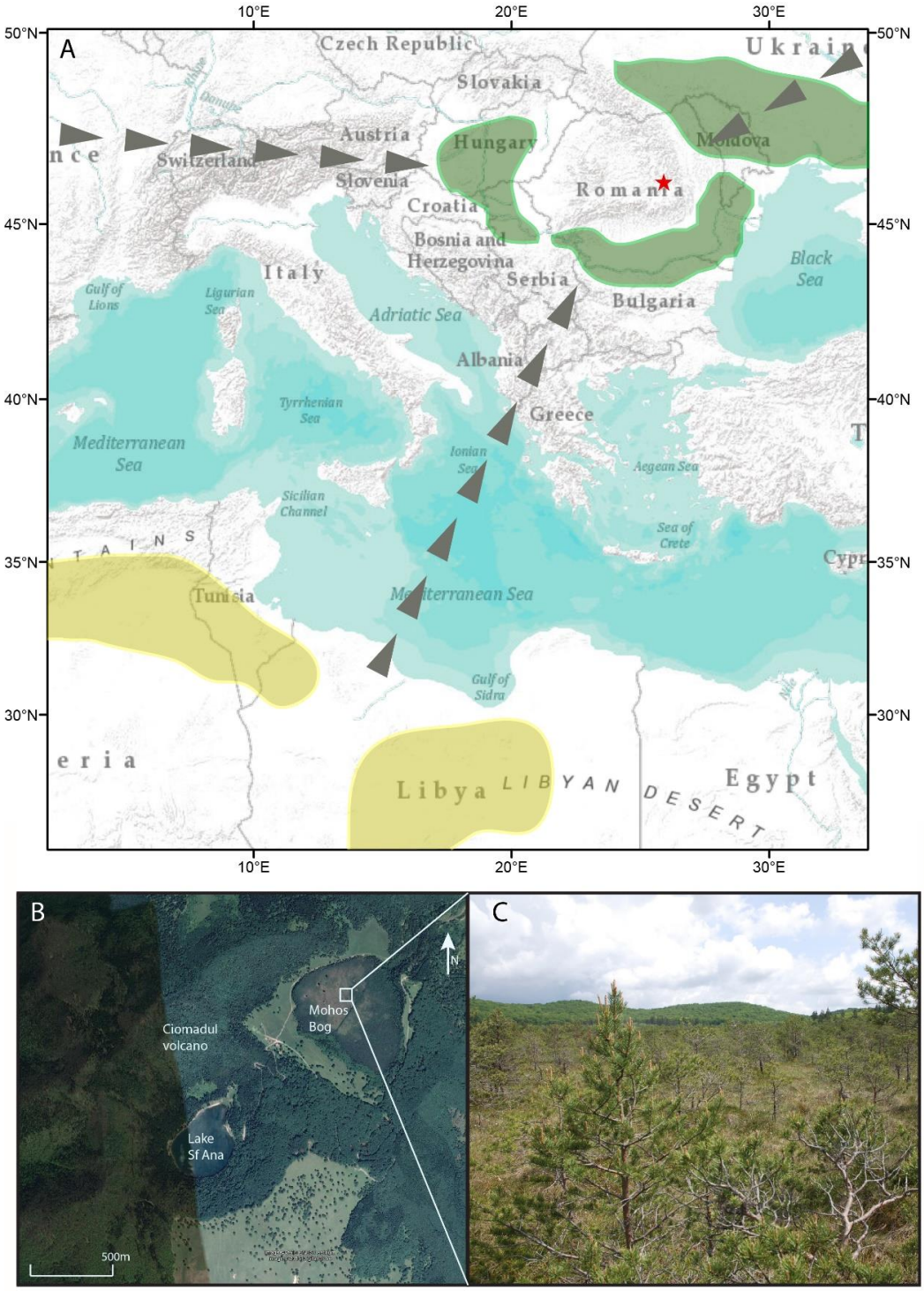

Figure 2.2: *A: Map of the Carpathian-Balkan region indicating location of Mohos peat bog (red star), in the south-eastern Carpathian Mountains. Predominant wind directions relating to air circulation patterns in the area are indicated by black arrows. Major Saharan dust source areas are indicated in yellow (Scheuvens et al., 2013) and local loess fields (including loess-derived alluvium) in green (Marković et al., 2015). B: Map of Mohos and neighbouring Lake Sf Ana, from Google Earth 6.1.7601.1 (June 10th 2016). Harghita County, Romania, 46°05'N ; 25°55'E, Eye altitude 3060m, CNES/Astrium, DigitalGlobe 2016. http://www.google.com/earth/index.html (Accessed January 23rd 2017). Coring location within white box. C: Photo of Mohos bog at the coring location with the crater rim visible in the distance.*

sediments in the lowermost part. Upon recovery, the material was wrapped in clingfilm, transported to the laboratory, described, imaged, and subjected to further analyses. Previous research in the area has produced a high-resolution pollen record from Mohos (Tanţău et al., 2003) reaching into the Late Glacial and multi-proxy palaeolimnological investigations on sediments from the neighbouring Lake St Ana (Magyari et al., 2009; 2014).

The climate is temperate continental, with average annual temperatures of 15°C and precipitation of 800mm (Kristó, 1995). The bog is typically covered with 5–15cm of water for much of the year. In terms of vegetation, local forests are composed of Serbian spruce (*Picea omorika*) alongside various other *Picea, Alnus, Fagus* and *Abies* species (Ćolić and Gigov, 1958).

2.1.3. Site 3: Crveni Potok

Crveni Potok (43°54'49.63"N; 19°25'11.08"E) is a small mire (<3 hectares) located in the Tara Mountains National Park, in western Serbia, at 1090m a.s.l. (Fig. 2.3), within the Dinaric Alps. The mire is heavily forested, with the majority of the tree cover consisting of

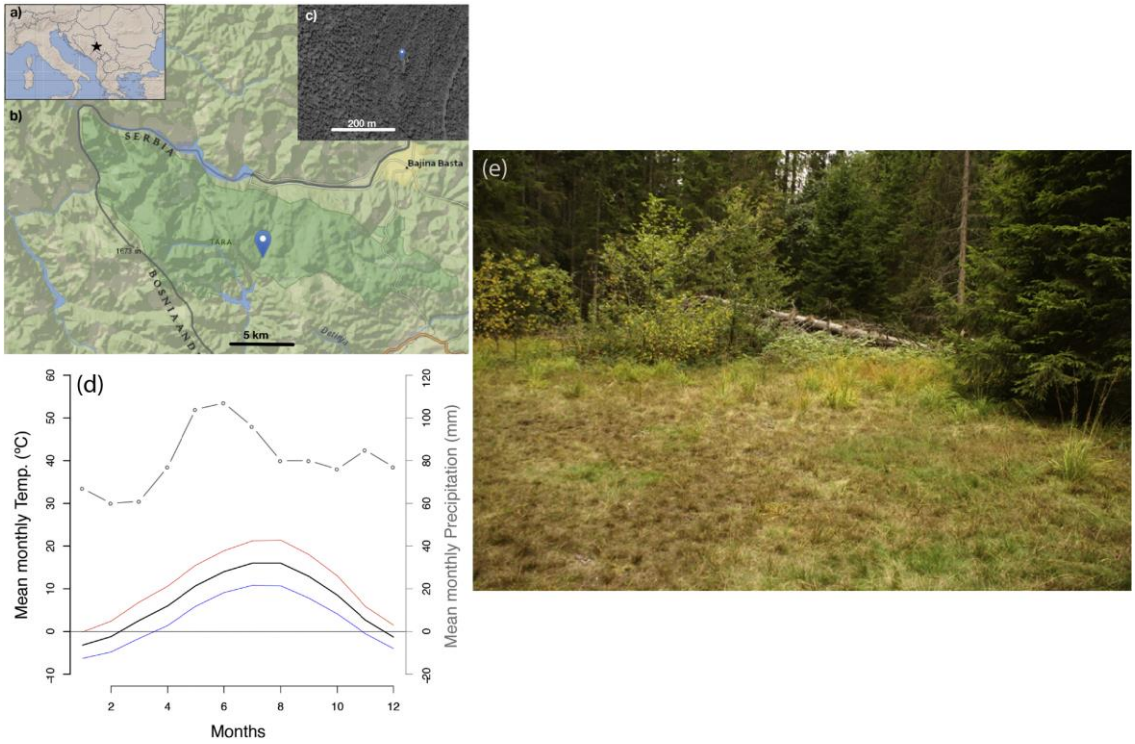

***Figure 2.3**: (A-B) Maps outlining location of Crveni Potok, alongside C) Aerial view of the site. D) Diagram indicating typical climate of the site, with mean monthly temperature (black: mean, blue: minimum, red: maximum) and mean monthly rainfall. E) Close up view of coring site. Figure adapted from Finsinger et al. (2017).*

conifers (*Abies alba* and *Picea abies*) and *Fagus sylvatica* (see Finsinger et al., 2017 for further detail), with a small local population of the rare Serbian spruce (*Picea omorika*). Geologically, the bedrock consists of Triassic age calcareous rock, with Cretaceous marbles and ultrabasic igneous bedrock located to the south-west of the site (Finsinger et al., 2017). Previous investigations into the site have yielded a detailed pollen, macrofossil and charcoal record (Finsinger et al., 2017).

270cm of sediment was collected via two overlapping and parallel cores extracted via Russian peat corer. Each drive was 1m, and the collected core was 8cm in diameter. The core was transferred to PVC tubes, wrapped and stored. Sampling for trace metal analysis was performed using plastic tools to ensure no contamination, with exactly $0.5cm^3$ of sediment analysed for each sample to allow for density calculations to be made.

The mean annual temperature foe the site is 7°C, with the mire receiving approximately 970mm of precipitation a year (Hijmans et al., 2005).

2.2. Coring Method

For high resolution palaeoenvironmental reconstructions, it is key the archive is collected as a continuous, uninterrupted core, covering the entire time period of interest. To ensure this, and to reduce the chance of compression all cores were collected with a Russian peat corer (Belokopytov and Beresnevich, 1955) with a cylinder 1m in length and 5cm across. All cores were immediately transferred to PVC tubes and wrapped for transport back to the laboratory. This corer provided the quickest method for taking long cores with enough sample for all necessary analyses (Givelet et al, 2004). In all cases, attempts to reach as deep as possible were made, with the underlying sediment the aim, but in most locations this was impossible due to lack of rods, or poor coring conditions.

2.3. Core Subsampling

Once the cores were transported back to the laboratory, they were immediately placed in cold storage, at 3ºC. When subsampling, the cores were initially cut at 1cm intervals using a ceramic knife. The top surface was scraped off using a glass slide, before from each section equal samples were taken for X-Ray Flourescence (XRF)/Inductively-Coupled Optical Emission Spectrometry (ICP-OES), Loss on Ignition (LOI), physical measurements & Pb isotopes. This was done using plastic spatulas, each one discarded after use, with the immediate 1mm section of core in contact with the PVC tube discarded. In selected cores, further samples were taken for pollen, testate amoeba and grain size analysis.

2.4. Radiocarbon Dating

In each core a number of radiocarbon dates were produced, to allow for age-depth models to be developed. Dating analyses were performed via accelerator mass spectrometry (AMS) at the ^{14}C CHRONO centre at Queen's University Belfast (6 of the dates for Sureanu bog), at HEKAL AMS Laboratory (8 from Sureanu, and 16 from Mohos), MTA ATOMKI Institute for Nuclear Research of the Hungarian Academy of Sciences in Debrecen (Molnár et al., 2013), and Poznan Radiocarbon Laboratory (9 dates from Crveni Potok).

Table 2.1: *Outline of different analyses carried out at each site*

	Sureanu	Mohos	Crveni Potok
Loss On Ignition	✓	✓	✓
Geochemistry (ICP-OES)	✓	✓	✓
Lead Isotope Geochemistry	✓		
Grain Size Analysis	✓		
Pollen	✓		✓ (Finsinger et al., 2017)
Testate Amoeba		✓	
ITRAX		✓	

Due to variations in atmospheric $^{14}C/^{12}C$ throughout the Holocene, AMS dating methods require calibrating. This was performed using a calibration curve to convert from raw age to calibrated years before present (cal yr BP). Throughout this work, calibration was performed using the INTCAL 13 curve (Reimer et al., 2013). For all cores, Bacon software for age-depth modelling was used (Blaauw and Christen, 2011).

2.5. Loss on Ignition

Every 1cm the water content, total organic carbon, inorganic carbon and residual components were measured via loss on ignition (LOI), as described by Heiri et al. (2001). In each of the cores, around 1g of sample was taken and weighed before being dried overnight at 105°C prior to weighing again to determine water content. This dry sample was then placed in a muffle furnace for 4 hours at 550°C before re-weighing. Finally, the samples were placed back into the furnace, this time at 950°C for 2 hours, before a final weighing.

The three weights may be used to calculate water content, total organic carbon and inorganic carbon, respectively, using the following formulas:

$$Water\ Content\ (\%) = \frac{WW - DW_{105}}{WW} \times 100 \text{ (Eq.1)}$$

Where WW is the wet weight of the sample being analysed for LOI, and DW_{105} is the weight after drying overnight at 105°C.

$$Organic\ Carbon\ (\%) = \left(\frac{DW_{105} - DW_{550}}{DW_{105}}\right) \times 100 \text{ (Eq. 2)}$$

Where DW_{550} is the weight of the sample after ignition at 550°C for 4 hours. This value indicates the amount of organic material in the sample.

$$Inorganic\ Carbon\ (\%) = \left(\frac{DW_{550} - DW_{950}}{DW_{105}}\right) \times 100 \text{ (Eq. 3)}$$

Where DW_{950} is the weight of the smaple after ignition at 950°C for 2 hours. This value indicates the amount of carbon dioxide evolved from the breakdown of carbonate minerals.

2.6. Density

For each sample analysed, exactly 1cm^3 of material was taken to allow for density calculations, using the following equation, with ρ=density, m= mass and V= volume to be made:

$$\rho = {}^{m}/_{V} \text{ (Eq.4)}$$

2.7. Geochemical Analyses

2.7.1. Acid Digestion

To allow the solid peat samples to be run via Inductively-Coupled Optical Emission Spectrometry ICP-OES, they first have to be dissolved into solution. Since peat is refractory and can be extremely hard to fully digest, a concentrated acid attack, under heat and pressure was used. Prior to all digestion, each section of peat was dried at 105ºC overnight before being homogenised using a pestle and mortar.

The initial attack on the organic component of the peat was performed using a strong oxidising agent. In this case it was nitric acid (HNO_3), in combination with hydrochloric acid (HCl), in a ratio of 3:1 (reverse aqua regia). During initial trials hydrogen peroxide (H_2O_2) was also used as an additional oxidiser, but it was found to have little overall effect on the completeness of the digestion, as so it was not used for actual analyses.

Due to the high levels of dust, and occasional pebble within some of the peat samples, and silicate fraction within lake sediments, it was determined that pseudototal dissolution would not occur unless additional hydrofluoric acid (HF) was added, meaning it was necessary to equip an HF-resistant introduction system, torch and spray chamber to the ICP-OES.

Digestion was performed on 0.2g of dried, crushed sample. In a Teflon digestion vessel equipped with a vent for gas, 12ml of reverse aqua regia (9ml of HNO3 & 3ml of HCl) was added to the sample, before addition of 1ml concentrated HF. Lids are then placed on these vessels before tightening with a wrench to ensure a tight seal during the reaction.

These vessels were then placed into a MARS (Microwave Accelerated Reaction System) microwave where they were heated under pressure. This happened gradually over 40 minutes, before cooling for a further 20 minutes. Due to the presence of HF, the samples were left for a further 30 minutes to ensure any reaction was complete before removal from the microwave. Samples were decanted into 50ml centrifuge vials, and diluted to the full 50ml with milli-Q deionized water.

2.7.2. ICP-OES

Inductively Coupled Plasma Optical Emission Spectrometer (ICP-OES), or -AES (Atomic Emission Spectrometer) may be used for the multi-element analysis of materials, in

gaseous, liquid or powdered form. For this work, all samples were in liquid form- solid peat and lake sediment samples digested using the hot acid microwave digestion method outlined above.

The instrument used was a Perkin Elmer Optima 8000 located at Northumbria University. From the 50ml vial, produced from acid digestion, 9ml of sample was added to 1ml of 10ppm Yttrium or Indium internal standard (producing a final solution containing 100ppm of the internal standard), dependent upon the elements being analysed for in that run. The internal standard is used to check for instrumental drift throughout a run. Results are reported alongside the analysed elements.

Before any analytical run, a range of calibrations standards were run. Depending on the elements being analysed in that run, a standard solution containing a known amount of each element is diluted to 8 concentrations; Blank (containing no calibration standard) 0.01; 0.1; 1; 2; 5; 10 and 20ppm. Added to this was 100ppm of internal standard - this defines the value to be checked for in each sample. These were run initially and a calibration curve was created, so as to ensure that the raw intensity values created by the instrument may be converted to reliable ppm concentrations. Due to the concentrations created, all samples must fall within this range - too high and they must be diluted, too low and they must be concentrated.

Alongside any sample run, a number of blanks and standards must be run. To check for any contamination, with every set of microwave digestions, a procedural blank was prepared. This consisted of the preparation of a digest without any sediment, to indicate any input of contaminants from the digestion vessels, centrifuge tubes, pipette tips or the instrument. Blanks were analysed periodically, and in each case, were at or below the detection limit for all elements, indicating negligible contamination from the method. Nevertheless, all data presented here is blank-subtracted, with raw counts per second values for the final blank prior to the first samples subtracted from subsequent analyses. The three standards, or certified reference materials (CRMs) used are Montana 2711 soil, Peat Standard NIMT/UOE/FM001, and IAEA-SL-1 Lake Sediment. All standards were digested using the same method as for the samples. These standards contain known concentrations of all the elements of interest, and are as close as possible in terms of matrix to the actual samples.

For the running of samples, it was first determined which wavelengths would be the best in terms of both detection limit and accuracy. This was performed by initial literature review,

and use of the instrument manual to determine recommended wavelengths, before checking with a digested CRM on these, and other wavelengths to determine the correct one for this specific instrument.

2.7.3. Micro-XRF Core Scanning

Non-destructive X-Ray fluorescence (XRF) analysis was performed on Mohos bog using an ITRAX core scanner equipped with a Si-drift chamber detector (Croudace et al., 2006) at the University of Cologne (Institute of Geology and Mineralogy). The analytical resolution employed a 2mm step size and 20s counting time using a Cr X-ray tube set to 30 kV and 30 mA. The method allowed for a wide range of elements to be analysed, from which we have selected Ti, K, and Si for further interpretation. To allow for better visibility, all XRF data sets were smoothed using a 9-point running average. Due to the methodological nature of XRF core scanning, the data are presented as counts per second (cps) and are therefore considered semi-quantitative. Due to the nature of fresh peat sediment (as opposed to once a peat sample is dried and homogenised), XRF-based analyses are hampered by backscatter-related problems. Fresh peat is highly refractive, organic-rich and typically exhibits an irregular surface. As a result, when an XRF core scanner analyses such substrate a large proportion of the incoming X-Rays are scattered, and are therefore not detected by the instrument. Practically, this means a dilution of the signal, and when elemental concentrations are low, the related fluorescent energies detected are also low. This results in difficulties when attempting to distinguish true elemental variations from noise. As such, only elements observed in high concentrations are investigated here. Further validation of the data presented is performed by comparison of qualitative ITRAX-derived values with quantitative ICP-OES-derived measurements. Such an approach ensures interpretations are made relative to fluctuations in the trends observed via both analytical methods.

Changes in substrate, or amount of backscatter (as is to be expected in peat sediment) will alter the overall fluorescent energy observed at each sampling point. As a result, when individual elements are interpreted, variability downcore may be observed, but such variability is truly related to the change in substrate. A simple example of this 'closed sum effect' is when moving from a gyttja, which has a much more homogenous and flat surface, and so lower backscatter, to a peat, where backscatter is higher (Davies et al., 2015). Across the transition, a decrease in one element may be observed, which is actually due to the increased dilution of the signal, and not due to a concentration change. To avoid such an issue, normalisation of ITRAX data is a standard approach. Here, the raw cps

values have been normalised with respect to total (incoherent + coherent) scattering. Such an approach has been used previously to mitigate the closed sum effect (Kylander et al., 2011).

2.8. Pollen Analysis

As a result of the resistant biopolymer sporopollenin present in the outer walls (exine) of pollen grains, they preserve very well, even through deposition and compaction. Sporopollenin is also extremely resistant to normal strong acids, but not to oxidising agents. This means an extraction procedure may be developed, which can remove the pollen from the background organic material, carbonates and silicates of the peat.

Samples of 1cm^3 sediment were taken throughout Sureanu core at roughly 10cm intervals, with a total of 65 samples. These were prepared following standard palynological methods with acetolysis and hydrofluoric acid digestion (Faegri and Iversen, 1989). *Lycopodium* marker spores were added, to allow for concentrations to be calculated (Stockmarr, 1971). At least 350 grains (including pollen, spores, fungi and unidentified grains) were counted in all samples, and pollen percentages were produced from the number of counts respective to the total pollen sum, not including aquatics, fungi, and unknown grains (of which there were less than 3 per sample). When presented, pollen percentages for aquatics were calculated from a separate pollen sum including aquatic taxa. Pollen and spores have been identified using literature (Beug, 2004; Demske et al., 2013) and the pollen reference collection held at Northumbria University. Graphs were drawn using the software Tilia (Grimm, 1990). Microscopic charcoal content was calculated using the point count method as outlined by Clark (1982). Local pollen assemblage zones (LPAZ) were delimited by stratigraphically constrained cluster analysis in CONISS (Grimm, 1987).

2.9. Testate Amoeba

A total of 44 samples of roughly 1-cm^3 were sampled from the Mohos core for testate amoeba analysis. These were disaggregated and sieved according to Booth et al. (2010), prior to mounting in water on slides. Two tablets of *Lycopodium* spores of known value were added to allow for calculation of test density. For each sample at least 150 tests were counted, with identification of taxa following Charman et al. (2000). To allow for interpretation within Mohos bog, two methods of determining wet and dry periods based on changes in testate amoeba assemblages were used. Firstly, a transfer function (Schnitchen et al., 2006) already applied to Carpathian bogs was used to reconstruct past

variations in the depth of the water table. Secondly, the main taxa were grouped into their affinity to wet or dry conditions according to Charman et al., (2000) and plotted as a function of percentage.

2.10. Grain Size Analysis

For granulometric analyses on Sureanu and Mohos bogs, approximately 1g of sample was taken, prior to removal of the organic fraction through the addition of 15ml H_2O_2. Samples were allowed to settle for 2 hours before heating on a hotplate at 200°C to dry down the remaining non-organic fraction. These dry samples were then resuspended in 40% Calgon using a sonicator before analysis via a Malvern Mastersizer Particle Size Analyser at Northumbria University. Results were analysed and presented using Mastersizer software prior to interpretation.

2.11. Numerical Analyses

2.11.1. Dust Flux

The dust flux delivered to an ombrotrophic bog via atmospheric loading may be calculated using the concentration of a lithogenic element, such as Ti (Allan et al., 2013a). Using the averaged occurrence of Ti in the upper continental crust (UCC values from Wedepohl, 1995), the density of the peat as well as the peat accumulation rate (PAR), was calculated using the fo following formula:

$$Dust\ Flux\ (\mathrm{g\ m^{-2}yr^{-1}}) = \left(\frac{[\mathrm{Ti}\ ]_{sample}}{[Ti]_{UCC}}\right) \times density \times PAR \times 10000 (Eq.5)$$

2.11.2. Wavelet Analysis

Continuous Morlet wavelet transform was used to identify non-stationary cyclicities in the Mohos ITRAX data (Grinsted et al., 2004; Torrence and Compo, 1998). For this analysis, the lithogenic normalised elemental data from ITRAX measurements (Ti, K, and Si) was interpolated to equal time steps of four years using a Gaussian window of 12 years.

2.11.3. Extraction of Anthropogenic Pollution Signal

To ensure only the anthropogenic, pollution-related Pb is considered in interpretation, a number of methods were applied to remove the natural (background erosion-related deposition) Pb from the overall signal. In all approaches utilising a conservative litogenic element, Zr has been used (Shotyk et al., 2000).

2.11.3.1. Enrichment Factor

Considering the expected values of the pollution element and the conservative element, from either the crust, or uncontaminated sediment, the Enrichment Factor (EF) may be calculated. This is a function of the difference between the expected ratio of the two elements, in uncontaminated (either crustal, or local uncontaminated values) and contaminated samples. Continental crust values, as defined by Wedepohl (1995) are used.

$$Enrichment\ Factor = \frac{{Pollutant_{Sample}}/{Lithogenic_{Sample})}}{{Pollutant_{Background}}/{Lithogenic_{Background})}} \text{ (Eq. 6)}$$

2.11.3.2. Anthropogenic/Lithogenic Component Extraction

This approach removes the lithogenic (natural) heavy metal component from the anthropogenic (Shotyk et al., 2000), using the following equations. Firstly, using the concentration of a conservative, lithogenic element (in this case Zr), and the expected composition of the UCC (from Wedepohl, 1995), the lithogenic fraction may be calculated:

$$Pb_{Lithogenic} = Zr_{Sample} \times (Pb_{UCC} \times Zr_{UCC}) \text{ (Eq. 7)}$$

This value is simply subtracted from the overall Pb concentration of the sample to provide the anthropogenic fraction:

$$Pb_{Anthropogenic} = Pb_{Sample} - Pb_{Lithogenic} \text{ (Eq. 8)}$$

2.12. Modelling

Pb isotope analysis was carried out on the Sureanu core, with the intention of sourcing the Pb pollution archived. Although results of such work is not presented here, a method for assessing source proportions via Bayesian modelling is proposed.

As the focus of the study is on the application of complex mixing models to Pb isotope values from bulk sediment samples and artefacts, the theory behind simple binary, or ternary mixing approaches is not outlined (See Faure & Mensing 2005 for an outline, and Brugam et al. 2011 and Álvarez-Iglesias et al. 2012 for Pb-specific examples). For disentangling multiple sources, however, two possible approaches are considered: 1) IsoSource, a mass balance-based multi-source mixing model (Phillips and Gregg, 2003) and 2) MixSIAR (Stock and Semmens, 2013), the latest iteration of a series of Bayesian mixing models (Parnell et al., 2010).

IsoSource examines all possible source contribution configurations, at user-defined intervals (e.g. 1%). These calculations rely upon the following equations, expressed below for a system with one isotope system and three sources:

$$X_M = f_A X_A + f_B X_B + f_C X_C \text{ (Eq. 9)}$$

$$1 = f_A + f_B + f_c \text{ (Eq. 10)}$$

where:

X =Isotopic signature of the mixture

f_A, f_B, f_C =Source proportions

X_A, X_B, X_C =Source isotopic signatures

This is an underdetermined system containing three unknowns and two equations, with no unique solution (Phillips and Gregg, 2003). However, the predicted mixture signature for each source combination can be compared to the observed mixture signature; if it matches, mass balance is achieved and the source combination is a feasible solution. Since combinations can only be examined in discrete steps, a small tolerance for deviation from exact matches is allowed (Phillips and Gregg, 2003). These equations make interpretation of datasets with n isotope systems and more than n+1 sources possible (Benstead et al., 2006; Phillips and Gregg, 2003; Soto-Jiménez and Flegal, 2009). Outputs are generally presented as range values, to ensure that all potential combinations are reported (See Benstead et al. 2006).

IsoSource may provide valuable model output, and prior to development of Bayesian isotopic mixing models, it was the main model for food web studies (Boecklen et al., 2011). However, IsoSource uses only mean isotopic signatures for sources and mixtures and does not directly account for errors related to measurement. Additionally, it is unable to take into consideration any variability in source ratios. Since ore bodies are typically heterogenous, ascribing a single value is a simplification.

Complex models have recently been developed which do incorporate these uncertainties within the framework of rigorous Bayesian statistics, utilising the same basic principles as outlined in equations 1 and 2 (see Parnell et al., 2010 for specific mathematics). Put simply, this approach allows the user to incorporate prior information about the system, including analytical error and source heterogeneity, and using a natural distribution (ie. Dirichlet distribution; see Forbes et al. 2011) allows the model to develop solutions, in terms of percentage contributions which sum to unity. The Dirichlet-defined distribution,

however, is intentionally vague, allowing for the model to be driven primarily by the user's data input. Model fits are developed via many Markov Chain Monte Carlo (MCMC) simulations, which produce simulations of plausible source proportions based upon the data, and probability densities. Any mixtures not probabilistically consistent with the data are discarded, and mixtures developed at the end of the run are required to be close to the early ones in terms of proportion, causing a Markov chain to be converged (Parnell et al., 2010). These, when combined with prior information (e.g. results of previous studies if available) produce posterior distributions; true probability distributions for each source (Parnell et al., 2010).

Models built around a Bayesian approach include MixSIAR (Stock and Semmens, 2013), which is a combination of MixSIR (Moore and Semmens, 2008) and SIAR (Parnell et al., 2010), as well as FRUITS (Fernandes et al., 2014), IsotopeR (Hopkins and Ferguson, 2012), and others, which are slightly varied approaches to the same problem.

Chapter 3. Detrital events and hydroclimate variability in the Romanian Carpathians during the mid-to-late Holocene

3.1. Introduction

The Carpathian Mountains and bordering lowlands are one of the most rapidly reacting regions of Europe to current climatic change, with droughts, and periods of short, intense precipitation becoming more common (IPCC, 2013; Micu et al., 2015). The wider region (the Carpathian-Balkans) is located at the confluence of major atmospheric circulation patterns, with the North Atlantic system towards the west, the Mediterranean to the south-west, and the Siberian High to the east (Obreht et al., 2016 and references therein; Panagiotopoulos et al., 2005). As a result, the region should be very sensitive in recording past climate variability resulting from periodic shifts in the dominant circulation pattern. The NAO, in particular, has a major control on winter precipitation (Bojariu and Giorgi, 2005; Stefan et al., 2004; Tomozeiu et al., 2005, see Fig. 2.1.C) and winter temperature (Bojariu and Giorgi, 2005) changes in the region.

The Carpathian-Balkan region is one of the longest-inhabited regions in Europe, with Neolithic cultures having interacted with the environment as far back as 9000 years before present (yr BP) (Bailey, 2000). An increasing number of studies have demonstrated the importance of the long-term impact of humans within the Carpathians, particularly via deforestation and high Alpine pasturing (Carozza et al., 2012; Feurdean et al., 2009; Feurdean and Astalos, 2005; Schumacher et al., 2016), activities which may have had a significant impact on an area's erosional regime (e.g. Arnaud et al., 2012). Indeed, the Balkan Peninsula was the earliest region in Europe to domesticate animals, roughly 9000 yr BP (Larson et al., 2007), and hosted the spread of agriculture from the south-east from 7000 yr BP on (Price, 2000; van Andel and Runnels, 1995). Additionally, the earliest known examples of extractive metallurgy (around 7000 yr BP) may be found throughout the region (Radivojević et al., 2010 and references therein); evidence for a long history of significant human impact.

Despite significant improvements in the last decades, high-resolution and especially multi-proxy palaeoclimate records from the Carpathian region in Romania are still rare (Buczkó et al., 2013; Magyari et al., 2009, 2014; Magyari et al., 2012). Individual proxies have been used to produce a number of long-term records, especially pollen (Feurdean et al., 2008;

***Figure 3.1**: Image of Sureanu lake, and connection to Sureanu peat bog. Indicated on image are the lake, the bog and the moraine which separates the two. Also indicated is a person, for scale.*

Schumacher et al., 2016; Tanţău et al., 2011) and references therein), speleothems (Constantin et al., 2007; Drăguşin et al., 2014; Onac et al., 2002) and other palaeoecological and geochemical proxies (Brückner et al., 2010; Magyari et al., 2013; Schnitchen et al., 2006; Tóth et al., 2015). Most studies display strong inter-site variability, even when in close proximity to one another (e.g. Feurdean et al., 2008), an indication of the complexity of the region's climate, one which has been defined primarily by natural controls (e.g. Tóth et al., 2015) but also influenced by major anthropogenic disturbances (Schumacher et al., 2016).

Furthermore, a tree ring reconstruction of summer temperatures over the past 1000 years in the Eastern Carpathians (Popa and Kern, 2009) shows an interesting lack of correlation to similar records from central Europe (e.g. Büntgen et al., 2011), particularly during periods of rapid climate change (e.g. MWP and LIA). This is indicative of strong regional forcing of climate in the Romanian Carpathians in particular and south-eastern Europe in general (Roberts et al., 2012). This is further evidenced by pollen-based reconstructions across the continent, which indicate a disconnection between Holocene temperature and precipitation changes in south-eastern Europe, and central and western Europe (Davis et al., 2003; Magny et al., 2013; Mauri et al., 2015). The location of the region, at the confluence of three major atmospheric pressure fields, may play a major role in this apparent discrepancy. Studies exploring this teleconnection between changes in the atmospheric system and the impact on the environment are sorely lacking in this area, as most studies have been focussed on the last 100 years (e.g. Bojariu and Giorgi 2005 for a review). These studies indicate the correlation of a low NAO index with high precipitation in the

region for the period of available meteorological data (Stefan et al., 2004; Tomozeiu et al., 2005; see Fig. 2.1.C), but it is unclear if this connection has persisted over a longer timescale.

To understand the link between changing atmospheric patterns and precipitation, records of sedimentation related to flooding events, common in central Europe, may be used (Czymzik et al., 2013; Magny et al., 2013; Swierczynski et al., 2013; Wirth et al., 2013). Using these long term high-resolution records in central Europe, a link between NAO variability and periods of flooding has been inferred (Wirth et al., 2013).

Determining the interactions between varying controls on the climate system is difficult when utilising single-proxy studies, particularly when attempting to put a region's history in the context of a changing climate and human occupation, and so more multi-proxy studies are needed (Veres and Mîndrescu, 2013). Here the first record of apparent flooding events from south-eastern Europe is presented, in the southern Romanian Carpathians throughout the mid-to-late Holocene. Alongside traditional loss-on-ignition parameters, proxies for organic matter and minerogenic contents, the viability of a novel geochemical proxy (namely the Rb/Sr ratio) is investigated as a proxy for minerogenic deposition in the bog, previously only utilised in loess and lake sediments (Jin et al., 2006; Vasskog et al., 2011).

3.2. Methods and Materials

3.2.1. Sample Information

Sureanu peat bog (45°34'51"N, 23°30'28"E), is a small bog in the Sureanu Mountains, Southern Carpathians (Romania) (Figs. 2.1, 3.1). 603cm of sediment was recovered, with recovery methods outlined in Chapter 2.

A total of 220 samples were analysed via ICP-OES for a suite of elements, whilst 603 samples were analysed via loss-on-ignition. In addition, 65 pollen samples (with at least 350 grains investigated in each sample) were counted, and 105 samples were analysed for grain size. See Chapter 2 for specific details of each method.

Table 3.1: *Radiocarbon dates used to build age model for Sureanu record. Sample DeA-5795, dated on wood, is likely an age outlier and was excluded from age model calculations.*

Lab No.	Depth	^{14}C age (± 1σ)	Minimum Calibrated Age (yr BP)	Maximum Calibrated Age (yr BP)	Mean Calibrated Age (yr BP)	Dated material	Observation
DeA-7256	34	-16 ± 22				bulk peat	
DeA-7257	57	236 ± 23	277	310	287	bulk peat	
DeA-7258	72	368 ± 22	319	500	441	bulk peat	
DeA-7259	104	805 ± 22	680	770	713	bulk peat	
DeA-7260	129	728 ± 21	660	690	675	bulk peat	
DeA-7261	163	1164 ± 25	989	1177	1090	bulk peat	
DeA-5795	172.5	3176 ± 26	3360	3450	3401	wood	outlier
DeA-7262	200	1417 ± 26	1290	1356	1319	bulk peat	
DeA-5796	209	1560 ± 27	1392	1528	1467	bulk peat	
DeA-7263	228	1809 ± 22	1634	1820	1750	bulk peat	
UBA-31373	252	2228 ± 44	2148	2339	2244	bulk peat	
UBA-31374	280	2202 ± 44	2119	2333	2226	bulk peat	
DeA-7264	314	2595 ± 24	2720	2759	2744	bulk peat	
UBA-31375	344	3023 ± 30	3141	3275	3207	bulk peat	
UBA-31376	378	3317 ± 50	3447	3645	3551	bulk peat	
DeA-7265	404	3638 ± 29	3868	4080	3949	bulk peat	
UBA-31377	454	4181 ± 32	4614	4706	4660	bulk peat	
DeA-5797	516	5301 ± 36	5950	6189	6083	bulk peat	
UBA-31378	603	6777 ± 54	7564	7702	7633	bulk peat	

3.2.2. Chronology

The age model for the core is based on 19 ^{14}C dates. From each sample, wood or moss fragments within bulk sediment were analysed (Table 3.1). These analyses were performed via AMS at the ^{14}C CHRONO centre at Queen's University Belfast, and at HEKAL AMS Laboratory, MTA ATOMKI Institute for Nuclear Research of the Hungarian Academy of Sciences in Debrecen (Molnár et al., 2013). The ^{14}C ages were converted into calendar years using the IntCal13 calibration curve (Reimer et al., 2013) and an age-depth model was generated using Bacon (Blaauw and Christen, 2011, Fig. 3.2). Sample DeA-5795 represents an outlier and therefore was excluded from age modelling. This is a wooden sample, which may be much older than surrounding sediment and was likely transported onto the bog from the surrounding slopes (Oswald et al., 2005; Schiffer, 1986).

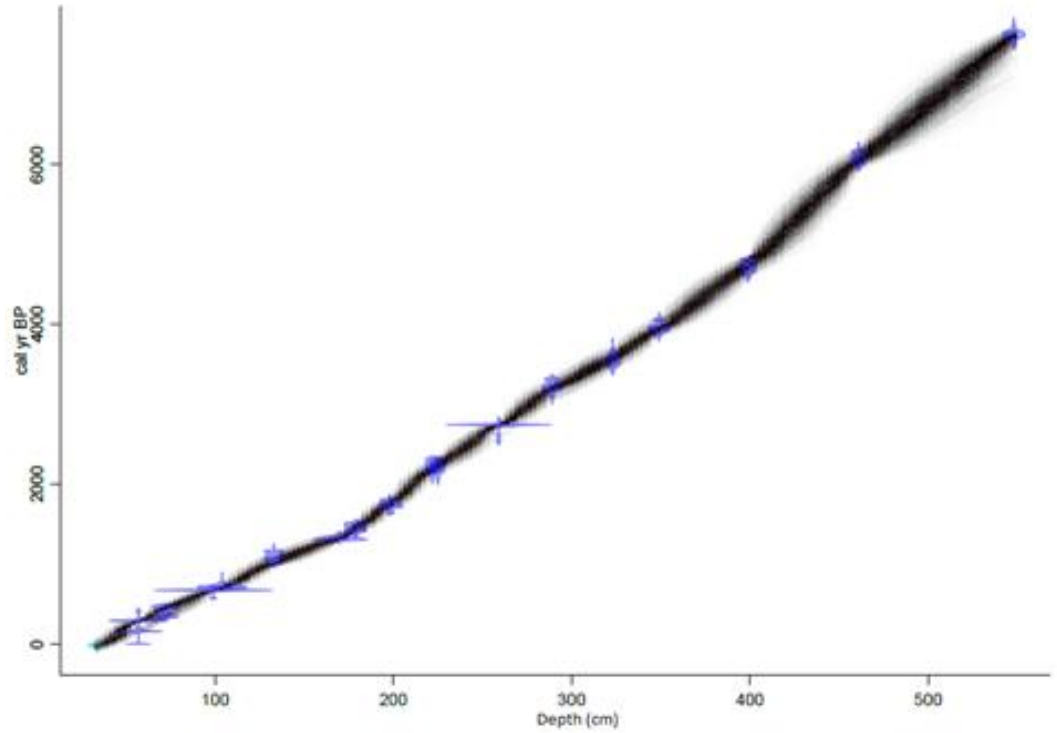

Figure3.2: *Age model for Sureanu record based on 18 ^{14}C dates, as calculated using Bacon (Blaauw and Christen, 2011).*

3.3. Results

3.3.1. Lithology and Sedimentology

The lower part (below 300cm) of the record consists of gyttja and fen peat, clearly documenting the gradual transformation of this basin into a raised bog throughout the mid-to-late Holocene (see Fig. 3.5). For the upper 4m, the record consists of Sphagnum-dominated peat, with a number of minerogenic layers, some of which are apparent upon visual inspection.

The age model (Fig. 3.2) indicates the time frame covered by this study is from roughly 7500 yr BP to the present day, with the uppermost peat (growing moss) dating from 2014. This means the time span between samples is roughly 10yrs for the LOI and grain size, 100yrs for the pollen and between 30–100yrs for the geochemistry. All ages quoted throughout the text are in calendar years BP (yr BP).

For the first 2000 years, the Sureanu record is characterised by low organic matter (OM) values (roughly 30%), indicative of a coarse gyttja-like, lacustrine sediment with occasional roots and fine gravel (Figs. 3.4, 3.5). After 5000 yr BP there is a shift towards a coarse, detritus-rich fen peat, with OM values stable around 50–60%, but with small high-organic excursions becoming more common throughout the period, pointing to the gradual

establishment of a raised bog. There is a clear transition into much more detritus-free peat at around 3300 yr BP, which follows on from a shift in the OM record to values of around 90% at 3500 yr BP. There are occasional sharp drops in the OM values however, but it is not until 2140 yr BP these become more frequent. In this section, the record consists of fine Sphagnum peat, with clear occasional root and sand/small pebbles incursions. This period is characterised by the first appearance of regular, sharp (in terms of boundaries) and rapid (in terms of deposition time) minerogenic depositional events within the peat. The first of these is seen in the OM record between 2140–2030 yr BP, with an excursion to OM values as low as 30%, before a short period of normal bog growth and subsequent minerogenic overprinting again around 1870 yr BP. This large event is followed by the final period of extended uninterrupted peat deposition, with OM values of 90% sustained until 1260 yr BP (Fig. 3.5.F).

Table 3.2: *Table of Certified Reference Material (CRM) values run alongside samples to ensure reliable data is produced from the ICP-OES system. Both CRMs were repeated five times within the runs. Recoveries (in %) are calculated relative to expected values, and standard deviations have been calculated.*

Montana Soil 2711	**Rb (ppm)**	**Sc (ppm)**	**Sr (ppm)**
	142.5	10.7	202.1
	137.3	9.1	239.3
	141.3	9.5	211.9
	107.5	7.1	222.6
	108.9	8.0	230.9
Average	127.5	8.9	221.3
Expected (ppm)	110.0	9.0	245.3
Recovery (%)	**115.9**	**99.6**	**90.2**
Std Deviation	17.7	1.3	14.7

IAEA Lake Sediment	**Rb (ppm)**	**Sc (ppm)**	**Sr (ppm)**
	135.2	17.6	101.5
	110.3	19.1	91.3
	128.5	17.4	91.4
	120.5	16.7	97.1
	128.4	16.4	95.9
Average	124.5	17.482	95.4
Expected (ppm)	113.0	17.3	80.0
Recovery (%)	**110.2**	**101.052**	**119.3**
Std Deviation	9.5	1.1	4.2

After 1260 yr BP there are 13 major high minerogenic content depositional events (see Fig. 3.5). These events are variable in their duration and their presumed effect on the bog growth. Most cover a fairly short period of time (roughly 5–10 years or even less), but show OM values as low as 10%. Some indicate OM of around 40% and last a little longer. A period of constant low OM is observed between 1100–850 yr BP, in which the values rarely rise above 80%. The sediment remains a detrital peat (still composed mainly of Sphagnum), with notable layers of minerogenic material, until 900 yr BP, when it becomes a coarse,

undecomposed peat, with similar gravel and sand layers distributed throughout the time period. Following on from this shift, there is one period of enhanced sedimentation rate, between 810–690 yr BP, where it rises to 0.22 cm/yr, as opposed to the normal rate of 0.1–0.15 cm/yr throughout the record.

The remainder of the core is characterised by several OM declines, a sign of near-constant minerogenic influx (Fig. 3.5). The OM record indicates values between 10– 40%, with no return to normal peat deposition, suggesting frequent mass wasting events, regular inundation of the bog, or a combination of both, between 350–100 yr BP. A very short period of high OM, fresh undecomposed peat is observed in the final 50 years, indicating a cessation of the major minerogenic deposition typical of much of the record (Fig. 3.5).

3.3.2. Pollen

The pollen assemblages have been grouped into Local Pollen Assemblage Zones (LPAZ), constraining major shifts in the local vegetation type (Figs. 3.3, 3.5, 3.6).

3.3.2.1. LPAZ 1: 7500– 5800 yr BP

This pollen zone is indicative of a mixed forest dominated by *Picea*, with typical percentages between 40– 50%, and a collection of more foothill representative taxa including *Alnus*, *Corylus* and *Quercus* typically making up 10% of the assemblage. *Carpinus* and *Ulmus* percentages are the highest of the core, with *Carpinus* making up as much as 15%, while *Ulmus* is typically 5% of the assemblage (Fig. 3.6). In addition to the tree taxa, high values for monolete spores are found throughout LPAZ 1, the only major component seen that is not arboreal.

3.3.2.2. LPAZ 2: 5800– 4300 yr BP

This zone is characterised by a dominance of subalpine forest taxa: *Picea* (up to 60%) and *Pinus*. There are lower abundances of foothill forest taxa pollen, although *Carpinus* still makes up 10%, Quercus roughly 10% and *Fagus*, for the first time, becomes a clear component of the vegetation. The appearance of *Fagus* follows on from the disappearance of *Ulmus* at around 4500 yr BP. At the start of this zone *Corylus* drops to around 5% and never recovers to the values seen previously. In terms of non-arboreal taxa, an increase in Chenopodiaceae, and decrease in undifferentiated monolete spores may be observed.

3.3.2.3. LPAZ 3: 4300– 3000 yr BP

Through this period, the coniferous pollen percentages begin to fall, with *Picea* dropping the most (to around 40% by the end of the zone), whilst *Fagus* (reaching 20% by the end of the zone), and *Quercus* increase. *Pinus*, which rises briefly early in the zone to 10%, drops back down to around 5% by the end. This occurs concurrently with an increase in *Sphagnum* and fungi spores, and a decrease in *Alnus* and undifferentiated monolete spores. *Carpinus* still makes up a fairly major component, with values of 10% common, until the end of the zone, where it disappears. *Dryopteris*, previously present in low percentages, disappears, and Poaceae, previously only observed in small pollen abundances, rises to 10%, by the end of the zone.

3.3.2.4. LPAZ 4: 3000–1900 yr BP

This period is characterised by another major decrease in *Picea* from 40% to 30% between 2750– 2500 yr BP, a value around which it hovers for the remainder of the record. This decline is offset by an increase in *Alnus*, up to over 20% and *Quercus* (circa 15%). At the same time, *Fagus* declines below 20%, and *Carpinus* disappears. Herb taxa, particularly Poaceae, Apiaceae, *Artemisia* and Asteraceae appear. The pollen data for this zone indicate further shifts away from conifer-dominated forests. *Alnus* and *Fagus* (both as high as 30%) are dominant throughout the period, with *Picea* making up the remainder, indicative of more local deciduous forest.

3.3.2.5. LPAZ 5: 1900–950 yr BP

The pollen record from this period is indicative of a deciduous forest but with a contribution from coniferous taxa. *Picea* (30%) and *Pinus* (5%) remain low, with *Alnus* (25%), and in particular *Fagus* (30% rising to 40%) make up the majority of the assemblage. The herb and shrub taxa are at the highest levels yet seen, indicating the least dense forest, alongside the initial appearance of a number of taxa related to anthropogenic activity. Indeed, throughout this period, the abundances of *Plantago* and Poaceae are high, and the first occurrences of *Papaver* (1100 yr BP) and *Cerealia* (1450 yr BP), unequivocally agriculture-related taxa, are seen. The concurrent increases in Apiaceae, Asteraceae, Chenopodiaceae, Ericaceae, all further indicate lower forest cover.

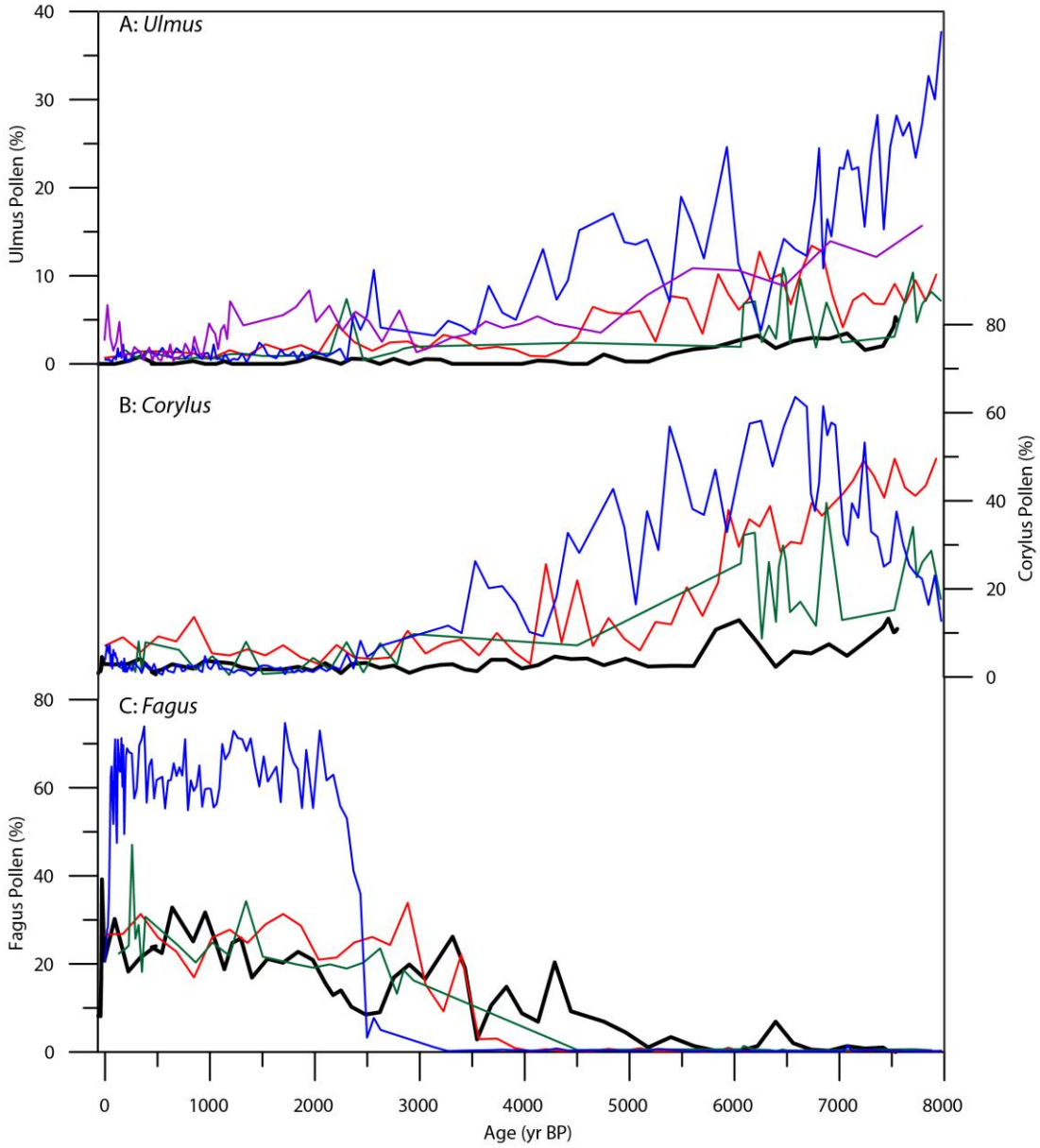

Figure 3.3: *Comparison of Sureanu pollen record to other sites in the Southern Carpathians. Presented are records of A: Ulmus, B: Corylus and C: Fagus. Sureanu (Bold black line) is compared to one eastern Carpathian site; Mohos peat bog (1050m, blue line, Tanţău et al., 2003) and three southern Carpathian sites; Taul Zanogutii peat bog (1840m, red line, Farcas et al., 1999), Avrig peat bog (400m, green line Tanţău et al., 2006)and Semenic peat bog (1440m, purple line, Rösch and Fischer, 2000)*

3.3.2.6. LPAZ 6: 950 yr BP to 0 yr BP

Within this zone the vegetation remains dominated by *Fagus*, composing up to 40% of the assemblage, prior to a major drop at the end of the zone, at the transition into LPAZ 7. *Alnus*, *Quercus* and *Picea* make up the remainder of the arboreal taxa.

3.3.2.7. LPAZ 7: 0 yr BP to Present

The period is notable, for the sharp increase in Poaceae (up to 15% by the end of the zone) and Chenopodiaceae percentages, recording the highest values of these taxa, and an extremely large spike in Cyperaceae, rising to 15%. Additionally, *Sphagnum* rises to 5%. The impact of this change may also be seen in the pollen concentrations which are at their lowest throughout the core (Fig. 3.6). Another notable feature is the highest abundances of *Cerealia*, *Papaver* and *Plantago*, all related directly or indirectly to agriculture or pasturing.

3.3.3. Charcoal

Between 7500–4550 yr BP, the microcharcoal record is characterised by high, but fluctuating values, between 100–450 cm^2/cm^3 before an extended period of low (<50 cm^2/cm^3) values until 2740 yr BP (Fig. 3.5B). After this point, values remain high, ranging between 100–300 cm^2/cm^3 until a recent drop to below 50 cm^2/cm^3 in the final 50 years of the record.

3.3.4. Geochemistry

For the first 2500 years of the record (Fig. 3.5), the lithogenic elements indicate elevated concentrations (Rb: 100 ppm, Sr: 110 ppm, Sc: 5–10 ppm), indicative of a lacustrine system, with Rb values ~100 ppm having been observed previously in Alpine lakes (e.g. Koinig et al., 2003). These are significantly lower for the subsequent period, between 5050–2650 yr BP (Rb: 25 ppm, Sr: 50 ppm, Sc: 3.5 ppm). After 2650 yr BP, the values increase indicating higher mineral input, potentially as a result of enhanced regional erosion. Additionally, in this zone some trends in the Rb/Sr ratio appear visually coupled with the organic matter record (see Fig. 3.8).

The concentrations for all elements remain generally high for the section 2650 yr BP to present, with values of Rb: 200 ppm, Sr: 200 ppm, Sc: 10 ppm common. Short periods of lower values may be seen between 1950– 1650 yr BP before high but fluctuating values between 1650–600 yr BP (Fig. 3.5). This is followed by periods of lower values with one peak at 750–650 yr BP. The values return to the low concentrations observed earlier towards the top of the record, but not before a short period of enrichment between 200–50 yr BP with Rb (100–200 ppm), Sr (100–150 ppm) and Sc (5–10 ppm) showing short-term increases.

3.3.5. Grain Size

Grain size analysis (Figs. 3.7, 3.8), performed on the last 2500 years of the record, indicates the difference in grain size distribution of various types of minerogenic deposition within Sureanu record. There appear to be three types of deposition, the first with medium to high uniformity (2–4 μm) and low d50 (average particle size; 30-50 μm, see Fig. 3.7A). and the second with average to high uniformity (2–4 μm) and medium d50 (50–65 μm, see Fig 3.7B). Finally are layers with low uniformity (0.5–1.5 μm) and generally high d50 (50–120 μm, see Fig.3.7B).

3.4. Discussion

3.4.1. Depositional events record

Sequential periods of peat growth (generally >80% organic matter) are interrupted by periodic, abrupt (in terms of boundaries) and short-term episodes of much lower OM (generally <60%, but reaching as low as 10%, Fig. 3.5F) values. Due to the low OM values reached without a clear change in the peat material (still dominated by Sphagnum remains), these layers may be associated with the input of minerogenic debris from a proximal source, and not just direct atmospheric deposition of fine-grained particulates/dust. If it were simply atmospheric dust deposited within a raised bog environment, the OM values would remain much higher (roughly around 90%; Shotyk, (2002).

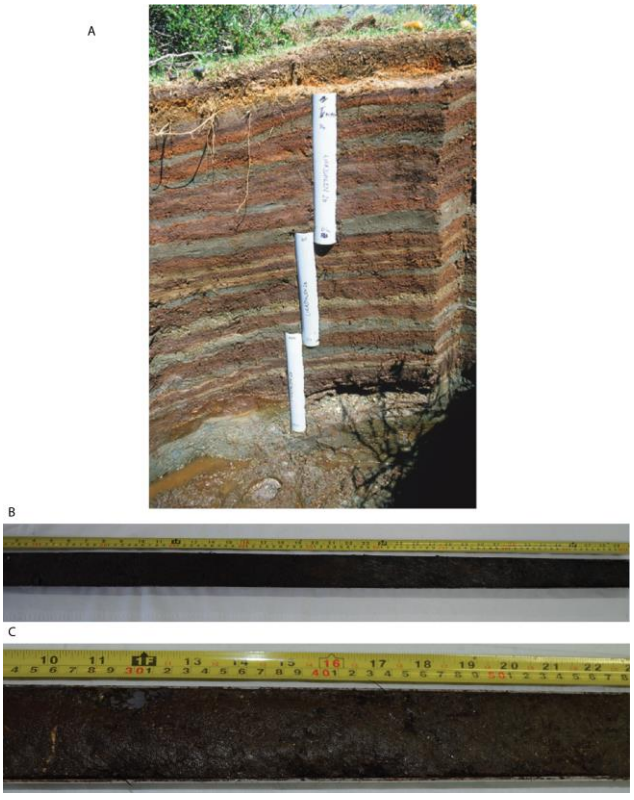

Figure 3.4*: A: Comparison of Sureanu peat bog with a peat bog with true minerogenic layers (Matthews et al., 2009; B is the top 1m of Sureanu, the most affected by minerogenic debris.C is a closer image of 25-58cm from the top 1m.*

The age model can be potentially complicated by these minerogenic layers. If these are indicative of rapid deposition through mass wasting then they may create incorrect sedimentation rates. However, the Sureanu pollen profile matches similar sites in the region

(See Fig. 3.3) and the sedimentation rate is relatively constant throughout (0.05–0.15cm/yr) suggesting that the minerogenic deposition has had little impact on the sedimentation rate for the past 2500 years. Furthermore, observations of the core indicate the minerogenic debris was generally made up of fine-grained particles, with only very occasional pebbles, and so it is reasonable to assume such events do not cause cessation of peat growth (see Fig. 3.4). To further evaluate the robustness of the age model, the pollen results from Sureanu are compared with other pollen records from similar sites, with emphasis on the timing of appearance and disappearance of key species (See Fig. 3.3). These approaches appear to indicate the Sureanu record is replicating the trends observed regionally and is therefore based on a well-constrained age model.

3.4.1.1. Interpretation of Minerogenic Event Layers

To understand the underlying source of the depositional events, grain size analysis has been performed on the top 2500 years of the record (since this section contains the majority of minerogenic debris layers), the sediment from the rocky shore of Iezerul Sureanu Lake, and a soil sample from the surrounding forested slopes between the lake and the bog (Figs. 2.1, 3.1). Peat intervals with high organic matter values (>80%), shows d50 values typically between 20–40µm, (Fig. 3.8). As the analytical method for determining grain size removes all organic material, and typically atmospheric dust particles are around 20um (Stuut and Prins, 2014), this can be considered the signature of normal atmospheric dust input.

Within minerogenic layers (as determined from the OM and the geochemical records) the grain size (compared to normal peat deposition) shifts, with d50 averaging around 40µm and reaching values as high as 130µm (Fig. 3.8). This shift indicates the clear input of a non-dust minerogenic fraction, with the site's location at the base of a cirque likely to be the cause. As the surrounding slopes are steep, and there are avalanche channels present, it is reasonable to assume the minerogenic debris present is related to slope activity.

It has been suggested (Nesje et al., 2007; Vasskog et al., 2011) that snow avalanches result in the deposition of coarse-grained sediment, as the snow pack breaks up and transports local rock as it moves downslope. When avalanches settle and the snow melts, these grains are deposited onto the substrate below (Nesje et al., 2007). Within Sureanu cirque, as the lake is regularly frozen during winter, avalanches would flow over and the debris settle on the frozen lake and bog. Additionally, mass wasting not related to snow action (i.e. landslides, rockfalls, flooding) would cause the same type of deposit as they break up the

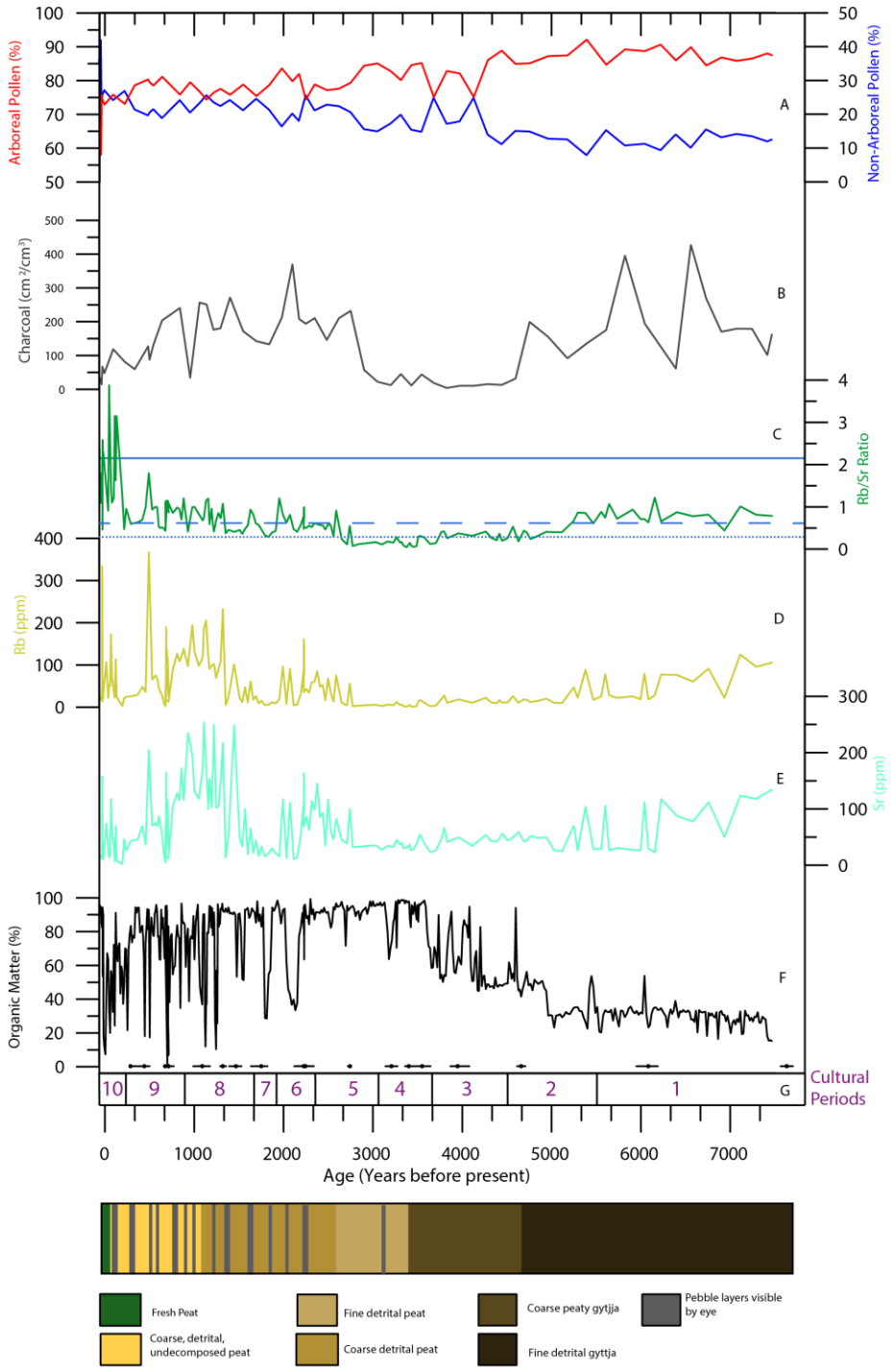

Figure 3.5: *Downcore variations in multiple proxies from Sureanu. Arboreal and non-arboreal pollen percentages (A) are presented alongside microcharcoal counts (B), the Rb/Sr ratio (C) and lithogenic (Rb, Sr) element concentrations (D and E). The blue lines in panel C denote the ratio from local soil (solid), lake sediment (dashed) and local rock (dotted). Panel F shows the organic matter as determined via loss-on-ignition. Cultural periods referenced in the text are indicated in panel G: 1: Neolithic, 2: Early Bronze Age, 3: Middle Bronze Age, 4: Late Bronze Age, 5: Iron Age, 6: Dacian State, 7: Roman Dacia, 8: Middle Ages, 9: Medieval Period, 10: Industrial to modern. In addition, a simple lithological diagram is presented. Calibrated radiocarbon dates and uncertainties are indicated at the base of the graph.*

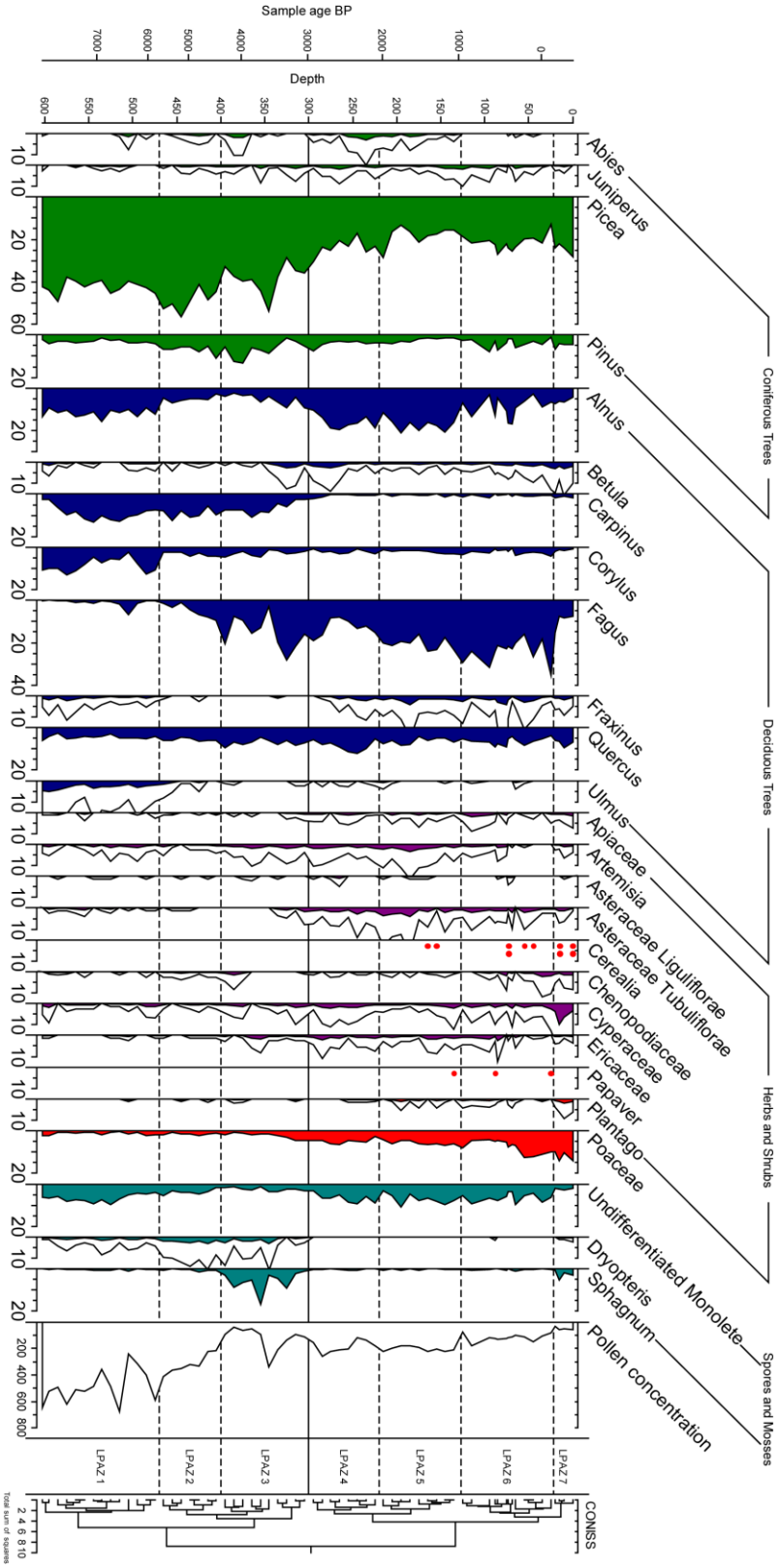

Figure 3.6: *Simplified pollen diagram showing percentages of selected taxa from Sureanu bog. Non-patterned, unshaded area represents five times exaggeration of percentages. Red circles are representative of one pollen grain. Percentages of pollen and spores were calculated based on the total pollen sum, excluding unidentified pollen/spores. Taxa used to reconstruct human impact have been highlighted in red.*

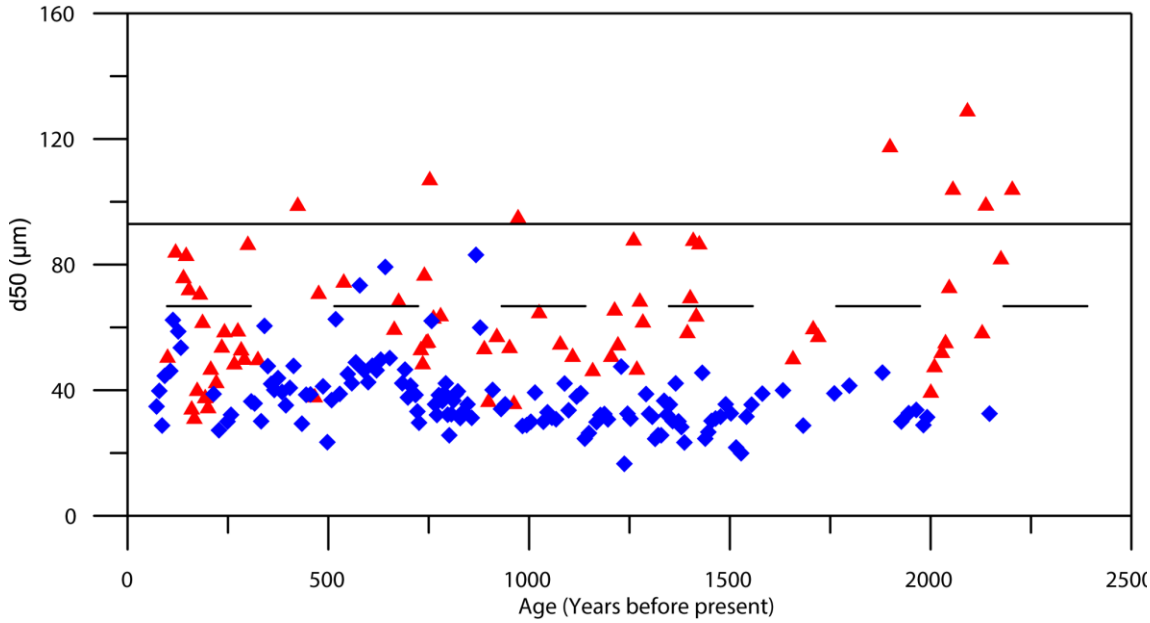

Figure 3.7: *Median grain size data (d50) for most recent 2500 years of Sureanu core. Samples taken from minerogenic (<65% OM) layers are indicated by red triangles, whilst those which are form normal (>65% OM) peat are indicated by blue diamonds. Also indicated are the d50 values for both the local soil (solid line) and lake sediment (dashed line).*

surrounding rocks into small particles as they flow down the slope (see Panek, 2015 for a review of dated landslides in sedimentary archives). Such activity is likely to be behind the shift toward larger particles during minerogenic layers. Deposits of this type would also result in the existence of large grains (>1mm), as seen in the grain size distributions, core observations (clear pebbles may be seen within minerogenic layers), and in the presence of boulders in the lake and surrounding area.

Other depositional events appear to indicate the influence of the local soil being washed into the bog. The local soil has d50 values above the typical peat d50, but below that of the lake sediments (Fig. 3.7). The simplest explanation for the presence of these deposits is the impact the hydrology of the nearby lake has on the site. When water levels in Iezerul Sureanu are high, the water overflows the bank on which the soil sample was taken, and washes into the bog, bringing with it sediment which has been entrained in the water, or picked up as the water flows over rock and soil.

3.4.1.2. Significance of the Depositional Record

For each of the methods of sediment delivery outlined above, water is a major control on their formation. For avalanches, the primary controller is high snowfall (Schweizer et al., 2003). The value of 30cm of fresh snowfall is regularly used as an indicator for an increased avalanche risk (McClung and Schaerer, 2006). Studies in Iceland (Keylock,

2003) and the Pyrenees (Esteban et al., 2005; García-Sellés et al., 2010; López-Moreno et al., 2011) have shown that periods of high snowfall, and even large-scale atmospheric precipitation controls, such as the NAO, play a large role in the frequency of avalanches. Additionally, intense, short periods of rainfall are one of the major factors in landslide formation (Crozier, 2010; Popescu, 2002; Zaruba and Mencl, 1982) with a clear correlation between precipitation and landslide frequency. Further connections between NAO-controlled precipitation and landslide frequency have been made in the Azores (Marques et al., 2008), and Portugal (Marques et al., 2008; Trigo et al., 2005). As such, the minerogenic depositional event record may be used as an indirect proxy for periods of high precipitation affecting Sureanu (both bog and lake), and catchment area.

3.4.2. Investigating the Potential of Rb/Sr Ratio as a Proxy for Grain Size

When investigating highly organic substrate such as peat, traditional grain size analyses are not easy to perform. Due to the high organic content, a large amount of sample is needed to extract a sufficient minerogenic fraction for analysis, as is performed here. Furthermore, such approaches (removal via H_2O_2 or ashing) may alter the minerogenic debris, and so particle size measurements are not routinely performed (Kylander et al., 2016). However, particle size analyses could be very useful for interpreting the provenance of both local (avalanche and mass wasting) and distal (dust) minerogenic inputs (Kylander et al., 2016; Vasskog et al., 2011).

The Rubidium/Strontium (Rb/Sr) ratio (Fig. 3.8A) has been used in lake sediments from China to indicate weathering in the catchment area (Jin et al., 2001, 2006), and then to estimate weathering intensity in loess-palaeosol deposits (Jin et al., 2006). This work was developed based on the behaviour of the two elements during weathering. Rubidium commonly substitutes for K in mineral lattices, and Sr commonly replaces Ca, due to similar ionic radii (Kabata-Pendias, 2010; Vasskog et al., 2011). Minerals containing K are much more resistant than Ca-bearing minerals, resulting in an enrichment in weathering products of Ca (Boggs, 2013; Kabata-Pendias, 2010; Simmons, 1998). Consequently, Sr should be enriched in glacigenic, and weathered material (Vasskog et al., 2011). In Norway, the proxy has been used to establish a preliminary record of mass wasting events from the slopes surrounding a lake (Vasskog et al., 2011).

The use of Rb/Sr ratio has been further refined, and it appears that the ratio also changes as a function of grain size (Kylander et al., 2011), or more precisely, correlates with the lack of clay in the layers of debris (Chawchai et al., 2016; Vasskog et al., 2012). This

hypothesis rests on the K-bearing minerals being derived primarily from finely crushed phyllosilicates, whilst Ca-bearing minerals are concentrated in coarser, more erosion-resistant grains, with plagioclase a common constituent. This results in low Rb/Sr ratios associated with large grain sizes.

The periods between 7500–2950 yr BP, and from 200 yr BP to present appear to show no direct coupling between the Rb/Sr and the organic matter record, other than the reduction in Rb/Sr at 5000 yr BP mirroring the increase in OM. This appears to indicate another major control on the distribution of these elements within the column during these times (Figs. 3.5, 3.8). The results appear to indicate the issues of applying a proxy previously utilised (Vasskog et al., 2011) where the influence of organic matter is negligible, to an organic-rich substrate.

Within the period 7500–2950 yr BP the Rb/Sr ratio is uncoupled from the OM, related to the lacustrine nature of the sediment, with high values to be expected. During this time, the clayey lacustrine sediment would be associated with fine grain sizes, and may explain the ratio shift. This is corroborated by the LOI record (Fig. 3.5), which indicates a shift towards clay-rich peat, and lower organic contents. The period of very low ratios between 300–375cm appears to be due to a natural shift into a gyttja-like sediment, at this time, which contains larger grain sizes (Fig. 3.5).

In the upper 50cm, the high Rb/Sr values may reflect the position of the water table, and the shift to more stable values could be indicative of the contact between the aerobic (acrotelm) and anaeorobic (catotelm) peat, with the shift from active to inactive peat controlling the elemental distribution. The decomposition process and transition from live material to inactive causes the increased migration (out of the layer of interest) of Rb relative to Sr (Tyler, 2005, 2004). Additionally, due to the ease with which Rb and Sr may be taken up by plants (Kabata-Pendias, 2010), it can be assumed that both elements will be affected by migration. The discrepancy could be a result of Rb being taken up more readily than Sr, and easily cycled by organic compounds due to its lower atomic weight and electronegativity (Tyler, 2005), and substitution for K in upper peat layers. Rb is particularly likely to be re-absorbed by the upper organic layers when the system is acidic (Folkeson et al., 1990), as it is the case of Sureanu bog. It has been demonstrated that acidity can exacerbate the uptake by causing K^+ leaching losses, resulting in replacement by Rb^+ where available (Nyholm and Tyler, 2000), especially when mediated by intense

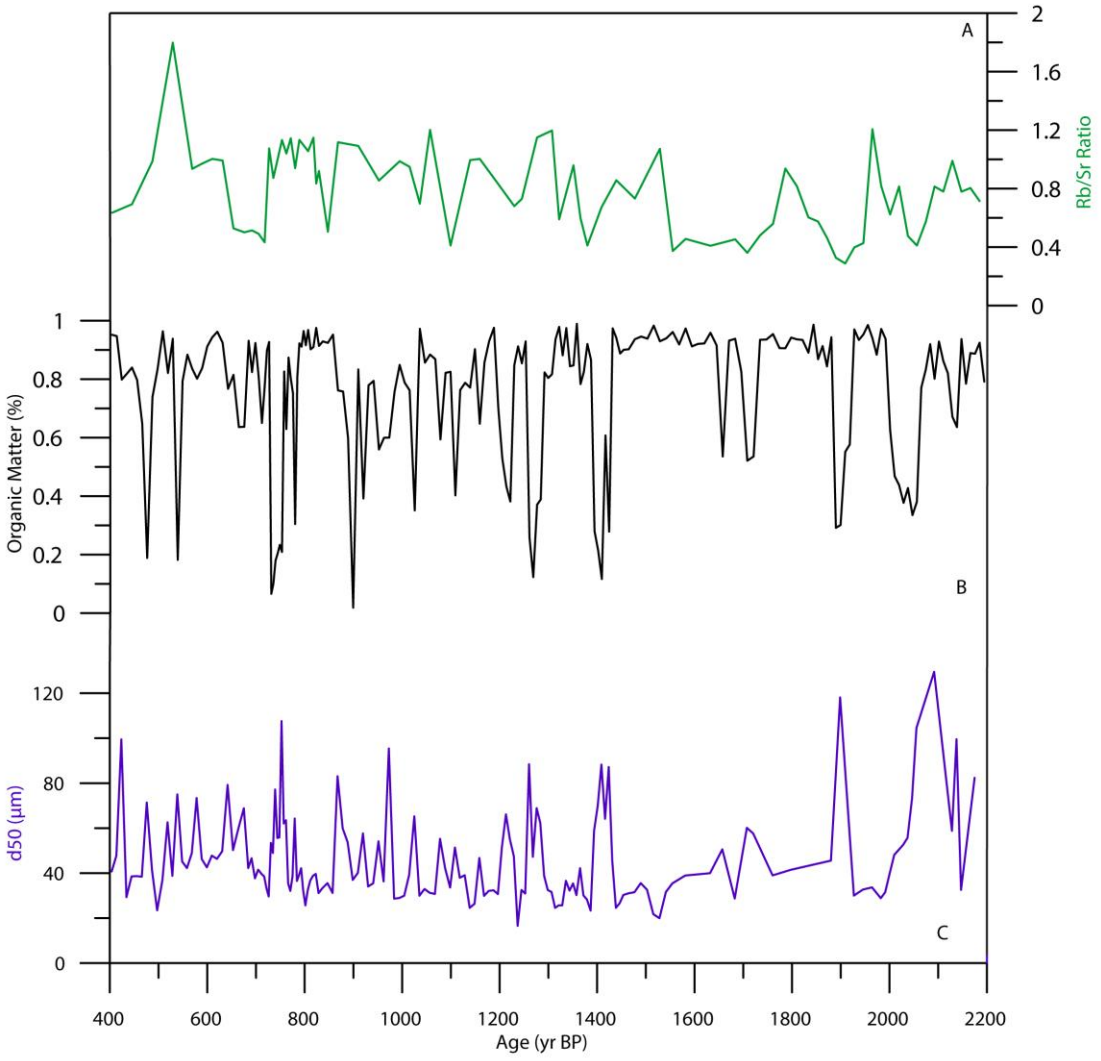

Figure 3.8: *Comparison of Rb/Sr ratio (A) to the organic matter record (B) and the grain size distribution (C) for the period 2200–400 yr BP, where tentative correlations may be made between the three methods for reconstructing grain-size variations.*

fungal activity (Vinichuk et al., 2010), which would be concentrated in the upper peat layers.

Between 2950–200 yr BP some similarities may be observed between Rb/Sr ratios and the OM content, with most of the major drops in the OM values corresponding with a lower Rb/Sr ratio (Fig. 3.8). Typically, the periods of highly organic, undisturbed peat produce Rb/Sr values around 1, with the ratio dropping to as low as 0.4 in the debris events. Therefore, for at least this part of the record, the Rb/Sr ratio anticorrelates with the OM record, or weathering products associated with mass wasting. To corroborate this, the Rb/Sr ratio of both the local lake deposits (0.55) and bedrock (0.35, calculated from values given by Rudnick and Gao (2013) from the average UCC) have a value close to the lower, debris event related values. This could indicate either directly weathered bedrock or lake

sediment entering the bog as a result of the mass wasting processes to be the source of the low Rb/Sr ratios.

However, quantitative comparisons indicate only a weak correlation between the Rb/Sr ratio and OM values, with an r^2 of 0.08 throughout the record, and 0.1 for the past 2500 years, although the p-value indicates significance. Further, wavelet coherence and cross wavelet analysis have been performed, indicating little clear correlation. This is to be expected, however, since Rb/Sr is perceived to be related to grain size fluctuations, and different types of minerogenic input (e.g. avalanches, flooding, see Fig. 3.8) each produce different Rb/Sr ratios, potentially complicating the geochemical signal, which is then compared to an 'averaged' minerogenic signal (the OM values). This is further evidenced by direct comparison of Rb/Sr with grain size, where no correlation (r^2= 0.042) is observed, likely due to the inability of the particle size analyser to provide any data on the very large grains (as its upper limit is 2mm), whereas the geochemical approach analyses the entire signal. As a result of the lack of statistical correlation, utilisation of Rb/Sr alone appears insufficient for reconstruction of grain size fluctuations in organic-rich sediment. However, the apparent visual similarities indicate some form of relationship. However, further validation is necessary to confirm this.

3.4.3. Palaeoenvironmental Reconstruction from Sureanu Bog

The mid Holocene (7500–4500 yr BP) is characterised by the absence of major detrital events and relatively little variability in the organic matter record (Fig. 3.5). Vegetation throughout this period consists primarily of conifers, with some input of pollen from lower altitude taxa, a combination which is indicative of the natural vegetation at this altitude in this region (Feurdean et al., 2010). Additionally, the undifferentiated monolete spore content is high, related to mosses and ferns, and potentially an indication of wet conditions, as also inferred at a nearby site for this period (Buczkó et al., 2013). These wet conditions are reflected in the deposition of gyttja at the site, and a shallow lake environment throughout this period.

After 5500 yr BP, conifer abundances increase further, indicative of a cooler climate than during the previous interval, with a lowering of the treeline likely to be responsible for the decreased influx of lowland pollen. Cooler conditions during this time are also seen in a chironomid-inferred temperature record from Retezat Mountains nearby (Tóth et al., 2015), and in the Maramures Mountains in NW Romania (Fărcaş et al., 2013), further indicating the increase in conifers is temperature-related. From about 4600 yr BP, there is a

stepwise change away from low-organic gyttja and the organic content increases gradually until c.3500 yr BP after which the OM remains high. Occasional high OM events present between 4500 and 3500 yr BP signal the initial development of peat bog, but are interrupted by transitions back to gyttja (Fig. 3.5).

At 3500 yr BP, there is a shift to coarse, detritus-rich peat, reflected in the decrease in lithogenic element (Rb, Sr) concentrations, likely reflecting the initiation of the gradual process of raised bog formation. This transition to ombrotrophy and raised bog formation results in subsequent sedimentation occurring above the water table, and accounts for the reduction in lithogenic elements, and increase in organic matter (Charman, 2002).

The change in sediment type is accompanied by a marked decrease in *Picea* values and an increased abundance of the mid-altitude taxa *Fagus*. This is a significant shift in vegetation composition, and represents a change seen in other regional studies (Feurdean et al., 2011b and references therein). It is possible that the decline in *Picea* was in response to regionally cooler summers and wetter conditions (Onac et al., 2002; Schnitchen et al., 2006; Feurdean and Willis, 2008; Magyari et al., 2009; Tóth et al., 2015; Drăguşin et al., 2014), superimposed on a slightly higher winter insolation relative to the early-mid-Holocene (Berger and Loutre, 1991). *Fagus* is much more sensitive to colder winters than *Picea* (Feurdean et al., 2011b), and increased winter insolation and associated warmer winters would have allowed its spread in the region. Its ability to thrive in shade during its juvenile stage allows for it to out-compete *Picea* during periods of climatic warming (Feurdean et al., 2011b).

Prominent and abrupt drops in OM values characterized the peat deposition after 3500 yr BP (Fig. 3.5). The values never drop below 50%, and always return to a baseline value of around 90% soon after, indicating that the bog environment went quickly back to normal peat formation, before the next minerogenic event occurred. If the mechanism for these isolated events is increased precipitation and subsequent inundation of the bog during Iezerul Sureanu Lake highstands, it would parallel the signal seen within local (Buczkó et al., 2013) and regional records (Cristea et al., 2013; Drăguşin et al., 2014; Gałka et al., 2016; Lotter and Birks, 2003; Magyari et al., 2009; Onac et al., 2015; Schnitchen et al., 2006). Alongside the appearance of detrital events, a rise in hydrophilic taxa (*Sphagnum* in particular) is observed as a reaction to this regional precipitation increase. Additionally, the charcoal record indicates a period of extremely low fire activity between 4000–2500 yr BP, which could also be the result of increased precipitation that limited biomass ignition. Prior

to this, regional fire activity was higher, but with large fluctuations in amount of charcoal deposited (Fig. 3.5) and so the onset of this low fire regime appears to be controlled by regional precipitation.

The period of wetness implied by the low fire regime is followed in the pollen record by an increase in *Alnus* and *Quercus* and a further decrease in the previously dominant *Picea* between 2500–2000 yr BP, indicating a decrease in conifer forests, as documented regionally (e.g. Finsinger et al., 2016), in response to local warming (Toth et al., 2015). The major shift away from a boreal forest to a more deciduous one, and in particular, the replacement of *Picea* with *Fagus* is a trend recorded in various other local and regional vegetation studies (Tanțău et al., 2006; 2011; Feurdean 2005; Feurdean et al., 2009, 2011, 2015; Magyari et al., 2009). Alongside this, the disappearance of *Dryopteris* - ferns typically found in the understory of dense forest appears to indicate a regional decline in forest cover. Alternatively, this may be related to a change in preservation conditions, resulting in the identification of *Dryopteris* spores as undifferentiated monolete spores (See Fig. 3.6).

After 2200 yr BP there is an increase in lithogenic elements, indicating higher mineral input, potentially as a result of enhanced local erosion, linked to precipitation-controlled weathering, a process that reduced tree coverage would exaggerate. In the Retezat Mountains, a temperature rise is observed at 2200 yr BP (Tóth et al., 2015), and it is therefore possible this ongoing change in vegetation (toward a more deciduous forest) could reflect the impact of the so-called Roman climatic optimum, a period of warm and dry conditions in the region (Büntgen et al., 2011). In addition to natural changes, warmer temperatures would allow increasing human use of uplands, for pasturing, thereby reducing forest cover, and increasing erosion. Furthermore the charcoal increase from 2500 yr BP onward may be linked to such increased human activity on the high mountain environments of Sureanu (Finsinger et al., 2016).

After 2500 yr BP, the minerogenic depositional events become more frequent and pronounced, becoming particularly regular after 1500 yr BP (Fig. 3.5). Much of the early part of this period corresponds to the MWP, with generally warm conditions seen in the Northern Hemisphere (Christiansen and Ljungqvist, 2012). Locally, the MWP is characterised by an increase in wetness (Feurdean et al., 2015). However, it is not reflected in the July temperature reconstruction from tree rings as presented by Popa and Kern (2009). At Sureanu, the period between 1150–850 yr BP is characterized by large-scale

mass wasting, with a large number of low OM events. As discussed earlier, a precipitation increase would increase weathering rates, and it is possible events through this period are associated with major rainfall leading to large-scale slope erosion, and flooding of the lake adjacent to Sureanu bog. This may be equivalent to an episode of intensified erosion signal seen within Sf Ana Lake in the Eastern Carpathians (Magyari et al., 2009), interpreted as a reflection of deforested slopes in the area.

A short period of normal peat growth follows, before the most pronounced period of minerogenic deposition between 350–100 yr BP. The initiation of this period of intense minerogenic deposition is closely correlated with the onset of the LIA (Mann et al., 2009) which is generally associated with cooler climate (Bradley and Jonest, 1993; McGregor et al., 2015). Regional palaeoclimate reconstructions indicate the initiation of this period at around 300 yr BP (Popa and Kern, 2009; Feurdean et al., 2015) (Fig. 3.5). The OM signal drops at almost exactly the same time, suggesting that the increased deposition of clastic material within the bog is associated with regional climate forcing. Increased erosion during the LIA has been observed in a number of places, from the Alps (Arnaud et al., 2012; Wilhelm et al., 2013, 2012) to mardels in Luxembourg (Slotboom and van Mourik, 2015), but not documented in the Carpathians before. The signal seen here therefore may be attributed to the cooler and wetter climate causing increased rainfall in summer and snow avalanches events in winter period. Other local studies do not define well the extent to which the LIA had an impact on the area. Pollen data for this time also do not indicate a clear shift in vegetation, echoing other vegetation and other palynomorph records, which generally indicate no specific signal (Tanţău et al., 2011; Buczkó et al., 2013; Tóth et al., 2015). Additionally, available speleothem isotopic proxies have too low a resolution to discern LIA-related changes (Onac et al., 2002; Drăguşin et al., 2014). A clear drying is indicated via testate amoebae (Schnitchen et al., 2006), and diatoms (Buczkó et al., 2013) but this drying does not appear to be specific to the LIA as in both cases it does not cease with the end of the period. Therefore, this may be the first clear indication of the impact the LIA had on the Sureanu bog record: a period of intense minerogenic deposition, from runoff-sourced erosion and lake flooding denoting increased precipitation rates.

3.4.4. Human Impact

Until 3650 yr BP human impact at the site appears minimal, with only sporadic *Plantago* (from 6200 yr BP onwards) and Poaceae (present from the base of the core) pollen indicating anthropogenic influence via deforestation. Indeed, it is plausible that humans had begun to clear forests for agriculture more regionally (Schumacher et al., 2016), but

not necessarily in the local environment, although the alpine environments in the Carpathians are to the current day heavily exploited for pasturing. Additionally, as the climate during this period appears fairly humid, high charcoal values (Fig. 3.5) could be an indication of man-driven, regional biomass burning. Human impact has been observed via the appearance of grass and crop taxa as far back as 8000 yr BP in the eastern Carpathians (Feurdean, 2005; Fărcaş et al., 2013) and 7500 yr BP in the nearby Transylvanian Depression (Tanțău et al., 2006), so it is possible these are the first hints at pasturing activities proximal to the site. However, it is unlikely humans had much of an impact through this period at Sureanu.

At 4200 yr BP, a large decrease in pollen concentration occurring at the same time as the first drop in *Picea* abundances, corresponds to the onset of the Middle Bronze Age in Romania (Bailey, 2000). This is somewhat earlier than most regional studies place the first major impact of humans in the region, with 3200 yr BP being typical in the Romanian Carpathians (Tantau et al., 2003; Feurdean et al., 2010; Tanţău et al., 2011). Due to the location of Sureanu bog near the upper edge of the treeline, it is possible that this site is more sensitive in recording traces of early small-scale deforestation than these other sites. At this time, the local Wittenberg and Verbicioara cultures are both known to have developed copper extraction and smelting (Gimbutas, 1965; Gogâltan, 1995), which would have required exploitation of other natural resources, including timber. This anthropogenic disturbance occurs concurrently with the climatic forcing previously mentioned.

The second decrease in *Picea* after 2900 yr BP (Fig. 3.6), is not seen in many other regional vegetation reconstructions, with *Picea* percentages remaining fairly stable after an initial drop at around 3000–4000 yr BP (Feurdean et al., 2011b; Tanţău et al., 2011). The use of *Picea* timber for building, and of denser wood like *Carpinus* and *Fagus* as fuel for metal smelting in the area (with the northern valleys draining Sureanu Mountains particularly rich in gold placers and tin) may explain these shifts, and potentially the disappearance of *Carpinus* and the drop of *Fagus* at this time. This initial drop is followed by further reductions in *Picea* abundances, (between 2900–2000 yr BP). It is possible this is related to climatic change, but it correlates well with the advance of Late Bronze Age and Dacian people, and the growth of their economy, based mainly on the mineral resources of the Carpathians, particularly gold, silver and iron (Anthony and Chi, 2009; Mountain, 1998) and also extensive agriculture. A strong human influence is expected at Sureanu as the Dacian capital, Sarmizegetusa Regia (a well-known centre for metal smelting in Antiquity), was established 15km to the west around 2200 yr BP at 1030 m

a.s.l (Oltean, 2007). This may also be inferred from the charcoal record, indicating a large shift at around 2900 yr BP from extremely low values to much higher levels which characterise most of the last 2000 years. The relatively stable climate over this period (Onac et al., 2002; Schnitchen et al., 2006; Buczkó et al., 2013) provide additional support for the anthropogenic influence on the observed changes in vegetation.

Soon after, the first large perturbations in the OM record occur, dated between 2200–1800 yr BP. This was a period of great upheaval in the history of the region, with the establishment of the Dacian Kingdom, with the nearby Sarmizegetusa Regia as its capital and part of a network of fortresses and high-altitude settlements encompassing the Sureanu Mountains on all sides, followed by the Trajan wars with Rome (AD101–106), and subsequent incorporation of Dacia into the Roman Empire (Bailey, 2000; Gudea, 1979). These large fluctuations in the OM record could be an indication of the local impact war had on the region, presumably with large-scale tree felling for weaponry and defences common (Hughes and Thirgood, 1982). Additionally, the charcoal record indicates the prevalence of fire events through this period; it is likely that many of these fire events were not natural. The remains of a Roman military castrum located on Varful lui Patru at 2100 m altitude, in the vicinity of the Sureanu bog, further supports evidence for a strong human impact at the time, even at such high altitudes. The mass wasting events do not cease until the final 100 years of the record, so it is likely the local environment never recovered fully from the deforestation and impact humans inflicted upon the site area starting in the Antiquity period.

After the collapse of Roman Dacia, in AD 271, the charcoal content decreases, suggesting a peak at around AD 200 is potentially an indication of a shift of the economy of the region from primarily mining and metal production towards agriculture (Poulter, 2007), which persisted throughout the Middle Ages. These pastoral communities are unlikely to have produced the same scale of clear-felling as major Roman or Dacian activity, and may explain the reduction in fire events throughout this period, and the relatively stable vegetation assemblage of the last 1800 years. The appearance of the first unequivocal agriculture-related *Cerealia* at 1400 yr BP confirms this shift toward widespread farming.

The pollen record for the final 500 years indicates the clearest human impact, with increased *Cerealia*, *Plantago*, Poaceae and other herb taxa (Fig. 3.6). This increase is particularly noticeable in the last 200 years, an indication of major forest clearance in the region, as noticed in many other regional studies (e.g. Feurdean et al., 2008; Tanţău et al.,

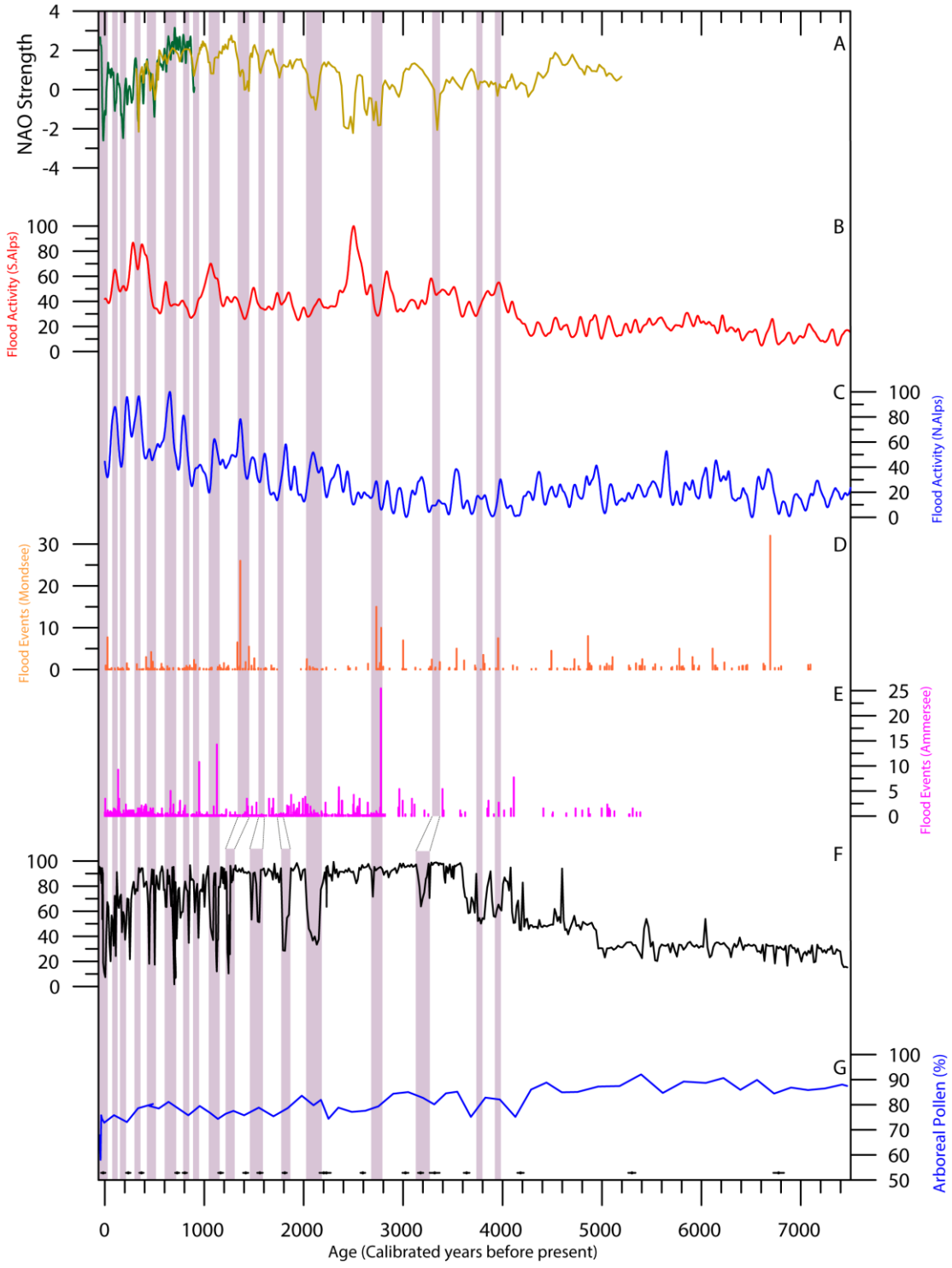

Figure 3.9: *Comparison of Sureanu minerogenic deposition record to mid-to-late Holocene climate forcing and records of palaeoflooding. Periods of low North Atlantic Oscillation (NAO) index and high minerogenic deposition are highlighted in purple, with correlations within radiocarbon dating uncertainty indicated using dashed lines. A: NAO Index as reconstructed by Trouet et al., (2009) in green and Olsen et al., (2012)in orange. Flood activity in the southern (B) and northern (C) Alps from Wirth et al. (2013); D: Flood events as indicated by Mondsee sediments (Swierczynski et al., 2013). .E: Flood events as indicated by Ammersee sediments (Czymzik et al., 2013); F) Sureanu organic matter record and G: Arboreal pollen (AP) percentages from Sureanu. Radiocarbon dates and uncertainties are indicated at the base of the graph.*

2011). The most recent section of the core (50 yr BP to present) indicates no clear minerogenic events (Fig. 3.5). The increase in temperatures seen over the last five decades has had a negative impact on the amount of snow in the region (Birsan and Dumitrescu, 2014) with an overall decreasing precipitation trend over the period. It is likely the reduced snowfall has led to a decrease in the number of avalanches and sudden snow-melt events, as, despite other causes, the primary controlling factor on mass wasting is still the amount of snow (Esteban et al., 2005). The warmer summers of this period (Popa and Kern, 2009) appear to have had no effect on the number of summer rainfall events. Additionally, regional reconstructions indicate clear drying throughout this time period (Schnitchen et al., 2006), explaining the cessation of mass wasting processes. The correlation of mass wasting ceasing and reduced winter snowfall indicates the likelihood that the main driving force behind the mass wasting processes around Sureanu bog is snow availability.

3.4.5. Comparison With Other Records of Palaeohydrology and Flooding

As it appears that the primary controller of the minerogenic deposition in this environment is precipitation-related mass wasting, with occasional lake flooding events, the flooding signal as reconstructed using the Sureanu record is compared with other palaeohydrological and flooding reconstructions (Fig. 3.9). As there are no such reconstructions from south-eastern Europe, comparison is made to a selection of central European records.

Within Sureanu bog flood layers appear to be rare prior to around 2000 yr BP. This sporadic flooding is similar to that which is observed in the Ammersee (Germany), the Mondsee (Germany) and Polish rivers at a similar time, with small, intermittent flood layers common in all sites (Czymzik et al., 2013; Starkel et al., 2006; Swierczynski et al., 2013). Clear intensification of the number of flood events is present from 2800 yr BP onwards in the Ammersee, 2000 yr BP in Poland and after 1500 yr BP in the Mondsee. Within Sureanu, this intensification may be seen at either 2000 yr BP (Figs. 3.5, 3.9), when the first large minerogenic input occurs, or at 1350 yr BP, when the onset of nearly constant deposition minerogenic is clearly documented. The central European flood records both ascribe the intensification to human activity and the effect deforestation had on the source area. The Sureanu pollen record shows that the major drop in tree taxa, and inferred deforestation earlier, roughly 3000 yr BP (Figs. 3.5, 3.6), and so it is sensible to assume the onset of minerogenic depositional events has presumably been mediated mainly by climatic factors.

After 2000 yr BP specific periods of enhanced flooding may be correlated to other records, with flood activity in the southern Alps appearing to show the same period of intense flooding between 1200 and 900 yr BP, and short-term fluctuations thereafter (Arnaud et al., 2012; Wirth et al., 2013). In addition, a clear correlation between minerogenic deposition in Sureanu and high flooding in the Alps may be seen between 500–50 yr BP, during the LIA. The correlation here is very good, with all records showing the initial intensification at 500 yr BP, a short period of less intense flooding, then a further increase before a drop at 50 yr BP (Fig. 3.9). Clearly the climatic controls between the two areas during the LIA are rather similar.

The flood records of the northern and southern Alps are interpreted by Wirth et al. (2013) to be indicative of fluctuations in the NAO. Due to the location of Sureanu, at the far eastern edge of Atlantic-influenced area, small shifts in the strength of the NAO should be also detectable in the bog record. Indeed, it appears many periods of intense flooding do correlate to periods of weakened NAO (Fig. 3.9). When the NAO is weaker, Mediterranean air masses become more dominant, with extreme summer rainfall in the Carpathians as a result of low pressure systems forming to the south of the site (Parajka et al., 2010). In Romania, a positive (negative) NAO index is associated with negative (positive) precipitation anomalies (Bojariu and Paliu 2001; see Fig. 2.1.C) and reductions in snowfall (Birsan and Dumitrescu, 2014).

Within the Sureanu record, and particularly the past 1500 years, flooding periods fluctuate in time with relatively small decreases in the NAO intensity. This is indicative of the sensitivity of the area to climatic fluctuations, in accordance with model predictions of sensitivity in this location and altitude (Bojariu and Giorgi, 2005) and the first demonstration of such a connection in this area over the late Holocene. Such an impact has been seen in the Southern Balkans, with NAO-controlled palaeoenvironment fluctuations observed in Lake Butrint (Morellón et al., 2016), but not in the northern section, like the Carpathians. It is clear, however, that not all enhanced flooding periods may be attributable solely to NAO fluctuations (e.g. 1100–1050 and 900–850 yr BP). These are likely to be related to the interplay between the NAO and other major climatic systems in the area, and indicate that unlike the Alps, the NAO is not the only major forcing factor at play in the Carpathian – Lower Danube area, and that its influence is periodically weakened; indeed it appears the eastern edge of dominant NAO influence is found at around 30°E (Krichak et al., 2002).

Signal from more than one major SLP pattern is to be expected, with sites to the south-east, including Lake Nar (Turkey) (Jones et al., 2006), Soreq (Bar-Matthews et al., 1997) and the Dead Sea (Migowski et al., 2006) showing no NAO-related connectivity, whilst sites further west show clear correlations (e.g. Wirth et al., 2013). The record therefore indicates the decreasing impact of the NAO on climate as one moves from western Europe east through to Eurasia. Furthermore, it provides a long time series showing evidence of the east-west climate see-saw in the Mediterranean (Magny et al., 2013; Roberts et al., 2012), with the reducing influence of the NAO being one of the major drivers behind it.

3.5. Conclusions

Using pollen alongside sedimentological and geochemical methods from a peatbog in the Southern Carpathians a regional record of the depositional environment and palaeoclimate has been produced.

The main findings are:

1. Both natural climatic fluctuations and human impacts are clear in the vegetation record of the site. Between 7500–4500 yr BP, there was a slow shift from relatively warm mixed forest towards cooler, conifer-dominated forest after 5000 yr BP, relating to natural increases in warmth and humidity in the region. From 4500 yr BP, the impact of human activity may be seen, with decreasing forest cover, and evidence for agricultural (mainly pasturing) activities in the high-mountain environment of Sureanu Mountains (from 3300 yr BP onward), alongside an inferred warming evidenced by the increase in deciduous taxa. This correlates with the onset of major agriculture in the region, and develops in time with shifts in local economy and development.
2. A record of minerogenic deposition is presented, likely forced by changes in hydroclimate, the first of its kind in this region. Sources of debris have been identified using grain size analysis, indicating input from periods of lake highstands, but with precipitation-related mass wasting being the main control. In addition, the Rb/Sr ratio has been utilised for the first time to determine depositional events within an organic-rich core, although the methods need further validation.
3. Particularly intense minerogenic deposition is observed during the Medieval Warm Period and the Little Ice Age, the first such indication of the effect these periods had in palaeoenvironmental records from the Carpathians. Warm and

dry conditions over the last 50 years have led to a cessation of mass wasting in the local environment, indicating the reduction in precipitation and snow coverage is a major driver in the control of erosion in this region.

4. A teleconnection with major atmospheric circulation patterns is inferred, as most fluctuations in flooding correlate to decreased NAO index values. This shows for the first time the long-term impact of the NAO in this region, which has previously only been predicted through modelling.

Chapter 4. Periodic input of dust over the Eastern Carpathians during the Holocene linked with Saharan desertification and human impact

4.1. Introduction

Atmospheric dust plays a major role in oceanic and lacustrine biogeochemistry and productivity (Jickells, 2005) by providing macronutrients to these systems (Mahowald et al., 2010). Furthermore, climatically dust plays a role in forcing precipitation (Ramanathan, 2001; Yoshioka et al., 2007) and in moderating incoming solar radiation. As such, reconstructions of past dust flux are an important tool to understand Holocene climate variability, biogeochemical cycles, and the planet's feedback to future changes in atmospheric dust loading.

The link between atmospheric circulation patterns and dust input has been studied intensively (Allan et al., 2013a; Kylander et al., 2013a; Le Roux et al., 2012; Marx et al., 2009) with clear evidence of climate variations linked with the dust cycle (Goudie and Middleton, 2006). Generally, dust is produced in arid zones (Grousset and Biscaye, 2005) and may be transported thousands of miles before deposition (Grousset et al., 2003). In addition, dust input into the atmosphere can increase significantly during droughts (e.g. Miao et al., 2007; Notaro et al., 2015; Sharifi et al., 2015). As such, fluctuations in dust loading may be indicative of both regional drying and long-distance transport (Le Roux et al., 2012).

Hydroclimatic fluctuations had a significant effect on the development of civilisations throughout the Holocene (Brooks, 2006; deMenocal and Peter, 2001; Sharifi et al., 2015), especially on those which relied heavily on agriculture and pastoralism, as was the case in the Carpathian-Balkan region (Schumacher et al., 2016). To understand the impact hydroclimatic changes had on the population of an area of such importance to European history, high-resolution palaeoclimate and palaeohydrological records are needed. This is especially important in the Carpathian region, given the extensive loess cover in the area (Marković et al., 2015) - a fundamental factor in sustaining high agricultural production. Additionally, the sensitivity of loess to moisture availability and water stress during dry periods may turn this region and other surrounding loess belts into major dust sources (Kok et al., 2014; Rousseau et al., 2014; Sweeney and Mason, 2013). This is particularly true under semi-arid (Edri et al., 2016), or agriculturally-altered conditions (Korcz et al., 2009), as is the case with the major dust fields of eastern Eurasia (Buggle et al., 2009; Smalley et

al., 2011; Újvári et al., 2012). Thus, the dust influx into the Carpathian-Balkan region should be extremely sensitive to relatively small changes in precipitation rates. This hydroclimatic sensitivity is enhanced due to the fact that the Carpathians and the surrounding lowlands are located at a confluence of three major atmospheric systems; the North Atlantic, the Mediterranean and the Siberian High (Obreht et al., 2016). Indeed, research appears to indicate the climate in Romania is controlled, at least in part, by NAO fluctuations (Bojariu and Giorgi, 2005; Bojariu and Paliu, 2001) but it is yet unclear how this relationship evolved in the past (Haliuc et al., 2017).

This research provides a record of periodic dry and/or dusty periods in Eastern Europe as indicated by reconstructed dust input, using an ombrotrophic bog from the Romanian Carpathians (Figs. 2.2, 4.1). As the only source of clastic material deposited within ombrotrophic bogs is via atmospheric loading, such records have been used convincingly as archives of dust deposition over the Holocene in western Europe and Australia (Allan et al., 2013a; Kylander et al., 2013a; Le Roux et al., 2012; Marx et al., 2010, 2009).

The record covers 10,800 years of deposition over 9.5m of peat, providing a valuable high-resolution record for this region. This research utilises both organic and inorganic proxies, with a high-resolution geochemical record of lithogenic elements (Ti, Si, and K), presented alongside the bog surface wetness as reconstructed using testate amoeba to understand dust source changes and the link between regional and extra regional hydroclimate variability and dust.

4.2. Methods and Materials

850cm of peat was recovered from Mohos bog (25°55'E; 46°05'N; 1050m altitude, Figs. 2.1, 4.1). See Chapter 2 for further details on the site, and the coring strategy. In terms of analyses, LOI was performed on 425 discrete samples (2cm resolution), with ICP-OES analysis (of Ti, to allow for dust flux calculations) carried out on 105 samples. Micro-XRF core scanning via ITRAX was carried out on the entire record. A further 44 samples were taken for testate amoeba analysis. On the ITRAX data, ontinuous Morlet wavelet transform was used to identify non-stationary cyclicities in the data (Grinsted et al., 2004; Torrence and Compo, 1998). For this analysis, the lithogenic normalised elemental data from ITRAX measurements (Ti, K, and Si) was interpolated to equal time steps of four years using a Gaussian window of 12 years.

The age model for the Mohos peat record is based on 16 radiocarbon dates on bulk peat (collected over less than 1cm depth interval per sample) consisting only of *Sphagnum* moss

remains (Table 4.1). These analyses were performed via Environ MICADAS accelerator mass spectrometry (AMS) at the Hertelendi Laboratory of Environmental Studies (HEKAL), Debrecen, Hungary, using the methodology outlined in Molnár et al. (2013). An outline of the age model development may be found in Chapter 3.

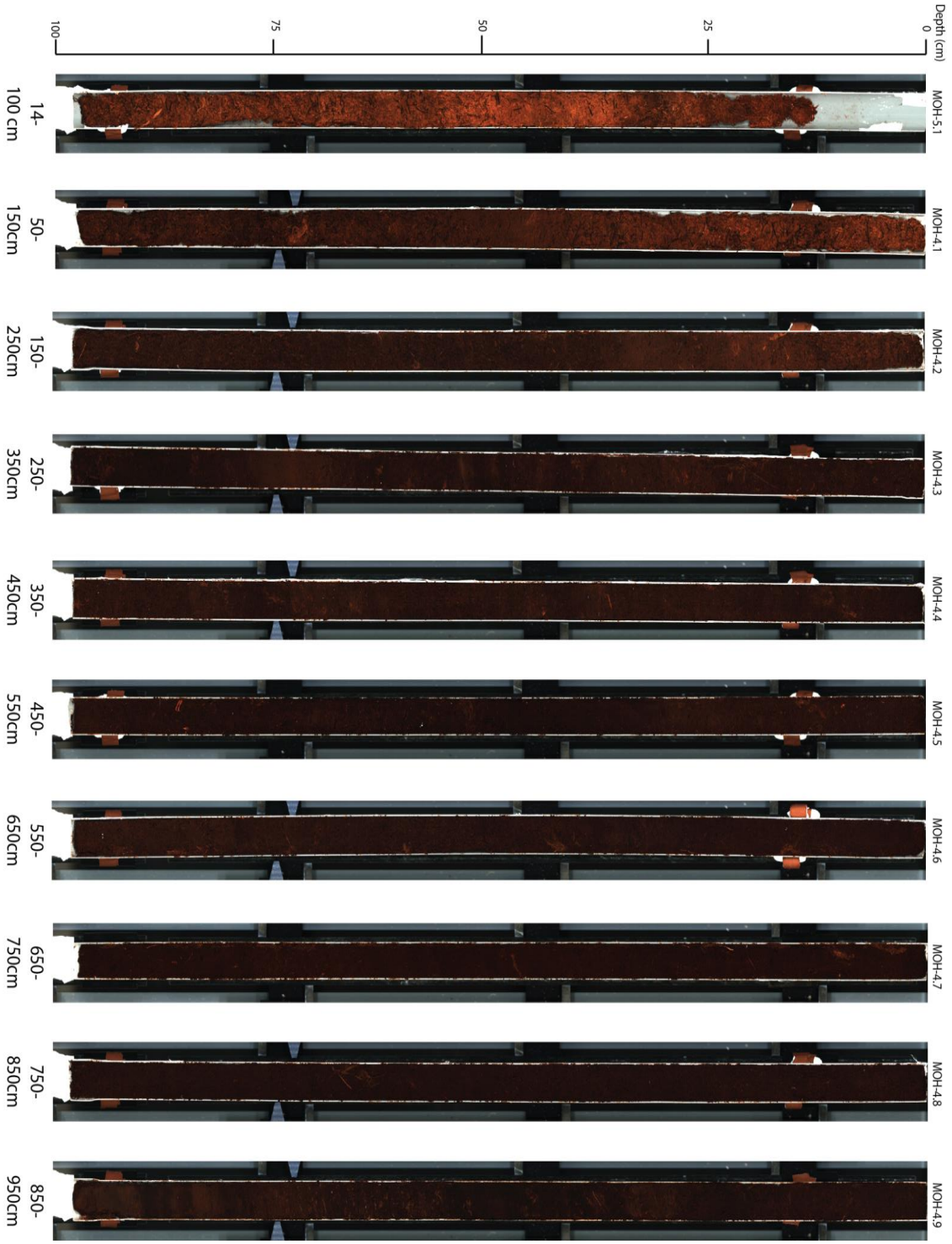

Figure 4.1: *Images of Mohos core, indicating the organic-rich nature of the sediment for the entirety of the 950cm-long core.*

Table 4.1: *Radiocarbon dates used to build the age model for Mohos peat record.*

Lab ID	Depth	^{14}C age (yr BP ± 1σ)	Calibrated age (cal yr BP ± 2σ)	Dated material
DeA-8343	50	**37±18**	37-65	bulk peat
DeA-8344	100	**838±19**	700-785	bulk peat
DeA-10111	150	**1174±28**	1049-1179	bulk peat
DeA-10112	175	**1471±26**	1309-1399	bulk peat
DeA-8345	200	**2022±21**	1921-2007	bulk peat
DeA-10137	225	**2155±27**	2048-2305	bulk peat
DeA-10138	280	**2530±28**	2495-2744	bulk peat
DeA-8346	300	**3112±23**	3249-3383	bulk peat
DeA-10139	350	**4110±31**	4523-4713	bulk peat
DeA-10140	380	**4641±54**	5282-5484	bulk peat
DeA-8347	400	**4638±26**	5372-5463	bulk peat
DeA-10141	500	**5949±36**	6677-6861	bulk peat
DeA-10142	600	**6989±43**	7785-7867	bulk peat
DeA-8348	700	**7909±33**	8600-8793	bulk peat
DeA-10143	800	**8687±45**	9539-9778	bulk peat
DeA-8349	900	**9273±36**	10369-10571	bulk peat

4.3. Results

4.3.1. Age Model and Lithology

The Mohos peat profile is 950 cm long (Fig. 4.1, 4.2), and reaches the transition to the underlying basal limnic clay (Tanţău et al., 2003). Between 950–890cm the record is composed of organic detritus (gyttja) and *Carex* peat deposited prior to the transition from a wetland into a bog, at roughly 10,330 yr BP. From 890cm upwards, the core is primarily *Sphagnum*-dominated peat (Fig. 4.3). The age-depth model (Fig.4.3) indicates the Mohos peat record covers almost 10,800 years of deposition, with the uppermost layer (growing moss) of the peat dating to 2014. Age model uncertainties range from 20 years in the uppermost sections to 150 years at the base of the core. Thus, the resolution for ITRAX data average ~5yr/sample and for ICP-OES roughly 100 yr/sample. The testate amoeba resolution is roughly 200 yr/sample. In the following, all quoted ages are given in calibrated years before present (cal yr BP).

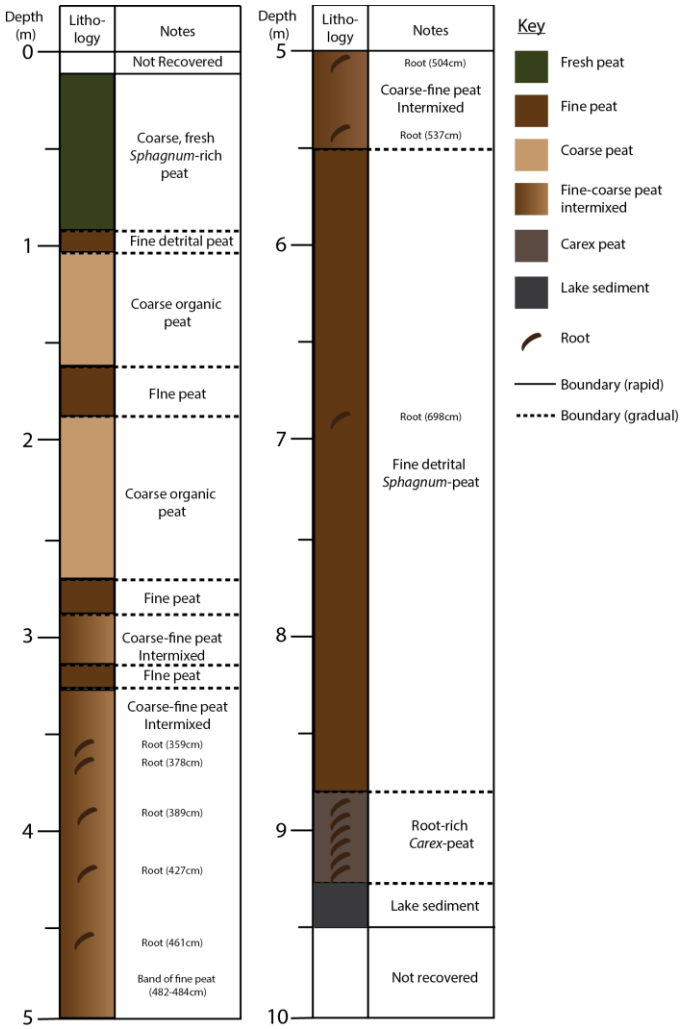

Figure 4.2: *Lithological description of Mohos core*

4.3.2. Dust indicators

4.3.2.1. Ti, K, and Si

Similar trends for the lithogenic elements Ti, and Si, and the mobile element K, are visible in the record (Fig. 4.4), with 10 main zones of higher counts above typical background values present. Such zones are identified as an increase in two or more of the elements above the background deposition (K > 0.001, Si > 0.001 and Ti > 0.004, see dashed line on Fig. 4.4).

These intervals are further discussed as reflecting major dust deposition events, and are referenced in the remainder of the text using the denotation D01-D10 (Fig. 4.4). Two exceptions, at the base of the core, close to the transition from lake to bog, and the last 1000 years, due to high noise, are not highlighted. The lithogenic, and therefore soil and rock derived Ti and Si have previously been used as proxies for dust input (e.g. Allan et al., 2013a; Sharifi et al., 2015), whilst K covaries with Si (R^2=0.9945) and so controlling factors on their deposition must be similar. For these elements, the periods with inferred non-dust deposition are characterised by values approaching the detection limit (150, 15 and 40 cps, respectively). A short period of very high values for all elements (10,000, 1300 and 8000 cps, respectively) is observed between 10,800-10,500 cal yr BP (not shown on diagram), reflecting the deposition of clastic sediments within the transition from lake to bog at the onset of the Holocene. Zones of elevated values (D1-D5), with average cps values roughly Ti=300, Si=30 and K=100 persisting for several centuries each, occur sporadically throughout the next 6000 years of the record, between 9500–9200, 8400–8100, 7720–7250, 6350–5900 and 5450–5050 cal yr BP (Fig. 4.4). Similarly long periods, but with much higher element counts (Ti=800, Si=60 and K=200 cps) occur

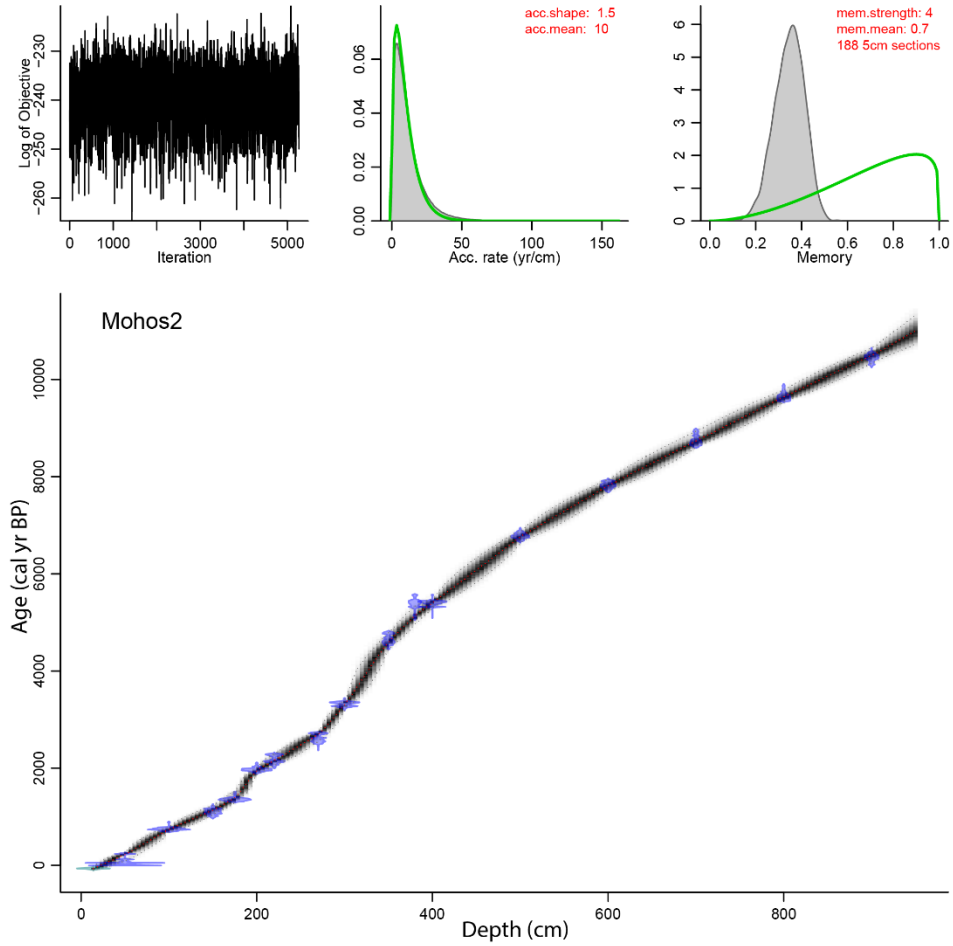

Figure 4.3: *Age-depth model of Mohos peat record, as determined via Bacon (Blaauw and Christen, 2011). Upper left graph indicates Markov Chain Monte Carlo iterations. Also on the upper panel are prior (green line) and posterior (grey histogram) distributions for the accumulation rate (middle) and memory (right). For the lower panel, calibrated radiocarbon ages are in blue. The age-depth model is outlined in grey, with darker grey indicating more likely calendar ages. Grey stippled lines show 95% confidence intervals, and the red curve indicates the single 'best' model used in this work.*

between 4130–3770, 3450–2850 and 2000–1450 cal yr BP (D6-8). Two final, short (roughly 100-year duration) but relatively large peaks (D9–10) may be seen in the last 1000 years, between 800–620 cal yr BP (with values Ti=300, Si=40 and K=100 cps) and 75 cal yr BP to present (Ti=300, Si=80 and K=400 cps, respectively).

4.3.2.2. Dust Flux

Using the quantitative ICP-OES values of Ti (in ppm) and PAR, the dust flux can be calculated (Fig. 4.4). The ICP-OES Ti record shows very good correlation with the Ti data derived through ITRAX analysis (Fig. 4.5). To facilitate comparison, both records are brought on to the same timescale using a Gaussian interpolation with 100 year time steps and a 300 year window. Pearson's r=0.2649, with a p-value of <0.001, indicative of a significant correlation. This further indicates the reliability of the XRF core scanning

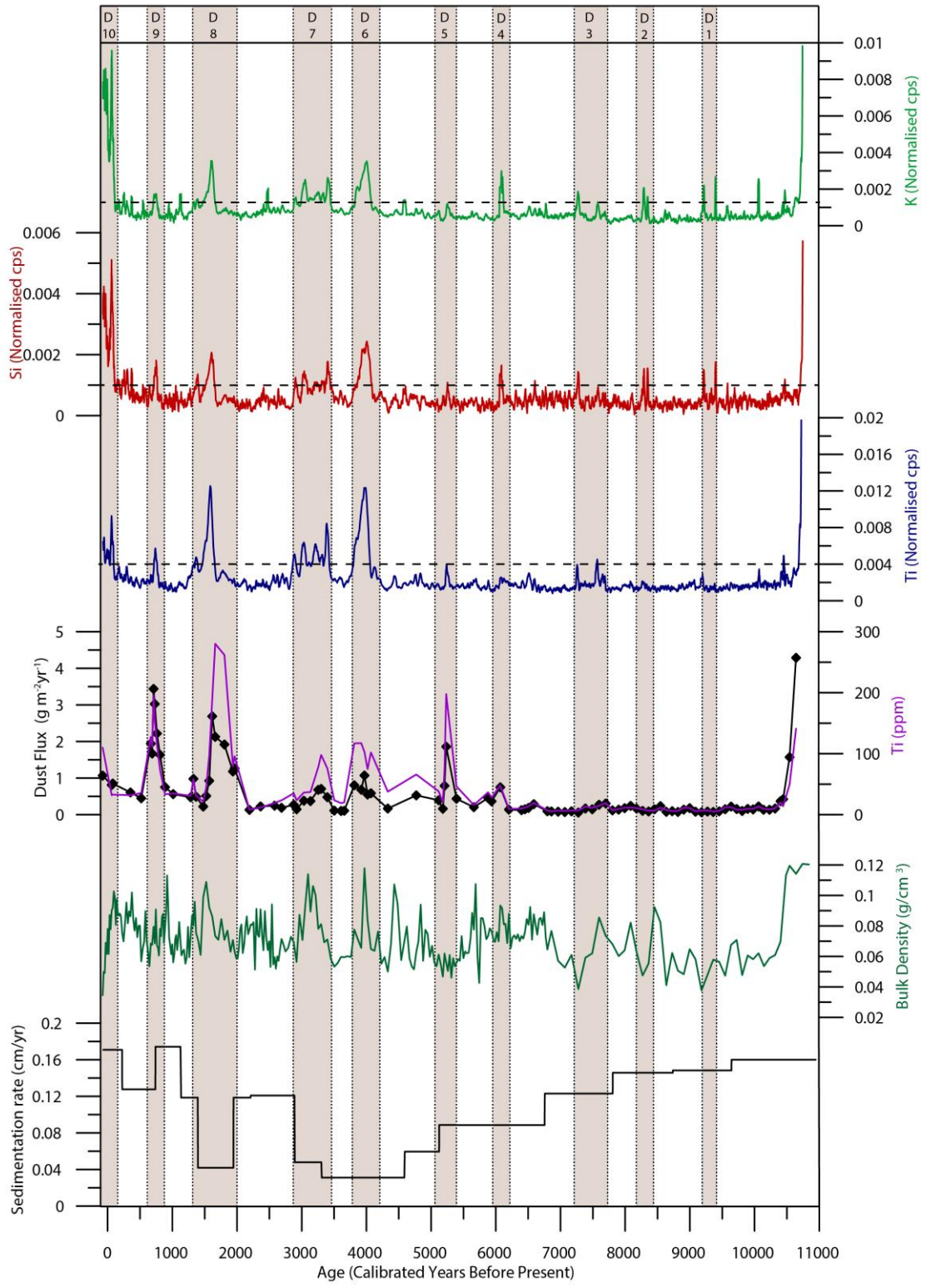

Figure 4.4: *ITRAX data of lithogenic elements (K, Si and Ti) concentration throughout the Mohos peat record, with all data smoothed using a 9-point moving average to eliminate noise. Alongside, dust flux as reconstructed from Ti concentration values (also displayed), and sedimentation rate is presented. Dust events (D0–D10), as identified from increases in at least two of the lithogenic elements under discussion, are highlighted in brown. Dashed lines on ITRAX data indicate the enrichment above which a dust event is denoted.*

method even for such highly organic sediments (as already suggested by Poto et al., 2014), and validates its usage as proxy for deriving dust flux (Figs. 4.4, 4.5).

It must be noted here that using Ti alone in dust flux calculations does not allow for reconstruction of all minerals related to dust deposition. Ti, which is lithogenic and conservative, is a major component in soil dust, particularly within clay minerals (Shotyk et al., 2002), but may not be associated with other dust-forming minerals, including phosphates, plagioclase and silicates (Kylander et al., 2016), although the records of K and Si may help indicate changes in deposition rates of these minerals (See Mayewski and Maasch, 2006). As a result, specific mineral-related changes may not be observed regarding the composition of dust. However, Ti alone will record changes in the intensity of deposition of the main dust-forming minerals (Sharifi et al., 2015; Shotyk et al., 2002), and variations in K and Si (particularly with local K- and Si-rich dacites a possible dust source) may further indicate the influx of minerals which are not associated with Ti. Such an approach has been applied successfully to studies of changing dust influx (e.g. Allan et al., 2013a; Sapkota et al., 2007; Sharifi et al., 2015), with each study able to identify periods of high and low dust deposition from Ti-derived dust flux alone.

The Ti-derived dust flux for most the record is below 1 g $m^{-2}yr^{-1}$, but with seven periods of dust deposition clearly identifiable for the last 6100 years, and several smaller fluctuations prior to that (mainly visible in the elemental data). The main peaks are similar in their timing to the ITRAX Ti trend, with three large peaks (dust flux >1.5 g $m^{-2}yr^{-1}$) located between 5400–5050, 2100–1450 and 800–620 cal yr BP, respectively (Fig. 4.4). Smaller peaks are present (dust flux 0.5–1 g $m^{-2}yr^{-1}$) at 6100–6000, 4150–3770, and 3500–2850 cal yr BP, respectively.

4.3.3. Density and Loss-on-Ignition

Density values are relatively stable throughout the core, with all samples ranging between 0.06-0.1 g/cm^3. This trend is different from the OM values, which typically oscillate around 90–100% over the entire record. The very base of the record is however an exception, denoting the gradual transition from limnic clays to the peat reaching OM values of 80–90% between 10,800–10,000 cal yr BP. Very occasional intervals with lower organic matter content (roughly 85%) may be observed at 5400, 4100–3900, 3300–3200, 1900–1800 and 900–800 cal yr BP, respectively (Fig. 4.4).

4.3.4. Testate Amoeba

Two methods of clarifying the paleoclimate signal derived through investigating testate amoeba (TA) assemblages have been used (Charman et al., 2000; Schnitchen et al., 2006),

with both indicating similar hydroclimatic trends. Reconstructions of depth-to-water table (DWT) values indicate three main trends within the record. The first, encompasses the time period between 10,800–7000 cal yr BP, and is characterised by highly fluctuating values, with four very dry periods (DWT ~20 cm) at 10,800–10,200, 9000–8800, 8600–7600, and 7400–6600 cal yr BP interspersed by wetter (DWT 15 cm) conditions (Fig. 4.7). After 7000 cal yr BP, values are much more stable, with DWT of 15cm until the final zone, the last 100 years, where DWT rises to 20cm. These fluctuations are in line with those seen in the wet/dry indicator species.

4.3.5. Wavelet Analysis

The wavelet analysis of K, Si and Ti show significant periodicities between 1000–2000 years within the past 6000 years (Fig. 4.11). Prior to this, there appears to be no major cyclicity in the ITRAX data. Within periods which display raised ITRAX counts, shorter frequency (50–200 year) cycles are seen. These persist only for the period in which each element is enriched, with such cycles particularly evident within the last 6000 years.

4.4. Discussion

4.4.1. Peat ombrotrophy

The relative intensities of the lithogenic elements analysed via ITRAX covary throughout the record (Fig. 4.4), despite their varying post-depositional mobility (Francus et al., 2009; Kylander et al., 2011). For example, the largely immobile Ti shows a very high correlation with that of redox sensitive Fe (R^2 = 0.962) and mobile K (R^2 = 0.970). This indicates the downcore distribution of these elements is mostly unaffected by post-depositional mobilisation via groundwater leaching and/or organic activity as documented in other studies (e.g. Novak et al., 2011; Rothwell et al., 2010), indicating the conservative behaviour of such elements in the studied peat. This, alongside the low clastic content (average organic matter of 91%), low density and domination of *Sphagnum* organic detritus, indicates the ombrotrophic nature of Mohos bog throughout time and validate the use of this record to reconstruct dust fluxes for the last ca. 10,000 years (Fig. 4.4).

4.4.2. The Dust Record

The record of inferred lithogenic (dust) input as indicated by Ti, K and/or Si documents 10 well-constrained periods of major and abrupt dust deposition (denoted D0–D10), with further small, short-term fluctuations (Figs. 4.4, 4.6). The dust influx onto the Mohos peat was accompanied by decreases in organic matter (OM) as indicated from the LOI profile, and higher density values (Fig. 4.4), particularly over the intervals covered by events D5–

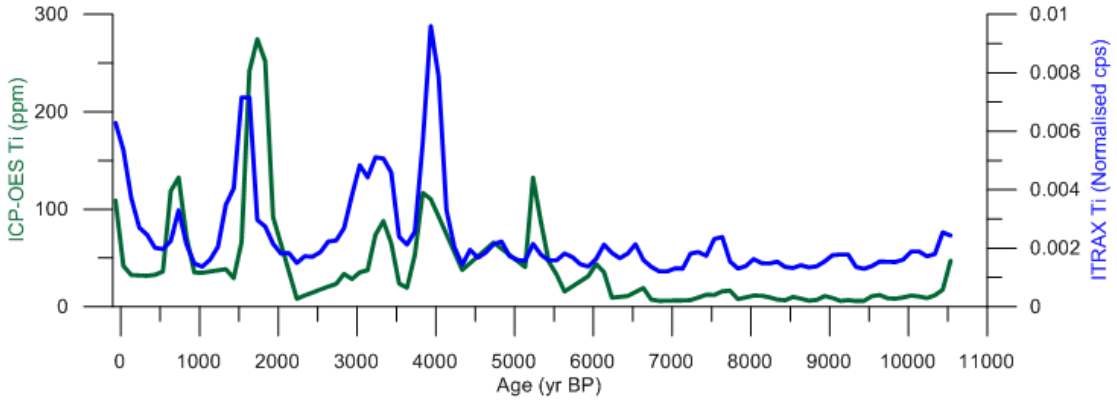

Figure 4.5: *Comparison graph of ICP-OES and ITRAX Ti data from Mohos core. To facilitate comparison, both data sets have been brought onto the same timescale via Gaussian interpolation at 100-year steps, using a 300-year window.*

D10. The major dust deposition events lasted from a few decades to centuries (Fig. 4.4, 4.6).

Firstly, it is noteworthy that five of the identified dust depositional events may be compared to periods of Rapid Climate Change (RCC) as outlined by Mayewski et al. (2004) from the Greenland GISP2 record (Fig. 4.8). However, despite apparent hemispheric-scale influences, the dust events identified within Mohos record have little correlation to reconstructed European paleoclimate changes during Holocene. For example, D8 between 3450-2800 cal yr BP falls Europe-wide cold period (Wanner et al., 2011). Such cold-related dust deposition has been observed previously in western Europe (Allan et al., 2013a; Le Roux et al., 2012). However, within Mohos such a compassion may not be drawn for the majority of dust events. For example, event D9 (860–650 cal yr BP) occurs during the MWP, a period of generally higher European temperatures (Mann et al., 2009) but also one of intense human impact on the environment through deforestation and agriculture (Arnaud et al., 2016; Kaplan et al., 2009). Furthermore, such events within the Misten record is Belgium (Fig. 4.8) (Allan et al., 2013a) were also linked to low humidity, whereas the Mohos TA (Fig. 4.7) record indicates locally wet conditions. This suggests that dust depositional events in this region are a result of a complex interplay of environmental conditions in the dust source areas, rather than simply reflecting locally warm or cold, or even wet or dry periods.

In addition to the North Atlantic, the impact of both the Mediterranean and the intertropical convergence zone (ITCZ) atmospheric systems influencing the Mohos dust record are apparent, including major climate changes in North Africa. D4 for example occurs within the chronological span of the 5900 cal yr BP event, a major cooling and drying period in Europe (Bond et al., 2001; Cremaschi and Zerboni, 2009; Shanahan et al., 2015). Increased

dust influx is also recorded around 5300 cal yr BP (D5, Fig. 4.4) which roughly correlates with the end of the African Humid Period and onset of Saharan desertification (deMenocal et al., 2000). The lack of dust flux perturbations prior to 6100 yr BP, and their prevalence thereafter at Mohos are consistent with a major shift in the controls of dust production and deposition at this time, a change observed in peat-derived dust records from western Europe (Allan et al., 2013a; Le Roux et al., 2012). The desertification of the Sahara around this time was the largest variation in dust production in the Northern Hemisphere (McGee et al., 2013; deMenocal et al., 2000).

Within the record, this initial dust flux increase was followed by a period of reduced dust loading, prior to a rapid, and apparently major event at 5400-5000 cal yr BP, displaying the highest dust flux values in the record prior to the most recent two millennia. Regionally, Saharan dust in Atlantic marine cores strongly increased at this time, with a 140% rise roughly at 5500 cal yr BP observed on the western Saharan margin (Adkins et al., 2006) with another study indicating a rise by a factor of 5 by 4900 cal yr BP in a selection of similarly-located sites (McGee et al., 2013). Furthermore, evidence from marine cores across the Mediterranean indicate decreasing Nile output and increasing dust fluxes into the eastern Mediterranean at this time (Box et al., 2011; Revel et al., 2010). The correlation of these data to the Mohos record appears indicative of the region-wide impact of North African desertification. It is noteworthy, as seen in Fig. 4.8, that the release of dust from the Sahara correlates well with increasing frequency and intensity of dust fluxes at Mohos after 6000 cal yr BP, with all major (dust flux >0.5 g $m^{-2}yr^{-1}$) Ti-derived dust flux peaks occurring after this time (Fig. 4.4). This record is the first indication of the impact the Mediterranean climate and movement of the ITCZ has had on the Carpathian-Balkan region (as simulated by Egerer et al. 2016 and Boos and Korty, 2016). Indeed, intermittent

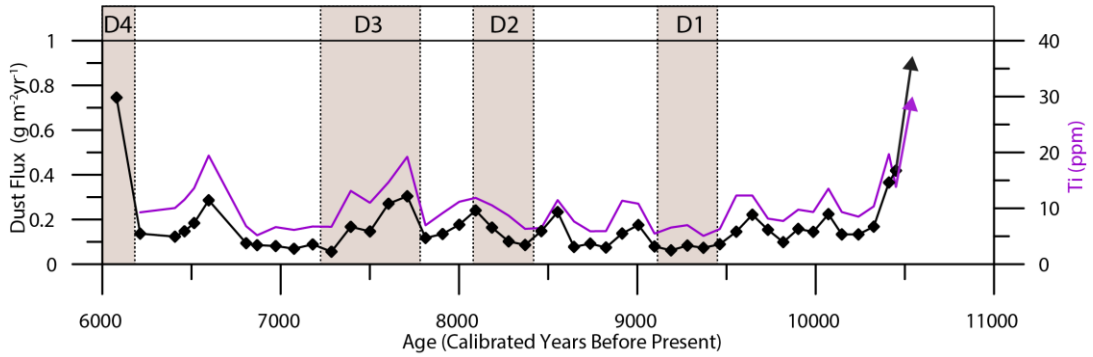

Figure 4.6: *Close-up of the dust flux and Ti ppm values for the period 10500–6000 yr BP. Also presented are dust events identified within this time, and highlighted in brown.*

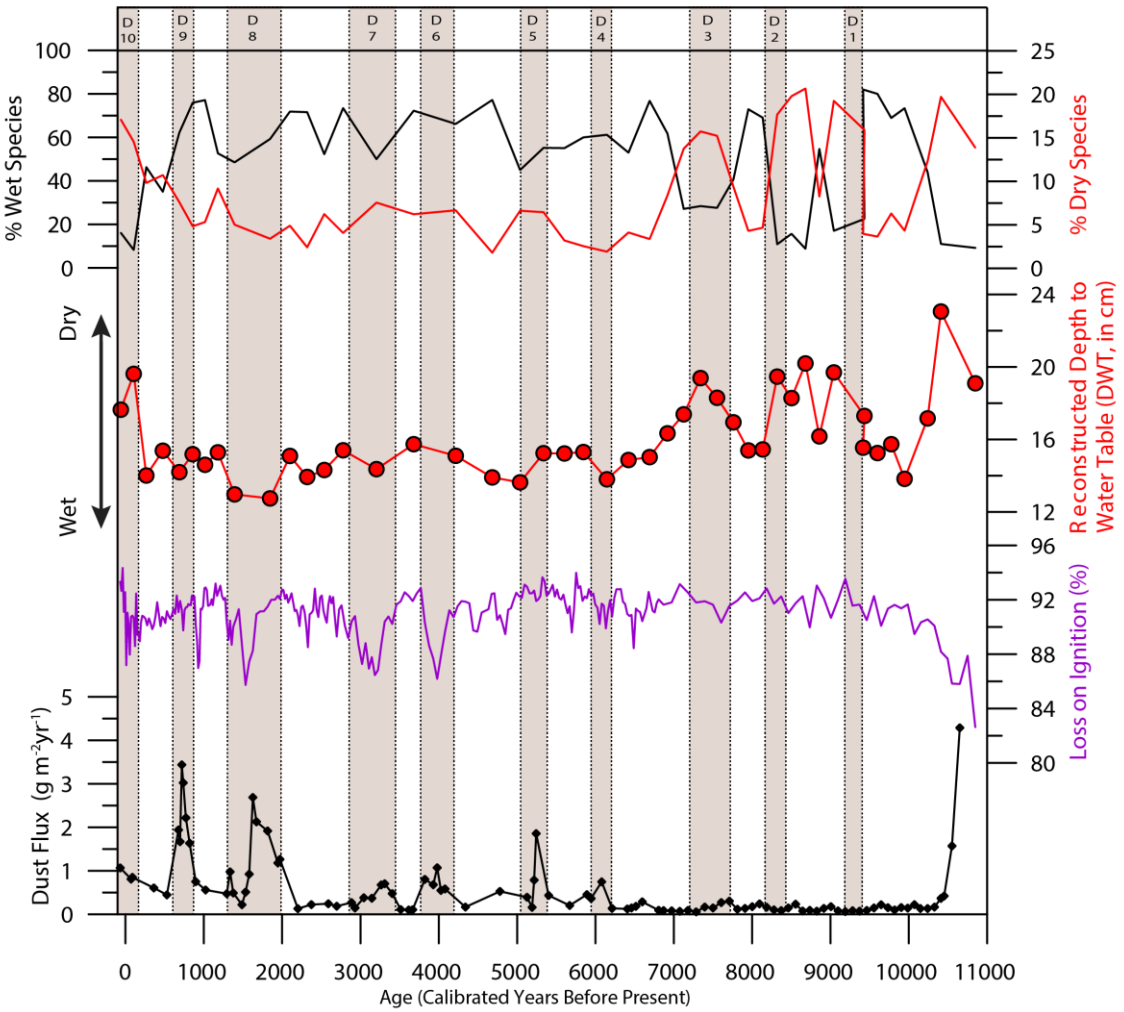

Figure 4.7: *Comparison of Ti-derived dust flux record with wet and dry Testate Amoeba (TA) indicator species percentage values, reconstructed Depth to Water Table (DWT) and organic matter (as indicated by Loss on Ignition). Vertical bars as in Figure 4.4.*

intrusions of Saharan dust over the Carpathian area have been well documented both through direct observations (Labzovskii et al., 2014; Varga et al., 2013), and through provenance studies of past Saharan dust contribution within interglacial soils in the region (Varga et al., 2016).

In addition to Saharan desertification, it is likely that early agriculture in the Carpathian-Balkan region contributed towards the increase in dust flux values at this time. It is known that advanced agriculture-based societies inhabited the Carpathian area in the mid-Holocene (Carozza et al., 2012), with evidence of farming seen in a number of pollen records (see Schumacher et al., 2016 for a compilation), including in Mohos itself at the end of the Chalcolithic period (Tanţău et al., 2003). Since agriculture and soil erosion may be linked, it is possible events D4 and D5 could also reflect to some extent dust input related to land disturbance by human activities, on a regional scale. However, such evidence for agriculture, particularly in the proximity of Mohos is limited to a few

Plantago and cereal pollen (Tanţău et al., 2003), whilst the majority of pollen studies in Romania at this time indicate no significant agricultural indicators (e.g. Magyari et al., 2010; Schumacher et al., 2016; Tanţău et al., 2014). As such, it seems unlikely agricultural activity is behind such a large change in the dust deposition record from Mohos.

4.4.3. Geochemical Evidence for a Dust Provenance Shift at 6100–6000 cal yr BP?

To better understand the nature of the shift in dust flux after 6100–6000 cal yr BP, a simple approach to disentangling the geochemical makeup of the reconstructed dust load is discussed below. Figure 4.9 displays the clustering of the lithogenic elements Ti and K (and Si, due to the similarity in the Si and K records) during dust events D1–D10. The data appear to show three main types of dust (and presumably sources), one with high values for both Ti and K (Type 1), one with relatively high values for K (Type 2), and one with relatively high Ti compared to K (Type 3). The values for Ti-K correlation, average Ti, and average K (in normalised cps) are listed in Table 2. Generally, the periods of no enrichment, and low K and Ti, do not show any correlation, indicative of natural background and instrumental detection limits.

Type 1 deposition occurs only in D10, and is characterised by Ti-K gradient of nearly 1, indicating similar values for both elements throughout the period, and a dust rich in both K and Ti. Type 2 deposition occurs in several dust events, particularly in D1–2, D4–5, and D7 (Fig. 4.9). The K enrichment which characterises these events is, evidenced by the Ti-K gradients <1 and low (even negative in the case of D2) correlations between the two elements. Finally, Type 3 events (D3, D6, and D8–9) are characterised by an increased Ti-K gradient, generally, around 0.2. The average Ti values during these events and the Ti-derived dust flux, are generally highest in these periods (Table 4.2). These groupings would indicate similar dust sources within grouped events, and may aid in identifying provenance.

Type 2 events typically occur in the older part of the record, except D7 (3400–3000 cal yr BP, Fig. 4.9). Such events are not visible in the Ti-derived dust flux values, indicative of the reduced impact of Ti-bearing dust particles deposited within the corresponding periods. The local rocks consist of K-rich dacites and pyroclastics (Szakács et al., 2015), with relatively low Ti concentrations and enriched in K (Vinkler et al., 2007). Therefore, the likely source of particulates deposited during these dust events is local or regional, with nearby (or even distal) loess and loess-like deposits as another potential source, since loess sediments in south-eastern Europe are generally depleted in Ti (Buggle et al., 2008). The

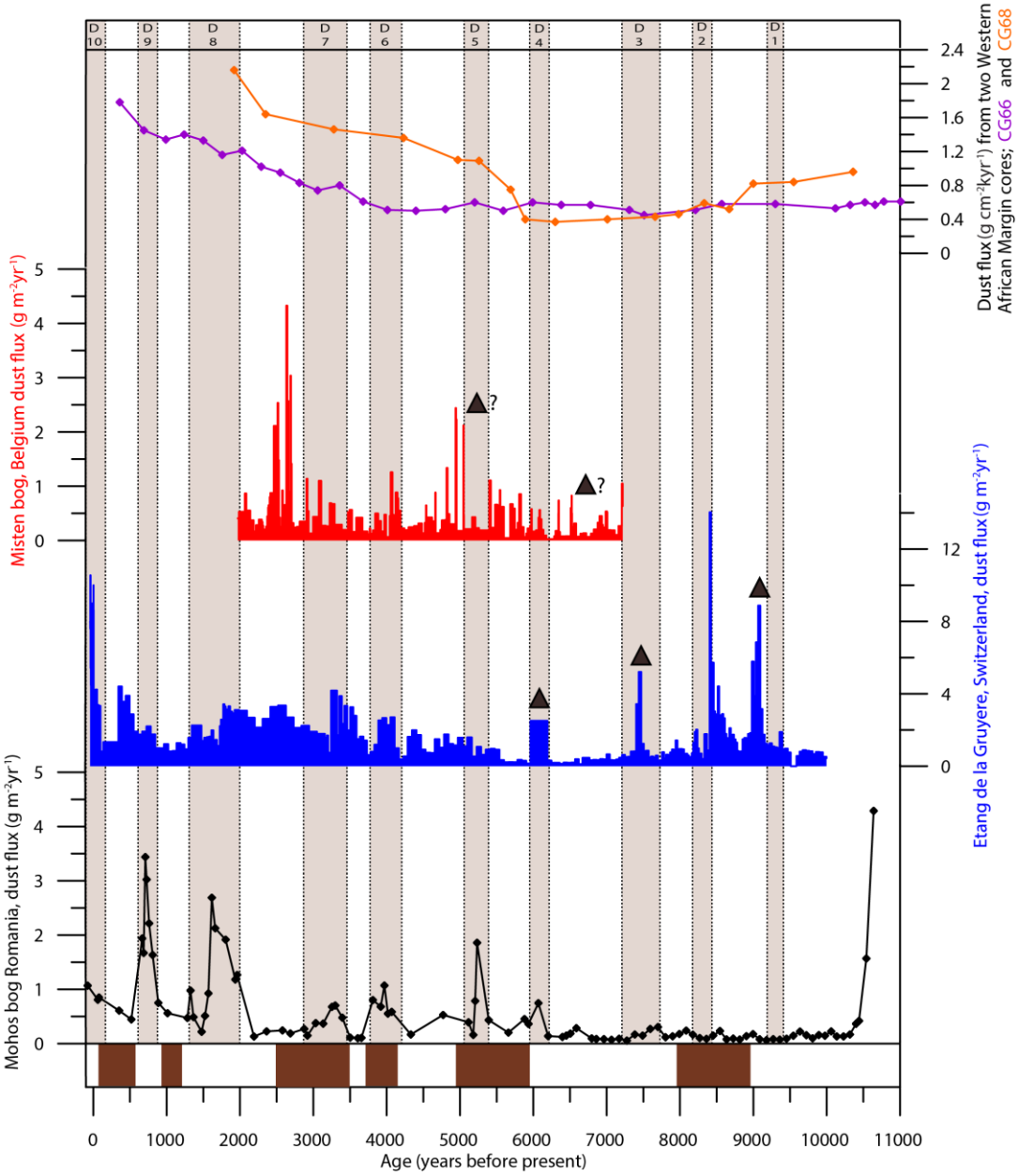

Figure 4.8: *Comparison of dust flux values as reconstructed from Mohos peat bog with similar records. Two western African dust flux records (GC 68 and 66) from marine cores (McGee et al., 2013), are presented alongside bog-based records from Misten bog in Belgium (Allan et al., 2013b), and Etang de la Gruyere in Switzerland (Le Roux et al., 2012), respectively. Indicated on these records are volcanic events as identified by the authors (brown triangles). These are presented alongside the dust flux record from Mohos (lower panel). Also shown, in brown, are periods of Rapid Climate Change derived from Greenland ice (Mayewski et al., 2004). Verticle bars as in Fig. 4.4.*

local nature of such deposition is emphasised by the similarity of the depositional signal to background values; the elemental composition outside of dust events. For all data points not considered to be related to dust (or the minerotrophic lowermost section), the Ti-K regression is low (r^2= 0.1513) with a gradient of 0.0863.

Type 3 events, conversely, appear Ti-enriched (Fig. 4.9), with contribution from a source away from the low-Ti dust of south-eastern European loess fields. These events typically

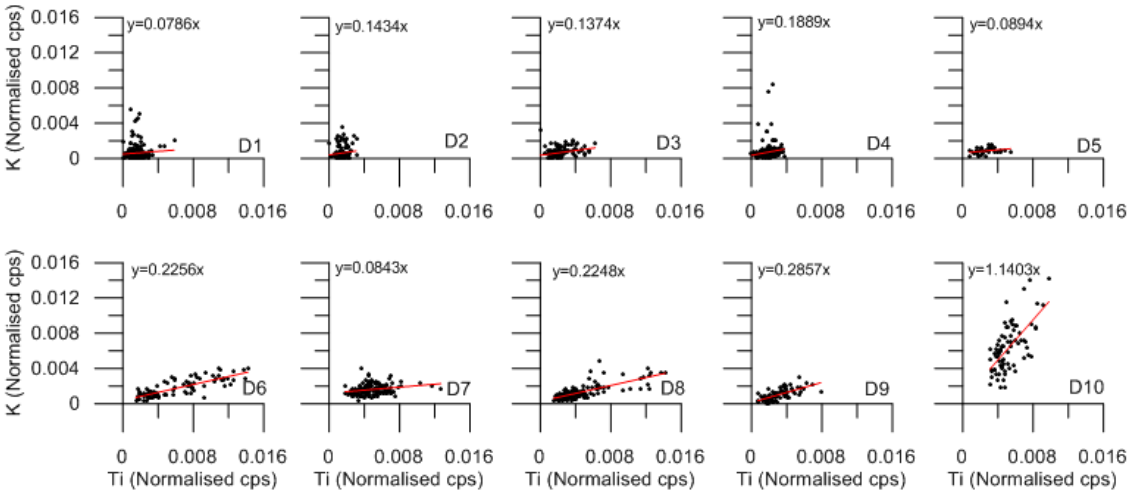

Figure 4.9: *Correlation graphs and gradients of normalised Ti versus normalised K for each of the dust events (D1–D10)*

occur after 6100 cal yr BP (Fig. 4.4). With the periodic influence of the Mediterranean air masses in the region (Apostol, 2008; R Bojariu and Paliu, 2001), Saharan dust must be considered as a potential source area, since it appears to play a major role in dust input into Europe today (e.g. Athanasopoulou et al., 2016). Geochemically, Saharan dust is typically Ti-enriched (Nicolás et al., 2008). In particular, the Bodélé depression, the single-largest dust source in the Sahara, exhibits extremely high Ti/Al and Ti enrichment (Bristow et al., 2010; Moreno et al., 2006). Since Ti enrichment does not show any regional trends, it is no use for determining exact source areas within the Sahara (Scheuvens et al., 2013), but the presence of Ti-enriched dust appears to reflect a signal of Saharan influence. Consequently, events of Type 3 may be considered to reflect, at least to a large extent, contribution of Saharan dust. Finally, the single Type 1 event (since 75 yr BP) may be attributable to a mixing of both local (resulting in high K) and distal (resulting in high Ti) sources, evidence for Saharan input and local soil erosion/deflation.

Previous work has indicated the input of Saharan dust in Eastern Europe, with evidence of such a source seen in Carpathian loess (Újvári et al., 2012; Varga et al., 2013) and soil-forming dust (Varga et al., 2016). Additionally, recent atmospheric satellite imagery has further confirmed the extent of Saharan dust outbreaks and depositional events over central-eastern Europe (Varga et al., 2013). However, the lack of long-term dust reconstructions in the region has so far precluded understanding of changing dust sources over the Holocene.

Previous studies across Europe indicate the complex input of dust from various sources over the mid-to late Holocene (e.g., Veron et al., 2014), but pertinently to the findings at Mohos, many examples exhibit a major shift in dust sources at roughly 5000–7000 cal yr

BP. In Belgium, Nd isotopes indicate a local source of dust from the input of European loess prior to, and Saharan dust after 6500 cal yr BP (Allan et al., 2013a). This is echoed by data from Le Roux et al. (2012) that implies a major shift in the Nd isotopic composition at 6000 cal yr BP, moving from a local to a mixed source, but with clear Saharan overprinting. The transition identified within the Mohos Ti-derived dust record at 6100–6000 cal yr BP, therefore, appears to echo the appearance of a Saharan dust element within other European bog-based dust reconstructions. However, it appears that input of Saharan dust was not limited to the onset of North African desertification, as indicated by input of likely Saharan derived dust within Mohos event D3 already by 7800–7200 cal yr BP. Further, even after 6100 cal yr BP, local sources still played a significant role, with D7 showing clear local or regional (e.g., loess-derived) signal.

D10 (since 75 yr BP) is interesting in that it appears to indicate even more K-rich dust sources. The D10 values are similar in compositional gradient to the lake sediments deposited prior to the onset of peat formation in the early Holocene (Gradient of samples pre-10,500 yr BP = 0.7429, D10= 1.0637). Since the surrounding dacites and pyroclastics are K-rich (Vinkler et al., 2007), and the sediment composition prior to peat formation reflects the natural signal of erosion into the lake, it is reasonable to assume this period is indicative of local slope erosion. This is potentially due to the decline of the local forest and agricultural intensification, identified in the most recent sections of the Mohos pollen record (Tanţău et al., 2003). It is sensible to assume the local deforestation (visible around the Mohos bog as meadows for hay harvesting) has caused local soil erosion and increased dust production from very proximal sources (Mulitza et al., 2010). This is a clear sign of the persistent human impact at local to regional scale during the early Holocene (Giosan et al., 2012; Schumacher et al., 2016) that is also mirrored in the nearby Lake St Ana record (Magyari et al., 2009). As indicated by regional studies (e.g., Labzovskii et al., 2014; Varga et al., 2013; Vukmirović et al., 2004) high levels of Ti indicate Saharan input does not cease through this period, but that it is matched by high-K local sources. The apparent higher water table of the Mohos bog as implied by the TA record and the increased Ti contents rather point towards an increasing Saharan influence rather than a major local dust source.

4.4.4. Correlation to Other European Dust Records

Comparison to similar dust records from peat cores in Western Europe (Allan et al., 2013a; Le Roux et al., 2012), and Atlantic margin sediments (McGee et al., 2013) reveals some interesting trends visible in all these records (Fig. 4.8), indicating comparable continent-

wide controls on past dust flux. Specifically, the major dust event as seen at 5400–5000 cal yr BP in Mohos, and subsequent increase in number and intensity of dust events is comparable with an intensification of dust deposition over Europe after 6000 cal yr BP (Le Roux et al., 2012), with concurrent increases in dust flux in the mid-Holocene documented in Belgium (Allan et al., 2013a). The authors suggest a cool period as the cause of this dust increase (Wanner et al.,

Table 4.2: *Ti-K correlation (R^2), alongside average cps for K and Ti for each of the dust events as identified within the Mohos core.*

Dust Event	D1	D2	D3	D4	D5	D6	D7	D8	D9	D10
Ti-K Correlation (R^2)	0.072	0.111	0.314	0.162	0.296	0.809	0.248	0.758	0.671	0.645
Average Ti (Normalised cps)	0.0015	0.0015	0.0022	0.0018	0.0026	0.0061	0.0048	0.0044	0.0031	0.0052
Average K (Normalised cps)	0.0006	0.0006	0.0006	0.0007	0.0009	0.0018	0.0016	0.0013	0.0011	0.0064

2011). In addition to the reconstructed cool environments in Western Europe, this period is characterised by increased dust production in the Sahara (McGee et al., 2013), which is also likely to have played a role in the increasing dust flux over Europe. After 5000 cal yr BP, it appears Mohos and central-western European records show a more concurrent trend, with comparable dust peaks in the Swiss record (Le Roux et al., 2012) between 4100–3800, 3600–3050, 850–600 and 75 cal yr BP also present in Mohos, and a similar dust peak at 3200–2800 cal yr BP identified in another bog record from Bohemia (Veron et al., 2014).

Despite some similarities between the records, there is also significant variability, highlighting the difference between climatic controls in western and central Europe and those in south-eastern Europe. The disconnection between Mohos and other records is particularly clear for the early Holocene, with a large dust flux peak identified in Switzerland between 9000–8400 cal yr BP, and other volcanic eruption-related dust (See Fig. 4.8), when there is little evidence of dust input into Mohos. This discrepancy could be indicative of the east-west (Davis et al., 2003; Mauri et al., 2015; Roberts et al., 2012) and north-south (Magny et al., 2013) hydroclimatic gradients in Europe throughout the Holocene. As other studies indicate, south-eastern Europe was mostly disconnected (in terms of both precipitation and temperature) from the rest of Europe in the early-mid Holocene (Davis et al., 2003; Drăguşin et al., 2014), clearly indicated by the trend in the

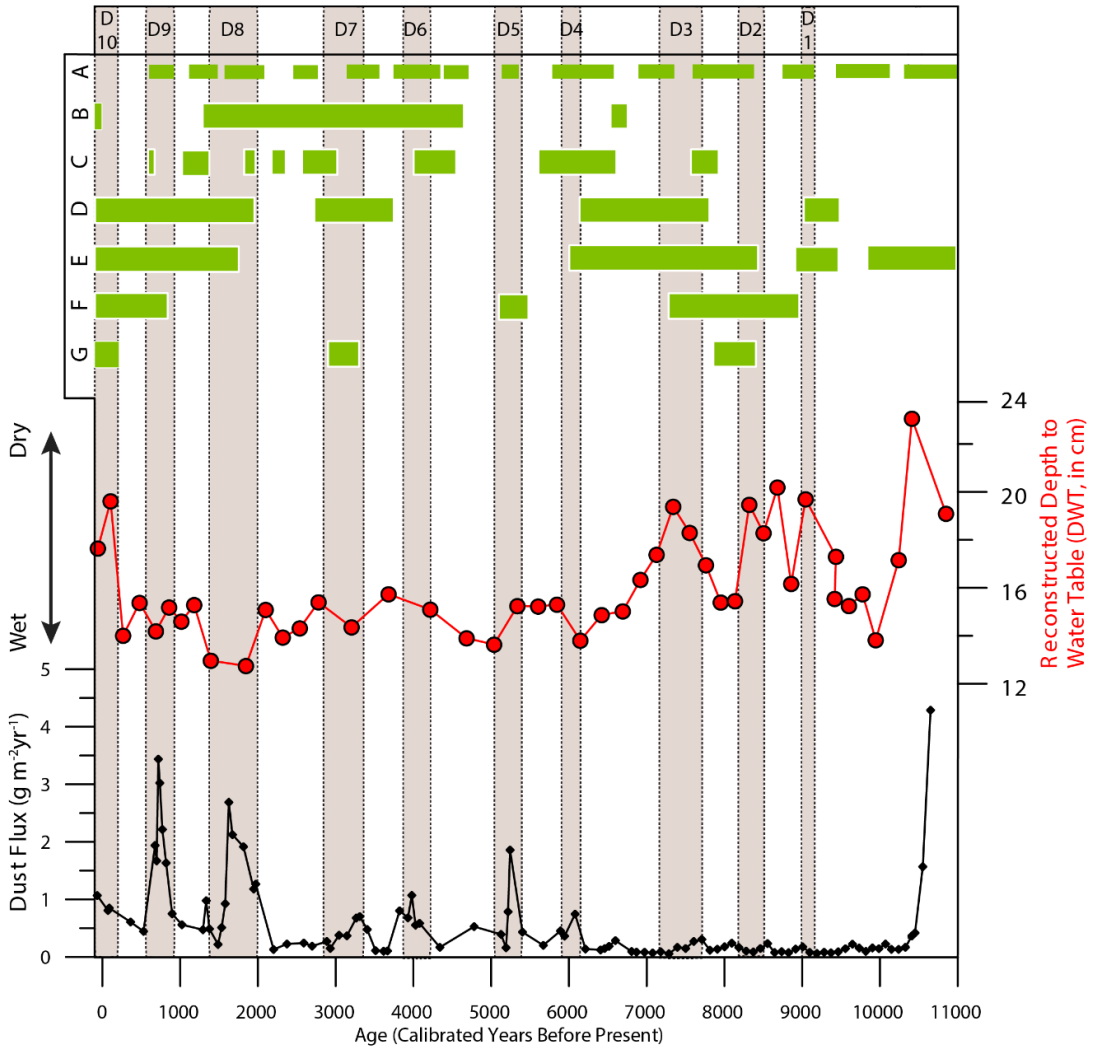

Figure 4.10: *Comparison of dust events and bog wetness as reconstructed from the Mohos record, to regional hydroclimate reconstructions. Data presented via green bars is drought/dry/low lake periods from the following publications. A: (Magny, 2004), B: Cristea et al. (2013), C: Gałka et al. (2016), D: Magyari et al. (2013), E: Buczkó et al., (2013), F: Magyari et al. (2009), G: Schnitchen et al, (2006). These are presented alongside the Mohos testate amoeba-derived Depth to Water Table (DWT) record, and Ti-derived dust flux.*

Mohos Ti-derived dust record. Since the Sahara had not undergone significant desertification by this time, no clear correlation with western records may be made, hinting at more local source for the earliest five dust events identified within the Mohos record (Fig. 4.4) likely related to local fluctuations in moisture availability, and Si and K rich soil dust.

4.4.5. Palaeoecological Proxy Record

To further investigate the difference between local and regional palaeoclimate signals within Mohos, and to reconstruct the local hydroclimate conditions throughout the record, the fossil assemblages of TA are used. These data, alongside comparisons to existing

Carpathian-Balkan and Mediterranean hydroclimate reconstructions (Fig. 4.10), may be used to further investigate the hypothesis of a distal (most likely Saharan) source for dust after 6100 cal yr BP. The earliest section in the TA record (10,800–6400 cal yr BP) is characterised by fluctuating dry/wet periods, indicative of large shifts in the local hydroclimatic environment (Fig. 4.10). The earliest identified dry period (10,800–10,000 cal yr BP) is linked to the shift away from a lacustrine to a palustrine environment as a result of local drying. Three subsequent dry periods may be identified in the TA record 9300–8800, 8500–8100, and 7800–7000 cal yr BP, all of which are also identifiable in the geochemical dust record (D1–D3) via peaks in K and Si. Between 10,200–7450 cal yr BP, dust flux at Mohos was low. Dust events during this time are mainly present in the K and Si records (Fig. 4.4), or in OM and density parameters (Fig. 4.7).

The first period of elevated dust proxies at roughly 10,300 cal yr BP (D0) correlates well with the 10,200 cal yr BP oscillation (Rasmussen et al., 2007), previously linked to a drop in water levels at nearby Sf. Ana Lake (Korponai et al., 2011; Magyari et al., 2012; Magyari et al., 2014). High *Difflugia pulex* and *Trigonopyxis arcula* values during D1 as indicator taxa for dry conditions (Allan et al., 2013a; Charman et al., 2000) appear to confirm local drying, observed across much of the Mediterranean (Berger et al., 2016; Buczkó et al., 2013; Magyari et al., 2013; Fig. 4.10). The D2 and D3 events may also be observed in both the TA record and the geochemical dust record, with D2 attributable to the 8200 cal yr BP event (Bond et al., 2001), a paleoclimatic event already identified in other local hydroclimate reconstructions (Buczkó et al., 2013; Magyari et al., 2013; Schnitchen et al., 2006). The transition to the next wet period at 8000 cal yr BP also mirrors the dust record, with a deeper water table occurring during the dust-free conditions between D2 and D3. This is prior to the bog undergoing dry conditions between 7800–7000 cal yr BP, roughly in line with D3, drying which has previously been observed in Romania (Gałka et al., 2016; Magyari et al., 2009; Fig 4.10). Due to the covariance between geochemical and palaeoecological proxies at this time, and the correlation to other local reconstructions, the early Holocene section of the record indicates a close linkage of local hydroclimate and dust input. These dust events, therefore, are likely the signal of remobilised material (Edri et al., 2016), from proximal or distal sources (including perhaps from loess-derived sediments, at the foot of Ciomadul volcano) as the climate locally appears to become more arid.

Between 6600–1200 cal yr BP, the TA indicate a shift to prolonged wet conditions, with only minor fluctuations and no clear correlation to the geochemically-derived dust record,

and so the dust events appear unrelated to local drying within this time period (Fig. 4.10). Such wetter conditions also limit local drought-related erosion, and so may be further evidence of distal dust input at this time (Allan et al., 2013a). Furthermore, this is indicative of a decoupling of the dust record from local climate reconstructions, with dry phases common throughout the mid-late Holocene in other Romanian sites (e.g., Magyari et al., 2009; Schnitchen et al., 2006; Fig. 4.10), and a distal dust source.

In the last millennium, there are two major dust events, with the first, D9, occurring between 850–650 cal yr BP. This episode falls within the late MWP, and could be related to human activity in the local area, as pollen from the Mohos bog indicate strong evidence for agriculture at roughly the same time (Tanţău et al., 2003). This may be seen in the intensity of the dust deposition at this time (dust flux >3 g $m^{-2}yr^{-1}$). This second event, D10, from 75 cal yr BP to present is certainly linked to such human influences, with the TA record echoing local studies, which display anthropogenically-altered conditions and intensive agriculture (Fig. 4.10) (Buczkó et al., 2013; Diaconu et al., 2016; Giosan et al., 2012; Magyari et al., 2009, 2013; Morellón et al., 2016; Schnitchen et al., 2006). This appears to validate the geochemical approach used earlier, as intensive farming is likely to result in local dust mobilisation, with K-rich dust present at this time, and local input potentially erasing some distal signals. This does not preclude Saharan input, however, as the dust is also Ti-rich.

4.4.6. Periodicity

To further understand the nature of the reconstructed dust events, cyclicity within the geochemical record was investigated using wavelet analysis (Fig. 4.11). The main elements of interest (Ti, Si and K) have no apparent cyclicity in the first half of the record (10,800-6000 cal yr BP) when there is low spectral power at all periods. In contrast, the last 6000 years display clear centennial and millennial-scale cycles. A number of other studies have identified cyclicity shifts at this time (Fletcher et al., 2013; Jiménez-Espejo et al., 2014; Morley et al., 2014), related to North Atlantic variability, but so far mainly in western Mediterranean records. From 6000 cal yr BP onwards, the geochemical record at Mohos preserves two main cyclicities; one millennial cycle (at c.1200–2000 years) and the second at c.600–800 years

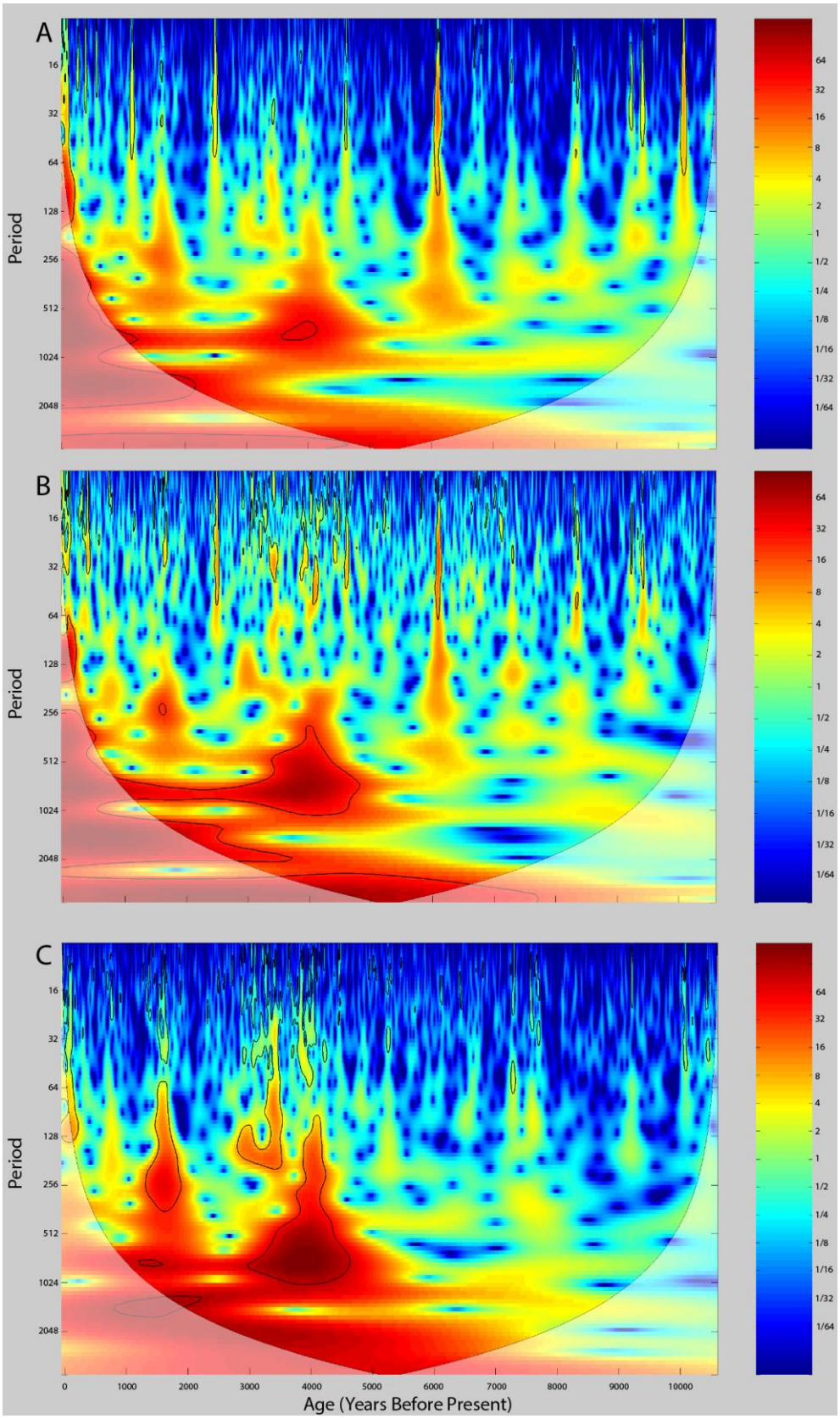

Figure 4.11: *Spectral analysis of Mohos ITRAX geochemical data for A: K, B: Si, C: Ti. Areas outlined in black are significant at the 95% confidence level. Shaded area indicates the cone of influence, outside of which results may be unreliable.*

(Fig. 4.11). A 715–775 year cycle has been determined as a harmonic of Bond event-related dry periods, present in other Northern hemisphere records (Springer et al., 2008) and in central Africa (Russell et al., 2003). The millennial scale cycle, in contrast, is within the envelope of a 1750 year cycle observed within the western Mediterranean, in pollen (Fletcher et al., 2013) and Saharan dust (Debret et al., 2007; Jiménez-Espejo et al., 2014), which is attributed to changes in North Atlantic atmospheric circulation.

Within the dust deposition events (Fig. 4.4), there is an overprinting of high-frequency cyclicity in the Ti record, especially within the last 5000 years (Fig. 4.11). These are particularly clear at 4200, 3400 and 1800 cal yr BP, but lower-power cyclicities may be seen in most dust deposition events. These are generally 100–200 years in length, and only last the extent of the dust outbreak. Cycles with lower than 140-year periodicities are possibly reflecting mainly background noise (Turner et al., 2016), but those longer in duration may be indicative of climatically forced fluctuations within drought events affecting the dust source areas. This suggests the reconstructed dust deposition events based on the Mohos record were not characterised by constant deposition of dust, but by periodic dust pulses. These short cycles could reflect solar forcing, with comparable 200-year cycles observed in humification profiles from peats (Swindles et al., 2012), sediments in the Baltic Sea (Yu, 2003), Pacific Ocean (Poore et al., 2004), and in North American peatland isotope records (Nichols and Huang, 2012). In many cases, such cycles have been linked to lower solar activity periods, low temperatures and increased precipitation oscillations, related to the De Vries/Suess 200 year cycle (Lüdecke et al., 2015). In the case of Mohos, these fluctuations may have manifested themselves as shifts in dust deposition, and could indicate the persistent effect solar dynamics has on all facets of climate system.

4.5. Conclusions

The first record of Holocene drought and dust input in a bog from Eastern Europe documents ten periods of high dust loading: 9500–9100, 8400–8100, 7720–7250, 6150–5900, 5450–5050, 4130–3770, 3450–2850, 2100–1450, 800–620 and 75 cal yr BP to present.

A major intensification in the number, and severity (as indicated by dust flux values) of dust events is observed after 6100 cal yr BP. The two intervals before and after this shift are indicative of an alteration in major dust controls. For the period prior to 6100 yr BP, dust input is reflective of more local controls, whilst the most recent 6100 yr BP of deposition may be linked to more distal forcings.

The timing of the major shift at 6100 cal yr BP is possibly related to the end of the African Humid Period, and the establishment of the Sahara Desert, pointing to significantly greater Saharan input within the regional dust loading after this time. This is corroborated by changes in cyclicity attributable to Saharan dust outbreaks, and a shift toward Ti-rich dust (a signal of Saharan rock and sediment) deposited onto the Mohos peat. This data is the first such indication of the impact Saharan dust has had across Eastern Europe, in line with enhanced deposition of dust across the Mediterranean region. A tentative dust provenance analysis based on a simple geochemical approach to disentangle the composition of the dust has been applied to confirm this, with three main types of deposition documented, indicating the interplay between local/regional (mainly loess-derived) and Saharan dust sources over the Holocene.

The most recent dust event, between 75 cal yr BP and today is geochemically indicative mainly of local erosion. This may be linked to the increasing human impact through deforestation, agriculture and recently tourism, and associated soil erosion, indicating a shift in the controls on drought and dust in the region.

Chapter 5. Exceptional Levels of Lead Pollution in the Balkans from the Early Metal Ages to the Industrial Revolution

5.1. Introduction

The discovery and refinement of metals and alloys has been fundamental to the development of our industrialised society (Killick and Fenn, 2012). The earliest use of metals in the form of native copper in Anatolia roughly 7000 BCE (Stech, 1999) preceded the invention of extractive metallurgy and alloying at around 5000 BCE (Radivojević et al., 2010). Evidence of intentional thermal treatment of metal ores and complex metalworking around this time has been uncovered in several places throughout the Balkans (Pernicka et al., 1993; Radivojević et al., 2013, 2010; Radivojević and Rehren, 2016) as well as in the Middle East (Roberts et al., 2009). Building on the discoveries of these early metalworking pioneers, humans have continuously employed metals in a wide range of applications, utilizing their adaptability to develop modern technologies and industries. However, the exploitation of mineral resources has had a broad range of environmental impacts, including metal-contaminated wastewater and chemical particulates being released from atmospheric pollution (More et al., 2017), mining (Csavina et al., 2012) and smelting (Dudka and Adriano, 1997). Further, human applications such as the use of toxic metals in tools, appliances and artefacts (e.g. lead in Roman water pipes) may directly input metals into the environment. As a result, the effects of highly toxic Pb poisoning on the broader ecosystem (Hoffman et al., 2003) and on human health during the past 2,000 years are well documented, particularly for the Roman Empire, where Pb was a highly sought metal commodity (Hernberg, 2000).

In central-western Europe, trends and amplitudes of mineral resource exploitation have been documented using mainly the geochemical composition of peat bog records, building on earlier work on polar ice cores (Hong et al., 1994; Rosman et al., 1997) and lake sediments (Brännvall et al., 1999; Bränvall et al., 2001; Renberg et al., 2001). Released to the atmosphere through mining and smelting, once deposited within peat or lake sediments, Pb is effectively immobile (Novak et al., 2011), resulting in its reliability as a proxy for reconstructing past pollution directly related to such anthropogenic activities (Hansson et al., 2015). Due in part to its immobility, and after the early detection (Gaël Le Roux et al., 2004) of a clear environmental Pb pollution peak from Roman times in British peat

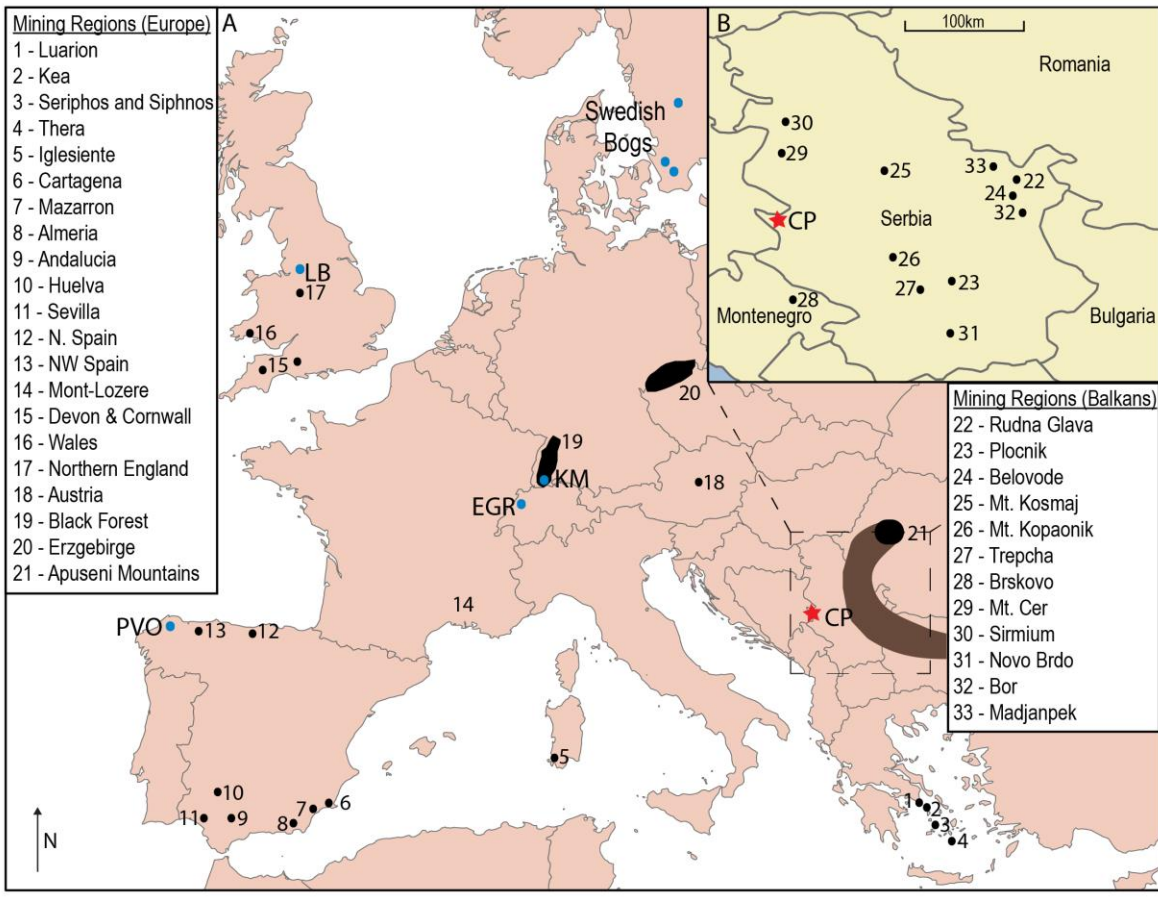

Figure 5.1: *Map of Europe indicating location of Crveni Potok (red star) and of other studies referenced in text; Lindow Bog (LB)* (Le Roux et al., 2004), *Penido Vello (PVO)*(Kylander et al., 2005), *Etang de la Gruyere (EGR)* (Shotyk et al., 1998), *Kohlhütte Moor (KM)* (Le Roux et al., 2005) *and three Swedish bogs* (Klaminder et al., 2003). *Also presented are locations of major metallogenic provinces exploited prior to 1800 CE* (Kylander et al., 2005) *and the Banatitic Magmatic and Metallogenic Belt (highlighted in brown). 5.1.B displays Serbia and surrounding countries, indicating the location of Crveni Potok with respect to the locations of mining and metal production sites as mentioned in text.*

records, much of the focus has been on this metal (Hansson et al., 2015). Traces of Roman Age Pb pollution have been found in records from much of Europe (Hansson et al., 2015), including Spain (García-Alix et al., 2013; Martínez Cortizas et al., 2012, 2002), Switzerland (Shotyk et al., 1998) and even areas outside the Roman Empire's reach such as Sweden (Klaminder et al., 2003) and Central Europe (Novák et al., 2003), all clearly documenting the far-reaching impact of such past metal resource exploitation.

Such results indicate the reality of atmospheric long-distance transport of Pb, although differences between records hint at strong regional differences in past pollution patterns (More et al., 2017), necessitating further investigation of pollution loading in regions with rich ore endowment and long history of metal use. Pertinently, long-term Pb pollution records for south-eastern Europe have not yet been investigated (Fig. 5.1), thereby limiting

the inference of past metal use, long-term environmental pollution and the likely impact on human health in this region and beyond. The rich archaeological heritage of the Carpathian-Balkan region includes the earliest known sites of extractive metallurgy in Europe (O'Brien, 2014), with processing centres and mines at Rudna Glava (Jovanović, 2009), Plocnik and Belovode in Serbia (Radivojević et al., 2013, 2010) and Ai Bunar (Chernyk, 1992) in Bulgaria dating prior to 5000 BCE (Fig. 5.1). These early activities ushered in significant metalworking activities for several millennia related mainly to the Vinca and other contemporaneous or successive material cultures (Jovanović, 2009; Radivojević et al., 2010). Metal production in the area further bloomed during the Copper Age and especially during the Bronze Age, with metallic artefacts reaching exceptional quantities and sophistication (Bugoi et al., 2013; Chernyk, 1992; Ling et al., 2014) after 3000/2800 BCE (Kienlin, 2014). Further significant metal exploitation was undertaken by the Romans and their Byzantine successors, with evidence of exploration and large-scale mining in the area at the time (Borcoş and Udubaşa, 2012; Petković, 2009). In addition, it has been suggested silver rich ores in modern-day Serbia were likely exploited since the Medieval period (Bálint, 2010; Paulinyi, 1981), although modern scale exploitation of mineral resources has largely destroyed old vestiges.

This 7000-year long history of mining and metallurgy in the Balkans has been facilitated by the significant endowment in polymetallic ores, very rich in base and precious metals (Fig. 5.1). In particular, the Apuseni mountains (western Romania) host the Metaliferi mining district, home to Europe's largest gold and silver (Au-Ag) deposits (Laznicka, 2006; Xun, 2015). In addition to this district, other mining areas are still being exploited on the 1500 km-long Banatitic Magmatic and Metallogenic Belt, which runs from Romania, through Serbia and into Bulgaria, and is the most important ore-bearing (particularly Cu, Au, and Pb-Zn) belt of the Alpine-Balkan-Carpathian realm (Ciobanu et al., 2002; Heinrich and Neubauer, 2002).

From an archaeological perspective, the inception of metallurgy is a hotly debated topic, and understanding it is key to understanding the ancient world. The beginning of metallurgy likely ushered in a new age of technology, with substantial social (e.g. new lifestyles) and cultural (e.g. use of metal as decoration) consequences, but it is unclear as to whether smelting diffused outward from the Middle East (Frame, 2004), Eastern Europe (Radivojević et al., 2010), or was it developed multiple times in multiple locations (Wertime, 1973). It is possible coherent records of pollution related to smelting from such locations could clarify this issue. Other contentious discussions may also be investigated in

this manner, with one such example the level of trade and mobility in Balkan Bronze Age cultures (Ling et al., 2014). Further, the impact of the fall of the Roman Empire on the technological development of Eastern Europe is uncertain. It is clear that in western Europe, the dark ages and associated migration period were indicative of greatly decreased technological and socio-economic development. However, in Eastern Europe, the maintenance of the Byzantine Empire east of the Danube (Treadgold, 1997) apparently led to the continuation of Roman metalworking activities (Edmondson, 1989). If evidence of continued metallurgical exploitation is observed, it would have profound implications on our understanding of development in the wake of the fallen Roman Empire.

Here a high-resolution record of past anthropogenic pollution based on the geochemical data from Crveni Potok peat bog (Fig. 2.3) is discussed, for the first-time reconstructing past metal-related environmental pollution linked to mineral resource exploitation in the Balkans. The approach delivers a valuable new view on the chronology of past mineral resource exploitation and related pollution load in south-eastern Europe. It allows for the gap between indirect geochemical inferences and direct archaeological evidence to be bridged in a region that has likely been crucial from the first steps of metal exploitation at the onset of human technological development, and through all of metallurgical history (O'Brien, 2014; Pernicka et al., 1993; Radivojević et al., 2013, 2010; Radivojević and Rehren, 2016).

5.2. Methods and Materials

Crveni Potok (43°54'49.63" N; 19°25'11.08" E) is a small bog (<3 ha) located in the Tara Mountains National Park, on Serbia's western border with Montenegro, at 1090 m a.s.l., within the Dinaric Alps (Fig. 2.3). See Chapter 2 for further details about the site.

Table 5.1: *Expected and observed recoveries for elements analysed within Crveni Potok core.*

CRM 1- NIMT/UOE/FM/001

(Yafa et al., 2004)

Overall Average

Element	Expected	Observed	**% Recovery**	Analysis 1	Analysis 2	Analysis 3	Analysis 4	Analysis 5
Cu	5.28	5.49	**104.01**	5.86	5.01	4.16	6.52	5.90
Cr	6.36	5.32	**83.70**	4.96	5.69	5.77	4.57	5.61
Ni	4.10	4.18	**101.96**	4.20	3.31	5.41	4.62	3.36
Pb	174.00	177.74	**102.14**	190.40	193.10	161.10	177.80	166.30
Ti	357.00	323.88	**90.72**	330.90	336.70	317.00	324.00	310.80
Zn	28.6	27.82	**97.30**	26.19	26.06	28.27	29.93	28.69

CRM 3- Montana Soil 2711

Overall Average

Element	Expected	Observed	**% Recovery**	Analysis 1	Analysis 2	Analysis 3	Analysis 4	Analysis 5
Sc	9.00	10.39	**115.51**	10.19	10.88	7.24	12.79	10.88
Sr	245.30	234.47	**95.58**	250.90	225.05	229.65	225.6	240.73
Zr	230.00	231.91	**100.83**	207.20	232.10	286.80	208.01	225.35

270 cm of sediment was recovered in overlapping cores. The age-depth model was developed using nine AMS ^{14}C dates calibrated using the IntCal 13 dataset (Reimer et al., 2013), and Clam age-depth modelling software (Blaauw, 2010) (Fig. 5.2). Subsamples were taken and trace metal analysis was performed on exactly 0.5 cm^3 of sediment to allow for density calculations. Each subsample was dried overnight prior to homogenization and digestion via a mixed acid (HNO_3-HCl-HF) microwave-assisted method (see Chapter 2 for further details). These solutions were analysed via a Perkin Elmer Optima 8000 ICP-OES system. Procedural blanks indicate negligible contamination, and two reference materials, run alongside the samples, indicate reliable recoveries (within 10% of the expected values in most runs) (Table 5.1).

HYSPLIT modelling suggests potential particle source areas are to the north-west and east, with periodic incursions from the south, which is reflected in prevailing wind directions (NW and SE (Gavrilov et al., 2017), and so the site is well located to record activity from a number of mining centres in the Balkan area (Fig. 5.1, 5.3), including ancient mining sites such as Sirmium or Rudna Glava (Merkel, 2007; Stojković, 2013), as well as central

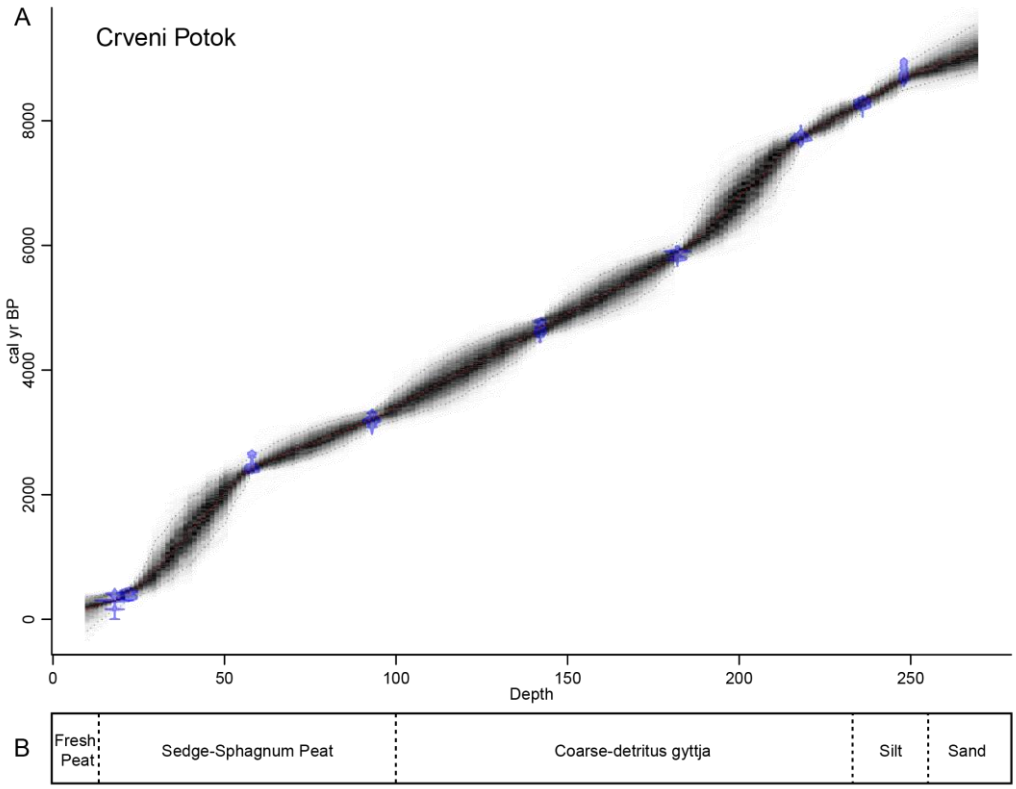

Figure 5.2: *A: Bacon-derived plot of age versus depth for the Crveni Potok sediment profile. B: simplified lithological diagram of the core from Crveni Potok.*

European mining areas including the Erzgebirge and eastern Alps (Fig. 5.1, 5.3). The vast majority of particles entering the site, however, appear local, with the densest source areas all within 100km of the site (Fig. 5.3).

Despite apparently low input from non-atmospheric metal sources including dust and runoff (Fig. 5.4), to derive a reliable picture of past metal loading related to anthropogenic activities it is necessary to extract the pollution-related Pb from the natural background. An approach which distinguishes the lithogenic (natural) heavy metal component from the

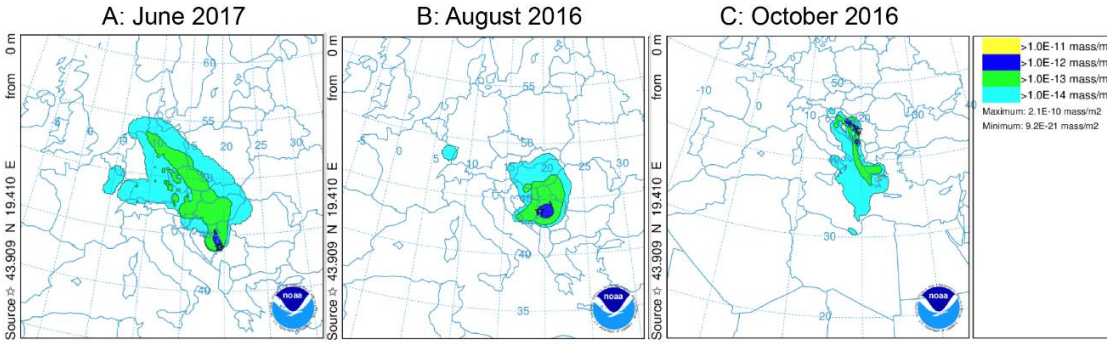

Figure 5.3: *84 hour back trajectory models carried out to interpret likely source areas for particles entering Crveni Potok.*

anthropogenic component (Shotyk et al., 2000) was used. This first calculates the

lithogenic component (by comparison with expected values in the upper continental crust) of the heavy metal contribution, prior to removal of this signal from the overall metal concentration. The remainder may be considered the anthropogenic component (Pb_{Anthro}). In addition to calculation of Pb_{Anthro}, we also present the enrichment factor (EF, Fig. 5.5C), and cumulative anthropogenic, atmospheric Pb (CAAPb, Fig. 5.5B), which clarifies exactly which times dominate the Pb depositional history. Finally, to allow for direct comparison to other records (Le Roux et al., 2005), the Pb accumulation rate (AR, Fig. 5.5.A) has been calculated (see Chapter 2 for details) (Kylander et al., 2005).

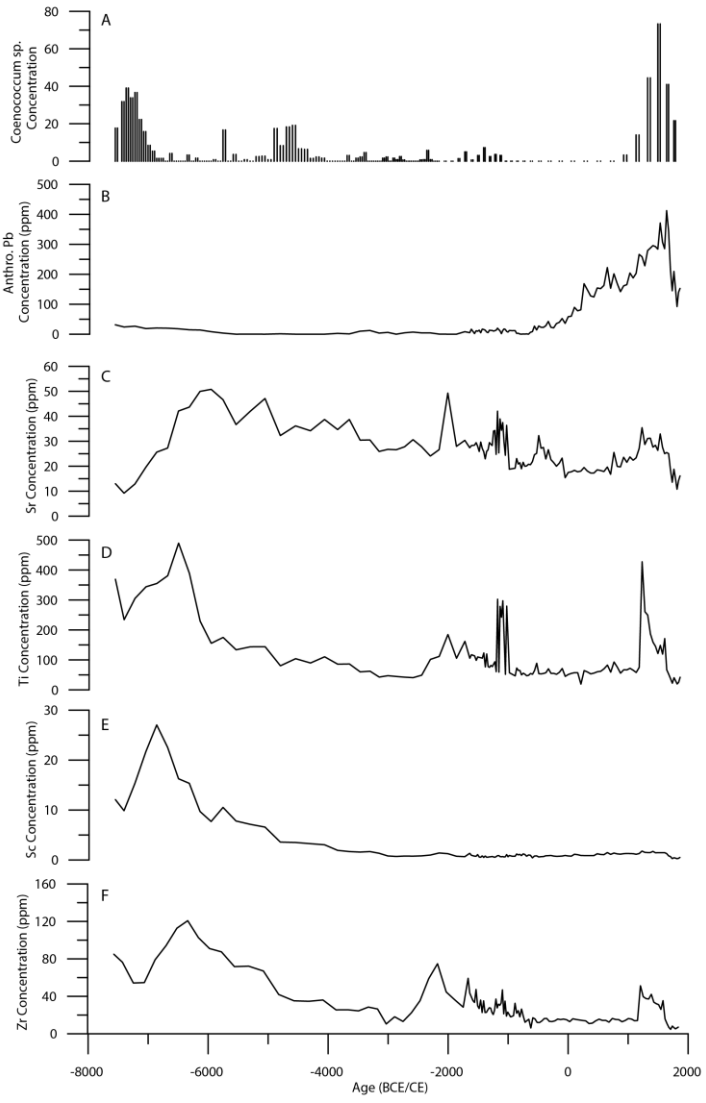

Figure 5.4: *Lithogenic Proxies used to determine potential input of non-pollution related metals to Crveni Potok. A is Coenococcum sp. (a fungi species generally related to soil erosion) concentrations. B: Anthropogenic Pb (Pb_{Anthro}). Panels C, D, E and F display lithogenic element concentrations; Sr, Ti, Sc and Zr, respectively.*

5.3. Results and Discussion

5.3.1. Ombrotrophy

Initial surveys at Crveni Potok indicate no evidence of inflow from permanent streams (Lazarević, 2013), suggesting mineral input to the mire is very rare from the surrounding gentle slopes, perhaps occurring only during periods of high rainfall. This was clear when describing the core, where no mineral matter was observable. Geochemically, low Sr concentrations (<20 ppm) have previously been used to fingerprint ombrotrophy of bogs (De Vleeschouwer et al., 2009a; Shotyk et al., 2002). The Sr concentration values measured at Crveni Potok are relatively low (15–35ppm, see Fig. 5.4) and suggest only little influence of runoff-derived Sr.

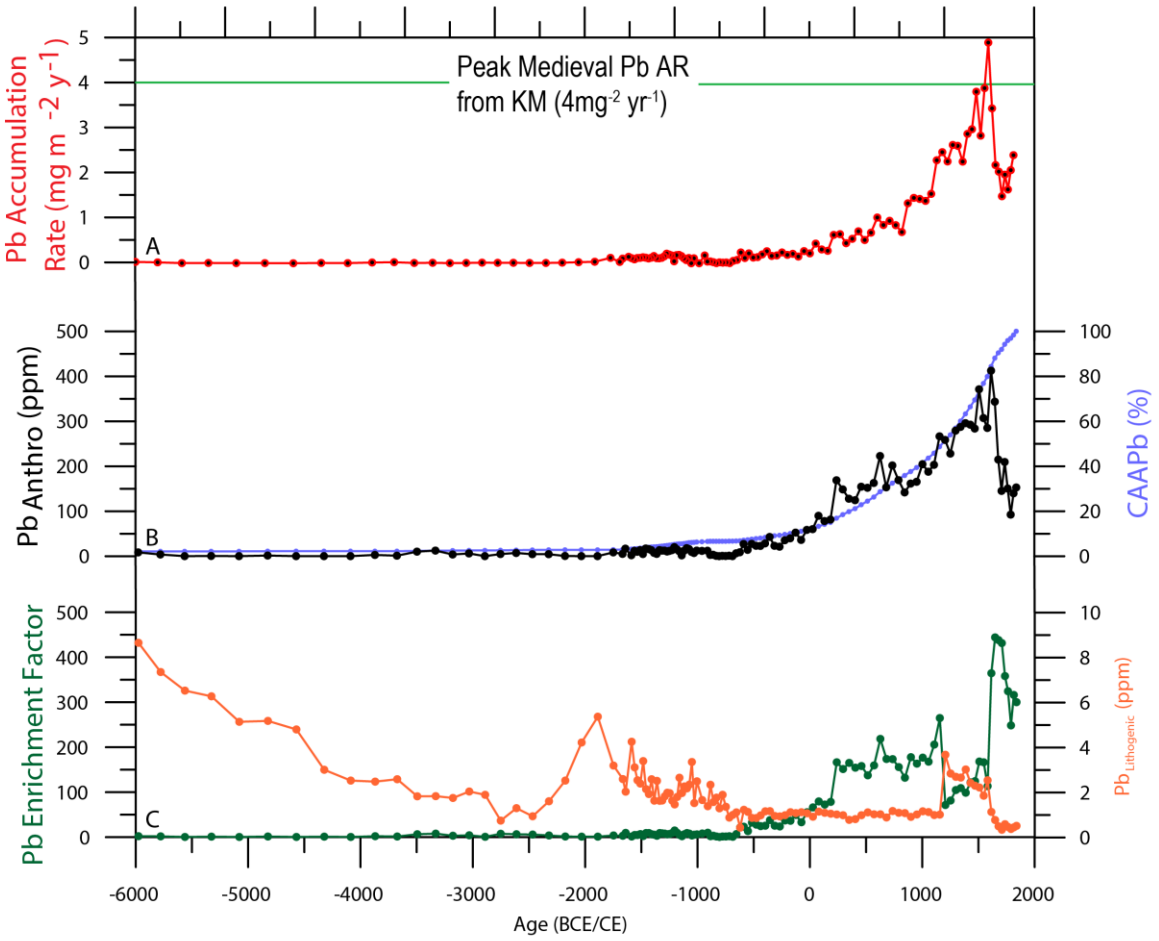

Figure 5.5: *Methods for elucidating the depositional history of Pb pollution at Crveni Potok. A: The Pb Accumulation Rate (Pb AR), presented alongside the peak medieval Pb AR from Kohlhutte Moor. B: Cumulative Anthropogenic, Atmospheric Pb (CAAPb), alongside the anthropogenic Pb component (Pb_{Anthro}). C: The lithogenic Pb component ($Pb_{Lithogenic}$) and Pb Enrichment Factor (EF).*

The trends in erosion and minerogenic debris indicators (Zr, Sc, Ti as well as *Coenococcum* sclerotia, Fig. 5.4) further hint at episodic/occasional inputs of minerogenic matter. In keeping with this, close inspection of the uppermost 100cm of the record indicates *Sphagnum*-dominated peat, rendering this part of the record typical of a spruce-forest mire (De Vleeschouwer et al., 2009a; Finsinger et al., 2017). Hence, it is very likely that the Crveni Potok peat has never been truly ombrotrophic. Other sources of Sr may potentially include dust from the extensive Danube loess fields (Marković et al., 2015), or from the underlying limestone.

Nevertheless, Sr concentrations are overall negligible when compared to other sites where regular influx of minerogenic debris from proximal slopes has been observed (Chapter 3). Further elemental indicators of minerogenic input (Zr and Sc, Fig 5.4) are also much lower than one would expect in a site influenced by regular runoff or flooding (see Chapter 3).

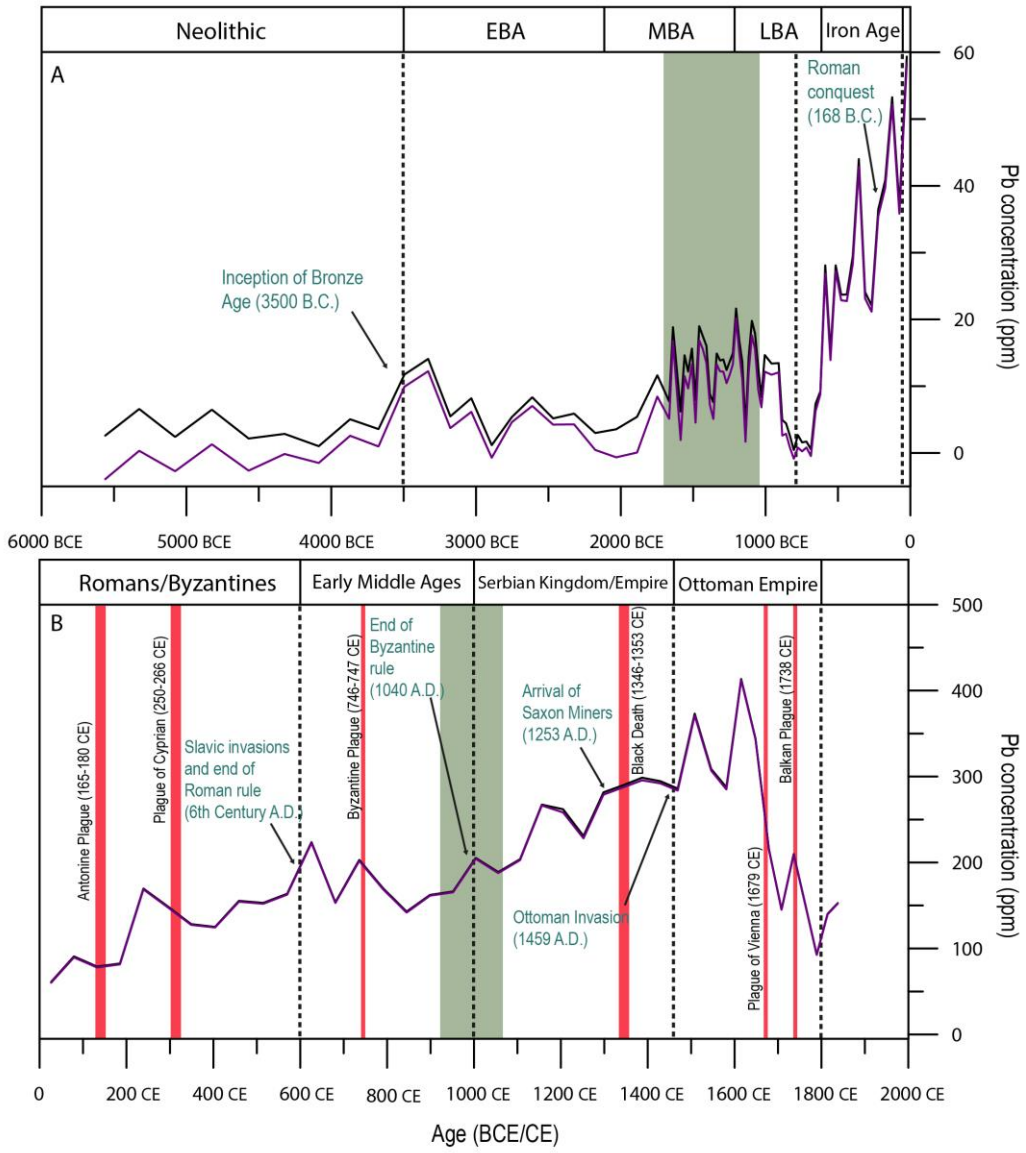

Figure 5.6: *Raw Pb concentration (black line) and calculated anthropogenic contribution (Pb_{Anthro}, purple line) for Crveni Potok core. Upper panel indicates earliest section of core, from 8000 BCE to 0 BCE/CE whilst the lower panel indicates the period from 0 BCE/CE to 2000 CE. Also indicated are major periods of socio-economic change in the region (green labels), and the timing of major European plagues (red rectangles). Changes in local development are indicated by black dashed lines. Green rectangles display periods of increased fire activity (Finsinger et al., 2017). Note panel A displays a smaller scale to panel B, to allow for variations in the older section to be observed.*

Furthermore, there are very low correlations between Pb and any of these elements (Pb-Zr= -0.151, Pb-Sc= -0.166, Pb-Sr= -0.19) and so it is unlikely any possible mineral influx is controlling Pb deposition.

Regardless, all Pb data interpreted have been normalized to a conservative element (Zr) in order to disentangle the natural Pb lithogenic contribution to the reconstructed anthropogenic Pb record of Crveni Potok (Fig. 5.5).

5.3.2. Reconstructing the History of Metal Pollution in the Central Balkans

The oldest section of the Crveni Potok record (7500 – 5600 BCE) is dominated by minerogenic deposition and therefore discussion of early metallurgical activities in the Balkans (Radivojević et al., 2010) prior to 5600 BCE is avoided. After 5600 BCE (Fig. 5.5.B, 5.6.A), Pb_{Anthro} record shows no enrichment until c.3700 BCE, indicative of background Pb deposition (Pb_{Litho}) from natural sources (Shotyk et al., 1998).

The first major rise of Pb_{Anthro} enrichment is found at around 3600–2500 BCE (Fig. 5.6.A), the earliest such evidence for environmental Pb pollution (Martínez-Cortizas et al., 2016). This correlates well with the inception of the Bronze Age in the Carpathian-Balkan region, with evidence for bronze production at this time being widespread (Pernicka et al., 1993) especially close to the Cu-rich deposits south of Danube (Pernicka et al., 1993), validating archaeological indications of the eastern European Bronze Age beginning 1000 years earlier than in central and western Europe (Stockhammer et al., 2015). Such artefacts are generally associated with the Vucedol culture, with eastern (Jovanović, 2009) and central Serbia as centres of metallurgy in the early Bronze Age, although evidence suggests a wide trading network at this time (Ling et al., 2014; O'Shea, 2011), with Cyprus considered as a major source of copper (Ling et al., 2014). In terms of tin (Sn), the other main constituent of bronze, a closer origin is possible, with deposits in western Serbia apparently an important source (Huska et al., 2014; McGeechan-Liritzis and Taylor, 1987).

Pb_{Anthro} values are lower (Fig. 5.6.A) during the Middle Bronze Age (2500 BCE–1750 BCE), echoing a non-local source (although possible local smelting) of metal for the numerous bronze artefacts within Serbia (Huska et al., 2014), and the neighbouring Carpathian Basin (Pernicka et al., 2016), with the Slovakian Ore Mountains and eastern Alps proposed as the most likely sources (Pernicka et al., 2016).

Pb_{Anthro} returns to high, but fluctuating values between 1750 BCE– 950 BCE (Fig. 3.A), a trend reflected also in the Cu, Zn and Cr records (Fig. 5.7). This correlates with the known rapid expansion of metal working in the Carpathian-Balkan region during the late Bronze Age (Chernyk, 1992), and the first major forest clearances attributed to human activity both locally, in the Dinaric Alps (Wolters et al., 2010) but also more regionally, over the Danube lowland basins (Giosan et al., 2012). Across the Balkans, a large number of metal artefacts have been documented, many attributed to the Vatin (Huska et al., 2014) and the Brnjica (Stojić, 2006) cultures of the late Bronze Age. This regional pollution is most likely linked to Sn mining and associated bronze manufacturing centres such as the area

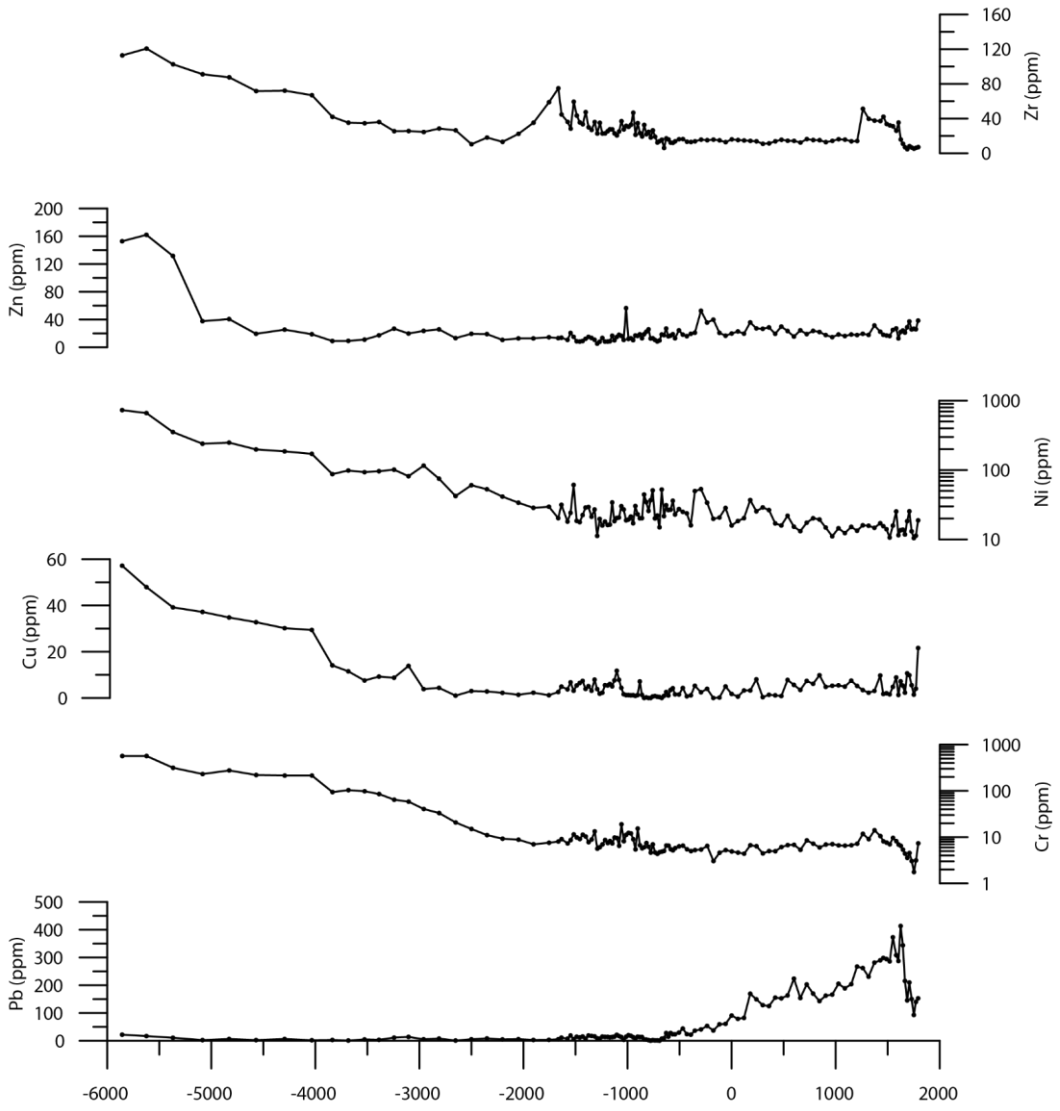

Figure 5.7: *Raw metallic elemental concentrations for Crveni Potok sediment sequence. Presented here are A: Zinc, B: Nickel, C: Copper, D: Chromium and E: Lead. Note logarithmic scale for Ni and Cr records*

around Mt. Cer (150km north of Crveni Potok), which was an important source of the Sn found within Serbian artefacts of the late Bronze Age (Mason et al., 2016). Additional evidence for increased anthropogenic disturbance at this time comes from Crveni Potok's enhanced fire activity centred around 1550 BCE (Fig 5.6, 5.7.B) (Finsinger et al., 2017). Further, land-use changes, likely associated to local human pressure and possible metal processing activities locally (Huska et al., 2014) may be inferred from the first appearance of coprophilous fungi (*Cercophora* and *Sporormiella,* Fig. 5.7.D), and increasing values for the anthropic pollen indicators (*Plantago lanceolata* and *Cerealia*-type, Fig. 5.7.C) in the Late Bronze Age at Crveni Potok.

The onset of the Iron Age is characterized by very low values for all elements (Figs. 5.6, 5.7), likely indicative of the disruptive impact the well-known socioeconomic Late Bronze

Age Collapse has had in the wider Balkan region (Dean et al., 2015; Drake, 2012). This period represents the last interval of peat deposition without significant evidence of enriched Pb_{Anthro} (Fig. 5.6.A). Remarkably, from roughly 600 BCE onwards the Crveni Potok record is indicative of near constant increases in the level of Pb_{Anthro} deposition through time, until 1700 CE. The first period of increased Pb_{Anthro} (600 BCE–200 BCE) is likely reflective of the ability of the local craftsmen (La Tène material cultures), including the Celtic Scordisci who occupied much of the western Balkans at this time, and the Thracians, Illyrians and Greeks in the rest of the Balkans, to mine and smelt metals. Indeed, the Scordisci were renowned for their ability to mint coins (Popovic, 1987), and are considered the craftsmen behind a large Pb ingot discovery at Valle Ponti (Dušanić, 2008), indicative of an advanced culture of metal working (Papazoglu, 1978). The source of the Pb ingot is thought to be Sirmium (located 200km north of Crveni Potok) (Fig. 5.1), an important early smelting center, prior to the Romans, exploiting Ag and Pb sources in the Dinaric Alps (Dušanić, 2008). The Crveni Potok record likely reflects contribution from regional Pb smelting, with rapid, stepwise increases in Pb_{Anthro} throughout Classical Antiquity and into the Roman period (600–150 BCE, Fig. 5.6). This economic activity is also reflected in regional forest clearance, as observed in Bosnia, 100km west of Sirmium (Dörfler, 2013), coincident with the increase in Pb_{Anthro} throughout Roman times, and the subsequent Medieval period. At Crveni Potok, no major decrease in forest cover is observed in the pollen record (Fig. 5.8.C, 5.8.D) (Finsinger et al., 2017), although the findings of anthropic taxa and of coprophilous *Cercophora* fungi are clear indicators of stronger local human pressure.

The Romans conquered much of the Balkan area between 200–100 BCE. As in other regions with rich mineral deposits (e.g. Hispania and later Dacia) the Romans systematically catalogued and mined the area (Dušanić, 2004). In the Crveni Potok record, Pb_{Anthro} increases dramatically to a peak at c.239 CE, with particularly sharp increases around 50 CE and 150 CE, reflecting the influence of Roman mining and smelting technology (Fig. 5.6). Illyricum and Moesia, south of Danube, became typical mining provinces, with a particular focus on Au and Pb deposits (Hirt, 2010). Moesia appears to have hosted two major mining regions, in the south (Dardania; now southern Serbia and Kosovo) and in the north (*ripa Danuvii;* near the Roman frontier along the Danube including the mineral-rich Timok valley) (Dušanić, 2004). In Dardania, famous examples of Roman mining have been excavated at Municipium Dardanorum (Westner, 2016), whilst the whole of the Balkans contains numerous traces of Roman metallurgy (Petković, 2009). Closer to Crveni Potok, it appears mineral resources within the Dinaric Alps were

also exploited, particularly at Mount Cer (150 km north of Crveni Potok). Other major mining areas included Mt Kosmaj near Belgrade (Merkel, 2007; Stojanović et al., 2015)

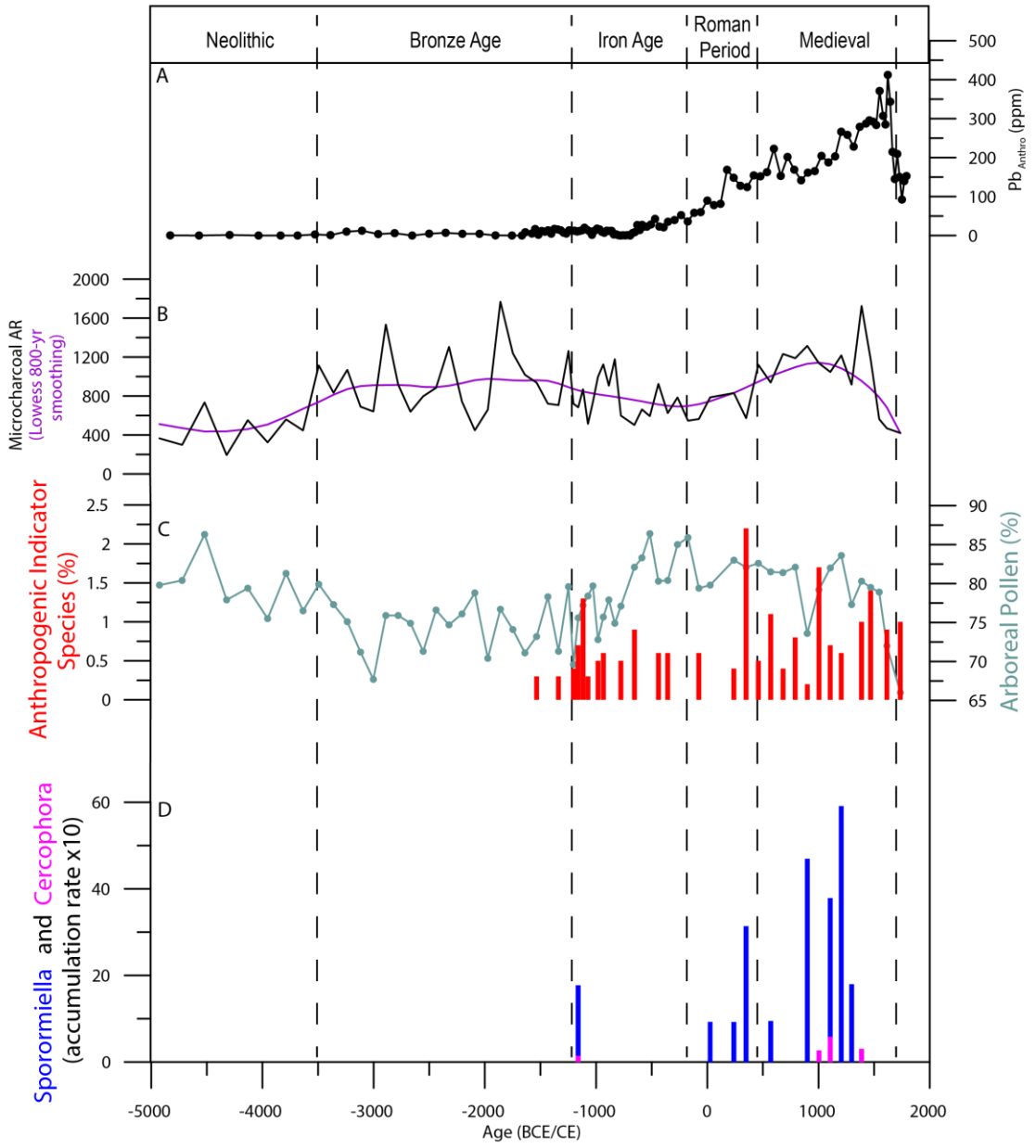

***Figure 5.8:**: Comparison of Anthropogenic Pb (Pb_{Anthro}) with other proxies of human activity from Crveni Potok for the past 7000 years.A is the Pb_{Anthro} curve as displayed in figure 5.5.B. B is microcharcoal accumulation rate, with both raw values (black line) and a smoothed curve (purple line), produced using a Lowess 800-year smoothing window. C displays the percentage values of anthropogenic indicator pollen species (Plantago lanceolata and Cerealia-type), alongside arboreal pollen percentages. D is a stacked bar chart of accumulation rates for two coprophilous fungi species (Cercophora and Sporomiella).*

and Mt Kopaonik in Kosovo (Westner, 2016)(Fig.5.1). From Kosmaj alone, the enormous quantities of ancient slag (1,000,000 tons) are testament to the massive-scale of Roman metal (primarily silver and lead) exploitation in the region (Merkel, 2007). Further evidence may be seen in the cumulative, atmospheric, anthropogenic Pb (CAAPb) percentage (relative to the entire Pb deposited within the core) deposited during this time at

Crveni Potok, nearly 20% (see Fig. 5.5.B), a significant fraction, especially once the large enrichment of the Medieval period is considered.

After a peak at around 239 CE, Pb_{Anthro} decreases (Fig. 5.6.B), possibly indicative of a slowdown in production, relating to the repeated invasions and upheavals that affected the Balkan area (Edmondson, 1989). However, subsequent increases after 400 CE indicate mineral exploitation in the region was continued by the Byzantine Empire which, contrary to Western Europe, reached its peak in economic and cultural development at this time (Treadgold, 1997). The decrease in Pb_{Anthro} evident after 736 CE and lasting up to 1000 CE echoes the gradual decrease in influence of the Byzantine Empire in the northern Balkans as documented in historical sources (Treadgold, 1997). After 1100 CE, and with the arrival of Saxon miners from 1253 CE onwards (Fine, 1994), the Serbian statehood developed into one of Europe's leading silver producers (Petrovic and Petrovic, 2010; Stojković, 2013), reflected in significant Pb_{Anthro} increases in the Crveni Potok record (Fig. 5.6.B). The major Balkan Medieval mining centers all opened between 1250 and 1300 CE, with Rudnik (1293 CE), Trepcha (1303 CE), and most pertinently to the Crveni Potok record, the Brskovo mines, which opened on the Tara Mountain in 1254 CE, 150 km to the south (Fig.5.1) (Ivanišević, 2001; Stojković, 2013). This development in Serbian mining is emphasized by the percentage of Pb deposited at Crveni Potok after 1000 CE; nearly 60% (Fig. 5.6B). The ongoing increase in Pb_{Anthro} from 1100 CE at Crveni Potok clearly reflects the continued regional opening of new mines and development of mining techniques throughout the early Medieval period (Stojković, 2013) to satisfy demand for silver in central Europe and the Middle East (Stojković, 2013). Post-Roman-conquest Pb_{Anthro} reaches a first peak at 1508 CE (Fig. 5.6.B), and just after the Ottoman conquest of Serbia in 1459 CE (Miljkovic, 2014). This was a period of rapid growth in mining output throughout Serbia and the Balkans, as most other European mines were in decline at the time - a "Golden Age of Serbian Medieval Metallurgy" (Vukovic and Weinstein, 2002). Under Ottoman rule, the mines of the region appear to continue to produce, even after the introduction of the Kanun-name (Ottoman law) regulating and restricting mining in 1536–1537 CE (Miljkovic, 2014), until Pb pollution peaked in 1615 CE (Fig. 5.6.B), by which time mines in the region were producing over 24.9 tons of silver per year (Malcolm, 2002; Vukovic and Weinstein, 2002).

The rapid decrease in Pb_{Anthro} at Crveni Potok after 1615 CE appears indicative of the restrictive impact of Ottoman laws and their taxation system, which became progressively more convoluted and inefficient through the 17th Century (Stojković, 2013).These onerous

laws and taxes, combined with the appearance of cheap and plentiful sources of silver in the new world, particularly Spanish America (Nriagu, 1996, 1994), meant that by 1690 CE silver production in the region had all but ceased, and did not recover until the end of Ottoman rule (Stojković, 2013; Vukovic and Weinstein, 2002). This is reflected in the Pb_{Anthro} record, with progressive decreases until 1789 CE (Fig. 5.6.B), a trend echoed also in the reduction in microcharcoal, and anthropogenic indicator pollen taxa at Crveni Potok (Fig. 5.8), pointing to region-wide economic stagnation as stated in historical records (Stojković, 2013).

The final section of the Crveni Potok core (1700 – 1820 CE, Fig. 5.6) indicates that the trend for decreasing metal pollution which characterized later Ottoman Serbia was reversed sometime in the early 19th Century, around the time of the Serbian Revolution (1804–1835 CE) (Mitev, 2010; Stavrianos, 1958). This Pb_{Anthro} upturn likely indicates the first impact of the Industrial Revolution in the Balkan area (Fig. 5.5.B).

5.3.3. Linkage with Plagues

It has been suggested by More et al. (2017) that metal production and environmental pollution is majorly perturbed by the occurrence of major plague epidemics such as the Black Death of 1346–1354 CE (Byrne, 2012). Within Crveni Potok this hypothesis has been tested, with evidence to suggest such a linkage is possible with a number of major pestilences which afflicted eastern and southern Europe (Fig. 5.6). These include the Cyprian Plague (Harper, 2015), believed to be smallpox related, which decimated numbers in the Roman army between 250–266 CE, and may be behind the decrease in Pb_{Anthro} at this time at Crveni Potok (Fig. 5.6). Other such epidemics, including the plague of Antonine (165–180 CE), Byzantine (746–747) and Vienna (1679 CE) (Alchon, 2004) are all associated with downturns in Pb_{Anthro}. Notable, however is the lack of apparent influence the Black Death had on Pb pollution, evidence for a much reduced influence in eastern Europe when compared to the west. It is plausible such an impact on western European metal production allowed the eastern European industry to flourish, and resulted in the major enrichment observed at Crveni Potok in the Medieval period.

5.3.4. Comparison with Western European Pollution Records

When comparison with western Europe is made, as expected, several similarities may be observed, suggestive of comparable continent-wide Pb production trends at times. Pb enrichment in the Bronze Age, although not as early as indicated in Crveni Potok; between 3600–2500 BCE and 1750–950 BCE, has previously been observed in Spain (García-Alix et al., 2013), France (Monna et al., 2004a) and the British Isles (Mighall et al., 2009), with

the oldest evidence previously from Spain 3030 BCE (Martínez-Cortizas et al., 2016). Furthermore, Roman-related pollution (as observed at Crveni Potok from 150 BCE onwards) has previously been documented continent-wide (Fig. 5.9), from Spain (Kylander et al., 2005; Martínez Cortizas et al., 2013) through central Europe (Forel et al., 2010; Le Roux et al., 2005; Shotyk et al., 2001) and as far from centres of occupation as the Faroe Islands (Shotyk et al., 2005) and Greenland (Hong et al., 1996; Rosman et al., 1994). Finally, the impact of Medieval pollution which is so well expressed in the Crveni Potok record has been observed previously, but primarily close to known mining areas in southern Germany (Le Roux et al., 2005; Shotyk et al., 2001) and northern England (Gaël Le Roux et al., 2004). Further from such metallurgically active areas, only small-scale Medieval pollution is typically observed (Fig. 5.9) (Shotyk et al., 2005).

It is not the similarities with western European records, which are most interesting, however, but the differences. Clearly the Roman Empire had a major influence on the pollution history of the Balkans, echoing a Roman Pb pollution peak observed across western Europe (Fig. 5.9) (Hansson et al., 2015). Unlike western Europe, however, it appears the end of the Roman period in central-western Europe did not bring a cessation of the mining activities in the Balkans (Fig. 5.6.B, 5.9). This is in contrast to western European records, which indicate major disruptions in metal exploitation and related Pb pollution after 300 CE in both Spain and Switzerland (Fig. 5.9). The dissimilarity between western and south-eastern Europe is evidence for the continued exploitation of Balkan metal ores by the Byzantines, validating previous archaeological indications (Edmondson, 1989), and confirming the so-called 'Dark Ages' of western Europe coincide with significant economic development in south-eastern Europe. High levels of metal environmental pollution in the Balkans throughout the Medieval period, and after the fall of the Byzantine Empire, indicates the knowledge and expertise of the local peoples, and the arrival of Saxon miners (from 1224 CE onward) further increased mining productivity (Fig. 5.6.B) (Stojković, 2013). Thus, it is demonstrated here that the Carpathian-Balkans acted as a major source for European metal pollution not only during Antiquity, but also during the early Medieval period and later.

These values undoubtedly attest to major mining and smelting industries operating in south-eastern Europe. The timing of the Medieval increase in Pb_{Anthro} is in line with the development in silver mining in Germany (Baron et al., 2009; Novák et al., 2003) and increased Pb pollution in a number of peat records across Europe (Hansson et al., 2015). However, in no other studies does the Pb pollution exceed that of the Roman period until

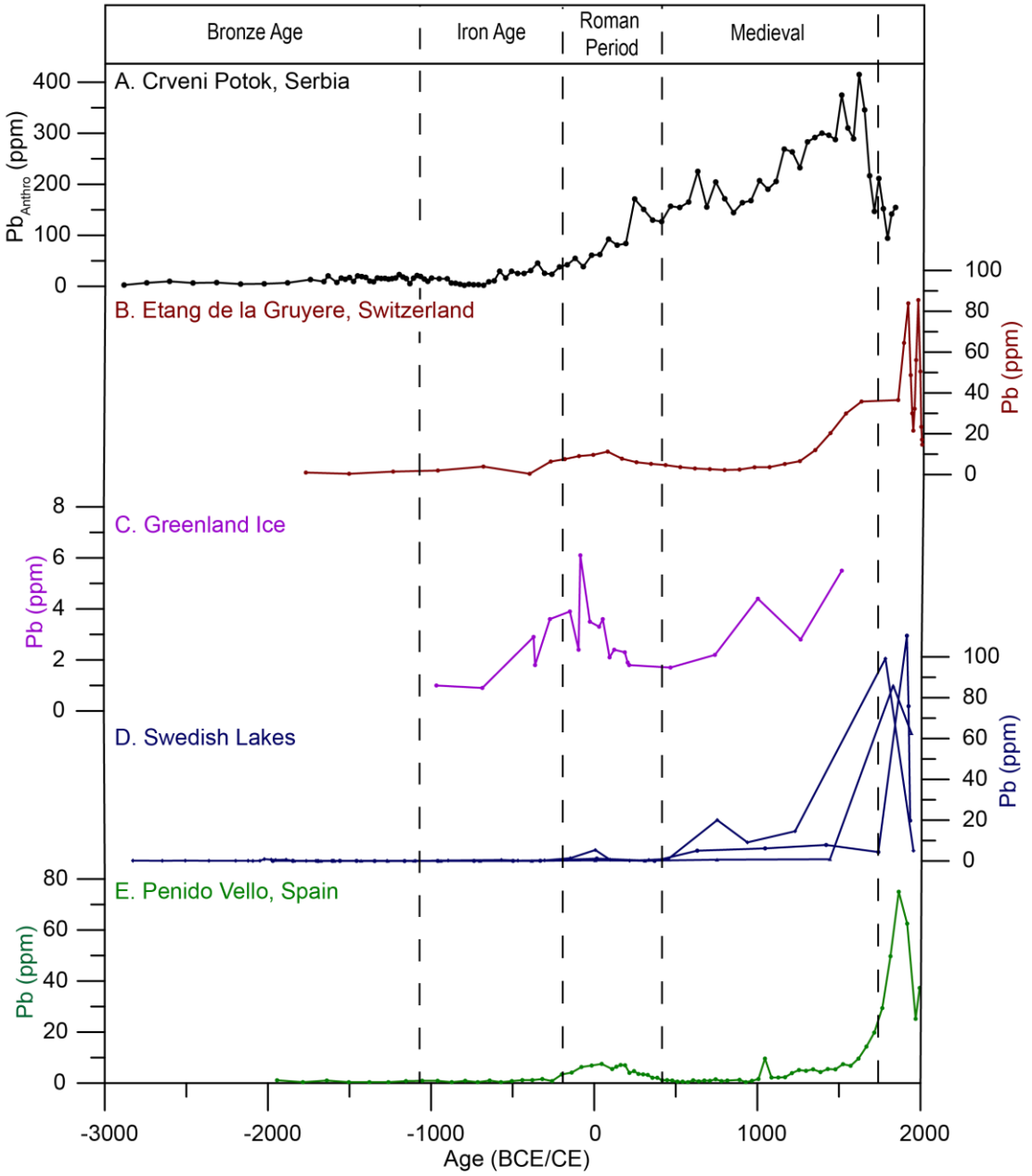

Figure 5.9: *Comparison of Anthropogenic Pb (Pb_{Anthro}) from Crveni Potok with other studies in western and northern Europe and Greenland. A: Crveni Potok. B: Northern Switzerland* (Shotyk et al., 2001). *C: Greenland ice* (Rosman et al., 1997). *D: Three peat records of Pb from southern Sweden* (Klaminder et al., 2003). *E: North-western Spain* (Kylander et al., 2005).

after 1800 CE, with major pollution associated with the inception of the Industrial Revolution (Gaël Le Roux et al., 2004; Shotyk et al., 2001). This further confirms the large extent and size of the metalworking industry in the Balkans during the late Medieval period.

The Crveni Potok record, therefore, provides the first evidence of a significantly different pollution history for south-eastern Europe when compared to the west. Previously, the

comparability of western European records, regardless of substrate (Hansson et al., 2015) has allowed for cohesive records of pollution to be put together. However, this new record shows that overall estimations of historical metal pollution (including Pb production) must be revised, to take into account the varied nature of development across Europe, and to consider the previously less well-constrained contribution of Balkan metallurgical history.

To allow for direct comparison of the Crveni Potok pollution record with other sites, and to remove intercomparison issues relating to sedimentation rates, Pb ARs have been calculated (Fig. 5.5.A). Despite the low sedimentation rates (Fig. 5.3), and the near-pristine natural local environment at Crveni Potok today (Finsinger et al., 2017), Pb ARs are for the past 2000 years, peaking during the late Medieval Period, generally reflecting the Pb_{Anthro} values.

Comparison with the Etang de la Gruère (EGR)(Shotyk et al., 1998) record in Switzerland's Jura Mountains, and that of Kohlhütte Moor (KM) (Le Roux et al., 2005) in south-western Germany provide the most pertinent evaluations (Fig. 5.1). Similarly to Crveni Potok, these are located in remote mountain areas with relatively low local human pressure during most of the Holocene. Further, geographically they are proximally located to pollution sources derived from centers of metallurgy: south-eastern France and the Eastern Alps, regions active from the Bronze Age onwards for EGR, and Black Forest Medieval mining centres for KM (Fig.5.1). The comparison reveals the similarity in the Crveni Potok and KM records throughout the Roman period, with both sites indicating Pb ARs between 0.5–1.5 mg m^{-2} y^{-1}, suggesting regional smelting activities were similarly extensive. However, in both KM and EGR, the Pb ARs do not exceed 2 mg m^{-2} y^{-1} until the Industrial Revolution. In contrast, in the Crveni Potok record, this threshold is reached eight centuries earlier (ca. by 1100 CE), rising to a peak of nearly 5 mg m^{-2} y^{-1} by 1615 CE (Fig. 5.5.A). The latter Pb AR peak is comparable to Pb-pollution flux levels reached three to four centuries later in the two central European bogs, which only reach this Pb contamination level by the early 20th Century (Le Roux et al., 2005; Shotyk et al., 1998). Another valid comparison may be made with Lindow bog (LB) near Manchester in north-western England (Le Roux et al., 2004). Here, at a site located within a region of rich medieval mining heritage, Pb ARs comparable to Crveni Potok are observed at roughly similar times, particularly during the Medieval period; at LB Pb ARs reach 1.24 mg m^{-2} y^{-1} in the period 1100–1500 CE, prior to a peak of roughly 4 mg m^{-2} y^{-1} by the 1450 CE.

The Pb pollution history inferred from the Crveni Potok record is reflective of major mining and smelting activity in the Balkan region for the last 7000 years, which peaks in

the 17th century. By this time, the mining activity was producing Pb pollution comparable to other known Medieval mining centers such as southern Germany and northern England. A major difference, however, is the fact that there is no evidence of proximal mining at Crveni Potok, suggesting the high Pb output recorded by this bog is either reflective of significant pollution region-wide, or noteworthy underestimation of the extent of Balkan metallurgy.

5.4. Conclusions

The Crveni Potok peat sequence provides an unprecedented 7000 years-long record documenting the impact of mining and smelting on atmospheric pollution in the wider Balkan region. The onset of clear signs of anthropogenic Pb enrichment is detected first during the Bronze Age, with two periods of high Pb pollution (3600–2500 BCE and 1750–950 BCE), correlating with well-constrained archaeological evidence of regional mining. The first of these is the earliest such evidence for Pb pollution in an environmental record worldwide.

Pb enrichments correspond to increases in fire activity and early deforestation, pointing to a causal link between mineral resource exploitation and land-use changes. Major Pb pollution is recorded from 600 BCE onwards, with gradually increasing values in anthropogenic Pb until a peak at 1615 CE. The record of ever-increasing pollution is indicative of a long and varied history of exploitation of metals in the area. Inhabitants, from the Neolithic-Bronze Age material cultures to the Romans, Byzantines and Serbs all appear to have promoted a strong metalworking culture in the Balkan region as indicated by archaeological and historical sources, with the Pb pollution record of Crveni Potok reflective of this. The influence of the Ottoman Empire during the pre-modern and modern periods appears clear, with rapidly decreasing Pb contamination from 1615 CE until the early 19th Century. Occasional, plague-related perturbations may be observed, with the negative influence of the plagues of Antonine and Cyprian, as well as the later plague of Vienna evident within the record. No impact, however, is observed from the Black Death, indicating its weak impact in eastern Europe.

The record discloses a significantly different pollution history in comparison to central-western European records, suggesting that the picture of European environmental impact through such activities is not complete without considering developments in south-eastern Europe, a region very rich in metal ores and a documented long history of mineral resource and land-use exploitation. No previous studies have displayed constant Pb enrichment

increases throughout the Medieval period, with most central-western European records peaking only during Roman and later during industrial times. Accumulation rate comparisons corroborate the scale of metallurgical activity in the region throughout the Medieval period, with values comparable only to sites located close to centers of mining and smelting today, indicative of the size and long-term persistence of the Pb pollution in the Balkans, for several millennia.

Chapter 6. Utilisation of Bayesian Mixing Models to Quantitatively Assess Proportions of Pb Sources in Isotopic Mixtures

6.1. Introduction

Lead (Pb), a toxic, non-essential metal for life, has been an important commodity for technological development (Killick and Fenn, 2012) and one of the most persistent anthropogenic pollutants through time (Hansson et al., 2015; Settle and Patterson, 1980). Lead may be released directly from the mining and smelting of Pb-containing ores (especially during argentiferous metallurgy), and more recently, through the extensive use of Pb-containing fuels, batteries, paints and other commodities (Komárek et al., 2008). Pb is one of the most well-studied pollutants, due in part to its toxicity, even at low levels, to multiple organ systems (Landrigan, 2002), and its particular danger to young children and developing foetuses (Lanphear et al., 2005). As such, understanding the sources, sinks and cycles of Pb are vital.

Evidence suggests humans have greatly impacted the natural biogeochemical cycle of Pb (Nriagu 1983; 1996), with records of pollution indicating anthropogenic influence of the Pb cycle as far back as the Bronze Age (Komárek et al., 2008; Gaël Le Roux et al., 2004; Shotyk et al., 1998). Particularly large amounts of Pb were released into the atmosphere during the Roman period in Europe, which left a clear imprint in peat records (Cloy et al., 2005; Kylander et al., 2010; Gaël Le Roux et al., 2004; Nriagu, 1983), and Greenland ice (Hong et al., 1994; Rosman et al., 1997). Further anthropogenic atmospheric Pb enrichment has been observed in records located close to centres of mining in Medieval times (Kempter and Frenzel, 2000; Gaël Le Roux et al., 2004; Veron et al., 2014), and upon the introduction of Pb-containing gasoline in the early 20th Century across the globe (Allan et al., 2013b; De Vleeschouwer et al., 2009b, 2007, Shotyk et al., 2005, 1998), even as far from mining centres as Antarctica (Chang et al., 2016).

Knowledge of the pollution activity at the sites of mining and smelting (Fig. 6.1), and assessment of contamination levels at different sites is not sufficient for firm conclusions regarding Pb provenance and contributions from changing sources through time. Analysis of ore bodies has indicated the variability of Pb isotope ratios depends on the type of ore, age, and style of mineralization (Komárek et al., 2008). A simple example is the difference observable between the $^{206}Pb/^{207}Pb$ ratio of very old ores (e.g. the Broken Hill ore, which was formed 1.6-1.8 billion years ago and used in European leaded petrol; $^{206}Pb/^{207}Pb$= 1.05

– 1.1, Grousset et al. 1994; Weiss et al. 1999) when compared to younger ores (most Jurassic to Miocene age fall within the range $^{206}Pb/^{207}Pb$= 1.18 – 1.25, Hansmann & Köppel 2000). Old ores (e.g., Proterozoic age) were formed, and the Pb isotope ratios were set, during an early stage of the Earth's evolution, and so the decay of Th and U contributed little to the Pb budget. Conversely, younger ores contain variable amounts of radiogenic lead, since time has allowed for more decay of parent isotopes (^{238}U, ^{235}U and ^{232}Th) to occur (Bacon, 2002; Farmer et al., 2000) prior to their incorporation into the ore.

Crucially for archaeometallurgical inferences, the Pb isotopic ratios are not severely altered by physical or chemical fractionation processes during ore processing, smelting, and casting, although some minor variations may occur (Baron et al., 2009). Therefore it can be assumed the lead isotope values of the pollution-related Pb are very similar to those of the parent ore bodies (Bollhöfer and Rosman, 2002). As such, precise isotopic ratios may be used to 'link' Pb deposited in a substrate (e.g. bogs, lakes and ice) to a certain ore (Bollhöfer and Rosman, 2002; Komárek et al., 2008). It has been demonstrated that records of Pb concentration from sedimentary archives such as peat bogs, lake sediments and ice cores may retain the isotopic signature of the original source of Pb, since once deposited within such environments, Pb is largely immobile (Novak et al., 2011). Such work has clearly indicated the impact of metal pollution from local sources (e.g. Shotyk et al. 2016), and long range atmospheric transport (e.g. Rosman et al. 1997; Le Roux et al. 2004; Shotyk et al. 1998) through time. However, the signal recorded within a bog or lake represents a mixture of many local, regional and extraregional inputs, including contribution from natural sources (dust, biomass burning, volcanoes, etc.) and disentangling these has proven challenging (Cheng and Hu, 2010).

Moreover, without a modelling component in interpreting Pb records from sedimentary archives, typical approaches may only be used to indicate likely sources, rather than infer quantitative apportionments. Traditionally, interpretation of Pb isotopic ratios is performed via a 3-isotope plot (Fig. 6.2; and Kylander et al. 2005), and comparing the location of the sink mixture data (the isotope signal recorded within the archive) to the isotopic signatures of known sources. More recent studies attempted modelling of the sink mixture (the isotopic signature of the substrate) as a way of quantitatively assessing the relationships between sinks, and sources (Álvarez-Iglesias et al., 2012; Brugam et al., 2011). Until now, Pb isotope mixing models have generally been limited to considering either two (e.g. Bird et al. 2010b; Monna et al. 2000; Brugam et al. 2011) or three (Álvarez-Iglesias et al., 2012) potential sources. This approach is adequate in a very well determined system, where only

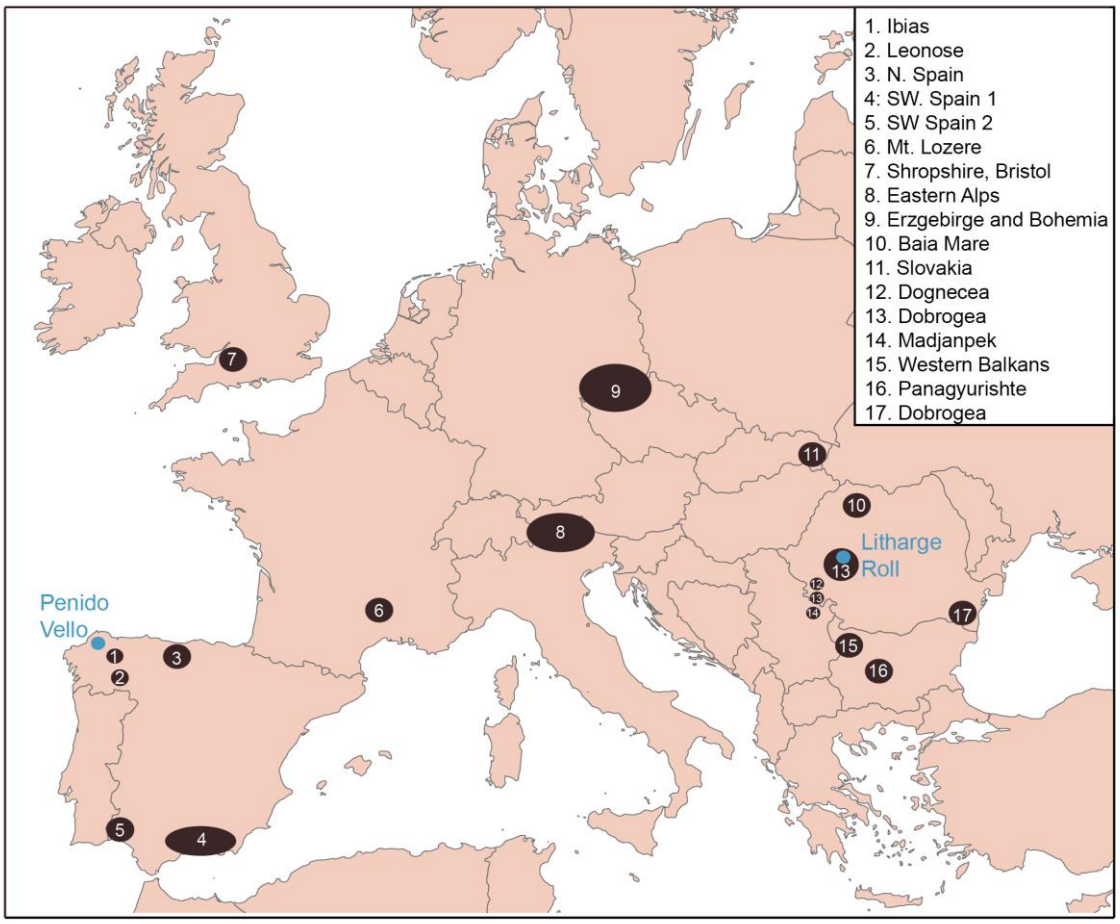

Figure 6.1*: Outline map of Europe displaying the location of the studies utilised in this Chapter; Penido Vello bog and a litharge roll from Rosia Montana (blue circles). Also shown are all mining regions modelled in the three example studies.*

a few possible sources may be considered, or only a couple of broad sources are of interest (e.g. Monna et al. 2000; Brugam et al. 2011). This approach allows identification of very general source inputs, such as anthropogenic vs lithogenic Pb, but the lack of further source consideration precludes defined provenance of such Pb to an ore body or mining region (Brugam et al., 2011). This is due to the limitations related to the models and the Pb isotope systems themselves, where generally only two or three isotope ratios (n) are interpreted, and such models are limited to n+1 sources. These types of models, therefore, may be useful, but the complexity of potential Pb inputs, particularly in an anthropogenically polluted world, cause such approaches to be likely oversimplifications, with only limited conclusions possible (Brugam et al., 2011).

In the field of biology, mixing models have long been used to apportion large numbers of prey sources within a predator's diet (e.g. Inger et al. 2006; Layman et al. 2012; Benstead et al. 2006), from stable isotope compositions using mixing models such as IsoSource (Phillips and Gregg, 2003) and MixSIAR (Parnell et al., 2010; Stock and Semmens, 2013).

When IsoSource was developed, an initial attempt to apply it to pollution sourcing via Pb isotopes was made (Phillips and Gregg, 2003). However, to our knowledge, little further work to apply this method to the field has been done (Soto-Jiménez and Flegal, 2009). Other approaches to Pb isotope modelling have been applied, with Euclidean distance calculation used to determine potential source(s) for archaeological artefacts (Ling et al., 2014; Stos, 2009). This method, however, simply indicates the most likely ores (or mines) within the database.

Application of more complex models to Pb isotope tracing, therefore, could provide a new approach to source apportionment, with potentially a better understanding of past pollution input than might be achieved solely through 3-isotope graphing or Euclidean distance modelling. In practice, this may be able to produce more reliable tracing of Pb in the environment, as far more potential sources can be considered, and less simplification of the system is necessary. This approach could be applied to the interpretation of indirect records (such as from peat, lake sediments and ice) of historical pollution, modern pollution, and even the origin of metal used in archaeological artefacts.

Here a best practice approach is proposed for applying a state-of-the-art Bayesian stable isotope mixing model (MixSIAR; see Chapter 2) to pollution sourcing and artefact tracing via Pb isotopes. Firstly the approach is applied to pre-anthropogenic samples from a peat bog in north-western Spain (Kylander et al., 2005) to track the changing influence of Saharan dust on the Pb isotope ratio. Secondly, an example utilises data from the same site but from a period of heavy pollution (namely the Roman period) to trace likely ore sources of Pb within the bog. Finally, the ability of MixSIAR to consider a very large number of sources is exploited to investigate sources of Pb in a litharge roll discovered in Romanian mine, dating back to the Roman period (Baron et al., 2011).

***Table 6.1**: Calculated atom weight percentages, and standard deviations for all sources investigated in this study. Also presented are the a priori groups used in examples 2 and 3.*

1A: Example, Pre Anthropogenic Dust Tracing							
	Calculated Atom Weight %			**Standard Deviation**			**Reference**
Source	$^{206}Pb/^{204}Pb$	$^{207}Pb/^{204}Pb$	$^{208}Pb/^{204}Pb$	$^{206}Pb/^{204}Pb$	$^{207}Pb/^{204}Pb$	$^{208}Pb/^{204}Pb$	
Local Soil	0.27909	0.20928	0.49836	<0.001	<0.001	<0.001	(Kylander et al., 2005)
Local Rock	0.24999	0.20875	0.52793	0.05250	0.01850	0.47250	(Kylander et al., 2005)
Saharan Dust	0.25495	0.20999	0.52171	0.10044	0.02426	0.14379	(Abouchami and Zabel, 2003)

Upper Continental Crust	0.25430	0.20879	0.52368	<0.001	<0.001	<0.001	(Kramers and Tolstikhin, 1997)

1B: Example 2, Anthropogenic Pollution Tracing in Peat

Source		**Calculated Atom Weight %**			**Standard Deviation**			**Reference**
A Priori Group	**Fields Included**	$^{206}Pb/^{204}Pb$	$^{207}Pb/^{204}Pb$	$^{208}Pb/^{204}Pb$	$^{206}Pb/^{204}Pb$	$^{207}Pb/^{204}Pb$	$^{208}Pb/^{204}Pb$	
SW Spain 1	Almeria, Andalusia, Mazarron & Cartagena	0.25204	0.21090	0.52361	0.00103	0.00058	0.00054	(Ruiz et al., 2002; Stos-Gale et al., 1995)
SW Spain 2	Huelva	0.24899	0.21397	0.52337	0.00011	0.00011	0.00013	(Pomiès et al., 1998; Stos-Gale et al., 1995)
N Spain	Reocin	0.25269	0.21140	0.52241	0.00011	0.00003	0.00009	(Velasco et al., 2003)
NW Spain 1	Ibias	0.24655	0.21502	0.52479	0.00058	0.00044	0.00096	(Arias et al., 1996)
NW Spain 2	Leonose	0.24637	0.21546	0.52436	0.00020	0.00003	0.00019	(Tornos et al., 1996)
Gaul	Mt Lozere	0.25042	0.21226	0.52379	0.00064	0.00034	0.00041	(Baron et al., 2006)
England	Shropshire, Bristol	0.24941	0.21340	0.52357	0.00105	0.00073	0.00037	(Rohl, 1996)
PPA		0.26291	0.20955	0.51421	<0.001	<0.001	<0.001	(Kylander et al., 2005)

1C: Example 3, Artefact Tracing

Source		**Calculated Atom Weight %**			**Standard Deviation**			**Reference**
A Priori Group	**Fields Included**	$^{206}Pb/^{204}Pb$	$^{207}Pb/^{204}Pb$	$^{208}Pb/^{204}Pb$	$^{206}Pb/^{204}Pb$	$^{207}Pb/^{204}Pb$	$^{208}Pb/^{204}Pb$	
Apuseni Epithermal	Baia de Aries, Sacarimb, Coranda, Rosia Montana	0.25195	0.21144	0.52310	0.00054	0.00009	0.00056	(Baron et al., 2011; Marcoux et al., 2002)
Apuseni Porphyry	Rosia Poieni, Balea Morii	0.25265	0.21159	0.52224	0.00011	0.00011	0.00021	(Marcoux et al., 2002)
Apuseni VMS	Vorta, Dealul Mare	0.25105	0.21223	0.52315	0.00002	0.00005	0.00007	(Marcoux et al., 2002)
Bohemia	Horní Slavkov, Příbram-Vrancice, Kutná Hora	0.24937	0.21382	0.52310	0.00098	0.00039	0.00056	(Niederschlag et al., 2003)
Central Erzgebirge	Bärenstein, Annaberg, Měděnec, Marienberg, Hora Sv. Kateřiny	0.24896	0.21372	0.52362	0.00110	0.00073	0.00037	(Niederschlag et al., 2003)
Dobrogea	Altan Tepe, Somova	0.25114	0.21298	0.52229	0.00081	0.00089	0.00041	Unpublished data
Dognacea	Dognacea	0.25144	0.21179	0.52324	0.00000	0.00000	0.00000	Unpublished data
Eastern Erzgebirge	Freiberg, Sadisdorf, Zinnwald	0.24865	0.21377	0.52386	0.00054	0.00038	0.00032	(Niederschlag et al., 2003)

Ghezuri	Ghezuri	0.25245	0.21094	0.52316	0.00012	0.00001	0.00013	(Marcoux et al., 2002)
Ilba	Ilba	0.25325	0.21056	0.52275	0.00011	0.00003	0.00010	(Marcoux et al., 2002)
Madjanpek	Madjanpek	0.25079	0.21299	0.52260	<0.001	<0.001	<0.001	(Amov, 1999)
Moldova Noua	Moldova Noua	0.25423	0.21119	0.52108	0.00000	0.00000	0.00001	Unpublished data
Northern Erzgebirge	Schönborn, Gersdorf	0.24948	0.21283	0.52405	0.00039	0.00033	0.00005	(Niederschlag et al., 2003)
Oberlausitz	Ludwigsdorf	0.24962	0.21284	0.52389	0.00021	0.00008	0.00026	(Niederschlag et al., 2003)
Pangyurishte	Vlaikov Vruh, Elshitsa, Radka, Assarel, Medet, Chelopech, Elasite	0.25103	0.21295	0.52241	0.00021	0.00015	0.00014	(Amov, 1999; Von Quadt et al., 2002)
SW Spain 1	Almeria, Andalusia, Mazarron & Cartagena	0.25204	0.21090	0.52361	0.00103	0.00058	0.00054	(Ruiz et al., 2002; Stos-Gale et al., 1995)
SW Spain 2	Huelva	0.24899	0.21397	0.52337	0.00011	0.00011	0.00013	(Pomiès et al., 1998; Stos-Gale et al., 1995)
Sasar	Sasar	0.25268	0.21078	0.52311	0.00006	0.00004	0.00011	(Marcoux et al., 2002)
Slovakia	Banska Stiavnica, Brehov, Rosalia	0.25288	0.21036	0.52334	0.00055	0.00012	0.00056	(Chernyshev et al., 2007)
Other Baia Mare	Baia Sprie, Cavnic, Herja, Suior	0.25322	0.21055	0.52279	0.00021	0.00010	0.00013	(Marcoux et al., 2002)
Eastern Alps	Calceranica, Vetriolo, Valle Imperina	0.24670	0.21515	0.52440	0.00043	0.00025	0.00020	Artioli et al., 2016
Vogtland	Schönbrunn, Lauterbach, Gottesberg, Mühlleithen, Klingenthal	0.24795	0.21387	0.52446	0.00166	0.00121	0.00051	(Niederschlag et al., 2003)
Western Balkans	Sedmochlinesti, Chiprovitsi, Berkovitsa	0.25094	0.21308	0.52234	0.00003	0.00004	0.00005	(Amov, 1999, 1983; Stos-Gale et al., 1998)

6.2. Methods and Materials

6.2.1. Why use MixSIAR?

The primary advantages using MixSIAR as opposed to more simple mixing models such as IsoSource, or distance-based models are related to the much more rigorous nature of the model. Bayesian statistics allow the incorporation of prior knowledge of a system into modelling of the system, and most pertinent to this approach, source variability. Within Pb isotope systems and models, this allows the user to input (where data is available) two prior components; error and concentration. The incorporation of error is of particular importance as it allows for models to compensate for both methodological error (instrument-derived standard deviations), and sampling 'error', or heterogeneity in the isotopic ratio of samples from the same site.

The use of MixSIAR also utilises a far more rigorous mathematical approach than more simple linear models. Firstly, the structure used to model source proportions is more complex, utilising an isometric log-ratio (ilr) approach to transform the raw data in the simplex into a vector space divided into orthogonal subspaces (Egozcue et al., 2003). Practically, this allows a simplex developed from widely ranging variables to be interpreted more simply, and removes issues relating to differing ranges for individual isotope ratios (Parnell et al., 2013). Secondly, the use of Gibbs sampling allows for a multivariate distribution to be considered in the sampling of possible mixtures in the vector space (Plummer, 2003), whilst not requiring the user to tune the data. Using the Just Another Gibbs Sampler (JAGS) framework written in R, Markov Chain Monte Carlo (MCMC) methods sample the (multivariate) posterior probability distribution and incorporate a number of tests to ensure the reliability of the data (Parnell et al., 2013). Running the model for longer improves the quality of the sample, and ensures it is representative of the true probability distribution (Plummer, 2003).

6.2.2. Pre-Modelling Preparation

Prior to any modelling (see Chapter 2 for methods), one must ensure that all potential sources (mining regions active during the period of study, active smelters, natural Pb sources) that may have contributed to the Pb isotope signal at the study site are considered in the analysis. For modern applications, the approach is complicated by the fact that potential sources will have changed over time, or that ores once actively mined may have been exhausted. Here, modelling results for bulk peat Pb isotope samples and of an artefact of mining are discussed, with possible sources that contributed to each site outlined in Table 6.1. All potential sources (with sufficient data available) must be considered, regardless of locality, including long-range transport of Pb. Further, for pollution tracing of

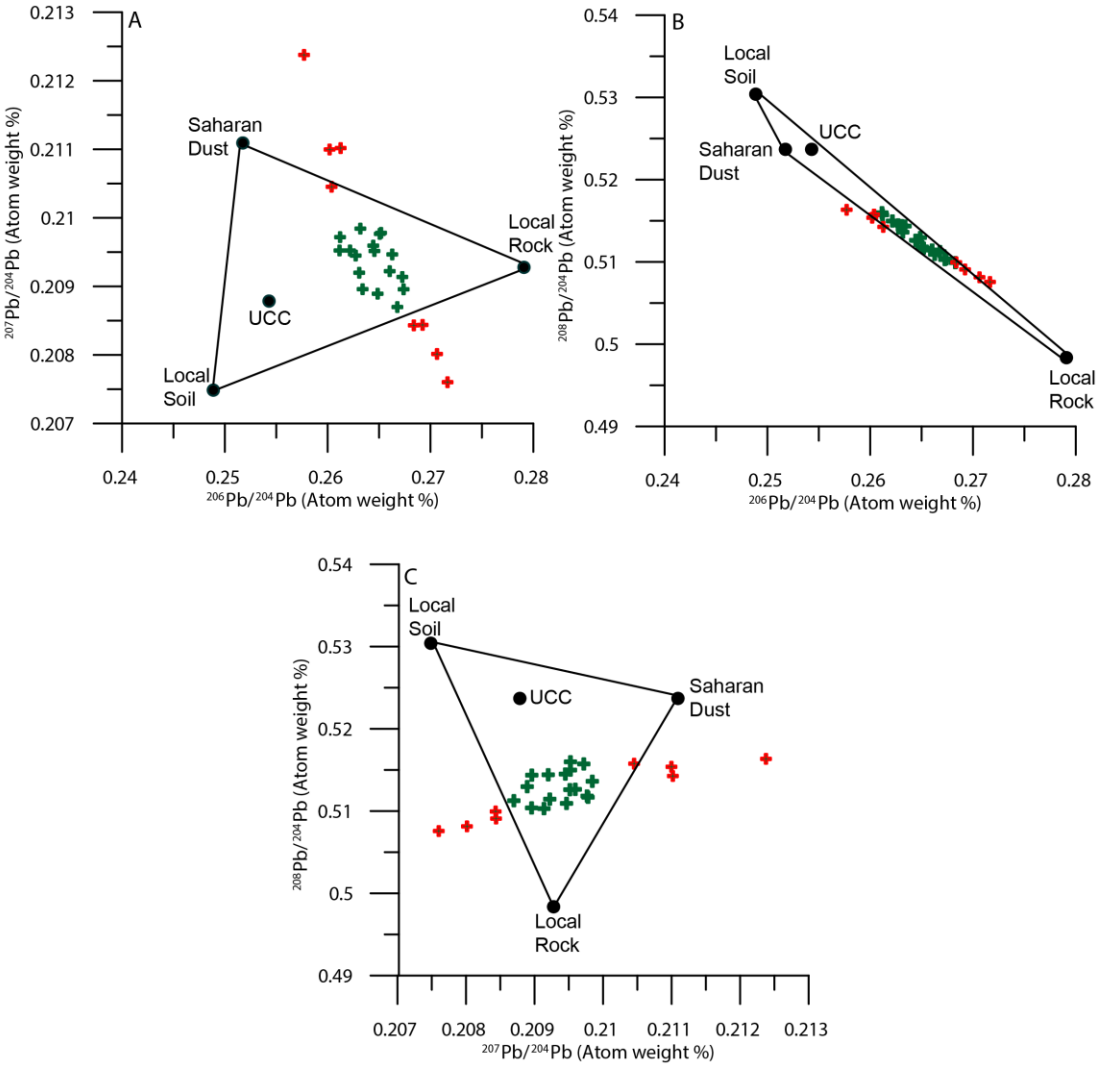

Figure 6.2*: Convex hulls from example 1 (pre-anthropogenic dust tracing). Each is a three-isotope plot displaying the four sources modelled in this example. Lines have been added to outline the mixing envelope. Also shown are the transformed isotope ratios from Penido Vello core between 5000–1200 BCE. Samples which fall within the convex hulls are marked in green whilst those which fall outside one or more are red, and have not been modelled.*

sediment samples, a local 'natural' Pb isotope signal should be introduced to the model, to ensure any such local minerogenic input of Pb is considered.

All data must be collated, and a database of all signatures prepared. As suggested by Garçon et al. (2012) and Baron et al. (2014), Pb isotope ratios relative to ^{204}Pb should be used (i.e. ^{208}Pb/^{204}Pb, ^{207}Pb/^{204}Pb and ^{206}Pb/^{204}Pb). This allows for as much of the possible variability in the isotopic signature to be considered as possible during the modelling. Since isotope ratios do not combine linearly, raw ratios should be converted into atom weight percentages at this point.

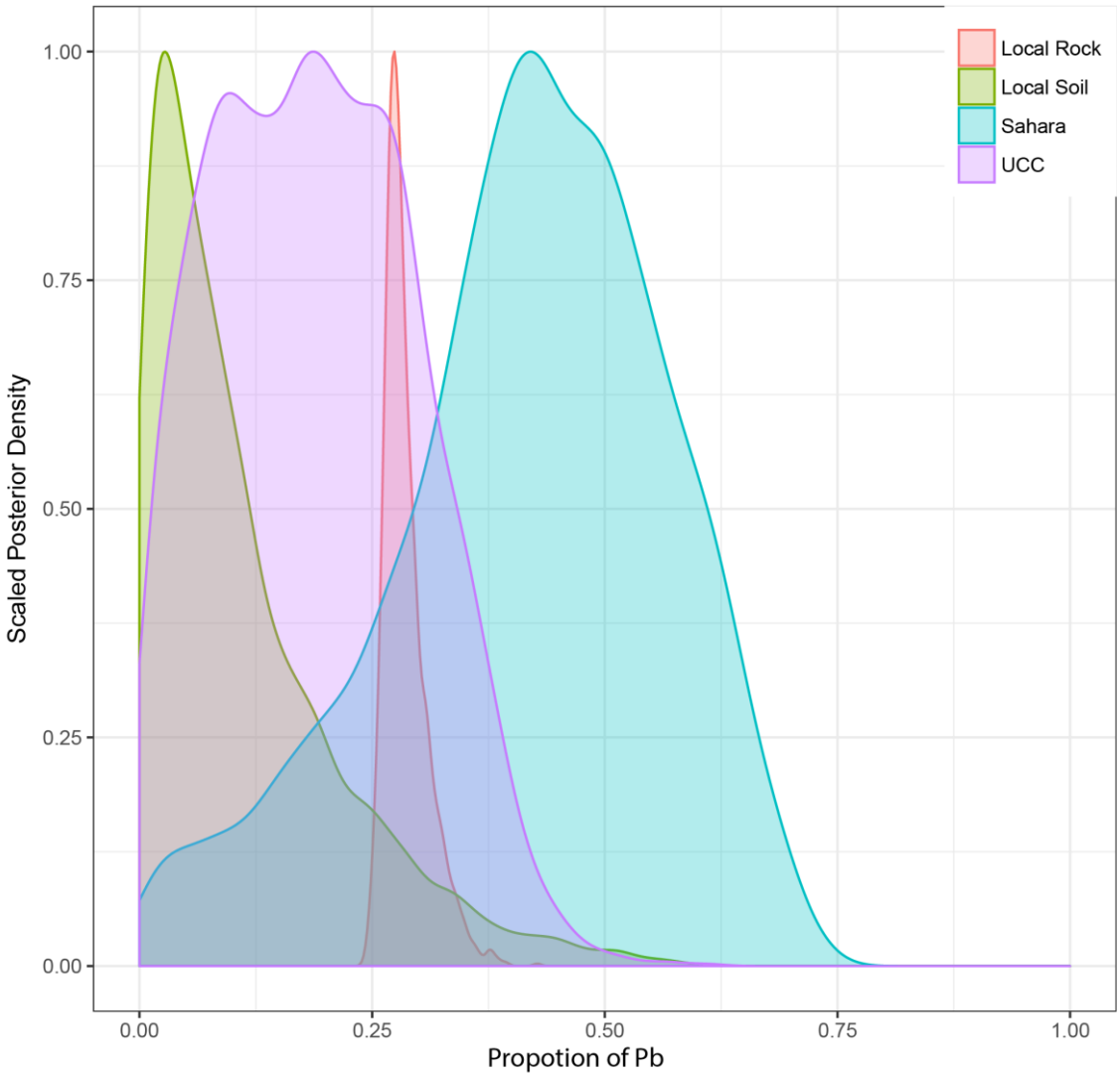

Figure 6.3: *Example posterior density graph as output from MixSIAR. The example shown here is from Penido Vello core at 1262 BCE.*

If several analyses are available for the same site, these data should be averaged and standard deviations calculated. Grouping, one of the most important parts of this analysis, should be approached robustly and can be done *a priori*, or *a posteriori* (Phillips et al., 2005). *A priori* grouping should be carried out to align sources (prior to the analysis) which are very similar in isotopic signature, or are all from the same ore field. Significance tests (see Phillips et al. 2014) may be performed, to ensure that the groups are significantly different. If not, they should be grouped together.

For the first two example model runs, characterising the likely sources of Pb deposited via atmospheric loading in a peatbog is of interest, using a list of potential sources as outlined in the original publication (Kylander et al., 2005). For analysis of the litharge roll, all

published local, regional, and extraregional potential sources of Pb that may have contributed were considered (See Table 6.1, Fig. 6.1).

Examples of *a priori* grouping has been performed on the litharge-roll related dataset (Table 6.1C), with examples observable from both the Apuseni and Baia Mare mining fields. The Apuseni data has been grouped using mineralisation type, with epithermal, porphyry and volcanogenic massive sulphides (VHMS) fields, respectively (Table 6.1C). Conversely, Baia Mare field have been grouped by isotopic signature, with the grouping of Suior, Baia Sprie, Cavnic, Herja fields, whilst the isotopically distinct Ghezuri, Ilba and Sasar fields are not grouped *a priori* (Table 6.1.C).

6.2.3. Pre-Run Checks

Prior to running any analyses, checks must be performed to ensure the mixture data falls within the mixing envelope (Phillips and Gregg, 2003) as determined via the sources identified. Due to the nature of MixSIAR (Stock and Semmens, 2013) results are produced even when these are not realistic. Thus, it is imperative convex hulls (Fig. 6.2) must be produced, and all mixtures must fall within them. If they do not, then it is a clear indication there is an issue in the analysis: either errors during measurement, or a significant source of Pb has been overlooked (Phillips and Gregg, 2003). Instances of this issue may be observed from the first example (Fig. 6.2), where a number of samples fall outside the designated potential sources, and so are not interpreted. As all sources must be considered, sources may fall within the convex hull (Fig. 6.2).

6.2.4. Post-Run Checks

Once all the preparation steps have been completed, the model should be run (see Chapter 2 for details). The model utilises Markov Chain Monte Carol (MCMC) statistics, which investigate probability distributions for variables (in this example the proportion of Pb coming from each source). From this 'posterior' distribution (see Fig. 6.3), descriptive statistics including mean, standard deviation and range may be produced. To ensure meaningful results, the MCMC chains must be long enough for convergence to be achieved. Convergence of the data may be checked via two diagnostics post-run: Gelman-Rubin and Gewecke tests (Phillips et al., 2014; Stock and Semmens, 2013). The Gelman-Rubin test requires at least one chain, and values will be near 1 at convergence, therefore high values indicate non-convergence. The Gewecke test compares the two halves of the MCMC chain, and develops z-scores to determine convergence. High z-scores are an immediate indicator of non-convergence, and so a longer run must be performed (Stock and Semmens, 2013).

In practice, with many sources and three isotope ratios, MixSIAR generally must be set to either 'long' or 'very long' MCMC chains to achieve satisfactory convergence. However, this may vary, and so it is a valuable exercise checking the post-run diagnostics, and in running the model at various lengths. For all models discussed here, 'long' or 'very long' MCMC chains have been run.

For the anthropogenically-influenced example mixtures, and particularly the litharge roll dataset (Table 1C), the large number of sources means distinct source apportionment is difficult, as all source regions display wide ranges (Table 6.2). However, when fewer sources are used, such as the pre-anthropogenic dust example, raw proportions show well-defined results, and so conclusions may be drawn without further grouping (Fig. 6.4).

6.2.5. A Posteriori Grouping

Pb isotope modelling generally considers many sources, and often the output from a model run will be disparate, and with few clear major contributors (Example 3, Table 2). At this point, further grouping *a posteriori* is suggested (Phillips et al., 2014). This combines raw contribution results in order to produce better-constrained (in terms of percentage) contributions, but at the expense of specificity of sources. In practice, this means a user will not be able to discern between ore bodies, but will be able to indicate more reliably which groups of ore bodies (or major mining regions) are significant contributors. As with *a priori* grouping, this should be performed on groups which are still isotopically similar, or are located close (in terms of distance, or isotopic composition) to each other, allowing for meaningful conclusions to be drawn, despite the simplification this approach causes.

Using these examples, it is clear further grouping is necessary for the litharge roll (Table 6.2), since each group has a wide possible range of contributions. Thus, *a posteriori* grouping has been performed on all examples, combining sources to minimise the number of possible end-members (Table 6.3). For each possible mixture, all sources to be grouped should be summed (Phillips et al., 2005). In the litharge roll example, this approach has resulted in clearer contributions. The combination of three Baia Mare groups, and the Slovakian group (all with similar mineralisation types and ages, and relatively small distances between fields), displays this (Table 6.3). As can be seen from the raw data (Table 6.2) these groups, when considered individually, did not have a significant contribution, but when they are combined, the signal of mining and smelting from this region becomes clearer (Table 6.3). This approach has its advantages in clarifying broad source areas. However, it does remove some of the certainty to the approach, as it requires further grouping, at times erasing distinct fields. Nevertheless, without grouping, it is

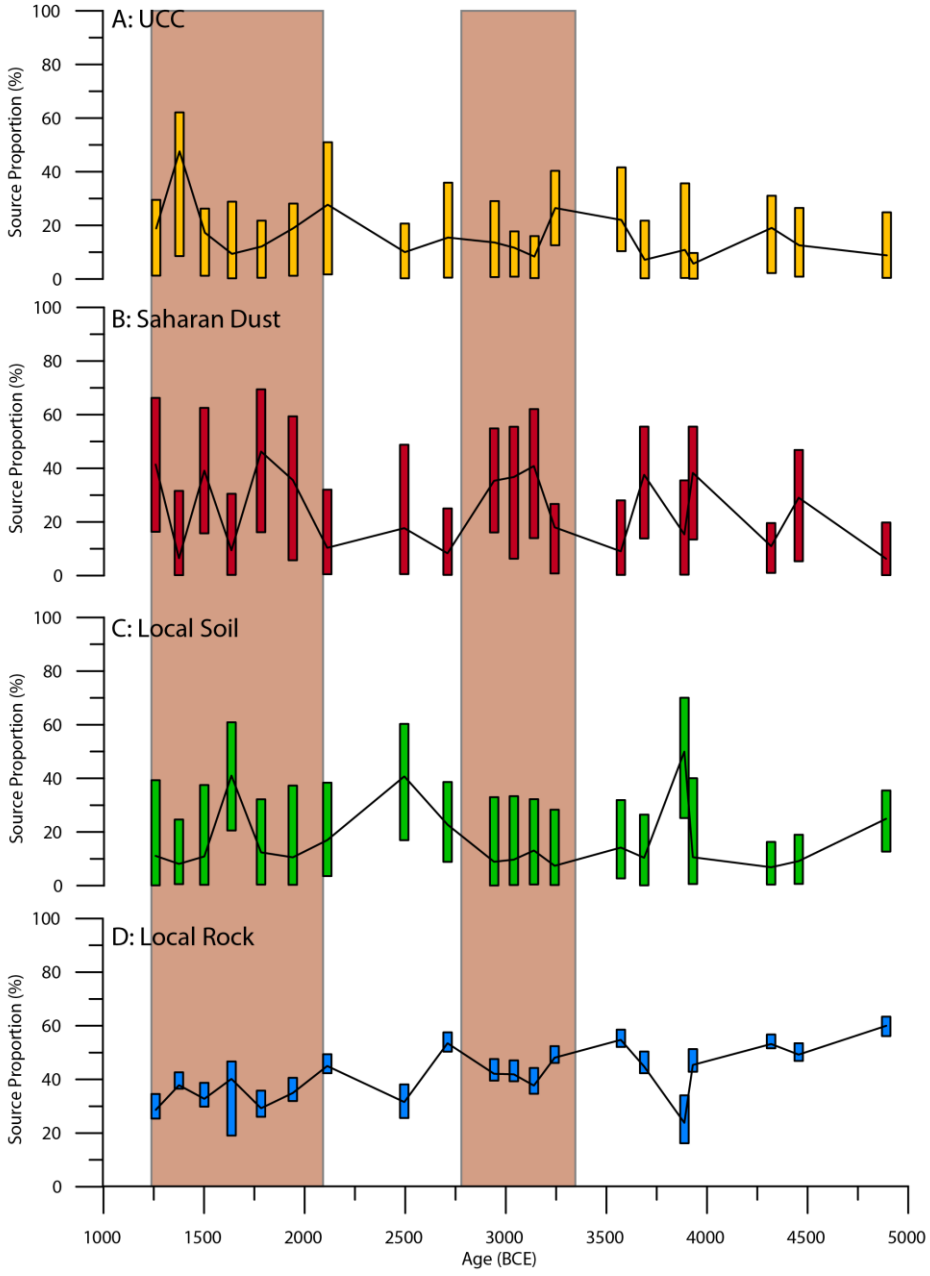

Figure 6.4: *Model output from the pre-anthropogenic samples at Penido Vello. In each case, the rectangle indicates the range of outputs, with the upper and lower bounds signifying the 2.5% and 97.5% confidence intervals, while black lines trace the mean value. Brown rectangle indicate periods of Saharan influence.*

difficult to say with any certainty that any of these fields provided meaningful contributions to the Pb isotope signature, and so *a posteriori* grouping is a valuable tool when interpreting data which initially appears unconstrained.

This data, once produced, should be presented either as it is here, in table form (e.g. Table 6.2, 6.3) or via figures (Fig. 6.4, 6.5, 6.6), but always outlining the entire range of results (see Phillips et al., 2014), and not simply the mean.

6.3. Results and Discussion

6.3.1. Example 1: Pre-Anthropogenic Dust Sourcing

Due to the prevalence of anthropogenic Pb in the biogeochemical system since the inception of metallurgy, Pb isotopes are an imperfect tracer of natural fluxes (Scheuvens et al., 2013). However, because of the ability of Pb isotopes to record source signatures, they have been applied to dust tracking studies (Grousset and Biscaye, 2005). Using a selection of natural geogenic sources, we attempt to indicate the source of pre-human lead in the geochemical cycle within Penido Vello, a peat bog in north-west Spain (Kylander et al., 2005), for the period 5000–1300 BCE. Using sources determined in the original publication, the isotopic ratio of local rock and the signal of local soil to represent local inputs is modelled, whilst also modelling input from potential Saharan sources (Abouchami and Zabel, 2003) and a general crustal value (Kramers and Tolstikhin, 1997). Since only four potential sources are considered here, no grouping has been performed *a priori* (Table 6.1.A), allowing for visualisation of posterior densities (Fig. 6.3).

Prior to modelling, mixing diagrams were developed (Fig. 6.2) indicating a number of samples fall outside of the mixing envelope. As such, models were developed only for those which fall within the envelope. Those which were modelled appear to show periodic influx of Saharan dust into the site, with two main periods of high Saharan proportions (3300 – 2800 BCE and 2100 – 1300 BCE). Outside of these times, the Pb isotope signal

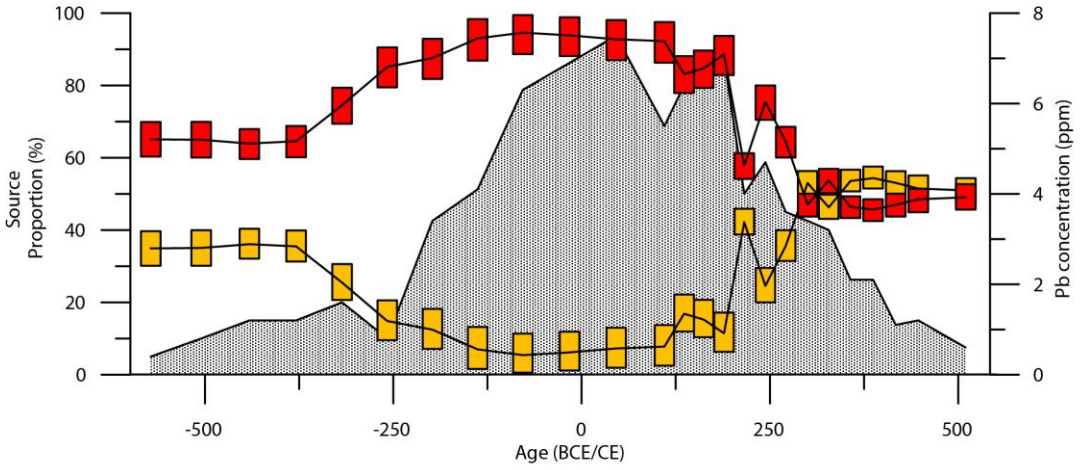

Figure 6.5: *Model output from PVO between 600 BCE and 550 CE. Red rectangles correspond to a posteriori grouping of all anthropogenic sources, while yellow rectangles are the modelled contribution from natural (Pre-pollution aerosol). Rectangles indicate upper and lower bounds as in figure 4, with black lines indicating the mean. Also shown (shaded black) is the raw Pb concentration for Penido Vello core throughout this period.*

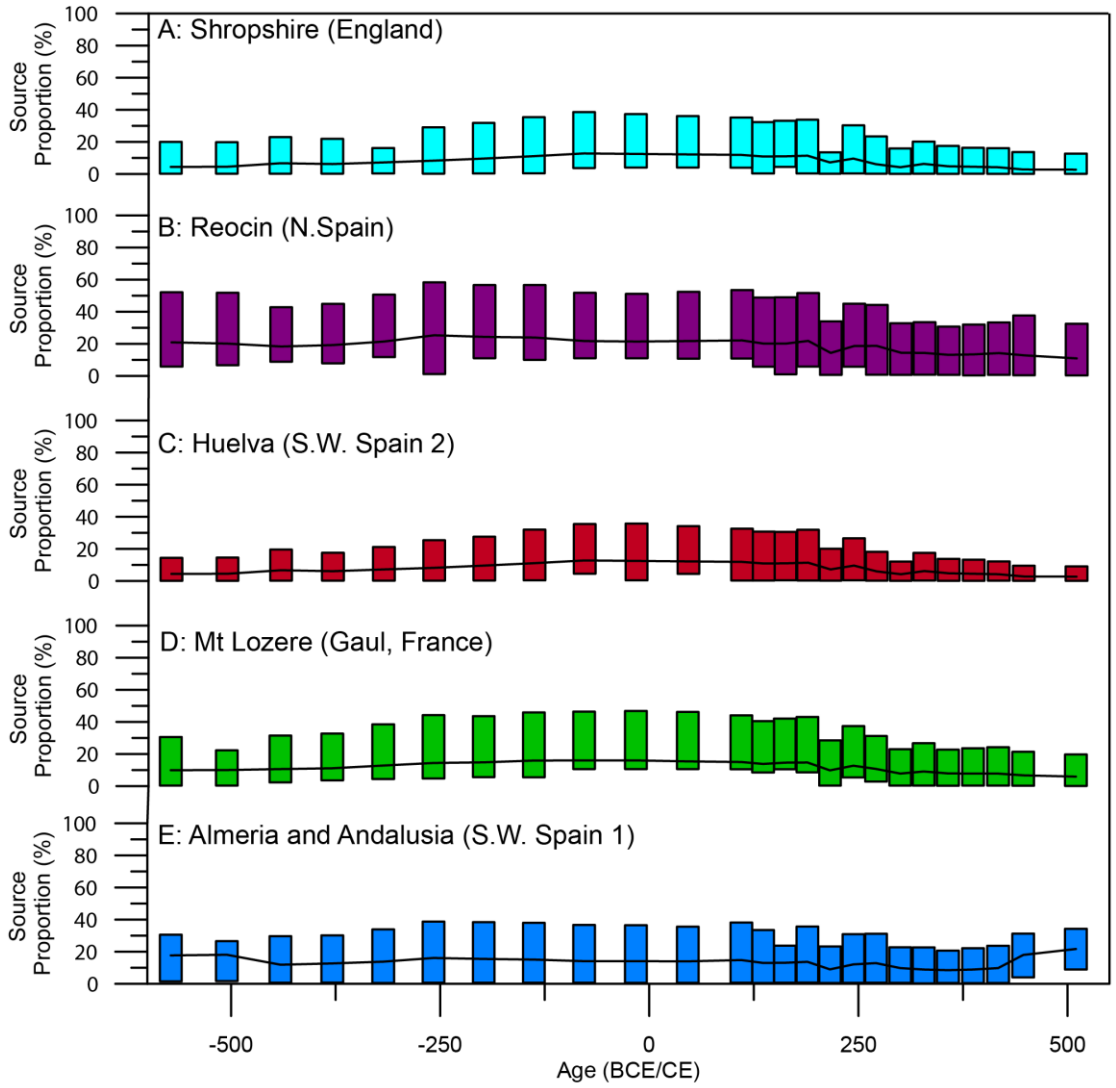

Figure 6.6: *Model output from Penido Vello between 600 BCE and 550 CE, displaying the contribution of individual mining regions. Again, rectangles indicate upper and lower bounds as in Figure 6.4, with black lines indicating the mean.*

appears to be a mixture of rock and soil, but with occasionally high UCC contributions (e.g. 1375 BCE).

This modelling corresponds well with the original publication, where simple distance-based modelling indicated clear Saharan input midway through the period (3300-2800 BCE) (Kylander et al., 2005). The model outputs also reflect previously observed increase in Saharan input towards the end of the phase (2100– 300 BCE). The first period of increased input correlates well with well-constrained desertification in the north-western Sahara and subsequent dust deposition (Albani et al., 2015; Egerer et al., 2016; McGee et al., 2013), whilst the second may be one of the periodic pulses of Saharan dust deposition common in the western Mediterranean (Debret et al., 2007; Jiménez-Espejo et al., 2014). A decreasing trend throughout the whole period for local rock (Fig. 6.4.D) and increasing

local soil proportions (Fig. 6.4.C) appears indicative of local soil erosion related to farming and agriculture, with an increase in intensity throughout the time period, echoing pollen records (Martínez Cortizas et al., 2005).

6.3.2. Example 2: Pollution Sourcing from Environmental Archives

To investigate possible anthropogenic sources to the same bog as above during a period of intense metallurgy (namely the Roman period), a series of likely sources has been determined (See Table 6.1.B), including a natural pre-pollution aerosol (PPA) value as determined by Kylander et al., 2005. Here, some *a priori* grouping was necessary due to the similar isotopic signal of a number of south-western Spanish ore bodies (Andalusia, Almeria and Cartagena, Table 6.1.A).

No *a posteriori* grouping was performed as it was possible to make conclusions from the raw results. However, the first main point of interest is the changing contribution of natural (as represented by PPA) and anthropogenic (the remainder) sources (Fig. 6.5). Early in the period anthropogenic sources make up ~60% of the Pb, prior to increasing values over the period 350 – 200 BCE, before plateauing at roughly 90 % between 100 BCE – 150 CE (Fig. 6.5). These values reflect the development of the Roman metal industry, from the acquisition of Hispania during the Punic wars by 146 BCE (Hoyos, 2011), through their exploitation, to the combined pressure of source exhaustion (Settle and Patterson, 1980) and repeated invasions of Hispania by the Moors from 170 CE onwards (Edmondson, 1989). The coherence of the modelled record with the raw concentration data (Fig. 6.5) indicates the reliability of the model and its ability to disentangle human sources from natural.

Unfortunately, due to overlapping fields, many of the modelled ore-related proportions are unconstrained. However, some conclusions are still possible, with Almerian and Andalusian contributions remaining fairly steady throughout (Fig. 6.6.F), indicating continuous exploitation, whilst all other mining regions reflect the developmental trend indicated by overall anthropogenic proportion changes (Fig. 6.6), confirming the Roman exploitation of a variety of sources. Reocin ore field (of the Basque-Cantabrian basin in Northern Spain) generally appears the largest contributor to Penido Vello mixtures, with around 20% of the Pb in most models attributable to this source. This corroborates previous indications of exploitation in the region during the Roman period (Irabien et al., 2012; Monna et al., 2004a), evidence for which has been destroyed by more recent utilisation.

Interestingly, mining outside of Spain appears to have also had an impact on the isotopic mixture recorded here, with both Gaul (southern France) and Shropshire (England) appearing to change from very low contribution values at the start of the period, with both peaking at roughly 15% contribution by 30BCE (Fig. 6.6.B, 6.6.E).

***Table 6.2**: Raw MixSIAR results for the litharge roll. Presented here are the source names, along with their modelled contribution. Data is presented here as a mean value, alongside lower and upper bounds, signifying the modelled range within 2.5–97.5% confidence.*

A Priori Group	Mean	2.50%	97.50%
Apuseni Epithermal	3.41%	0.10%	13.39%
Apuseni Porphyry	5.54%	0.14%	19.53%
Apuseni VMS	2.90%	0.08%	10.33%
Bohemia	2.12%	0.07%	7.48%
Central Erzgebirge	1.86%	0.05%	6.41%
Dobrogea	3.14%	0.08%	11.11%
Dognacea	3.03%	0.09%	10.49%
Eastern Erzgebirge	1.83%	0.05%	6.19%
Ghezuri	3.61%	0.09%	12.38%
Ilba	4.67%	0.15%	14.61%
Madjanpek	2.95%	0.07%	10.19%
Moldova Noua	33.09%	21.73%	41.95%
Northern Erzgebirge	1.92%	0.04%	6.51%
Oberlausitz	1.96%	0.04%	7.19%
Pangyurishte	3.26%	0.08%	11.04%
SW Spain 1	2.91%	0.10%	10.71%
SW Spain 2	2.22%	0.07%	7.60%
Sasar	3.64%	0.10%	12.12%
Slovakia	3.51%	0.08%	11.67%

6.3.3. Example 3: Modelling of Artefact Provenance

Another potential application of MixSIAR and isotope mixing is the interpretation of the Pb isotope signal as recorded in individual metal artefacts. Determining the provenance of metal artefacts is of crucial importance in archaeology, and Pb isotopes have previously been utilised to this end in several previous studies (e.g. Stos-Gale et al. 1995; Ling et al. 2014; Pernicka et al. 2016). Here MixSIAR is applied, in much the same way as applied above to a substrate mixture, to the Pb isotope mixture of a litharge roll recovered from a Roman-age mining site in Romania. To determine source contributions, a dataset of potential sources has been put together (Table 6.1.C, Fig. 6.1).

Due to the large number of sources, initial results indicate a wide range of potential origins for the Pb, but with Moldova Noua apparently the clearest single source (Table 6.2). To interpret the data more easily, *a posteriori* grouping has been performed. Here, sources have generally been grouped by proximity (e.g. Baia Mare fields, and German fields). However, others have been grouped by mineralisation and similar isotopic signature. An example of this is the inclusion of Apuseni Volcanogenic Massive Sulphides with other ores from the same mineralisation

belt; the Banatic Metallogenic Province (von Quadt et al., 2005) such as Moldova Nuoa and Madjanpek (Table 6.3, Fig. 6.1).

From the grouped results it is clear Banatites make up the majority of the Pb in the litharge roll, with an average of nearly 50%, whilst Baia Mare Pb appears to contribute much of the remainder. Interestingly, the Apuseni group, which contains the Rosia Montana deposit where the litharge roll was discovered, does not constitute a major proportion (Table 6.3). This is very much in line with the original publication's conclusions, as Baron et al. (2011), deduce the lead contained within the artefact was not from the Apuseni Mountains. The model appears to suggest a Banatic source is dominant, and within that, Moldova

Table 6.3: *A posteriori grouping of raw MixSiar results as displayed in Table 6.2, from the Litharge Roll.*

A Posteriori **Group**	**Included *a priori* groups**	**Mean**	**2.50%**	**97.50%**
Apuseni	**Apuseni Epithermal, Apuseni Porphyry**	8.94%	1.14%	24.54%
Banatites	**Apuseni VMS, Dognecea, Moldova Nuoa, Madjanpek, Panagyurishte, Western Balkans**	48.56%	34.38%	60.98%
Germany	**Bohemia, All Erzgerbirge (Central, Eastern. Northern), Oberlausitz, Vogtland**	9.26%	3.55%	16.62%
Baia Mare	**Ghezuri, Ilba, Sasar, Slovakia, Other Baia Mare**	19.88%	9.77%	30.76%
Spain	**SW Spain 1, SW Spain 2**	6.92%	1.64%	16.19%
Eastern Alps	**Eastern Alps**	1.37%	0.04%	4.64%

Nuoa as the most likely single location. Evidence for mining in the Banat region is widespread, with Moldova Noua falling within the so-called 'Golden Quadrilateral' of Au mineralisation (Vlad and Orlandea, 2012), extensively exploited during the Roman period (Borcoş and Udubaşa, 2012).

6.3.4. Period Pollution

One of the further advantages of MixSIAR is that it was developed to investigate populations of species, and not just individuals. As such it allows the user to analyse more than one mixture at a time, and provide overall results for the dataset. In practice, this can allow a user not just to obtain proportions at discrete points in time, but to get an overall indication for an entire period. In the examples used here, all mixtures have been run separately, and increases and decreases in certain sources may be observed. When all mixtures are run together, a much broader picture of pollution over a longer period may be

produced. This is a faster process than modelling each individual mixture, and therefore may be useful for getting a better understanding of the dataset, or for comparing a few datasets covering a short period.

6.4. Conclusions

Bayesian mixing models, as developed for food-web studies, may be used to understand sources of pollution via Pb isotopes. In a system where many sources are likely, they are a much more realistic approximation of the real world than the simple binary or ternary mixing currently utilised for such studies. Furthermore, they allow for incorporation of errors, and as such provide a more complex and exhaustive approach.

The model results, of course, depend on the quality of the data input. As such, it is vital thorough literature reviews are carried out prior to any analysis, and that all potential sources are considered. This is likely to produce very wide range values, for many sources. In terms of best practice, the approach described here, outlining both *a priori* and *a posteriori* grouping is only essential when first working on a dataset. An *a posteriori* grouping approach as outlined here therefore may be applied to clarify what are likely to be the main sources, albeit at the cost of some specificity. Once groups have been determined, it is necessary to perform only one of the grouping methods on each mixture. Some systems, however, will not produce clear results. If the isotopic range for sources overlap, or are very close, the model may be unable to distinguish separate inputs to the mixture. In other cases, unknown and uncharacterised sources may result in the mixture falling outside the mixing envelope, after which any results are meaningless. A rigorous approach to source characterisation and model parametrisation, however, may rule out errors such as these. Finally, as good as the models may be, they will only ever be approximations, and as such, using them alongside more traditional provenance methods is recommended (e.g. 3-isotope plotting of all data). Such a dual method approach is likely to produce the most reliable source characterisation.

Chapter 7. Conclusions and Outlook

7.1. Summary of the Research Project

This research project investigated, via a number of Carpathian and Balkan bogs and a multi-proxy approach, the Holocene history, both natural and human, of the Carpathian-Balkan region. Specifically, detrital events and their linkage to major atmospheric pressure systems in southern Romania (Chapter 3), periodic inputs of dust and their Saharan source to an eastern Carpathian site (Chapter 4), metal pollution and human history in western Serbia (Chapter 5) and the use of a Bayesian mixing model to assess sources of Pb pollution (Chapter 6) were investigated. Since the region, one of long-term human occupation and particularly sensitive to climate change, had previously been understudied, such work can help to advance our understanding of the interaction between humans and climate. This provides much needed information on how such interactions have occurred in the past, and how they may continue in the future. Since humans have long inhabited the Carpathian-Balkan region, their impact on climate and the environment is vital when understanding its history, and the lack of any long-term pollution records preclude understanding the scale of impact metallurgy and technological development has had. With specific reference to metal pollution, it is vital to understand exactly where its sources are, and so a method for quantitatively making such an assessment is valuable.

7.1.1. Detrital Events and Hydroclimate Variability in the Romanian Carpathians During the Mid-to Late Holocene

Loss-on-ignition results, alongside geochemistry and pollen abundances from a 7500-year long record Sureanu peat bog (southern Carpathians, Romania) reveal a long history of minerogenic matter entering the site (Chapter 3). Such events may be linked with periods of extreme precipitation (lake flooding and mass wasting) and so the record may be used as a proxy for hydroclimatic variability. Results suggest an intensification of such events as a result of both natural climatic changes (e.g. Medieval Warm Period) and at times of social upheavals (e.g. Roman invasion of Dacia). Pollen results display a shift (at roughly 4500 yr BP) from more natural controls on the nature of vegetation cover in the early Holocene to greater human influence through the late Holocene. Also presented is a novel geochemical approach to reconstructing detrital influence over the peat bog development (relying on Rb/Sr ratio as a proxy for grain size), which appears to parallel the LOI results under certain conditions.

Despite clear human impact, the overriding control on palaeoenvironment appears to be natural climate variability, with atmospheric circulation changes the main driver behind the intensification of regional erosion. In particular, the influence of the NAO, which has previously been observed in rainfall records over recent times, is clear within the detrital record at Sureanu. The results validate model predictions of a weakened NAO causing increased rainfall in the Carpathian-Balkan region.

7.1.2. Periodic Input of Dust over the Eastern Carpathians During the Holocene Linked with Saharan Desertification and Human Impact

Using high-resolution qualitative (ITRAX) and quantitative (ICP-OES) geochemical data in conjunction with a new palaeoecological record of local wetness (based on testate amoeba), periods of sustained influx of dust to Mohos peat bog (eastern Carpathians, Romania) have been indicated over a 10,800-year long time interval, the first such research focus in the Carpathian region (Chapter 4). During the early Holocene, results indicate a coupling of dust flux to local bog wetness, and so an apparently local input of dust into the site, mainly controlled by local droughts and related soil (and loess) erosion in the Carpathian-Balkan region.

After 6100 yr BP, however, the number of, and intensity of such events increases dramatically. This is accompanied by a decoupling of dust flux and local wetness, and the appearance of clear cyclicity within the record. All these factors point to a transition away from the local dust regimes which characterised the early Holocene. With the dust shift to more titanium-rich, the cyclicities indicate a likely Saharan source for dust after 6100 yr BP. The timing of this shift, and further intensification after 5000 yr BP is in line with reconstructions of Saharan desertification, representing the shift from relatively lush grassland to the desert present today. This record is the first such evidence of the impact Saharan desertification had on the palaeoenvironment of eastern Europe.

7.1.3. Exceptional Levels of Lead Pollution in the Balkans from the Early Metal Ages to the Industrial Revolution

Via geochemical analysis of Crveni Potok peat core (western Serbia), the first record of long-term heavy metal pollution in a Balkan bog is reconstructed (Chapter 5). This documents the growth of metallurgy in a region rich in archaeological evidence, bridging the gap between such findings and environmental evidence. The first signs of metal pollution are observed in the very earliest Bronze Age (3500 BCE), the earliest environmental evidence of such activity discovered worldwide, and testament to the advanced nature of local civilisations, and the arrival of the Bronze Age 1000 years earlier

than in western Europe. After the later Iron Age (600 BCE) an almost linear increase in Pb pollution is observed until the Medieval period (c.1600 CE). This is indicative of the metallurgical activity of successive local cultures, from the Romans/Byzantines who first organised and exploited local metal resources in great quantities, through the Serbs (with help from imported Saxon miners) and into the period of Ottoman control. The record also clearly shows how increased Ottoman bureaucracy negatively impacted mining after 1615 CE. Furthermore, the impact of major plagues may be observed, with many such pestilences (including the Plagues of Antonine and Cyprian) appearing to result in reduced metal pollution. Interestingly, there is no such reduction as a result of the Black Death.

The record is at odds with western European records, which document a major drop in metal production after the fall of the Roman Empire, with most locations not observing regeneration of metallurgical industries until Medieval times. Clearly eastern Europe underwent a separate developmental trajectory from the west, and so current Pb pollution budgets and models should be reconsidered, factoring in a much greater influence from the east.

7.1.4. Utilisation of Bayesian Mixing Models to Quantitatively Assess Proportions of Pb Sources in Isotopic Mixtures

Records such as the one presented in Chapter 5 are valuable contributions to our understanding of past metal pollution and human development. A number of studies now utilise Pb isotopes, and their ability to fingerprint pollution sources. Such attribution is generally performed via basic models or simply graphing the data. Here a novel approach to source apportionment is presented, applying a mixing model which utilises rigorous Bayesian statistics in an attempt to quantitatively investigate sources of pollution (Chapter 6).

The mixing model used, MixSIAR, is the latest iteration of a number of approaches developed in the field of ecology to determine predator diets. It was developed to utilise stable isotopic signatures of both the sources' (prey) and sink's (predator) tissue. Such an approach meticulously investigates potential solutions which could have resulted in the isotopic ratio recorded in the predator, from the isotopic ratios recorded in various prey. Using real world data from a peat bog in Spain, the ability of Pb isotopes within a substrate to record their relative source contributions is investigated, and a best practice is developed. These example studies indicate the viability of such an approach for understanding the source of Pb in the peat bog during both pre-human times and during the Roman period. Further, the approach is applied to the field of archaeology, using the same

principles to investigate sources of Pb to an archaeological artefact discovered within a Roman mining system in Romania.

7.2. Outlook

This research has provided three new long-term geochemical and palaeoecological datasets from a range of peat bogs in Romania and Serbia. In addition, it has presented a new approach to apportioning sources of Pb pollution, utilising the isotopic signature of a mixture, and state of the art Bayesian modelling. Implications for further research are outlined below:

- The record of detrital events indicates for the first time a persistent (at least for the past 2000 years) linkage between a weakened NAO and heavy rainfall over the southern Carpathians. To confirm such a hypothesis, further studies in the region are needed, to assess whether the NAO does indeed play a significant role in the timing of such heavy rainfall events.
- The record of strong dust depositional events reconstructed from a bog in Romania indicates for the first time the clear impact desertification in North Africa had on the environments of eastern Europe. With climate change likely to cause further desertification, and with dust playing a major role in biogeochemical and energy balance cycles, it is imperative further similar studies are performed, to assess the continent-wide impact of major desertification events occurring elsewhere. This would allow to further test regional teleconnections between climate response and forcing factors. Further, it would be extremely useful to be able to categorically confirm a Saharan source of the dust in Mohos (and other locations), and so examination of isotopic tracers (Nd and Sr for example) should be performed. This would allow for more reliable tracing of dust loading within peat records, with a clearer view on its origin.
- The Pb pollution record from Crveni Potok in Serbia fills a blank spot in the European pollution picture, evidencing a strong difference between economic developments in the east on one hand and the west on the other hand, particularly after the fall of the Roman Empire. Further peat records must be investigated to confirm the extent of this variability, and to assess how metallurgical development varied throughout the past 5000 years in the Balkans. Since the record presented here does not cover the very earliest years of metallurgy, it would be valuable to analyse a peat (or lake) record which investigates (in high resolution) such a time

period in direct comparison with the existing archaeological evidence for such activities

- Pb isotope data should be modelled using MixSIAR, as suggested in Chapter 6. This approach, alongside more traditional methods for isotopic tracing, would allow future studies of Balkan Pb pollution to more precisely indicate sources of pollution and mining fields that contributed to the overall Pb pollution budget at any given time. Changes in main source region and proportions of natural lead as determined via modelling would provide valuable new insights to the metallurgical history of the region. Of course, this approach shall not be limited to the Balkans, and it should be tried and tested in further studies of Pb pollution worldwide.

References

Aaby, B., 1976. Cyclic palaeoclimatic variations and the future. Newsletters Stratigr. 5, 66–69.

Aaby, B., Tauber, H., 1975. Rates of peat formation in relation to degree of humification and local environment, as shown by studies of a raised bog in Deninark. Boreas 4, 1–17. doi:10.1111/j.1502-3885.1975.tb00675.x

Abouchami, W., Zabel, M., 2003. Climate forcing of the Pb isotope record of terrigenous input into the Equatorial Atlantic. Earth Planet. Sci. Lett. 213, 221–234. doi:10.1016/S0012-821X(03)00304-2

Adkins, J., DeMenocal, P., Eshel, G., 2006. The "African humid period" and the record of marine upwelling from excess 230Th in Ocean Drilling Program Hole 658C. Paleoceanography 21, 1–14. doi:10.1029/2005PA001200

Aebischer, S., Cloquet, C., Carignan, J., Maurice, C., Pienitz, R., 2015. Disruption of the geochemical metal cycle during mining: Multiple isotope studies of lake sediments from Schefferville, subarctic Québec. Chem. Geol. 412, 167–178. doi:10.1016/j.chemgeo.2015.07.028

Akinyemi, F.O., Hutchinson, S.M., Mîndrescu, M., Rothwell, J.J., 2013. Lake sediment records of atmospheric pollution in the Romanian Carpathians. Quat. Int. 293, 105–113. doi:10.1016/j.quaint.2012.01.022

Albani, S., Mahowald, N.M., Winckler, G., Anderson, R.F., Bradtmiller, L.I., Delmonte, B., François, R., Goman, M., Heavens, N.G., Hesse, P.P., Hovan, S.A., Kang, S.G., Kohfeld, K.E., Lu, H., Maggi, V., Mason, J.A., Mayewski, P.A., McGee, D., Miao, X., Otto-Bliesner, B.L., Perry, A.T., Pourmand, A., Roberts, H.M., Rosenbloom, N., Stevens, T., Sun, J., 2015. Twelve thousand years of dust: The Holocene global dust cycle constrained by natural archives. Clim. Past 11, 869–903. doi:10.5194/cp-11-869-2015

Alchon, S.A., 2004. A Pest in the Land: New World Epidemics in a Global Perspective (review). Americas (Engl. ed). doi:10.1353/tam.2004.0178

Alderton, D.H.M., Fallick, A.E., 2000. The nature and genesis of gold-silver-tellurium mineralization in the Metaliferi Mountains of western Romania. Econ. Geol. 95, 495–515. doi:10.2113/gsecongeo.95.3.495

Allan, M., Fagel, N., Van Rampelbergh, M., Baldini, J., Riotte, J., Cheng, H., Edwards, R.L., Gillikin, D., Quinif, Y., Verheyden, S., 2015. Lead concentrations and isotope ratios in speleothems as proxies for atmospheric metal pollution since the industrial revolution. Chem. Geol. 401, 140–150. doi:10.1016/j.chemgeo.2015.02.035

Allan, M., Le Roux, G., De Vleeschouwer, F., Bindler, R., Blaauw, M., Piotrowska, N., Sikorski,

J., Fagel, N., 2013a. High-resolution reconstruction of atmospheric deposition of trace metals and metalloids since AD 1400 recorded by ombrotrophic peat cores in Hautes-Fagnes, Belgium. Environ. Pollut. 178, 381–394. doi:10.1016/j.envpol.2013.03.018

Allan, M., Le Roux, G., Piotrowska, N., Beghin, J., Javaux, E., Court-Picon, M., Mattielli, N., Verheyden, S., Fagel, N., 2013b. Mid- and late Holocene dust deposition in western Europe: The Misten peat bog (Hautes Fagnes – Belgium). Clim. Past 9, 2285–2298. doi:10.5194/cp-9-2285-2013

Álvarez-Iglesias, P., Rubio, B., Millos, J., 2012. Isotopic identification of natural vs. anthropogenic lead sources in marine sediments from the inner Ría de Vigo (NW Spain). Sci. Total Environ. 437, 22–35. doi:10.1016/j.scitotenv.2012.07.063

Amov, B.G., 1999. Lead isotope data for ore deposits from Bulgaria and the possibility for their use in archaeometry. Berlin Beitr Archäom 16, 5–19.

Amov, B.G., 1983. Evolution of uranogenic and thorogenic lead, 1. A dynamic model of continuous isotopic evolution. Earth Planet. Sci. Lett. 65, 61–74. doi:10.1016/0012-821X(83)90190-5

Andrei, S., Roman, I., 2012. Severe weather phenomena in southern romania in association with blocking circulation over euro-atlantic area during the cold season. Rom. Reports Phys. 64, 246–262.

Anthony, D.W., 2010. The Horse, the Wheel, and Language: How Bronze-Age Riders from the Eurasian Steppes Shaped the Modern World. Princeton University Press, Princeton. doi:10.1086/268620

Anthony, D.W., Chi, J., 2009. The lost world of old Europe : the Danube valley, 5000-3500 BC. Princeton University Press, New York.

Antonovic, D., 2009. Prehistoric copper tools from the territory of Serbia. J. Min. Metall. Sect. B Metall. 45, 165–174. doi:10.2298/JMMB0902165A

Apostol, L., 2008. The Mediterranean cyclones: the role in ensuring water resources and their potential of climatic risk, in the east of Romania. Present Environ. Sustain. Dev. 2, 143–163.

Arias, D., Corretgé, L.G., Suárez, O., Villa, L., Cuesta, A., Gallastegui, G., 1996. Lead and sulfur isotope compositions of the ibias gold vein system (NW Spain): Genetic implications. Econ. Geol. 91, 1292–1297. doi:10.2113/gsecongeo.91.7.1292

Arnaud, F., Révillon, S., Debret, M., Revel, M., Chapron, E., Jacob, J., Giguet-Covex, C., Poulenard, J., Magny, M., 2012. Lake Bourget regional erosion patterns reconstruction reveals Holocene NW European Alps soil evolution and paleohydrology. Quat. Sci. Rev. 51, 81–92. doi:10.1016/j.quascirev.2012.07.025

Athanasopoulou, E., Protonotariou, A., Papangelis, G., Tombrou, M., Mihalopoulos, N., Gerasopoulos, E., 2016. Long-range transport of Saharan dust and chemical transformations over the Eastern Mediterranean. Atmos. Environ. 140, 592–604. doi:10.1016/j.atmosenv.2016.06.041

Aurelian, F., Georgescu, D.P., Popescu, M., Florescu, M.S., 2007. Environmental impact assessment of the uranium mining activity in the Bihor district (Bucharest, Romania), in: Cidu, R., Frau, F. (Eds.), IMWA Symposium 2007: Water in Mining Environments, 27th–31st May, 2007. Mako Edizioni, Cagliari, p. 477.

Bachman, R.D., 1989. Romania: A Country Study, 2nd ed. Library of Congress, Washington.

Bacon, J.R., 2002. Isotopic characterisation of lead deposited 1989-2001 at two upland Scottish locations. J. Environ. Monit. 4, 291–9. doi:10.1039/B109731H

Bailey, D.W., 2000. Balkan Prehistory: Exclusion, Incorporation and Identity. Routledge, London and New York.

Bálint, C., 2010. Avar Goldsmiths' Work from the Perspective of Cultural History, in: Entwistle, C., Adams, N. (Eds.), Intelligible Beauty. Recent Research on Byzantine Jewellery. British Museum Press, London, pp. 146–160.

Bar-Matthews, M., Ayalon, A., Kaufman, A., 1997. Late Quaternary Paleoclimate in the Eastern Mediterranean Region from Stable Isotope Analysis of Speleothems at Soreq Cave, Israel. Quat. Res. 47, 155–168. doi:10.1006/qres.1997.1883

Barber, K.E., 1981. Peat Stratigraphy and Climate Change. Balkema, Rotterdam.

Barnston, A.G., Livezey, R.E., 1987. Classification, Seasonality and Persistence of Low-Frequency Atmospheric Circulation Patterns. Mon. Weather Rev. 115, 1083–1126. doi:10.1175/1520-0493(1987)115<1083:CSAPOL>2.0.CO;2

Baron, S., Carignan, J., Laurent, S., Ploquin, A., 2006. Medieval lead making on Mont-Lozere Massif (Cevennes-France): Tracing ore sources using Pb isotopes. Appl. Geochemistry 21, 241–252. doi:10.1016/j.apgeochem.2005.09.005

Baron, S., Le-Carlier, C., Carignan, J., Ploquin, A., 2009. Archaeological reconstruction of medieval lead production: Implications for ancient metal provenance studies and paleopollution tracing by Pb isotopes. Appl. Geochemistry 24, 2093–2101. doi:10.1016/j.apgeochem.2009.08.003

Baron, S., Tâmaş, C.G., Cauuet, B., Munoz, M., 2011. Lead isotope analyses of gold-silver ores from Roşia Montanâ (Romania): A first step of a metal provenance study of Roman mining activity in Alburnus Maior (Roman Dacia). J. Archaeol. Sci. 38, 1090–1100. doi:10.1016/j.jas.2010.12.004

Baron, S., Tămaş, C.G., Le Carlier, C., 2014. How Mineralogy and Geochemistry Can Improve the Significance of Pb Isotopes in Metal Provenance Studies. Archaeometry 56, 665–680. doi:10.1111/arcm.12037

Barrett, M.B., 2013. Prelude to Blitzkrieg : the 1916 Austro-German Campaign in Romania. Indiana University Press.

Barta, G., Köpeczi, B., 1994. History of Transylvania. Akadémiai Kiadó, Budapest.

Bartlein, P.J., Harrison, S.P., Brewer, S., Connor, S., Davis, B.A.S., Gajewski, K., Guiot, J., Harrison-Prentice, T.I., Henderson, A., Peyron, O., Prentice, I.C., Scholze, M., Seppä, H., Shuman, B., Sugita, S., Thompson, R.S., Viau, A.E., Williams, J., Wu, H., 2011. Pollen-based continental climate reconstructions at 6 and 21 ka: a global synthesis. Clim. Dyn. 37, 775–802. doi:10.1007/s00382-010-0904-1

Behr, E., 1991. Kiss the hand you cannot bite : the rise and fall of the Ceauşescus. Villard Books.

Belokopytov, I., Beresnevich, V., 1955. Giktorf's peat borers. Torfyanaya Promyshlennost 8, 9–10.

Ben Israel, M., Enzel, Y., Amit, R., Erel, Y., 2015. Provenance of the various grain-size fractions in the Negev loess and potential changes in major dust sources to the Eastern Mediterranean. Quat. Res. 83, 105–115. doi:10.1016/j.yqres.2014.08.001

Benstead, J.P., March, J.G., Fry, B., Ewel, K.C., Pringle, C.M., 2006. Testing isosource: Stable isotope analysis of a tropical fishery with diverse organic matter sources. Ecology 87, 326–333. doi:10.1890/05-0721

Berger, A., Loutre, M.F., 1991. Insolation values for the climate of the last 10 million years. Quat. Sci. Rev. 10, 297–317. doi:10.1016/0277-3791(91)90033-Q

Berger, J.F., Lespez, L., Kuzucuoğlu, C., Glais, A., Hourani, F., Barra, A., Guilaine, J., 2016. Interactions between climate change and human activities during the Early to Mid Holocene in the East Mediterranean basins. Clim. Past Discuss. 1–42. doi:10.5194/cp-2016-4

Beug, H.-J., 2004. Leitfaden der Pollenbestimmung für Mitteleuropa und angrenzende Gebiete. Dr. Friedrich Pfeil, Munich.

Bindler, R., Renberg, I., Anderson, N.J., Appleby, P.G., Emteryd, O., Boyle, J., 2001. Pb isotope ratios of lake sediments in West Greenland: inferences on pollution sources. Atmos. Environ. 35, 4675–4685. doi:10.1016/s1352-2310(01)00115-7

Bindler, R., Renberg, I., Klaminder, J., Emteryd, O., 2004. Tree rings as Pb pollution archives? A comparison of 206Pb/ 207Pb isotope ratios in pine and other environmental media. Sci. Total Environ. 319, 173–183. doi:10.1016/S0048-9697(03)00397-8

Bird, G., Brewer, P.A., Macklin, M.G., Nikolova, M., Kotsev, T., Mollov, M., Swain, C., 2010a.

Pb isotope evidence for contaminant-metal dispersal in an international river system: The lower Danube catchment, Eastern Europe. Appl. Geochemistry 25, 1070–1084. doi:10.1016/j.apgeochem.2010.04.012

Bird, G., Brewer, P. a, Macklin, M.G., Nikolova, M., Kotsev, T., Mollov, M., Swain, C., 2010b. Quantifying sediment-associated metal dispersal using Pb isotopes: application of binary and multivariate mixing models at the catchment-scale. Environ. Pollut. 158, 2158–69. doi:10.1016/j.envpol.2010.02.020

Birsan, M.-V., Dumitrescu, A., 2014. Snow variability in Romania in connection to large-scale atmospheric circulation. Int. J. Climatol. 34, 134–144. doi:10.1002/joc.3671

Björkman, L., Feurdean, A., Wohlfarth, B., 2003. Late-Glacial and Holocene forest dynamics at Steregoiu in the Gutaiului Mountains, Northwest Romania. Rev. Palaeobot. Palynol. 124, 79–111. doi:10.1016/S0034-6667(02)00249-X

Blaauw, M., 2010. Methods and code for "classical" age-modelling of radiocarbon sequences. Quat. Geochronol. 5, 512–518. doi:10.1016/j.quageo.2010.01.002

Blaauw, M., Christen, J.A., 2011. Flexible paleoclimate age-depth models using an autoregressive gamma process. Bayesian Anal. 6, 457–474. doi:10.1214/ba/1339616472

Blais, J.M., Rosen, M.R., Smol, J.P., 2015. Environmental Contaminants, Developments in Paleoenvironmental Research Volume 18. doi:10.1007/978-94-017-9541-8

Blytt, A., 1876. Essay on the immigration of the Norwegian Flora during alternating rainy and dry periods. Christiania.

Boecklen, W.J., Yarnes, C.T., Cook, B.A., James, A.C., 2011. On the Use of Stable Isotopes in Trophic Ecology. Annu. Rev. Ecol. Evol. Syst. 42, 411–440. doi:10.1146/annurev-ecolsys-102209-144726

Boggs, S., 2013. Principles of Sedimentology and Stratigraphy, 5th ed. Pearson, London.

Bojariu, R., Giorgi, F., 2005. The North Atlantic Oscillation signal in a regional climate simulation for the European region. Tellus 57A, 641–653. doi:10.1111/j.1600-0870.2005.00122.x

Bojariu, R., Paliu, D.-M., 2001. North Atlantic Oscillation Projection on Romanian Climate Fluctuations in the Cold Season, in: India, M.B., Bonillo, D.L. (Eds.), Detecting and Modelling Regional Climate Change and Associated Impacts. Springer Berlin Heidelberg, Berlin Heidelburg, pp. 345–356.

Bojariu, R., Paliu, D.-M.D.-M., 2001. North Atlantic Oscillation Projection on Romanian Climate Fluctuations in the Cold Season, in: India, M.B., Bonillo, D.L. (Eds.), Detecting and Modelling Regional Climate Change and Associated Impacts. Springer Berlin Heidelberg,

Berlin and Heidelberg, pp. 345–356. doi:10.1007/978-3-662-04313-4_29

Bollhöfer, A., Rosman, K.J.R., 2002. The temporal stability in lead isotopic signatures at selected sites in the Southern and Northern Hemispheres. Geochim. Cosmochim. Acta 66, 1375–1386. doi:10.1016/S0016-7037(01)00862-6

Bond, G., Kromer, B., Beer, J., Muscheler, R., Evans, M.N., Showers, W., Hoffmann, S., Lotti-Bond, R., Hajdas, I., Bonani, G., 2001. Persistent solar influence on North Atlantic climate during the Holocene. Science 294, 2130–2136. doi:10.1126/science.1065680

Bonsall, C., Boroneanţ, A., Soficaru, A., McSweeney, K., Higham, T., Mirițoiu, N., Pickard, C., Cook, G., 2012. Interrelationship of age and diet in Romania's oldest human burial. Naturwissenschaften 99, 321–325. doi:10.1007/s00114-012-0897-1

Bonsall, C., Macklin, M.G., Boroneanţ, A., Pickard, C., Bartosiewicz, L., Cook, G.T., Higham, T.F.G., 2015. Holocene climate change and prehistoric settlement in the lower Danube valley. Quat. Int. 378, 14–21. doi:10.1016/j.quaint.2014.09.031

Borcoş, M., Udubaşa, G., 2012. Chronology and characterisation of mining development in Romania. Rom. J. Earth Sci. 86, 17–26.

Boric, D., 2009. Absolute dating of metallurgical innovations in the Vinča Culture of the Balkans. Met. Soc. Stud. honour Barbar. S. Ottaway, Univ. zur prähistorischen Archäologie 169, 191–245.

Boric, D., 2002. The Lepenski Vir conundrum: reinterpretation of the Mesolithic and Neolithic sequences in the Danube Gorges. Antiquity 76, 1026–1039.

Boroffka, N., Nessel, B., Prange, M., Ciugudean, H., Takacs, M., Takács, M., 2015. Neues Licht auf alte Fragen – Einige besondere Metallobjekte aus dem Depotfund von Aiud, Kreis Alba, Rumänien, in: Bartelheim, M., Horejs, B., Krauss, R. (Eds.), VON BADEN BIS TROIA RESSOURCENNUTZUNG, METALLURGIE UND WISSENSTRANSFER EINE JUBILÄUMSSCHRIFT FÜR ERNST PERNICKA. VERLAG MARIE LEIDORF GMBH, Rahden/Westf., pp. 399–421.

Boroneanţ, V., Bonsall, C., McSweeney, K., Payton, R., Macklin, M., 1999. A Mesolithic burial area at Schela Cladovei, Romania. L'Europe des derniers Chass. épipaléolithique Mésolithique 385–390.

Box, M.R., Krom, M.D., Cliff, R.A., Bar-Matthews, M., Almogi-Labin, A., Ayalon, A., Paterne, M., 2011. Response of the Nile and its catchment to millennial-scale climatic change since the LGM from Sr isotopes and major elements of East Mediterranean sediments. Quat. Sci. Rev. 30, 431–442. doi:10.1016/j.quascirev.2010.12.005

Bozhinova, E., 2012. THRACE BETWEEN EAST AND WEST: THE EARLY IRON AGE

CULTURES IN THRACE., in: ANCIENT NEAR EASTERN STUDIES ANATOLIAN IRON AGES 7 The Proceedings of the Seventh Anatolian Iron Ages. pp. 19–24.

Bradley, R.S., Jonest, P.D., 1993. "Little Ice Age" summer temperature variations: their nature and relevance to recent global warming trends. The Holocene 3, 367–376. doi:10.1177/095968369300300409

Brännvall, M.L., Bindler, R., Renberg, I., Emteryd, O., Bartnicki, J., Billström, K., 1999. The medieval metal industry was the cradle of modern large-scale atmospheric lead pollution in northern Europe. Environ. Sci. Technol. 33, 4391–4395. doi:10.1021/es990279n

Bränvall, M.-L., Bindler, R., Emteryd, O., Renberg, I., 2001. Four thousand years of atmospheric lead pollution in northern Europe: a summary from Swedish lake sediments. J. Paleolimnol. 25, 421–435. doi:10.1023/A:1011186100081

Bristow, C.S., Hudson-Edwards, K.A., Chappell, A., 2010. Fertilizing the Amazon and equatorial Atlantic with West African dust. Geophys. Res. Lett. 37, L14807. doi:10.1029/2010GL043486

Bronson, B., 1986. The making and selling of wootz, a crucible steel of India. Archeomaterials 1, 13–51.

Brooks, N., 2006. Cultural responses to aridity in the Middle Holocene and increased social complexity. Quat. Int. 151, 29–49. doi:10.1016/j.quaint.2006.01.013

Brückner, H., Kelterbaum, D., Marunchak, O., Porotov, A., Vött, A., 2010. The Holocene sea level story since 7500 BP – Lessons from the Eastern Mediterranean, the Black and the Azov Seas. Quat. Int. 225, 160–179. doi:10.1016/j.quaint.2008.11.016

Brugam, R.B., Ketterer, M., Maines, L., Lin, Z.Q., Retzlaff, W. a., 2011. Application of a simple binary mixing model to the reconstruction of lead pollution sources in two Mississippi River floodplain lakes. J. Paleolimnol. 47, 101–112. doi:10.1007/s10933-011-9562-5

Buczko, K., Magyari, E.K., Bitusik, P., Wacnik, A., 2009. Review of dated Late Quaternary palaeolimnological records in the Carpathian Region, east-central Europe. Hydrobiologia 631, 3–28. doi:10.1007/s10750-009-9800-2

Buczkó, K., Magyari, E.K., Braun, M., Bálint, M., 2013. Diatom-inferred lateglacial and Holocene climatic variability in the South Carpathian Mountains (Romania). Quat. Int. 293, 123–135. doi:10.1016/j.quaint.2012.04.042

Budja, M., 2001. The transition to farming in Southeast Europe: perspectives from pottery. Doc. Praehist. 28, 27–47.

Buggle, B., Glaser, B., Zöller, L., Hambach, U., Marković, S., Glaser, I., Gerasimenko, N., 2008.

Geochemical characterization and origin of Southeastern and Eastern European loesses (Serbia, Romania, Ukraine). Quat. Sci. Rev. 27, 1058–1075. doi:10.1016/j.quascirev.2008.01.018

Buggle, B., Hambach, U., Glaser, B., Gerasimenko, N., Marković, S., Glaser, I., Zöller, L., 2009. Stratigraphy, and spatial and temporal paleoclimatic trends in Southeastern/Eastern European loess–paleosol sequences. Quat. Int. 196, 86–106. doi:10.1016/j.quaint.2008.07.013

Bugoi, R., Constantinescu, B., Popescu, A.D., Munnik, F., 2013. Archaeometallurgical Studies of Bronze Age Objects from the Romanian Cultural Heritage. Rom. Reports Phys. 65, 1234–1245.

Büntgen, U., Tegel, W., Nicolussi, K., McCormick, M., Frank, D., Trouet, V., Kaplan, J.O., Herzig, F., Heussner, K.-U., Wanner, H., Luterbacher, J., Esper, J., 2011. 2500 Years of European Climate Variability and Human Susceptibility. Science. 331, 578–582. doi:10.1126/science.1197175

Buzatu, G., 2002. A History of Romanian Oil Volume 1. Mica Valahie Publishing House, Bucharest.

Buzon, M., 2009. What does it mean the migrations in the Roman province of Pannonia. Stud. Antiq. Archaeol. XV, 41–70.

Byrne, J.P., 2012. Encyclopedia of the Black Death. ABC-CLIO, Santa Barbara.

Carozza, J.-M., Micu, C., Mihail, F., Carozza, L., 2012. Landscape change and archaeological settlements in the lower Danube valley and delta from early Neolithic to Chalcolithic time: A review. Quat. Int. 261, 21–31. doi:10.1016/j.quaint.2010.07.017

Chambers, F.M., Booth, R.K., De Vleeschouwer, F., Lamentowicz, M., Le Roux, G., Mauquoy, D., Nichols, J.E., van Geel, B., 2012. Development and refinement of proxy-climate indicators from peats. Quat. Int. 268, 21–33. doi:10.1016/j.quaint.2011.04.039

Chang, C., Han, C., Han, Y., Hur, S. Do, Lee, S., Motoyama, H., Hou, S., Hong, S., 2016. Persistent Pb Pollution in Central East Antarctic Snow: A Retrospective Assessment of Sources and Control Policy Implications. Environ. Sci. Technol. 50, 12138–12145. doi:10.1021/acs.est.6b03209

Chapman, J., 2000. Fragmentation in archaeology : people, places, and broken objects in the prehistory of south eastern Europe. Routledge.

Chapman, J., 1981. The Vinča culture of South-East Europe: studies in chronology, economy and society. Br. Archaeol. Reports 117.

Charman, D.J., 2002. Peatlands and Environmental Change. John Wiley & Sons, Ltd, New York.

Charman, D.J., Hendon, D., Woodland, W., 2000. The identification of testate amoebae (Protozoa: Rhizopoda) in peats, QRA Techni. ed. Quaternary Research Association, London.

Chawchai, S., Kylander, M.E., Chabangborn, A., Löwemark, L., Wohlfarth, B., 2016. Testing commonly used X-ray fluorescence core scanning-based proxies for organic-rich lake sediments and peat. Boreas 45, 180–189. doi:10.1111/bor.12145

Chen, M., Boyle, E.A., Switzer, A.D., Gouramanis, C., 2016. A century long sedimentary record of anthropogenic lead (Pb), Pb isotopes and other trace metals in Singapore. Environ. Pollut. doi:10.1016/j.envpol.2016.02.040

Cheng, H., Hu, Y., 2010. Lead (Pb) isotopic fingerprinting and its applications in lead pollution studies in China: A review. Environ. Pollut. 158, 1134–1146. doi:10.1016/j.envpol.2009.12.028

Chernyk, E., 1992. Ancient Metallurgy in the USSR. Cambridge Univ. Press.

Chernyshev, I. V., Chugaev, a. V., Shatagin, K.N., 2007. High-precision Pb isotope analysis by multicollector-ICP-mass-spectrometry using 205Tl/203Tl normalization: Optimization and calibration of the method for the studies of Pb isotope variations. Geochemistry Int. 45, 1065–1076. doi:10.1134/S0016702907110018

Christiansen, B., Ljungqvist, F.C., 2012. The extra-tropical Northern Hemisphere temperature in the last two millennia: reconstructions of low-frequency variability. Clim. Past 8, 765–786. doi:10.5194/cp-8-765-2012

Cioacă, A., Dinu, M.S., 2010. Romanian Carpathian Landscapes and Cultures, in: Martini, I.P., Chesworth, W. (Eds.), Landscapes and Societies. Springer Netherlands, Dordrecht, pp. 257–269.

Ciobanu, C.L., Cook, N.J., Stein, H., 2002. Regional setting and geochronology of the Late Cretaceous Banatitic Magmatic and Metallogenetic Belt. Miner. Depos. 37, 541–567. doi:10.1007/s00126-002-0272-9

Ciugudean, H., 2012. Ancient gold mining in Transylvania: the Roşia Montană - Bucium area. Caiet. Ara. Arhit. Restaurare, Arheol. 3, 219–232.

Clark, R.L., 1982. Point count estimation of charcoal in pollen preparations and thin sections of sediments. Pollen et spores 25, 523–535.

Cloy, J.M., Farmer, J.G., Graham, M.C., MacKenzie, A.B., Cook, G.T., Billström, K., Losno, R., Richard, H., Lèvêque, J., Chateau, C., Handley, M.J., Norton, S.A., Krachler, M., Shotyk, W., Li, X.D., Martinez-Cortizas, A., Pulford, I.D., MacIver, V., Schweyer, J., Steinnes, E., Sjøbakk, T.E., Weiss, D., Dolgopolova, A., Kylander, M., 2005. A comparison of antimony and lead profiles over the past 2500 years in Flanders Moss ombrotrophic peat bog, Scotland.

J. Environ. Monit. 7, 1137. doi:10.1039/b510987f

Coles, J.M., Harding, A.F., 2014. The Bronze Age in Europe: An Introduction to the Prehistory of Europe C. 2000-700 Bc. Routledge, Abingdon.

Čolić, D., Gigov, A., 1958. Community with Serbian Spruce (Picea omorika) on a swampy site (in Serbian). Biol. Inst. F.R. Serbia.

Connor, S.E., Ross, S.A., Sobotkova, A., Herries, A.I.R., Mooney, S.D., Longford, C., Iliev, I., 2013. Environmental conditions in the SE Balkans since the Last Glacial Maximum and their influence on the spread of agriculture into Europe. Quat. Sci. Rev. 68, 200–215. doi:10.1016/j.quascirev.2013.02.011

Constantin, S., Bojar, A.-V., Lauritzen, S.-E., Lundberg, J., 2007. Holocene and Late Pleistocene climate in the sub-Mediterranean continental environment: A speleothem record from Poleva Cave (Southern Carpathians, Romania). Palaeogeogr. Palaeoclimatol. Palaeoecol. 243, 322–338. doi:10.1016/j.palaeo.2006.08.001

Constantinescu, B., Bugoi, R., Cojocaru, V., Radtke, M., Calligaro, T., Salomon, J., Pichon, L., Röhrs, S., Ceccato, D., Oberländer-Târnoveanu, E., 2008. Micro-SR-XRF and micro-PIXE studies for archaeological gold identification – The case of Carpathian (Transylvanian) gold and of Dacian bracelets. Nucl. Instruments Methods Phys. Res. Sect. B Beam Interact. with Mater. Atoms 266, 2325–2328. doi:10.1016/j.nimb.2008.03.054

Constantinescu, B., Bugoi, R., Cojocaru, V., Simon, R., Grambole, D., Munnik, F., Oberländer-Târnoveanu, E., 2009. Elemental analysis through X-ray techniques applied in archeological gold authentication — the case of Transylvanian gold and of the Dacian bracelets. Spectrochim. Acta Part B At. Spectrosc. 64, 1198–1203. doi:10.1016/j.sab.2009.08.007

Constantinescu, M., 1971. Unification of the Romanian National State: The Union of Transylvania with Old Romania. Publishing House of the Academy of the Socialist Republic of Romania, Bucharest.

Cooke, C.A., Abbott, M.B., Wolfe, A.P., Kittleson, J.L., 2007. A millennium of metallurgy recorded by lake sediments from morococha, Peruvian Andes. Environ. Sci. Technol. 41, 3469–3474. doi:10.1021/es062930+

Cremaschi, M., Zerboni, A., 2009. Early to Middle Holocene landscape exploitation in a drying environment: Two case studies compared from the central Sahara (SW Fezzan, Libya). Comptes Rendus - Geosci. 341, 689–702. doi:10.1016/j.crte.2009.05.001

Cristea, G., Cuna, S.M., Farcas, S., Tantau, I., Dordai, E., Magdas, D.A., 2013. Carbon isotope composition as indicator for climatic changes during the middle and late Holocene in a peat bog from Maramures Mountains (Romania). The Holocene 24, 15–23.

doi:10.1177/0959683613512166

Cristea, V., 1993. Fitosociologie şi vegetaţia României. Babes-Bolyai University Press, Cluj Napoca.

Croitoru, A.-E.E., Drignei, D., Holobaca, I.-H.H., Dragota, C.S., 2012. Change-point analysis for serially correlated summit temperatures in the Romanian Carpathians. Theor. Appl. Climatol. 108, 9–18. doi:10.1007/s00704-011-0508-7

Croudace, I.W., Rindby, A., Rothwell, R.G., 2006. ITRAX: description and evaluation of a new multi-function X-ray core scanner. Geol. Soc. London 267, 51–63. doi:10.1144/GSL.SP.2006.267.01.04

Crozier, M.J., 2010. Deciphering the effect of climate change on landslide activity: A review. Geomorphology 124, 260–267. doi:10.1016/j.geomorph.2010.04.009

Csavina, J., Field, J., Taylor, M.P., Gao, S., Landázuri, A., Betterton, E.A., Sáez, A.E., 2012. A review on the importance of metals and metalloids in atmospheric dust and aerosol from mining operations. Sci. Total Environ. 433, 58–73. doi:10.1016/j.scitotenv.2012.06.013

Curta, F., 2008. The other Europe in the Middle Ages : Avars, Bulgars, Khazars, and Cumans. Brill.

Czymzik, M., Brauer, A., Dulski, P., Plessen, B., Naumann, R., von Grafenstein, U., Scheffler, R., 2013. Orbital and solar forcing of shifts in Mid- to Late Holocene flood intensity from varved sediments of pre-alpine Lake Ammersee (southern Germany). Quat. Sci. Rev. 61, 96–110. doi:10.1016/j.quascirev.2012.11.010

Czymzik, M., Muscheler, R., Brauer, A., 2016. Solar modulation of flood frequency in central Europe during spring and summer on interannual to multi-centennial timescales. Clim. Past 12, 799–805. doi:10.5194/cp-12-799-2016

Davies, S.J., Lamb, H.F., Roberts, S.J., 2015. Micro-XRF Core Scanning in Palaeolimnology: Recent Developments, in: Micro-XRF Studies of Sediment Cores2. pp. 189–226.

Davis, B.A.S., Brewer, S., Stevenson, A.C., Guiot, J., 2003. The temperature of Europe during the Holocene reconstructed from pollen data. Quat. Sci. Rev. 22, 1701–1716. doi:10.1016/S0277-3791(03)00173-2

Dean, J.R., Jones, M.D., Leng, M.J., Noble, S.R., Metcalfe, S.E., Sloane, H.J., Sahy, D., Eastwood, W.J., Roberts, C.N., 2015. Eastern Mediterranean hydroclimate over the late glacial and Holocene, reconstructed from the sediments of Nar lake, central Turkey, using stable isotopes and carbonate mineralogy. Quat. Sci. Rev. 124, 162–174. doi:10.1016/j.quascirev.2015.07.023

De Vleeschouwer, F., Fagel, N., Cheburkin, A., Pazdur, A., Sikorski, J., Mattielli, N., Renson, V., Fialkiewicz, B., Piotrowska, N., Le Roux, G., 2009a. Anthropogenic impacts in North Poland over the last 1300years — A record of Pb, Zn, Cu, Ni and S in an ombrotrophic peat bog. Sci. Total Environ. 407, 5674–5684. doi:10.1016/j.scitotenv.2009.07.020

De Vleeschouwer, F., Gérard, L., Goormaghtigh, C., Mattielli, N., Le Roux, G., Fagel, N., 2007. Atmospheric lead and heavy metal pollution records from a Belgian peat bog spanning the last two millenia: Human impact on a regional to global scale. Sci. Total Environ. 377, 282–295. doi:10.1016/j.scitotenv.2007.02.017

De VleeSchouwer, F., Le Roux, G., Shotyk, W., 2010. Peat as an archive of atmospheric pollution and environmental change: A case study of lead in Europe. PAGES Mag. 18, 20–22.

De Vleeschouwer, F., Piotrowska, N., Sikorski, J., Pawlyta, J., Cheburkin, A., Le Roux, G., Lamentowicz, M., Fagel, N., Mauquoy, D., 2009b. Multiproxy evidence of `Little Ice Age' palaeoenvironmental changes in a peat bog from northern Poland. The Holocene 19, 625–637. doi:10.1177/0959683609104027

De Vleeschouwer, F., Vanneste, H., Mauquoy, D., Piotrowska, N., Torrejón, F., Roland, T., Stein, A., Le Roux, G., 2014. Emissions from Pre-Hispanic Metallurgy in the South American Atmosphere. PLoS One 9, e111315. doi:10.1371/journal.pone.0111315

Debret, M., Bout-Roumazeilles, V., Grousset, F., Desmet, M., McManus, J.F., Massei, N., Sebag, D., Petit, J.-R., Copard, Y., Trentesaux, A., 2007. The origin of the 1500-year climate cycles in Holocene North-Atlantic records. Clim. Past Discuss. 3, 679–692. doi:10.5194/cpd-3-679-2007

Demenocal, P., Ortiz, J., Guilderson, T., Adkins, J., Sarnthein, M., Baker, L., Yarusinsky, M., 2000. Abrupt onset and termination of the African Humid Period: Rapid climate responses to gradual insolation forcing, in: Quaternary Science Reviews. pp. 347–361. doi:10.1016/S0277-3791(99)00081-5

deMenocal, P.B., Peter, B., 2001. Cultural Responses to Climate Change During the Late Holocene. Science. 292, 667–673. doi:10.1126/science.1059287

Demske, D., Tarasov, P.E., Nakagawa, T., 2013. Atlas of pollen, spores and further non-pollen palynomorphs recorded in the glacial-interglacial late Quaternary sediments of Lake Suigetsu, central Japan. Quat. Int. 290, 164–238. doi:10.1016/j.quaint.2012.02.002

Diaconu, A.-C., Grindean, R., Panait, A., Tanţău, I., 2016. Late Holocene palaeohydrological changes in a *Sphagnum* peat bog from NW Romania based on testate amoebae. Stud. UBB Geol. 60. doi:http://dx.doi.org/10.5038/1937-8602.60.1.1285

Dörfler, W., 2013. Prokoško Jezero: An environmental record from a subalpine lake in Bosnia-

Herzegovina, in: Müller, J., Rassmann, K., Hofmann, R. (Eds.), Okolište 1 – Untersuchungen Einer Spätneolithischen Siedlungskammer in Zentralbosnien. Dr. Rudolf Habelt GmbH, Bonn, pp. 311–340.

Drăguşin, V., Staubwasser, M., Hoffmann, D.L., Ersek, V., Onac, B.P., Veres, D., 2014. Constraining Holocene hydrological changes in the Carpathian–Balkan region using speleothem δ18O and pollen-based temperature reconstructions. Clim. Past 10, 1363–1380. doi:10.5194/cp-10-1363-2014

Drake, B.L., 2012. The influence of climatic change on the Late Bronze Age Collapse and the Greek Dark Ages. J. Archaeol. Sci. 39, 1862–1870. doi:10.1016/j.jas.2012.01.029

Dudka, S., Adriano, D.C., 1997. Environmental Impacts of Metal Ore Mining and Processing: A Review. J. Environ. Qual. 26, 590. doi:10.2134/jeq1997.00472425002600030003x

Dušanić, S., 2008. The Valle Ponti Lead Ingots: Notes on Roman Notables' Commercial Activities in Free Illyricum at the Beginning of the Principate. Starinar 107–118.

Dušanić, S., 2004. Roman Mining in Illyricum: Historical Aspects, in: Urso, G. (Ed.), Dall'Adriatico Al Danubio. L'Illirico Nell'età Greca E Romana. Atti Del Convengo Intenazionale Cividale Del Friuli, 25-27 Settembre 2003. Pisa, pp. 247–270.

Edmondson, J.C., 1989. Mining in the Later Roman Empire and beyond: Continuity or Disruption? J. Rom. Stud. 79, 84–102.

Edri, A., Dody, A., Tanner, S., Swet, N., Katra, I., 2016. Variations in dust-related PM10 emission from an arid land due to surface composition and topsoil disturbance. Arab. J. Geosci. 9, 607. doi:10.1007/s12517-016-2651-z

Egerer, S., Claussen, M., Reick, C., Stanelle, T., 2016. The link between marine sediment records and changes in Holocene Saharan landscape: Simulating the dust cycle. Clim. Past 12, 1009–1027. doi:10.5194/cp-12-1009-2016

Eggert, R.G., 1994. Mining and the environment : international perspectives on public policy. Resources for the Future.

Egozcue, J.J., Pawlowsky-Glahn, V., Mateu-Figueras, G., Barceló-Vidal, C., 2003. Isometric Logratio Transformations for Compositional Data Analysis. Math. Geol. 35, 279–300. doi:10.1023/A:1023818214614

Engel, P., 2005. The realm of St. Stephen : a history of medieval Hungary, 895-1526. I.B. Tauris.

Esteban, P., Jones, P.D., Martín-Vide, J., Mases, M., 2005. Atmospheric circulation patterns related to heavy snowfall days in Andorra, Pyrenees. Int. J. Climatol. 25, 319–329. doi:10.1002/joc.1103

Faegri, K., Iversen, J., 1989. Textbook of pollen analysis, 4th ed. The Blackburn Press, Caldwell.

Fărcaş, I., Sorocovschi, V., 1992. The climate of the Retezat Mountains, in: Popovici, I. (Ed.), The Retezat National Park, Ecological Studies. West Side Computers, Braşov, pp. 13–20.

Farcas, S., de Beaulieu, J.-L., Reille, M., Coldea, G., Diaconeasa, B., Goeury, C., Goslar, T., Jull, T., 1999. First 14C datings of Late Glacial and Holocene pollen sequences from Romanian Carpathes. Comptes Rendus l'Académie des Sci. - Ser. III - Sci. la Vie 322, 799–807. doi:10.1016/S0764-4469(00)80039-6

Fărcaş, S., Tanţâu, I., Mîndrescu, M., Hurdu, B., 2013. Holocene vegetation history in the Maramureş Mountains (Northern Romanian Carpathians). Quat. Int. 293, 92–104. doi:10.1016/j.quaint.2012.03.057

Farmer, J.G., Eades, L.J., Graham, M.C., Bacon, J.R., Shuster, E.L., Chaky, D.A., Walsh, D.C., Choy, C.C., Tolley, L.-R., Yarme, A., 2000. The changing nature of the 206Pb/207Pb isotopic ratio of lead in rainwater, atmospheric particulates, pine needles and leaded petrol in Scotland, 1982–1998. J. Environ. Monit. 2, 49–57. doi:10.1039/a907558e

Faure, G., Mensing, T.M., 2005. Isotopes : principles and applications, 3rd Edition. Wiley-Blackwell, Hoboken, NJ, USA.

Fernandes, R., Millard, A.R., Brabec, M., Nadeau, M.-J., Grootes, P., 2014. Food Reconstruction Using Isotopic Transferred Signals (FRUITS): A Bayesian Model for Diet Reconstruction. PLoS One 9, e87436. doi:10.1371/journal.pone.0087436

Ferrat, M., Weiss, D.J., Spiro, B., Large, D., 2012. The inorganic geochemistry of a peat deposit on the eastern Qinghai-Tibetan Plateau and insights into changing atmospheric circulation in central Asia during the Holocene. Geochim. Cosmochim. Acta 91, 7–31. doi:10.1016/j.gca.2012.05.028

Feurdean, A., 2010. Forest conservation In a changing world: natural or cultural? Example from the Western Carpathians forests, Romania. Stud. Univ. Babes-Bolyai, Geol. 55, 45–48. doi:10.5038/1937-8602.55.1.6

Feurdean, A., 2005. Holocene forest dynamics in northwestern Romania. The Holocene 15, 435–446. doi:10.1191/0959683605hl803rp

Feurdean, A., Astalos, C., 2005. The impact of human activities in the Gutâiului Mountains, Romania. Stud. Univ. Babes-Bolyai 50, 63–72. doi:10.5038/1937-8602.50.1.7

Feurdean, A., Galka, M., Kuske, E., Tantau, I., Lamentowicz, M., Florescu, G., Liakka, J., Hutchinson, S.M., Mulch, A., Hickler, T., 2015. Last Millennium hydro-climate variability in Central-Eastern Europe (Northern Carpathians, Romania). The Holocene 25, 1179–1192. doi:10.1177/0959683615580197

Feurdean, A., Gałka, M., Tanţău, I., Geantă, A., Hutchinson, S.M., Hickler, T., 2016. Tree and timberline shifts in the northern Romanian Carpathians during the Holocene and the responses to environmental changes. Quat. Sci. Rev. 134, 100–113. doi:10.1016/j.quascirev.2015.12.020

Feurdean, A., Klotz, S., Mosbrugger, V., Wohlfarth, B., 2008. Pollen-based quantitative reconstructions of Holocene climate variability in NW Romania. Palaeogeogr. Palaeoclimatol. Palaeoecol. 260, 494–504. doi:10.1016/j.palaeo.2007.12.014

Feurdean, A., Mosbrugger, V., Onac, B.P., Polyak, V., Veres, D., 2007. Younger Dryas to mid-Holocene environmental history of the lowlands of NW Transylvania, Romania. Quat. Res. 68, 364–378. doi:10.1016/j.yqres.2007.08.003

Feurdean, A., Perşoiu, A., Pazdur, A., Onac, B.P., 2011a. Evaluating the palaeoecological potential of pollen recovered from ice in caves: A case study from Scărişoara Ice Cave, Romania. Rev. Palaeobot. Palynol. 165, 1–10. doi:10.1016/j.revpalbo.2011.01.007

Feurdean, A., Tămaş, T., Tanţău, I., Fărcaş, S., 2012. Elevational variation in regional vegetation responses to late-glacial climate changes in the Carpathians. J. Biogeogr. 39, 258–271. doi:10.1111/j.1365-2699.2011.02605.x

Feurdean, A., Tantau, I., 2017. The Evolution of Vegetation from the Last Glacial Maximum Until the Present, in: Radoane, M., Vespremeanu-Stroe, A. (Eds.), Landform Dynamics and Evolution in Romania. Springer International Publishing, pp. 67–83. doi:10.1007/978-3-319-32589-7

Feurdean, A., Tanţâu, I., Fârcaş, S., 2011b. Holocene variability in the range distribution and abundance of Pinus, Picea abies, and Quercus in Romania; implications for their current status. Quat. Sci. Rev. 30, 3060–3075. doi:10.1016/j.quascirev.2011.07.005

Feurdean, A., Willis, K.J., 2008. The usefulness of a long-term perspective in assessing current forest conservation management in the Apuseni Natural Park, Romania. For. Ecol. Manage. 256, 421–430. doi:10.1016/j.foreco.2008.04.050

Feurdean, A., Willis, K.J., Astalos, C., 2009. Legacy of the past land-use changes and management on the "natural" upland forest composition in the Apuseni Natural Park, Romania. The Holocene 19, 967–981. doi:10.1177/0959683609337358

Feurdean, A., Willis, K.J., Parr, C.L., Tantau, I., Farcas, S., 2010. Post-glacial patterns in vegetation dynamics in Romania: Homogenization or differentiation? J. Biogeogr. 37, 2197–2208. doi:10.1111/j.1365-2699.2010.02370.x

Feurdean, a., Liakka, J., Vannière, B., Marinova, E., Hutchinson, S.M., Mosburgger, V., Hickler, T., 2013. 12,000-Years of fire regime drivers in the lowlands of transylvania (Central-Eastern

Europe): A data-model approach. Quat. Sci. Rev. 81, 48–61. doi:10.1016/j.quascirev.2013.09.014

Filipova-Marinova, M., Pavlov, D., Coolen, M., Giosan, L., 2013. First high-resolution marinopalynological stratigraphy of Late Quaternary sediments from the central part of the Bulgarian Black Sea area. Quat. Int. 293, 170–183. doi:10.1016/j.quaint.2012.05.002

Fine, J.V.A., 1994. The late medieval Balkans a critical survey from the late twelfth century to the Ottoman conquest. The Univ. of Michigan Press, Michigan.

Finné, M., Holmgren, K., Sundqvist, H.S., Weiberg, E., Lindblom, M., 2011. Climate in the eastern Mediterranean, and adjacent regions, during the past 6000 years – A review. J. Archaeol. Sci. 38, 3153–3173. doi:10.1016/j.jas.2011.05.007

Finsinger, W., Fevre, J., Orbán, I., Pál, I., Vincze, I., Hubay, K., Birks, H.H., Braun, M., Tóth, M., Magyari, E.K., 2016. Holocene fire-regime changes near the treeline in the Retezat Mts. (Southern Carpathians, Romania). Quat. Int. doi:10.1016/j.quaint.2016.04.029

Finsinger, W., Morales-Molino, C., Gałka, M., Valsecchi, V., Bojovic, S., Tinner, W., 2017. Holocene vegetation and fire dynamics at Crveni Potok, a small mire in the Dinaric Alps (Tara National Park, Serbia). Quat. Sci. Rev. 167, 63–77. doi:10.1016/j.quascirev.2017.04.032

Fletcher, W.J., Debret, M., Goni, M.F.S., 2013. Mid-Holocene emergence of a low-frequency millennial oscillation in western Mediterranean climate: Implications for past dynamics of the North Atlantic atmospheric westerlies. The Holocene 23, 153–166. doi:10.1177/0959683612460783

Fodor, P., Dávid, G., 2000. Ottomans, Hungarians and Habsburgs in Central Europe : the military confines in the era of Ottoman conquest. Brill.

Folkeson, L., I.Nyholm, N.E., Tyler, G., 1990. Influence of acidity and other soil properties on metal concentration in forest plants and animals. Sci. Total Environ. 96, 211–233. doi:10.1016/0048-9697(90)90075-6

Forbes, C., Evans, M., Hastings, N., Peacock, B., 2011. Statistical distributions. Wiley.

Forel, B., Monna, F., Petit, C., Bruguier, O., Losno, R., Fluck, P., Begeot, C., Richard, H., Bichet, V., Chateau, C., 2010. Historical mining and smelting in the Vosges Mountains (France) recorded in two ombrotrophic peat bogs. J. Geochemical Explor. 107, 9–20. doi:10.1016/j.gexplo.2010.05.004

Forray, F.L., Onac, B.P., Tanţău, I., Wynn, J.G., Tămaş, T., Coroiu, I., Giurgiu, A.M., 2015. A Late Holocene environmental history of a bat guano deposit from Romania: an isotopic, pollen and microcharcoal study. Quat. Sci. Rev. 127, 141–154. doi:10.1016/j.quascirev.2015.05.022

Frame, L., 2004. Investigations at Tal-i Iblis : evidence for copper smelting during the Chalcolithic period.

Francus, P., Lamb, H., Nakagawa, T., Marshall, M., Brown, E., Members, S. 2006 P., 2009. The potential of high-resolution X-ray fluorescence core scanning : Applications in paleolimnology. PAGES news 17, 93–95.

Fu, Q., Hajdinjak, M., Moldovan, O.T., Constantin, S., Mallick, S., Skoglund, P., Patterson, N., Rohland, N., Lazaridis, I., Nickel, B., Viola, B., Prüfer, K., Meyer, M., Kelso, J., Reich, D., Pääbo, S., 2015. An early modern human from Romania with a recent Neanderthal ancestor. Nature 524, 216–219. doi:10.1038/nature14558

Gałka, M., Tanţău, I., Ersek, V., Feurdean, A., 2016. A 9000year record of cyclic vegetation changes identified in a montane peatland deposit located in the Eastern Carpathians (Central-Eastern Europe): Autogenic succession or regional climatic influences? Palaeogeogr. Palaeoclimatol. Palaeoecol. 449, 52–61. doi:10.1016/j.palaeo.2016.02.007

Gallon, C., Tessier, A., Gobeil, C., Carignan, R., 2006. Historical perspective of industrial lead emissions to the atmosphere from a Canadian smelter. Environ. Sci. Technol. 40, 741–747. doi:10.1021/es051326g

Garaba, L., Sfîcă, L., 2015. Climatic Features of the Romanian Territory Generated By the Action of Mediterranean Cyclones. Lucr. Semin. Geogr. "Dimitrie Cantemir" 11–24.

García-Alix, a., Jimenez-Espejo, F.J., Lozano, J. a., Jiménez-Moreno, G., Martinez-Ruiz, F., García Sanjuán, L., Aranda Jiménez, G., García Alfonso, E., Ruiz-Puertas, G., Anderson, R.S., Sanjuán, L.G., Aranda Jiménez, G., García Alfonso, E., Ruiz-Puertas, G., Anderson, R.S., 2013. Anthropogenic impact and lead pollution throughout the Holocene in Southern Iberia. Sci. Total Environ. 449, 451–460. doi:10.1016/j.scitotenv.2013.01.081

García-Sellés, C., Peña, J.C., Martí, G., Oller, P., Martínez, P., 2010. WeMOI and NAOi influence on major avalanche activity in the Eastern Pyrenees. Cold Reg. Sci. Technol. 64, 137–145. doi:10.1016/j.coldregions.2010.08.003

Garçon, M., Chauvel, C., Chapron, E., Faïn, X., Lin, M., Campillo, S., Bureau, S., Desmet, M., Bailly-Maître, M.-C., Charlet, L., 2012. Silver and lead in high-altitude lake sediments: Proxies for climate changes and human activities. Appl. Geochemistry 27, 760–773. doi:10.1016/j.apgeochem.2011.12.010

Gavrilov, M.B., Marković, S.B., Schaetzl, R.J., Tošić, I., Zeeden, C., Obreht, I., Sipos, G., Ruman, A., Putniković, S., Emunds, K., Perić, Z., Hambach, U., Lehmkuhl, F., 2017. Prevailing surface winds in Northern Serbia in the recent and past time periods; modern- and past dust deposition. Aeolian Res. 0–13. doi:10.1016/j.aeolia.2017.07.008

Geantă, A., Gałka, M., Tanţău, I., Hutchinson, S.M., Mîndrescu, M., Feurdean, A., 2014. High mountain region of the Northern Romanian Carpathians responded sensitively to Holocene climate and land use changes: A multi-proxy analysis. The Holocene 24, 944–956. doi:10.1177/0959683614534747

Geantă, A., Tanțău, I., Tămaş, T., Johnston, V.E., 2012. Palaeoenvironmental information from the palynology of an 800year old bat guano deposit from M??gurici Cave, NW Transylvania (Romania). Rev. Palaeobot. Palynol. 174, 57–66. doi:10.1016/j.revpalbo.2011.12.009

Gimbutas, M., 1982. The gods and goddesses of old Europe, 7000 to 3500 BC; myths, legends and cult images. University of California Press.

Gimbutas, M., 1965. Bronze Age cultures in Central and Eastern Europe. De Gruyer Mouton, Berlin and Boston.

Giosan, L., Coolen, M.J.L., Kaplan, J.O., Constantinescu, S., Filip, F., Filipova-Marinova, M., Kettner, A.J., Thom, N., 2012. Early Anthropogenic Transformation of the Danube-Black Sea System. Sci. Rep. 2, 1–6. doi:10.1038/srep00582

Gogâltan, F., 2015. The Early and Middle Bronze Age Chronology on the Eastern Frontier of the Carpathian Basin. Revisited after 15 Years, Bronze Age Chronology in the Carpathian Basin. Proceedings of the International Colloquium from Târgu Mureş 2–4 October 2014.

Gogâltan, F., 1998. Early and middle bronze age chronology in south-west Romania. General aspects, in: The Early and Middle Bronze Age in the Carpathian Basin. pp. 191–212.

Gogâltan, F., 1995. Die Frühe Bronzezeit im Südwesten Rumäniens. Stand der Forschung (Early Bronze Age in the Southwest of Romania. State of the Research). Thraco-Dacia 16, 55–79.

Goudie, A.S., Middleton, N.J., 2006. Desert Dust in the Global System. Springer Berlin Heidelberg, Berlin & Heidelburg. doi:10.1007/3-540-32355-4

Grayson, R.P., Plater, A.J., 2008. A lake sediment record of Pb mining from Ullswater, English Lake District, UK. J. Paleolimnol. 42, 183–197. doi:10.1007/s10933-008-9270-y

Grimm, E.C., 1990. TILIA and TILIAGRAPH. PC spreadsheet and graphics software for pollen data. INQUA Work. Gr. Data Handl. Methods, Newsl. 4, 5–7.

Grimm, E.C., 1987. CONISS: a FORTRAN 77 program for stratigraphically constrained cluster analysis by the method of incremental sum of squares. Comput. Geosci. 13, 13–35. doi:10.1016/0098-3004(87)90022-7

Grindean, R., Tanţău, I., Fărcaş, S., Panait, A., 2014. Middle to Late Holocene vegetation shifts in the NW Transylvanian lowlands (Romania). Stud. Univ. Babes-Bolyai, Geol. 59, 29–37.

Grinsted, A., Moore, J.C., Jevrejeva, S., 2004. Application of the cross wavelet transform and

wavelet coherence to geophysical time series. Nonlinear Process. Geophys. 11, 561–566.

Grousset, F.E., Biscaye, P.E., 2005. Tracing dust sources and transport patterns using Sr, Nd and Pb isotopes. Chem. Geol. 222, 149–167. doi:10.1016/j.chemgeo.2005.05.006

Grousset, F.E., Ginoux, P., Bory, A., Biscaye, P.E., 2003. Case study of a Chinese dust plume reaching the French Alps. Geophys. Res. Lett. 30, 1277. doi:10.1029/2002GL016833

Grousset, F.E., Quetel, C.R., Thomas, B., Buat-Menard, P., Donard, O.F., Bucher, a, 1994. Transient pb isotopic signatures in the Western European atmosphere. Environ. Sci. Technol. 28, 1605–8. doi:10.1021/es00058a011

Gudea, N., 1979. The Defensive System of Roman Dacia. Britannia 10, 63–87. doi:10.2307/526045

Gulson, B., 2008. Stable lead isotopes in environmental health with emphasis on human investigations. Sci. Total Environ. 400, 75–92. doi:10.1016/j.scitotenv.2008.06.059

Haliuc, A., Veres, D., Hubay, K., Brauer, A., Hutchinson, S.M., Begy, R., Hubay, K., Hutchinson, S.M., Begy, R., Braun, M., 2017. Palaeohydrological changes over mid and late Holocene in the Carpathian area , central-eastern Europe. Glob. Planet. Change 1–43. doi:10.1016/j.gloplacha.2017.02.010

Hansen, S., 2013. Innovative Metals: Copper, Gold and Silver in the Black Sea Region and the Carpathian Basin During the 5th and 4th Millennium BC, in: Burmeister, S., Hansen, S., Kunst, M., Müller-Scheeßel, N. (Eds.), Metal Matters: Innovative Technologies and Social Change in Prehistory and Antiquity. VML Vlg Marie Leidorf, Rahden/Westf., pp. 138–167.

Hansmann, W., Köppel, V., 2000. Lead-isotopes as tracers of pollutants in soils. Chem. Geol. 171, 123–144. doi:10.1016/S0009-2541(00)00230-8

Hansson, S. V., Bindler, R., De Vleeschouwer, F., 2015. Using Peat Records as Natural Archives of Past Atmospheric Metal Deposition. Springer Netherlands, pp. 323–354. doi:10.1007/978-94-017-9541-8_12

Harangi, S., Molnar, M., Vinkler, A.P., Kiss, B., Jull, A.J.T., Leonard, A.G., 2010. Radiocarbon Dating of the Last Volcanic Eruptions of Ciomadul Volcano, Southeast Carpathians, Eastern-Central Europe. Radiocarbon 52, 1498–1507. doi:dx.doi.org/10.2458/azu_js_rc.52.3648

Harper, K., 2015. Pandemics and passages to late antiquity: rethinking the plague of c.249–270 described by Cyprian. J. Rom. Archaeol. 28, 223–260. doi:10.1017/S1047759415002470

Haynes, W., 2014. CRC Handbook of Chemistry and Physics. CRC Press. doi:10.1136/oem.53.7.504

Heinrich, C.A., Neubauer, F., 2002. Cu - Au - Pb - Zn - Ag metallogeny of the Alpine - Balkan -

Carpathian - Dinaride geodynamic province. Miner. Depos. 37, 533–540. doi:10.1007/s00126-002-0271-x

Heiri, O., Brooks, S.J., Renssen, H., Bedford, A., Hazekamp, M., Ilyashuk, B., Jeffers, E.S., Lang, B., Kirilova, E., Kuiper, S., Millet, L., Samartin, S., Toth, M., Verbruggen, F., Watson, J.E., van Asch, N., Lammertsma, E., Amon, L., Birks, H.H., Birks, H.J.B., Mortensen, M.F., Hoek, W.Z., Magyari, E., Muñoz Sobrino, C., Seppä, H., Tinner, W., Tonkov, S., Veski, S., Lotter, A.F., Renssen, H., Isarin, R.F.B., Clark, P.U., Fischer, H., Clark, P.U., Björck, S., Grafenstein, U. von, Erlenheuser, H., Brauer, A., Jouzel, J., Johnsen, S., Rach, O., Brauer, A., Wilkes, H., Sachse, D., Renssen, H., Bogaart, P.W., Liu, Z., Menviel, L., Timmermann, A., Timm, O.E., Mouchet, A., Lotter, A.F., Eggermont, H., Heiri, O., Brooks, S.J., Korhola, A., Olander, H., Blom, T., Heiri, O., Birks, H.J.B., Brooks, S.J., Velle, G., Willassen, E., Levesque, A.J., Cwynar, L.C., Walker, I.R., Thornalley, D.J.R., Barker, S., Broecker, W.S., Elderfield, H., McCave, I.N., Renssen, H., Vandenberghe, J., McManus, J.F., Francois, R., Gherardi, J.-M., Keigwin, L.D., Brown-Leger, S., Heiri, O., Brooks, S.J., Birks, H.J.B., Lotter, A.F., Rasmussen, S.O., Brooks, S.J., Langdon, P.G., Heiri, O., Braak, C.J.F. ter, Juggins, S., Heiri, O., Lotter, A.F., New, M., Lister, D., Hulme, M., Makin, I., Livingstone, D.M., Lotter, A.F., Walker, I.R., Renssen, H., 2014. Validation of climate model-inferred regional temperature change for late-glacial Europe. Nat. Commun. 5, 4914. doi:10.1038/ncomms5914

Helwing, B., 2008. 4 An Age of Heroes ? Some Thoughts on Early Bronze Age Funerary Customs in Northern Mesopotamia. (Re-)Constructing Funer. Ritual. Anc. Near East.

Hernberg, S., 2000. Lead Poisoning in a Historical Perspective. Am. J. Ind. Med. 38, 244–254.

Hervella, M., Rotea, M., Izagirre, N., Constantinescu, M., Alonso, S., Ioana, M., Lazar, C., Ridiche, F., Soficaru, A.D., Netea, M.G., De-la-Rua, C., 2015. Ancient DNA from South-East Europe Reveals Different Events during Early and Middle Neolithic Influencing the European Genetic Heritage. PLoS One 10, e0128810. doi:10.1371/journal.pone.0128810

Higham, T., Chapman, J., Slavchev, V., Gaydarska, B., Honch, N., Yordanov, Y., Dimitrova, B., 2007. New perspectives on the Varna cemetery (Bulgaria) – AMS dates and social implications. Antiquity 81, 640–654. doi:10.1017/S0003598X00095636

Hijmans, R.J., Cameron, S.E., Parra, J.L., Jones, P.G., Jarvis, A., 2005. Very high resolution interpolated climate surfaces for global land areas. Int. J. Climatol. 25, 1965–1978. doi:10.1002/joc.1276

Hillman, A.L., Abbott, M.B., Valero-Garcés, B., Morellon, M., Barreiro-Lostres, F., Bain, D.J., 2017. Lead pollution resulting from Roman gold extraction in northwestern Spain. The Holocene 95968361769390. doi:10.1177/0959683617693903

Hirt, A.M., 2010. Imperial Mines and Quarries in the Roman World. Oxford University Press. doi:10.1093/acprof:oso/9780199572878.001.0001

Hoffman, D.J., Rattner, B.A., Burton, G.A., Cairns, J., 2003. Handbook of ecotoxicology, 2nd edition. Lewis Publishers, Boca Raton.

Hong, S., Candelone, J.-P., Patterson, C.C., Boutron, C.F., 1996. History of Ancient Copper Smelting Pollution During Roman and Medieval Times Recorded in Greenland Ice. Science. doi:10.1126/science.272.5259.246

Hong, S., Candelone, J.P., Patterson, C.C., Boutron, C.F., 1994. Greenland ice evidence of hemispheric lead pollution two millennia ago by greek and roman civilizations. Science 265, 1841–1843. doi:10.1126/science.265.5180.1841

Hopkins, J.B., Ferguson, J.M., 2012. Estimating the diets of animals using stable isotopes and a comprehensive Bayesian mixing model. PLoS One. doi:10.1371/journal.pone.0028478

Hoyos, B.D., 2011. A companion to the Punic Wars. Wiley-Blackwell, Hoboken, NJ, USA. doi:10.1002/9781444393712

Hughes, J.D., Thirgood, J.V., 1982. Deforestation, Erosion, and Forest Management in Ancient Greece and Rome. J. For. Hist. 26, 60–75. doi:10.2307/4004530

Hurrell, J.W., 2005. North Atlantic Oscillation, in: Encyclopedia of World Climatology. Springer Netherlands, pp. 536–539. doi:10.1007/1-4020-3266-8_150

Huska, A., Powell, W., Mitrovi??, S., Bankoff, H.A., Bulatovi??, A., Filipovi??, V., Boger, R., 2014. Placer Tin Ores from Mt. Cer, West Serbia, and Their Potential Exploitation during the Bronze Age. Geoarchaeology 29, 477–493. doi:10.1002/gea.21488

Hutchinson, S.M., Akinyemi, F.O., Mîndrescu, M., Begy, R., Feurdean, A., 2016. Recent sediment accumulation rates in contrasting lakes in the Carpathians (Romania): impacts of shifts in socio-economic regime. Reg. Environ. Chang. 16, 501–513. doi:10.1007/s10113-015-0764-7

Iancu, V., Berza, T., Seghedi, A., Gheuca, I., Hann, H.P., 2005. Alpine polyphase tectono-metamorphic evolution of the South Carpathians: A new overview. Tectonophysics 410, 337–365. doi:10.1016/j.tecto.2004.12.038

Inger, R., Ruxton, G.D., Newton, J., Colhoun, K., Robinson, J.A., Jackson, A.L., Bearhop, S., 2006. Temporal and intrapopulation variation in prey choice of wintering geese determined by stable isotope analysis. J. Anim. Ecol. 75, 1190–1200. doi:10.1111/j.1365-2656.2006.01142.x

IPCC, 2013. The Physical Science Basis. Working Group I Contribution to the Fifth Assessment Report of the Intergovernmental Panel on Climate Change, Cambridge, United Kingdom and

New York, USA.

Irabien, M.J., Cearreta, A., Urteaga, M., 2012. Historical signature of Roman mining activities in the Bidasoa estuary (Basque Country, northern Spain): an integrated micropalaeontological, geochemical and archaeological approach. J. Archaeol. Sci. 39, 2361–2370. doi:10.1016/j.jas.2012.02.023

Ivanišević, V., 2001. Novčarstvo srednjovekovne Srbije (Serbian medieval coinage). Stubovi kulture, Beograd.

Jakab, G., Sumegi, P., 2004. The macrobotanical remains from Baláta-tó, in: Environmental History of Transdanubia. Varia Archaeologica Hungarica 20, pp. 247–250.

Jickells, T.D., 2005. Global Iron Connections Between Desert Dust, Ocean Biogeochemistry, and Climate. Science. 308, 67–71. doi:10.1126/science.1105959

Jiménez-Espejo, F.J., García-Alix, A., Jiménez-Moreno, G., Rodrigo-Gámiz, M., Anderson, R.S., Rodríguez-Tovar, F.J., Martínez-Ruiz, F., Giralt, S., Delgado Huertas, A., Pardo-Igúzquiza, E., 2014. Saharan aeolian input and effective humidity variations over western Europe during the Holocene from a high altitude record. Chem. Geol. 374, 1–12. doi:10.1016/j.chemgeo.2014.03.001

Jin, Z., Wang, S., Shen, J.I., Zhang, E., Li, F., Ji, J., Lu, X., 2001. Chemical Weathering Since the Little Ice Age Recorded in Lake Sediments : a High-Resolution Proxy of Past Climate. Earth Surf. Process. Landforms 782, 775–782. doi:10.1002/esp.224

Jin, Z.D., Cao, J.J., Wu, J.L., Wang, S.M., 2006. A Rb/Sr record of catchment weathering response to Holocene climate change in Inner Mongolia. Earth Surf. Process. Landforms 31, 285–291. doi:10.1002/esp.1243

Jones, M.D., Roberts, C.N., Leng, M.J., Türkeş, M., 2006. A high-resolution late Holocene lake isotope record from Turkey and links to North Atlantic and monsoon climate. Geology 34, 361–364. doi:10.1130/G22407.1

Jovanović, B., 2009. Beginning of the metal age in the central Balkans according to the results of the archeometallurgy. J. Min. Metall. Sect. B Metall. 45, 143–148. doi:10.2298/JMMB0902143J

Judt, T., 2005. Postwar : a history of Europe since 1945. Penguin Press.

Kabata-Pendias, A., 2010. Trace Elements in Soils and Plants, 4th ed. CRC Press, Boca Raton.

Kacanski, A., Carmi, I., Shemesh, A., Kronfeld, J., Yam, R., Flexer, A., 2006. Late Holocene climatic change in the Balkans; speleothem isotopic data from Serbia. Radiocarbon 43, 647–658. doi:10.2458/AZU_JS_RC.43.3896

Kaniewski, D., Van Campo, E., Guiot, J., Le Burel, S., Otto, T., Baeteman, C., 2013. Environmental roots of the late bronze age crisis. PLoS One 8, e71004. doi:10.1371/journal.pone.0071004

Kaplan, J.O., Krumhardt, K.M., Zimmermann, N., 2009. The prehistoric and preindustrial deforestation of Europe. Quat. Sci. Rev. 28, 3016–3034. doi:10.1016/j.quascirev.2009.09.028

Karátson, D., Wulf, S., Veres, D., Magyari, E.K., Gertisser, R., Timar-Gabor, A., Novothny, Telbisz, T., Szalai, Z., Anechitei-Deacu, V., Appelt, O., Bormann, M., Jánosi, C., Hubay, K., Schäbitz, F., 2016. The latest explosive eruptions of Ciomadul (Csomád) volcano, East Carpathians - A tephrostratigraphic approach for the 51-29 ka BP time interval. J. Volcanol. Geotherm. Res. 319, 29–51. doi:10.1016/j.jvolgeores.2016.03.005

Kellogg, F., 1995. The road to Romanian independence. Purdue University Press, West Lafayette.

Kempter, H., Frenzel, B., 2000. The Impact of Early Mining and Smelting on the Local Tropospheric Aerosol Detected in Ombrotrophic Peat Bogs in the Harz, Germany. Water. Air. Soil Pollut. 121, 93–108. doi:10.1023/A:1005253716497

Keylock, C.J., 2003. The North Atlantic Oscillation and snow avalanching in Iceland. Geophys. Res. Lett. 30, n/a-n/a. doi:10.1029/2002GL016272

Kienlin, T.L., 2014. Aspects of Metalworking and Society from the Black Sea to the Baltic Sea from the Fifth to the Second Millennium BC, in: Roberts, B.W., Thornton, C.P. (Eds.), Archaeometallurgy in Global Perspective: Methods and Syntheses. Springer, New York, pp. 1–868. doi:10.1007/978-1-4614-9017-3

Killick, D., Fenn, T., 2012. Archaeometallurgy: The Study of Preindustrial Mining and Metallurgy. Annu. Rev. Anthropol. 41, 559–575. doi:10.1146/annurev-anthro-092611-145719

Klaminder, J., Renberg, I., Bindler, R., Emteryd, O., 2003. Isotopic trends and background fluxes of atmospheric lead in northern Europe: Analyses of three ombrotrophic bogs from south Sweden. Global Biogeochem. Cycles 17, 19–1. doi:10.1029/2002GB001921

Kok, J.F., Mahowald, N.M., Fratini, G., Gillies, J.A., Ishizuka, M., Leys, J.F., Mikami, M., 2014. An improved dust emission model – Part 1: Model description and comparison against measurements. Atmos. Chem. Phys 14, 13023–13041. doi:10.5194/acp-14-13023-2014

Komárek, M., Ettler, V., Chrastný, V., Mihaljevič, M., 2008. Lead isotopes in environmental sciences: A review. Environ. Int. 34, 562–577. doi:10.1016/j.envint.2007.10.005

Korcz, M., Fudała, J., Kliś, C., 2009. Estimation of wind blown dust emissions in Europe and its vicinity. Atmos. Environ. 43, 1410–1420. doi:10.1016/j.atmosenv.2008.05.027

Korponai, J., Magyari, E.K., Buczkó, K., Iepure, S., Namiotko, T., Czakó, D., Kövér, C., Braun,

M., 2011. Cladocera response to Late Glacial to Early Holocene climate change in a South Carpathian mountain lake. Hydrobiologia 676, 223–235. doi:10.1007/s10750-011-0881-3

Kramers, J.D., Tolstikhin, I.N., 1997. Two terrestrial lead isotope paradoxes, forward transport modelling, core formation and the history of the continental crust. Chem. Geol. 139, 75–110. doi:10.1016/S0009-2541(97)00027-2

Krichak, S.O., Kishcha, P., Alpert, P., 2002. Decadal trends of main Eurasian oscillations and the Eastern Mediterranean precipitation. Theor. Appl. Clim. 72, 209–220. doi:10.1007/s007040200021

Kristiansen, K., Larsson, T.B., 2005. The rise of Bronze Age society : travels, transmissions and transformations. Cambridge University Press.

Kristó, A., 1995. A Csomád hegycsoport. A Szent-Anna tó természetvédelmi területe (The Nature Reserve of Lake Saint Ana). Kristó András emlékére (In Rememb. András Kristó). Balat. Akadémia Könyvek 13, 38–45.

Kulkarni, C., Peteet, D., Boger, R., Heusser, L., 2016. Exploring the role of humans and climate over the Balkan landscape: 500 years of vegetational history of Serbia. Quat. Sci. Rev. 144, 83–94. doi:10.1016/j.quascirev.2016.05.021

Kylander, M.E., Ampel, L., Wohlfarth, B., Veres, D., 2011. High-resolution X-ray fluorescence core scanning analysis of Les Echets (France) sedimentary sequence: New insights from chemical proxies. J. Quat. Sci. 26, 109–117. doi:10.1002/jqs.1438

Kylander, M.E., Bindler, R., Cortizas, A.M., Gallagher, K., Mörth, C.M., Rauch, S., 2013. A novel geochemical approach to paleorecords of dust deposition and effective humidity: 8500 years of peat accumulation at Store Mosse (the "Great Bog"), Sweden. Quat. Sci. Rev. 69, 69–82. doi:10.1016/j.quascirev.2013.02.010

Kylander, M.E., Klaminder, J., Bindler, R., Weiss, D.J., 2010. Natural lead isotope variations in the atmosphere. Earth Planet. Sci. Lett. 290, 44–53. doi:10.1016/j.epsl.2009.11.055

Kylander, M.E., Martínez-Cortizas, A., Bindler, R., Greenwood, S.L., Mörth, C.-M., Rauch, S., Mart??nez-Cortizas, A., Bindler, R., Greenwood, S.L., M??rth, C.M., Rauch, S., 2016. Potentials and problems of building detailed dust records using peat archives: An example from Store Mosse (the ???Great Bog???), Sweden. Geochim. Cosmochim. Acta 190, 156–174. doi:10.1016/j.gca.2016.06.028

Kylander, M.E., Weiss, D.J., Kober, B., 2009. Two high resolution terrestrial records of atmospheric Pb deposition from New Brunswick, Canada, and Loch Laxford, Scotland. Sci. Total Environ. 407, 1644–1657. doi:10.1016/j.scitotenv.2008.10.036

Kylander, M.E., Weiss, D.J., Martínez Cortízas, A., Spiro, B., Garcia-Sanchez, R., Coles, B.J.,

2005. Refining the pre-industrial atmospheric Pb isotope evolution curve in Europe using an 8000 year old peat core from NW Spain. Earth Planet. Sci. Lett. 240, 467–485. doi:10.1016/j.epsl.2005.09.024

Labzovskii, L., Toanca, F., Nicolae, D., 2014. Determination of Saharan dust properties over Bucharest, Romania. Part 2: Study cases analysis. Rom. J. Phys. 59, 1097–1108.

Landrigan, P.J., 2002. The worldwide problem of lead in petrol. Bull. World Heal. Organ. 80, 768.

Lanphear, B.P., Hornung, R., Khoury, J., Yolton, K., Baghurst, P., Bellinger, D.C., Canfield, R.L., Dietrich, K.N., Bornschein, R., Greene, T., Rothenberg, S.J., Needleman, H.L., Schnaas, L., Wasserman, G., Graziano, J., Roberts, R., 2005. Low-level Environmental Lead Exposure and Children's Intellectual Function: An International Pooled Analysis. Environ. Health Perspect. 113, 894–899. doi:10.1289/ehp.7688

Lantzy, R.J., Mackenzie, F.T., 1979. Atmospheric trace metals: global cycles and assessment of man's impact. Geochim. Cosmochim. Acta. doi:10.1016/0016-7037(79)90162-5

Larson, G., Albarella, U., Dobney, K., Rowley-Conwy, P., Schibler, J., Tresset, A., Vigne, J.-D., Edwards, C.J., Schlumbaum, A., Dinu, A., Balaçsescu, A., Dolman, G., Tagliacozzo, A., Manaseryan, N., Miracle, P., Van Wijngaarden-Bakker, L., Masseti, M., Bradley, D.G., Cooper, A., 2007. Ancient DNA, pig domestication, and the spread of the Neolithic into Europe. Proc. Natl. Acad. Sci. U. S. A. 104, 15276–15281. doi:10.1073/pnas.0703411104

Layman, C.A., Araujo, M.S., Boucek, R., Hammerschlag-Peyer, C.M., Harrison, E., Jud, Z.R., Matich, P., Rosenblatt, A.E., Vaudo, J.J., Yeager, L.A., Post, D.M., Bearhop, S., 2012. Applying stable isotopes to examine food-web structure: an overview of analytical tools. Biol. Rev. 87, 545–562. doi:10.1111/j.1469-185X.2011.00208.x

Lazarević, P.M., 2013. Mires of Serbia - Distribution characteristics. Bot. Serbica 37, 39–48.

Lazarovici, G., Merlini, M., 2005. New archaeological data refering to Tartaria tablets. Doc. Praehist. XXXII 32, 205–219.

Laznicka, P., 2006. Giant Metallic Deposits. Springer, Berlin & Heidelburg. doi:10.1007/3-540-33092-514

Le Roux, G., Aubert, D., Stille, P., Krachler, M., Kober, B., Cheburkin, A., Bonani, G., Shotyk, W., 2005. Recent atmospheric Pb deposition at a rural site in southern Germany assessed using a peat core and snowpack, and comparison with other archives. Atmos. Environ. 39, 6790–6801. doi:10.1016/j.atmosenv.2005.07.026

Le Roux, G., Fagel, N., De Vleeschouwer, F., Krachler, M., Debaille, V., Stille, P., Mattielli, N., van der Knaap, W.O., van Leeuwen, J.F.N., Shotyk, W., 2012. Volcano- and climate-driven changes in atmospheric dust sources and fluxes since the Late Glacial in Central Europe.

Geology 40, 335–338. doi:10.1130/g32586.1

Le Roux, G., Weiss, D., Grattan, J., Givelet, N., Krachler, M., Cheburkin, A., Rausch, N., Kober, B., Shotyk, W., 2004. Identifying the sources and timing of ancient and medieval atmospheric lead pollution in England using a peat profile from Lindow bog, Manchester. J. Environ. Monit. 6, 502–510.

Le Roux, G., Weiss, D., Grattan, J., Givelet, N., Krachler, M., Cheburkin, A., Rausch, N., Kober, B., Shotyk, W., 2004. Identifying the sources and timing of ancient and medieval atmospheric lead pollution in England using a peat profile from Lindow bog, Manchester. J. Environ. Monit. 6, 502–510. doi:10.1039/b401500b

Levanič, T., Popa, I., Poljanšek, S., Nechita, C., 2013. A 323-year long reconstruction of drought for SW Romania based on black pine (Pinus Nigra) tree-ring widths. Int. J. Biometeorol. 57, 703–714. doi:10.1007/s00484-012-0596-9

Ling, J., Stos-Gale, Z., Grandin, L., Billström, K., Hjärthner-Holdar, E., Persson, P.O., 2014. Moving metals II: Provenancing Scandinavian Bronze Age artefacts by lead isotope and elemental analyses. J. Archaeol. Sci. 41, 106–132. doi:10.1016/j.jas.2013.07.018

Livezeanu, I., 1995. Cultural politics in Greater Romania : regionalism, nation building & ethnic struggle, 1918-1930. Cornell University Press.

López-Moreno, J.I., Goyette, S., Vicente-Serrano, S.M., Beniston, M., 2011. Effects of climate change on the intensity and frequency of heavy snowfall events in the Pyrenees. Clim. Change 105, 489–508. doi:10.1007/s10584-010-9889-3

Lotter, A.F., Birks, H.J.B., 2003. The Holocene palaeolimnology of Sägistalsee and its environmental history – a synthesis. J. Paleolimnol. 30, 333–342. doi:10.1023/A:1026091511403

Lüdecke, H.-J., Weiss, C.O., Hempelmann, A., 2015. Paleoclimate forcing by the solar De Vries/Suess cycle. Clim. Past Discuss. 11, 279–305. doi:10.5194/cpd-11-279-2015

Luterbacher, J., García-Herrera, R., Akcer-On, S., Allan, R., Alvarez-Castro, M.C., Benito, G., Booth, J., Büntgen, U., Cagatay, N., Colombaroli, D., Davis, B., Esper, J., Felis, T., Fleitmann, D., Frank, D., Gallego, D., Garcia-Bustamante, E., Glaser, R., Gonzalez-Rouco, F.J., Goosse, H., Kiefer, T., Macklin, M.G., Manning, S.W., Montagna, P., Newman, L., Power, M.J., Rath, V., Ribera, P., Riemann, D., Roberts, N., Sicre, M.A., Silenzi, S., Tinner, W., Tzedakis, P.C., Valero-Garcés, B., van der Schrier, G., Vannière, B., Vogt, S., Wanner, H., Werner, J.P., Willett, G., Williams, M.H., Xoplaki, E., Zerefos, C.S., Zorita, E., 2012. A review of 2000 years of paleoclimatic evidence in the mediterranean, The Climate of the Mediterranean Region. doi:10.1016/B978-0-12-416042-2.00002-1

Luttwak, E., 1976. The grand strategy of the Roman Empire from the first century A.D. to the third. Johns Hopkins University Press.

MacKendrick, P., 2000. The Dacian Stones Speak. University North Carolina Press, Chapel Hill.

Magny, M., 2004. Holocene climate variability as reflected by mid-European lake-level fluctuations and its probable impact on prehistoric human settlements. Quat. Int. 113, 65–79. doi:10.1016/S1040-6182(03)00080-6

Magny, M., Combourieu-Nebout, N., De Beaulieu, J.L., Bout-Roumazeilles, V., Colombaroli, D., Desprat, S., Francke, A., Joannin, S., Ortu, E., Peyron, O., 2013. Geoscientific Instrumentation Methods and Data Systems North–south palaeohydrological contrasts in the central Mediterranean during the Holocene: tentative synthesis and working hypotheses. Clim. Past 9, 2043–2071. doi:10.5194/cp-9-2043-2013

Magyari, E., Buczkó, K., Jakab, G., Braun, M., Pál, Z., Karátson, D., Pap, I., 2009. Palaeolimnology of the last crater lake in the Eastern Carpathian Mountains: a multiproxy study of Holocene hydrological changes, Hydrobiologia. doi:10.1007/s10750-009-9801-1

Magyari, E.K., Chapman, J., Fairbairn, A.S., Francis, M., Guzman, M., 2012. Neolithic human impact on the landscapes of North-East Hungary inferred from pollen and settlement records. Veg. Hist. Archaeobot. 21, 279–302. doi:10.1007/s00334-012-0350-6

Magyari, E.K., Chapman, J.C., Passmore, D.G., Allen, J.R.M., Huntley, J.P., Huntley, B., 2010. Holocene persistence of wooded steppe in the Great Hungarian Plain. J. Biogeogr. 37, 915–935. doi:10.1111/j.1365-2699.2009.02261.x

Magyari, E.K., Demény, A., Buczkó, K., Kern, Z., Vennemann, T., Fórizs, I., Vincze, I., Braun, M., Kovács, J.I., Udvardi, B., Veres, D., 2013. A 13,600-year diatom oxygen isotope record from the South Carpathians (Romania): Reflection of winter conditions and possible links with North Atlantic circulation changes. Quat. Int. 293, 136–149. doi:10.1016/j.quaint.2012.05.042

Magyari, E.K., Jakab, G., Bálint, M., Kern, Z., Buczkó, K., Braun, M., 2012. Rapid vegetation response to Lateglacial and early Holocene climatic fluctuation in the South Carpathian Mountains (Romania). Quat. Sci. Rev. 35, 116–130. doi:10.1016/j.quascirev.2012.01.006

Magyari, E.K., Veres, D., Wennrich, V., Wagner, B., Braun, M., Jakab, G., Karátson, D., Pál, Z., Ferenczy, G., St-Onge, G., Rethemeyer, J., Francois, J.-P., von Reumont, F., Schäbitz, F., 2014. Vegetation and environmental responses to climate forcing during the Last Glacial Maximum and deglaciation in the East Carpathians: attenuated response to maximum cooling and increased biomass burning. Quat. Sci. Rev. 106, 278–298. doi:10.1016/j.quascirev.2014.09.015

Mahowald, N., Albani, S., Kok, J.F., Engelstaeder, S., Scanza, R., Ward, D.S., Flanner, M.G., 2014. The size distribution of desert dust aerosols and its impact on the Earth system. Aeolian Res. 15, 53–71. doi:10.1016/j.aeolia.2013.09.002

Mahowald, N.M., Kloster, S., Engelstaedter, S., Moore, J.K., Mukhopadhyay, S., Mcconnell, J.R., Albani, S., Doney, S.C., Bhattacharya, A., Curran, M.A.J., Flanner, M.G., Hoffman, F.M., Lawrence, D.M., Lindsay, K., Mayewski, P.A., Neff, J., Rothenberg, D., Thomas, E., Thornton, P.E., Zender, C.S., 2010. Observed 20th century desert dust variability: impact on climate and biogeochemistry. Atmos. Chem. Phys. Atmos. Chem. Phys. 10, 10875–10893. doi:10.5194/acp-10-10875-2010

Makkay, J., 1995. The Rise and Fall of Gold Metallurgy in the Copper Age of the Carpathian Basin: The Background of the Change, in: Prehistoric Gold in Europe. Springer Netherlands, Dordrecht, pp. 65–76. doi:10.1007/978-94-015-1292-3_7

Malcolm, N., 2002. Kosovo : a short history. Pan, London.

Mann, M.E., Zhang, Z., Rutherford, S., Bradley, R.S., Hughes, M.K., Shindell, D., Ammann, C., Faluvegi, G., Ni, F., 2009. Global Signatures and Dynamical Origins of the Little Ice Age and Medieval Climate Anomaly. Science. 326, 1256–1260. doi:10.1126/science.1177303

Manske, S., Hedenquist, J., O'Connor, G., Tămaş, C., Cauuet, B., Leary, S., Minut, A., 2006. Roşia Montană, Romania: Europe's largest gold deposit. SEG Newsl. 64, 1–15.

Marcoux, E., Grancea, L., Lupulescu, M., Milési, J., 2002. Lead isotope signatures of epithermal and porphyry-type ore deposits from the Romanian Carpathian Mountains. Miner. Depos. 37, 173–184. doi:10.1007/s00126-001-0223-x

Marković, S.B., Stevens, T., Kukla, G.J., Hambach, U., Fitzsimmons, K.E., Gibbard, P., Buggle, B., Zech, M., Guo, Z., Hao, Q., Wu, H., O'Hara Dhand, K., Smalley, I.J., Újvári, G., Sümegi, P., Timar-Gabor, A., Veres, D., Sirocko, F., Vasiljević, D.A., Jary, Z., Svensson, A., Jović, V., Lehmkuhl, F., Kovács, J., Svirčev, Z., 2015. Danube loess stratigraphy — Towards a pan-European loess stratigraphic model. Earth-Science Rev. 148, 228–258. doi:10.1016/j.earscirev.2015.06.005

Marques, R., Zêzere, J., Trigo, R., Gaspar, J., Trigo, I., 2008. Rainfall patterns and critical values associated with landslides in Povoação County (São Miguel Island, Azores): relationships with the North Atlantic Oscillation 22, 478–494. doi:10.1002/hyp.6879

Martínez-Cortizas, A., López-Merino, L., Bindler, R., Mighall, T., Kylander, M.E., 2016. Early atmospheric metal pollution provides evidence for Chalcolithic/Bronze Age mining and metallurgy in Southwestern Europe. Sci. Total Environ. 545–546, 398–406. doi:10.1016/j.scitotenv.2015.12.078

Martinez-Cortizas, A., Pontevedra-Pombal, X., Novoa Munoz, J.C., Garcia-Rodeja, E., 1997. Four thousand years of atmospheric Pb, Cd, and Zn deposition recorded by the ombotrophic peat bog of Penido Vello (Northwestern Spain).pdf. Water. Air. Soil Pollut. 100, 387–403.

Martínez Cortizas, A., López-Merino, L., Bindler, R., Mighall, T., Kylander, M., 2013. Atmospheric Pb pollution in N Iberia during the late Iron Age/Roman times reconstructed using the high-resolution record of La Molina mire (Asturias, Spain). J. Paleolimnol. 50, 71–86. doi:10.1007/s10933-013-9705-y

Martínez Cortizas, A., Mighall, T., Pontevedra Pombal, X., Novoa Munfoz, J.C., Peiteado Varela, E., Piñeiro Rebolo, R., 2005. Linking changes in atmospheric dust deposition, vegetation change and human activities in northwest Spain during the last 5300 years. The Holocene 15, 698–706. doi:10.1191/0959683605hl834rp

Martínez Cortizas, A., Peiteado Varela, E., Bindler, R., Biester, H., Cheburkin, A., 2012. Reconstructing historical Pb and Hg pollution in NW Spain using multiple cores from the Chao de Lamoso bog (Xistral Mountains). Geochim. Cosmochim. Acta 82, 68–78. doi:10.1016/j.gca.2010.12.025

Martínez Cortizas, a., García-Rodeja, E., Pontevedra Pombal, X., Nóvoa Muoz, J.C., Weiss, D., Cheburkin, a., 2002. Atmospheric Pb deposition in Spain during the last 4600 years recorded by two ombrotrophic peat bogs and implications for the use of peat as archive. Sci. Total Environ. 292, 33–44. doi:10.1016/S0048-9697(02)00031-1

Marx, S.K., Kamber, B.S., McGowan, H. a., Zawadzki, A., 2010. Atmospheric pollutants in alpine peat bogs record a detailed chronology of industrial and agricultural development on the Australian continent. Environ. Pollut. 158, 1615–1628. doi:10.1016/j.envpol.2009.12.009

Marx, S.K., McGowan, H.A., Kamber, B.S., 2009. Long-range dust transport from eastern Australia: A proxy for Holocene aridity and ENSO-type climate variability. Earth Planet. Sci. Lett. 282, 167–177. doi:10.1016/j.epsl.2009.03.013

Marx, S.K., Rashid, S., Stromsoe, N., 2016. Global-scale patterns in anthropogenic Pb contamination reconstructed from natural archives. Environ. Pollut. 213, 283–298. doi:10.1016/j.envpol.2016.02.006

Mason, A.H., Powell, W.G., Bankoff, H.A., Mathur, R., Bulatovi??, A., Filipovi??, V., Ruiz, J., 2016. Tin isotope characterization of bronze artifacts of the central Balkans. J. Archaeol. Sci. 69, 110–117. doi:10.1016/j.jas.2016.04.012

Matthews, J. a., Dahl, S.O., Dresser, P.Q., Berrisford, M.S., Lie, O., Nesje, a., Owen, G., 2009. Radiocarbon chronology of Holocene colluvial (debris-flow) events at Sletthamn, Jotunheimen, southern Norway: a window on the changing frequency of extreme climatic

events and their landscape impact. The Holocene 19, 1107–1129. doi:10.1177/0959683609344674

Mauri, A., Davis, B.A.S., Collins, P.M., Kaplan, J.O., 2015. The climate of Europe during the Holocene: a gridded pollen-based reconstruction and its multi-proxy evaluation. Quat. Sci. Rev. 112, 109–127. doi:10.1016/j.quascirev.2015.01.013

Mayewski, P. a, Rohling, E., Curtstager, J., Karlén, W., Maasch, K., Davidmeeker, L., Meyerson, E., Gasse, F., Vankreveld, S., Holmgren, K., 2004. Holocene climate variability. Quat. Res. 62, 243–255. doi:10.1016/j.yqres.2004.07.001

McClung, D., Schaerer, P., 2006. The Avalanche Handbook. The Mounaineers Books, Seattle.

McGee, D., DeMenocal, P.B., Winckler, G., Stuut, J.B.W., Bradtmiller, L.I., 2013. The magnitude, timing and abruptness of changes in North African dust deposition over the last 20,000 yr. Earth Planet. Sci. Lett. 371–372, 163–176. doi:10.1016/j.epsl.2013.03.054

McGeechan-Liritzis, V., Taylor, J.W., 1987. Yugoslavian Tin Deposits and the Early Bronze AGe Industries of the Aegean Region. Oxford J. Archaeol. 6, 287–300. doi:10.1111/j.1468-0092.1987.tb00158.x

McGregor, H. V., Evans, M.N., Goosse, H., Leduc, G., Martrat, B., Addison, J.A., Mortyn, P.G., Oppo, D.W., Seidenkrantz, M.-S., Sicre, M.-A., Phipps, S.J., Selvaraj, K., Thirumalai, K., Filipsson, H.L., Ersek, V., 2015. Robust global ocean cooling trend for the pre-industrial Common Era. Nat. Geosci. 8, 671–677. doi:10.1038/ngeo2510

Merkel, J.F., 2007. Imperial roman production of lead and silver in the northern part of upper moesia (mt. kosmaj area). J. Serbian Archaeol. Soc. 23, 39–78.

Miao, X., Mason, J.A., Swinehart, J.B., Loope, D.B., Hanson, P.R., Goble, R.J., Liu, X., 2007. A 10,000 year record of dune activity, dust storms, and severe drought in the central Great Plains. Geology 35, 119. doi:10.1130/G23133A.1

Micu, D., Dumitrescu, A., Cheval, S., Birsan, M.-V., 2015. Projections of Future Changes in Climate of the Romanian Carpathians, in: Climate of the Romanian Carpathians: Variability and Trends. Springer, New York, pp. 199–205. doi:10.1007/978-3-319-02886-6

Mighall, T., Cortizas, A.M., Sanchez, N.S., Foster, I.D.L., Singh, S., Bateman, M., Pickin, J.T., 2014. Identifying evidence for past mining and metallurgy from a record of metal contamination preserved in an ombrotrophic mire neat Leadhills, SW Scotland, UK. The Holocene 1–12. doi:10.1177/0959683614551228

Mighall, T.M., Foster, I.D.L., Crew, P., Chapman, A.S., Finn, A., 2009. Using mineral magnetism to characterise ironworking and to detect its evidence in peat bogs. J. Archaeol. Sci. 36, 130–139. doi:10.1016/j.jas.2008.07.015

Mighall, T.M., Timberlake, S., Foster, I.D.L., Krupp, E., Singh, S., 2009. Ancient copper and lead pollution records from a raised bog complex in Central Wales, {UK}. J. Archaeol. Sci. 36, 1504–1515. doi:16/j.jas.2009.03.005

Migowski, C., Stein, M., Prasad, S., Negendank, J.F.W., Agnon, A., 2006. Holocene climate variability and cultural evolution in the Near East from the Dead Sea sedimentary record. Quat. Res. 66, 421–431. doi:10.1016/j.yqres.2006.06.010

Miljkovic, E., 2014. Ottoman Heritage in the Balkans: The Ottoman Empire in Serbia, Serbia in the Ottoman Empire. Süleyman Demirel Üniversitesi Fen-Edebiyat Fakültesi Sos. Bilim. Derg. 129–137.

Miller, D.E., Van Der Merwe, N.J., 1994. Early Metal Working in Sub-Saharan Africa: A Review of Recent Research. J. Afr. Hist. 35, 1. doi:10.1017/S0021853700025949

Mitev, P., 2010. Empires and peninsulas : Southeastern Europe between Karlowitz and the Peace of Adrianople, 1699-1829. LIT, Munster.

Molnár, M., Rinyu, L., Veres, M., Seiler, M., Wacker, L., Synal, H.-A., 2013. EnvironMICADAS : a mini 14C AMS with enhanced gas ion source. Radiocarbon 55, 338–344. doi:10.2458/azu_js_rc.55.16331

Monna, F., Galop, D., Carozza, L., Tual, M., Beyrie, A., Marembert, F., Chateau, C., Dominik, J., Grousset, F.E., 2004a. Environmental impact of early Basque mining and smelting recorded in a high ash minerogenic peat deposit. Sci. Total Environ. 327, 197–214. doi:10.1016/j.scitotenv.2004.01.010

Monna, F., Hamer, K., Lévêque, J., Sauer, M., 2000. Pb isotopes as a reliable marker of early mining and smelting in the Northern Harz province (Lower Saxony, Germany). J. Geochemical Explor. 68, 201–210. doi:10.1016/S0375-6742(00)00005-4

Monna, F., Petit, C., Gulllaumet, J.P., Jouffroy-Bapicot, I., Blanchot, C., Dominik, J., Losno, R., Richard, H., Lévêque, J., Chateau, C., 2004b. History and Environmental Impact of Mining Activity in Celtic Aeduan Territory Recorded in a Peat Bog (Morvan, France). Environ. Sci. Technol. 38, 665–673. doi:10.1021/es034704v

Moore, J.W., Semmens, B.X., 2008. Incorporating uncertainty and prior information into stable isotope mixing models. Ecol. Lett. 11, 470–480. doi:10.1111/j.1461-0248.2008.01163.x

More, A.F., Spaulding, N.E., Bohleber, P., Handley, M.J., Hoffmann, H., Korotkikh, E. V., Kurbatov, A. V., Loveluck, C.P., Sneed, S.B., McCormick, M., Mayewski, P.A., 2017. Next generation ice core technology reveals true minimum natural levels of lead (Pb) in the atmosphere: insights from the Black Death. GeoHealth. doi:10.1002/2017GH000064

Morellón, M., Anselmetti, F.S., Ariztegui, D., Brushulli, B., Sinopoli, G., Wagner, B., Sadori, L.,

Gilli, A., Pambuku, A., 2016. Human–climate interactions in the central Mediterranean region during the last millennia: The laminated record of Lake Butrint (Albania). Quat. Sci. Rev. 136, 134–152. doi:10.1016/j.quascirev.2015.10.043

Moreno, T., Querol, X., Castillo, S., Alastuey, A., Cuevas, E., Herrmann, L., Mounkaila, M., Elvira, J., Gibbons, W., 2006. Geochemical variations in aeolian mineral particles from the Sahara–Sahel Dust Corridor. Chemosphere 65, 261–270. doi:10.1016/j.chemosphere.2006.02.052

Morley, A., Rosenthal, Y., DeMenocal, P., 2014. Ocean-atmosphere climate shift during the mid-to-late Holocene transition. Earth Planet. Sci. Lett. 388, 18–26. doi:10.1016/j.epsl.2013.11.039

Mountain, H., 1998. The Celtic Encyclopedia. Universal, Boca Raton.

Mulitza, S., Heslop, D., Pittauerova, D., Fischer, H.W., Meyer, I., Stuut, J.-B., Zabel, M., Mollenhauer, G., Collins, J.A., Kuhnert, H., Schulz, M., 2010. Increase in African dust flux at the onset of commercial agriculture in the Sahel region. Nature 466, 226–228. doi:10.1038/nature09213

Nagler, T., 2005. Transylvania between 900 and 1300, in: Pop, I.-A., Nagler, T. (Eds.), The History of Transylvania Volume 1: Until 1541. Romanian Cultural Institute, Cluj Napoca, p. 389.

Nesje, A., Bakke, J., Olaf Dahl, S., Lie, Ø., Bøe, A.-G., 2007. A continuous, high-resolution 8500-yr snow-avalanche record from western Norway. The Holocene 17, 269–277. doi:10.1007/s13398-014-0173-7.2

Neubauer, F., Ebner, F., Wallbrecher, E., 1995. Geological evolution of the internal Alps, Carpathians and of the Pannonian basin: an introduction. Tectonophysics 242, 1–4.

Nichols, J.E., Huang, Y., 2012. Hydroclimate of the northeastern United States is highly sensitive to solar forcing. Geophys. Res. Lett. 39, n/a-n/a. doi:10.1029/2011GL050720

Nicholson, P.T., Shaw, I., 2000. Ancient Egyptian materials and technology. Cambridge University Press.

Nicolás, J., Chiari, M., Crespo, J., Orellana, I.G., Lucarelli, F., Nava, S., Pastor, C., Yubero, E., 2008. Quantification of Saharan and local dust impact in an arid Mediterranean area by the positive matrix factorization (PMF) technique. Atmos. Environ. 42, 8872–8882. doi:10.1016/j.atmosenv.2008.09.018

Niederschlag, E., Pernicka, E., Seifert, T., Bartelheim, M., 2003. The Determination of Lead Isotope Ratios by Multiple Collector Icp-Ms: A Case Study of Early Bronze Age Artefacts and their Possible Relation With Ore Deposits of the Erzgebirge*. Archaeometry 45, 61–100. doi:10.1111/1475-4754.00097

Nikolova, L., with contributions by, Manzura, I. V., Schuster, C.C., 1999. The Balkans in later prehistory : periodization, chronology and cultural development in the Final Copper and Early Bronze Age (fourth and third millennia BC), BAR International Series ; 791. J. and E. Hedges.

Nissen, K.M., Leckebusch, G.C., Pinto, J.G., Ulbrich, U., 2014. Mediterranean cyclones and windstorms in a changing climate. Reg. Environ. Chang. 14, 1873–1890. doi:10.1007/s10113-012-0400-8

Norgate, T., Haque, N., 2010. Energy and greenhouse gas impacts of mining and mineral processing operations. J. Clean. Prod. 18, 266–274. doi:10.1016/j.jclepro.2009.09.020

Notaro, M., Yu, Y., Kalashnikova, O. V., 2015. Regime shift in Arabian dust activity, triggered by persistent Fertile Crescent drought. J. Geophys. Res. Atmos. 120, 10,229-10,249. doi:10.1002/2015JD023855

Novák, M., Emmanuel, S., Vile, M. a., Erel, Y., Véron, A., Pačes, T., Wieder, R.K., Vaněček, M., Štěpánová, M., Břízová, E., Hovorka, J., 2003. Origin of lead in eight central European peat bogs determined from isotope ratios, strengths, and operation times of regional pollution sources. Environ. Sci. Technol. 37, 437–445. doi:10.1021/es0200387

Novak, M., Zemanova, L., Voldrichova, P., Stepanova, M., Adamova, M., Pacherova, P., Komarek, A., Krachler, M., Prechova, E., 2011. Experimental Evidence for Mobility/Immobility of Metals in Peat. Environ. Sci. Technol. 45, 7180–7187. doi:10.1021/es201086v

Nriagu, J., 1996. A History of Global Metal Pollution. Science. 272, 11–12.

Nriagu, J.O., 1994. Mercury pollution from the past mining of gold and silver in the Americas. Sci. Total Environ. 149, 167–181. doi:10.1016/0048-9697(94)90177-5

Nriagu, J.O., 1983. Saturnine Gout among Roman Aristocrats. N. Engl. J. Med. 308, 660–663. doi:10.1056/NEJM198303173081123

Nriagu, J.O., Pacyna, J.M., 1988. Quantitative assessment of worldwide contamination of air, water and soils by trace metals. Nature 333, 134–139. doi:10.1038/333134a0

Nyholm, N.E.I., Tyler, G., 2000. Rubidium content of plants, fungi and animals closely reflects potassium and acidity conditions of forest soils. For. Ecol. Manage. 134, 89–96. doi:10.1016/S0378-1127(99)00247-9

O'Brien, W., 2014. Prehistoric copper mining in Europe: 5500-500 BC. Oxford University Press, Oxford.

O'Shea, J.M., 2011. A River Runs Through It: Landscape and the Evolution of Bronze Age

Networks in the Carpathian Basin. J. World Prehistory 24, 161–174.

Obreht, I., Hambach, U., Veres, D., Zeeden, C., Bösken, J., Stevens, T., Marković, S.B., Klasen, N., Brill, D., Burow, C., Lehmkuhl, F., 2017. Shift of large-scale atmospheric systems over Europe during late MIS 3 and implications for Modern Human dispersal. Sci. Rep. 7, 5848. doi:10.1038/s41598-017-06285-x

Obreht, I., Zeeden, C., Hambach, U., Veres, D., Marković, S. b., Bösken, J., Svirčev, Z., Bačević, N., Gavrilov, M.B., Lehmkuhl, F., 2016. Tracing the influence of Mediterranean climate on Southeastern Europe during the past 350,000 years. Sci. Rep. 6, 36334. doi:10.1038/srep36334

Olsen, J., Anderson, N.J., Knudsen, M.F., 2012. Variability of the North Atlantic Oscillation over the past 5,200 years. Nat. Geosci. 5, 1–14. doi:10.1038/ngeo1589

Oltean, I.A., 2007. Dacia : landscape, colonisation, and Romanisation. Routledge, London.

Onac, B.P., Constantin, S., Lundberg, J., Lauritzen, S.E., 2002. Isotopic climate record in a Holocene stalagmite from Ursilor Cave (Romania). J. Quat. Sci. 17, 319–327. doi:10.1002/jqs.685

Onac, B.P., Forray, F.L., Wynn, J.G., Giurgiu, A.M., 2014. Guano-derived ??13C-based paleo-hydroclimate record from Gaura cu Musca Cave, SW Romania. Environ. Earth Sci. 71, 4061–4069. doi:10.1007/s12665-013-2789-x

Onac, B.P., Hutchinson, S.M., Geantă, A., Forray, F.L., Wynn, J.G., Giurgiu, A.M., Coroiu, I., 2015. A 2500-yr late Holocene multi-proxy record of vegetation and hydrologic changes from a cave guano-clay sequence in SW Romania. Quat. Res. 83, 437–448. doi:10.1016/j.yqres.2015.01.007

Oprea, E.G., Oprea, C., 2015. Dacic Ancient Astronomical Research in Sarmizegetuza. Dialogo 2, 226–230. doi:10.18638/dialogo.2015.2.1.24

Oswald, W.W., Anderson, P.M., Brown, T.A., Brubaker, L.B., Hu, F.S., Lozhkin, A. V., Tinner, W., Kaltenrieder, P., 2005. Effects of sample mass and macrofossil type on radiocarbon dating of arctic and boreal lake sediments. The Holocene 15, 758–767. doi:10.1191/0959683605hl849rr

Oudbashi, O., Mohammadamin Emami, S., Davami, P., 2012. Bronze in Archaeology: A Review of the Archaeometallurgy of Bronze in Ancient Iran, in: Collini, L. (Ed.), Copper Alloys - Early Applications and Current Performance - Enhancing Processes. InTech, Rijeka, pp. 153–178. doi:10.5772/60142

PAGES 2k Consortium, 2017. A global multiproxy database for temperature reconstructions of the Common Era. Sci. Data 4, 1–33. doi:DOI: 10.1038/sdata.2017.88

PAGES 2k Consortium, 2013. Continental-scale temperature variability during the past two millennia. Nat. Geosci. 6, 339–346. doi:10.1038/NGEO1797

Pal, I., Magyari, E.K., Braun, M., Vincze, I., Palfy, J., Molnar, M., Finsinger, W., Buczko, K., 2016. Small-scale moisture availability increase during the 8.2-ka climatic event inferred from biotic proxy records in the South Carpathians (SE Romania). The Holocene 26, 8150. doi:10.1177/0959683616640039

Panagiotopoulos, F., Shahgedanova, M., Hannachi, A., Stephenson, D.B., Panagiotopoulos, F., Shahgedanova, M., Hannachi, A., Stephenson, D.B., 2005. Observed Trends and Teleconnections of the Siberian High: A Recently Declining Center of Action. J. Clim. 18, 1411–1422. doi:10.1175/JCLI3352.1

Panait, A., Diaconu, A., Galka, M., Grindean, R., Hutchinson, S., Hickler, T., Lamentowicz, M., Mulch, A., Tanţău, I., Werner, C., Feurdean, A., 2017. Hydrological conditions and carbon accumulation rates reconstructed from a mountain raised bog in the Carpathians: A multi-proxy approach. CATENA 152, 57–68. doi:10.1016/j.catena.2016.12.023

Panek, T., 2015. Recent progress in landslide dating: A global overview. Prog. Phys. Geogr. 39, 168–198. doi:10.1177/0309133314550671

Papazoglu, F., 1978. The Central Balkan Tribe in Pre-Roman Times: Triballi, Autariatae, Dardanians, Scordisci and Moesians. Hakkert, Amsterdam.

Parajka, J., Kohnová, S., Bálint, G., Barbuc, M., Borga, M., Claps, P., Cheval, S., Dumitrescu, A., Gaume, E., Hlavčová, K., Merz, R., Pfaundler, M., Stancalie, G., Szolgay, J., Blöschl, G., 2010. Seasonal characteristics of flood regimes across the Alpine-Carpathian range. J. Hydrol. 394, 78–89. doi:10.1016/j.jhydrol.2010.05.015

Parnell, A.C., Inger, R., Bearhop, S., Jackson, A.L., Macleod, H., 2010. Source Partitioning Using Stable Isotopes: Coping with Too Much Variation. PLoS One 5, e9672. doi:10.1371/journal.pone.0009672

Parnell, A.C., Phillips, D.L., Bearhop, S., Semmens, B.X., Ward, E.J., Moore, J.W., Jackson, A.L., Grey, J., Kelly, D.J., Inger, R., 2013. Bayesian stable isotope mixing models. Environmetrics 24, 387–399. doi:10.1002/env.2221

Patil, A.J., Bhagwat, V.R., Patil, J.A., Dongre, N.N., Ambekar, J.G., Jailkhani, R., Das, K.K., 2006. Effect of Lead (Pb) Exposure on the Activity of Superoxide Dismutase and Catalase in Battery Manufacturing Workers (BMW) of Western Maharashtra (India) with Reference to Heme biosynthesis. Int. J. Environ. Res. Public Health 3, 329–337. doi:10.3390/ijerph2006030041

Patterson, C.C., 1971. Native copper, silver, and gold accessible to early metallurgists. Am. Antiq.

36, 286–321.

Paulinyi, O., 1981. The Crown Monopoly of the Refining Metallurgy of Precious Metals and the Technology of the Cameral Refineries in Hungary and transylvania in the Period of Advanced and Late Feudalism (1325-1700) with Data and Output, in: Kellenbenz, H. (Ed.), Precious Metals in the Age of Expansion. Papers of the XIVth International Congress of the Historical Sciences. Klett-Cotta, Nurnberg.

Pernicka, E., Begemann, F., Schmitt-Strecker, S., Wagner, G.A., Hedges, R.E.M., Radovanović, I., Dimitrova, B., 1993. Eneolithic and Early Bronze Age copper artefacts from the Balkans and their relation to Serbian copper ores. Praehist. Zeitschrift 68, 1–54. doi:10.1515/prhz.1993.68.1.1

Pernicka, E., Nessel, B., Mehofer, M., Safta, E., 2016. Lead Isotope Analyses of Metal Objects from the Apa Hoard and Other Early and Middle Bronze Age Items from Romania. Archaeol. Austriaca 1, 57–86. doi:10.1553/archaeologia100s57

Perşoiu, A., Onac, B.P., Wynn, J.G., Blaauw, M., Ionita, M., Hansson, M., 2017. Holocene winter climate variability in Central and Eastern Europe. Sci. Rep. 7, 1196. doi:10.1038/s41598-017-01397-w

Petković, S., 2009. The traces of roman metallurgy in eastern Serbia. J. Min. Metall. Sect. B Metall. 45, 187–196. doi:10.2298/JMMB0902187P

Petrovic, G.G., Petrovic, V., 2010. Human Capital and Serbian Mining, in: Engel, J., Grujic, M., Rybar, P. (Eds.), Mining in Central Europe. University of Belgrade, Belgrade, pp. 31–39.

Phillips, D.L., Gregg, J.W., 2003. Source partitioning using stable isotopes: Coping with too many sources. Oecologia 136, 261–269. doi:10.1007/s00442-003-1218-3

Phillips, D.L., Inger, R., Bearhop, S., Jackson, A.L., Moore, J.W., Parnell, A.C., Semmens, B.X., Ward, E.J., 2014. Best practices for use of stable isotope mixing models in food web studies. Can. J. Fish. Aquat. Sci. 835, 823–835. doi:10.1139/cjz-2014-0127

Phillips, D.L., Newsome, S.D., Gregg, J.W., 2005. Combining sources in stable isotope mixing models: alternative methods. Oecologia 144, 520–527. doi:10.1007/s00442-004-1816-8

Photos, E., 1989. The question of meteoritic versus smelted nickel-rich iron: Archaeological evidence and experimental results. World Archaeol. 20, 403–421. doi:10.1080/00438243.1989.9980081

Pichat, S., Abouchami, W., Galer, S.J.G., 2014. Lead isotopes in the Eastern Equatorial Pacific record Quaternary migration of the South Westerlies. Earth Planet. Sci. Lett. 388, 293–305. doi:10.1016/j.epsl.2013.11.035

Pierre, S., Bruno, W., Francesco, F.G., Fanny, M., Jérôme, P., Anne-Lise, D., Adeline, B., Wentao, C., Cécile, P., Jean-Louis, R., Ludovic, G., Manon, B., Yves, P., Emmanuel, M., Pierre, T., Fabien, A., 2017. 6-kyr record of flood frequency and intensity in the western Mediterranean Alps – Interplay of solar and temperature forcing. Quat. Sci. Rev. 170, 121–135. doi:10.1016/j.quascirev.2017.06.019

Plummer, M., 2003. JAGS: A program for analysis of Bayesian graphical models using Gibbs sampling. Proc. 3rd Int. Work. Distrib. Stat. Comput. (DSC 2003) 20–22. doi:10.1.1.13.3406

Pokhrel, L.R., Dubey, B., 2013. Global Scenarios of Metal Mining, Environmental Repercussions, Public Policies, and Sustainability: A Review. Crit. Rev. Environ. Sci. Technol. 43, 2352–2388. doi:10.1080/10643389.2012.672086

Pomiès, C., Cocherie, A., Guerrot, C., Marcoux, E., Lancelot, J., 1998. Assessment of the precision and accuracy of lead-isotope ratios measured by TIMS for geochemical applications: example of massive sulphide deposits (Rio Tinto, Spain). Chem. Geol. 144, 137–149. doi:10.1016/S0009-2541(97)00127-7

Poore, R.Z., Quinn, T.M., Verardo, S., 2004. Century-scale movement of the Atlantic Intertropical Convergence Zone linked to solar variability. Geophys. Res. Lett. 31, n/a-n/a. doi:10.1029/2004GL019940

Pop, E., 1960. Mlaştinile de turbă din Republica Populară Română (Peat bogs from Romania). Editura Academiei Republicii Populare Române, Bucharest.

Pop, I., 1999. Romanians and Romania: A brief history. East European Monographs.

Pop, I.-A., 2005. Transylvania in the 14th century and the first half of the 15th century (1300 - 1456), in: Pop, I.-A., Nagler, T. (Eds.), The History of Transylvania Volume 1: Until 15412. Romanian Cultural Institute, Cluj Napoca, p. 389.

Popa, I., Bouriaud, O., 2014. Reconstruction of summer temperatures in Eastern Carpathian Mountains (Rodna Mts, Romania) back to AD 1460 from tree-rings. Int. J. Climatol. 34, 871–880. doi:10.1002/joc.3730

Popa, I., Kern, Z.Z., 2009. Long-term summer temperature reconstruction inferred from tree-ring records from the Eastern Carpathians. Clim. Dyn. 32, 1107–1117. doi:10.1007/s00382-008-0439-x

Popescu, M., 2002. Landslide causal factors and landslide remedial options, in: Proceedings of the Third International Conference on Landslides, Slope Stability and Safety of Infrastructures. Singapore, pp. 61–81.

Popovic, P., 1987. Le Monnayage des Scordisques. Les Monnaies et la circulation monetaire dans le centre des Balkans. Novi Sad University, Beograd/Novi Sad.

Poto, L., Gabrieli, J., Crowhurst, S., Agostinelli, C., Spolaor, A., Cairns, W.R.L., Cozzi, G., Barbante, C., 2014. Cross calibration between XRF and ICP-MS for high spatial resolution analysis of ombrotrophic peat cores for palaeoclimatic studies. Anal. Bioanal. Chem. 407, 379–385. doi:10.1007/s00216-014-8289-3

Poulter, A. (Ed.), 2007. The Transition to Late Antiquity, on the Danube and Beyond. Oxford University Press/British Academy, Oxford. doi:10.5871/bacad/9780197264027.001.0001

Price, T.D., 2000. Europe's First Farmers: an introduction, in: Price, T.D. (Ed.), Europe's First Farmers. Cambridge University Press, Cambridge.

Pundt, H., 2012. Mining Culture in Roman Dacia: Empire, Community, and Identity at the Gold Mines of Alburnus Maior ca.107-270 C.E. Diss. Theses.

Radivojević, M., Rehren, T., 2016. Paint It Black: The Rise of Metallurgy in the Balkans. J. Archaeol. Method Theory 23, 200–237. doi:10.1007/s10816-014-9238-3

Radivojević, M., Rehren, T., Kuzmanović-Cvetković, J., Jovanović, M., Northover, J.P., 2013. Tainted ores and the rise of tin bronzes in Eurasia , c . 6500 years ago. Antiquity 87, 1030–1045. doi:10.1017/S0003598X0004984X

Radivojević, M., Rehren, T., Pernicka, E., Šljivar, D., Brauns, M., Borić, D., 2010. On the origins of extractive metallurgy: New evidence from Europe. J. Archaeol. Sci. 37, 2775–2787. doi:10.1016/j.jas.2010.06.012

Radulescu, G., 2004. Bistritz - die glänzende Stadt im Schatten von Rodenau, in: Slotta, R., Wollmann, V., Dordea, I. (Eds.), Silber Und Salz in Siebenbürgen. Veröffentlichungen aus dem Deutschen Bergbau-Museum Bochum, Bochum, pp. 143–201.

Ramanathan, V., 2001. Aerosols, Climate, and the Hydrological Cycle. Science. 294, 2119–2124. doi:10.1126/science.1064034

Rasmussen, P.E., 1998. Long-range atmospheric transport of trace metals: the need for geoscience perspectives. Environ. Geol. 33, 96–108. doi:10.1007/s002540050229

Rasmussen, S.O., Vinther, B.M., Clausen, H.B., Andersen, K.K., 2007. Early Holocene climate oscillations recorded in three Greenland ice cores. Quat. Sci. Rev. 26, 1907–1914. doi:10.1016/j.quascirev.2007.06.015

Reimann, C., Flem, B., Fabian, K., Birke, M., Ladenberger, A., Négrel, P., Demetriades, A., Hoogewerff, J., 2012. Lead and lead isotopes in agricultural soils of Europe – The continental perspective. Appl. Geochemistry 27, 532–542. doi:10.1016/j.apgeochem.2011.12.012

Reimer, P., Bard, E., Bayliss, A., Beck, J.W., Blackwell, P.G., Bronk Ramsey, C., Buck, C.E., Cheng, H., Edwards, R.L., Friedrich, M., Grootes, P.M., Guilderson, T.P., Haflidason, H.,

Hajdas, I., Hatté, C., Heaton, T.J., Hoffmann, D.L., Hogg, A.G., Hughen, K.A., Kaiser, K.F., Kromer, B., Manning, S.W., Niu, M., Reimer, R.W., Richards, D.A., Scott, E.M., Southon, J.R., Staff, R.A., Turney, C.S.M., van der Plicht, J., 2013. IntCal13 and Marine13 Radiocarbon Age Calibration Curves 0–50,000 Years cal BP. Radiocarbon 55, 1869–1887. doi:10.2458/azu_js_rc.55.16947

Renberg, I., Bindler, R., Brannvall, M.L., 2001. Using the historical atmospheric lead-deposition record as a chronological marker in sediment deposits in Europe. Holocene 11, 511–516. doi:10.1191/095968301680223468

Renberg, I., Brännvall, M.L., Bindler, R., Emteryd, O., 2002. Stable lead isotopes and lake sediments - A useful combination for the study of atmospheric lead pollution history. Sci. Total Environ. 292, 45–54. doi:10.1016/S0048-9697(02)00032-3

Renberg, I., Persson, M.W., Emteryd, O., 1994. Pre-industrial atmospheric lead contamination detected in Swedish lake sediments. Nature 368, 323–326. doi:10.1038/368323a0

Revel, M., Ducassou, E., Grousset, F.E., Bernasconi, S.M., Migeon, S., Revillon, S., Mascle, J., Murat, A., Zaragosi, S., Bosch, D., 2010. 100,000 Years of African monsoon variability recorded in sediments of the Nile margin. Quat. Sci. Rev. 29, 1342–1362. doi:10.1016/j.quascirev.2010.02.006

Rîmbu, N., Boroneanţ, C., Buţă, C., Dima, M., Rimbu, N., Boroneant, C., Buta, C., 2002. Decadal variability of the Danube river flow in the lower basin and its relation with the North Atlantic Oscillation. Int. J. Climatol. 22, 1169–1179. doi:10.1002/joc.788

Rimbu, N., Stefan, S., Necula, C., 2015. The variability of winter high temperature extremes in Romania and its relationship with large-scale atmospheric circulation. Theor. Appl. Climatol. 121, 121–130. doi:10.1007/s00704-014-1219-7

Roberts, B.W., Thornton, C.P., Pigott, V.C., 2009. Development of metallurgy in Eurasia. Antiquity 83, 1012–1022.

Roberts, N., Eastwood, W.J., Kuzucuoglu, C., Fiorentino, G., Caracuta, V., 2011. Climatic, vegetation and cultural change in the eastern Mediterranean during the mid-Holocene environmental transition. The Holocene 21, 147–162. doi:10.1177/0959683610386819

Roberts, N., Moreno, A., Valero-Garcés, B.L., Corella, J.P., Jones, M., Allcock, S., Woodbridge, J., Morellón, M., Luterbacher, J., Xoplaki, E., Türkeş, M., 2012. Palaeolimnological evidence for an east-west climate see-saw in the Mediterranean since AD 900. Glob. Planet. Change 84–85, 23–34. doi:10.1016/j.gloplacha.2011.11.002

Rohl, B., 1996. Lead isotope data from the isotrace laboratory, Oxford: Archaeometry data base 2, galena from Britain and Ireland. Archaeometry 38, 165–180. doi:10.1111/j.1475-

4754.1996.tb00769.x

Rösch, M., Fischer, E., 2000. A radiocarbon dated Holocene pollen profile from the Banat mountains (Southwestern Carpathians, Romania). Flora (Jena) 195, 277–286.

Rösch, M., Fischer, E., Rosch, M., Fischer, E., 2000. A radiocarbon dated Holocene pollen profile from the Banat mountains (Southwestern Carpathians, Romania), Flora. doi:10.1016/S0367-2530(17)30981-7

Rose, N.L., Cogălniceanu, D., Appleby, P.G., Brancelj, A., Camarero, L., Fernández, P., Grimalt, J.O., Kernan, M., Lami, A., Musazzi, S., Quiroz, R., Velle, G., 2009. Atmospheric contamination and ecological changes inferred from the sediment record of Lacul Negru in the Retezat National park, Romania. Adv. Limnol. doi:10.1127/advlim/62/2009/319

Rosman, K., 2000. A two century record of lead isotopes in high altitude Alpine snow and ice. Earth Planet. Sci. Lett. 176, 413–424. doi:10.1016/S0012-821X(00)00013-3

Rosman, K.J.R., Chisholm, W., Boutron, C.F., Candelone, J.P., Hong, S., 1994. Isotopic evidence to account for changes in the concentration of lead in Greenland snow between 1960 and 1988. Geochim. Cosmochim. Acta 58, 3265–3269. doi:10.1016/0016-7037(94)90054-X

Rosman, K.J.R., Chisholm, W., Hong, S., Candelone, J.P., Boutron, C.F., 1997. Lead from Carthaginian and Roman Spanish mines isotopically identified in Greenland ice dated from 600 B.C. to 300 A.D. Environ. Sci. Technol. 31, 3413–3416. doi:10.1021/es970038k

Rossi, L., Toynbee, J.M.C., 1971. Trajan's Column and the Dacian wars, Documenta Praehistorica. doi:10.2307/526125

Rothwell, J.J., Taylor, K.G., Chenery, S.R.N., Cundy, A.B., Evans, M.G., Allott, T.E.H., 2010. Storage and behavior of As, Sb, Pb, and Cu in ombrotrophic peat bogs under contrasting water table conditions. Environ. Sci. Technol. 44, 8497–8502. doi:10.1021/es101150w

Rousseau, D.D., Chauvel, C., Sima, A., Hatté, C., Lagroix, F., Antoine, P., Balkanski, Y., Fuchs, M., Mellett, C., Kageyama, M., Ramstein, G., Lang, A., 2014. European glacial dust deposits: Geochemical constraints on atmospheric dust cycle modeling. Geophys. Res. Lett. 41, 7666–7674. doi:10.1002/2014GL061382

Rudnick, R.L., Gao, S., 2013. Composition of the Continental Crust. Treatise Geochemistry Second Ed. 4, 1–51. doi:10.1016/B978-0-08-095975-7.00301-6

Ruiz, C., Arribas, A., Arribas, A., 2002. Mineralogy and geochemistry of the Masa Valverde blind massive sulphide deposit, Iberian Pyrite Belt (Spain). Ore Geol. Rev. 19, 1–22. doi:10.1016/S0169-1368(01)00037-3

Russell, J.M., Johnson, T.C., Talbot, M.R., 2003. A 725 yr cycle in the climate of central Africa

during the late Holocene. Geology 31.

Sălăgean, T., 2005. Romanian Society in the Early Middle Ages (9th–14th Centuries AD), in: Pop, I.-A., Bolovan, I. (Eds.), History of Romania: Compendium. Insitutul Cultural Roman, Cluj Napoca, pp. 133–207.

Salomons, W., 1995. Environmental impact of metals derived from mining activities: Processes, predictions, prevention. J. Geochemical Explor. 52, 5–23. doi:10.1016/0375-6742(94)00039-E

Sarnowski, T., 2015. Danubian Provinces, in: Le Bohec, Y. (Ed.), The Encyclopedia of the Roman Army. Wiley-Blackwell, Hoboken, NJ, USA, pp. 277–347. doi:10.1002/9781118318140.wbra0449

Scheuvens, D., Schütz, L., Kandler, K., Ebert, M., Weinbruch, S., 2013. Bulk composition of northern African dust and its source sediments — A compilation. Earth-Science Rev. 116, 170–194. doi:10.1016/j.earscirev.2012.08.005

Schiffer, M.B., 1986. Radiocarbon dating and the "old wood" problem: The case of the Hohokam chronology. J. Archaeol. Sci. 13, 13–30. doi:10.1016/0305-4403(86)90024-5

Schmitz, M., 2005. The Dacian Threat, 101-106 A.D. Caeros Publishing, Armidale, New South Wales.

Schnitchen, C., Charman, D.J., Magyari, E., Braun, M., Grigorszky, I., Tóthmérész, B., Molnár, M., Szántó, Z., 2006. Reconstructing hydrological variability from testate amoebae analysis in Carpathian peatlands. J. Paleolimnol. 36, 1–17. doi:10.1007/s10933-006-0001-y

Schumacher, M., Schier, W., Sch??tt, B., 2016. Mid-Holocene vegetation development and herding-related interferences in the Carpathian region. Quat. Int. 415, 253–267. doi:10.1016/j.quaint.2015.09.074

Schweizer, J., Bruce Jamieson, J., Schneebeli, M., 2003. Snow avalanche formation. Rev. Geophys. 41, 1016. doi:10.1029/2002RG000123

Sebestyen, V., 2010. Revolution 1989 : the fall of the Soviet empire. Phoenix.

Sernander, R., 1908. On the evidences of Postglacial changes of climate furnished by the peat-mosses of Northern Europe. Geol. Foereningan i Stock. Foerhandlingar 30, 465–473. doi:10.1080/11035890809445601

Settle, D., Patterson, C., 1980. Lead in albacore: guide to lead pollution in Americans. Science. 207.

Shanahan, T.M., McKay, N.P., Hughen, K.A., Overpeck, J.T., Otto-Bliesner, B., Heil, C.W., King, J., Scholz, C.A., Peck, J., 2015. The time-transgressive termination of the African Humid

Period. Nat. Geosci. 8, 140–144. doi:10.1038/ngeo2329

Sharifi, A., Pourmand, A., Canuel, E.A., Ferer-Tyler, E., Peterson, L.C., Aichner, B., Feakins, S.J., Daryaee, T., Djamali, M., Beni, A.N., Lahijani, H.A.K., Swart, P.K., 2015. Abrupt climate variability since the last deglaciation based on a high-resolution, multi-proxy peat record from NW Iran: The hand that rocked the Cradle of Civilization? Quat. Sci. Rev. 123, 215–230. doi:10.1016/j.quascirev.2015.07.006

Shotyk, W., 2002. The chronology of anthropogenic, atmospheric Pb deposition recorded by peat cores in three minerogenic peat deposits from Switzerland. Sci. Total Environ. 292, 19–31. doi:10.1016/S0048-9697(02)00030-X

Shotyk, W., 1996. Natural and anthropogenic enrichments of As, Cu, Pb, Sb, and Zn in ombrotrophic versus minerotrophic peat bog profiles, Jura Mountains, Switzerland. Water. Air. Soil Pollut. 90, 375–405. doi:10.1007/BF00282657

Shotyk, W., Blaser, P., Grünig, a., Cheburkin, a. K., 2000. A new approach for quantifying cumulative, anthropogenic, atmospheric lead deposition using peat cores from bogs: Pb in eight Swiss peat bog profiles. Sci. Total Environ. 249, 281–295. doi:10.1016/S0048-9697(99)00523-9

Shotyk, W., Goodsite, M.E., Roos-Barraclough, F., Givelet, N., Le Roux, G., Weiss, D., Cheburkin, A.K., Knudsen, K., Heinemeier, J., van Der Knaap, W.O., Norton, S.A., Lohse, C., 2005. Accumulation rates and predominant atmospheric sources of natural and anthropogenic Hg and Pb on the Faroe Islands. Geochim. Cosmochim. Acta 69, 1–17. doi:10.1016/j.gca.2004.06.011

Shotyk, W., Krachler, M., Martinez-Cortizas, A., Cheburkin, A.K., Emons, H., 2002. A peat bog record of natural, pre-anthropogenic enrichments of trace elements in atmospheric aerosols since 12 370 14C yr BP, and their variation with Holocene climate change. Earth Planet. Sci. Lett. 199, 21–37. doi:10.1016/S0012-821X(02)00553-8

Shotyk, W., Rausch, N., Nieminen, T.M., Ukonmaanaho, L., Krachler, M., 2016. Isotopic Composition of Pb in Peat and Porewaters from Three Contrasting Ombrotrophic Bogs in Finland: Evidence of Chemical Diagenesis in Response to Acidification. Environ. Sci. Technol. 50, 9943–9951. doi:10.1021/acs.est.6b01076

Shotyk, W., Rausch, N., Outridge, P.M., Krachler, M., 2016. Isotopic evolution of atmospheric Pb from metallurgical processing in Flin Flon, Manitoba: Retrospective analysis using peat cores from bogs. Environ. Pollut. 218, 338–348. doi:10.1016/j.envpol.2016.07.009

Shotyk, W., Weiss, D., Kramers, J.D., Frei, R., Cheburkin, A.K., Gloor, M., Reese, S., 2001. Geochemistry of the peat bog at Etang de la Gruère, Jura Mountains, Switzerland, and its

record of atmospheric Pb and lithogenic trace metals (Sc, Ti, Y, Zr, and REE) since 12,370 14C yr BP. Geochim. Cosmochim. Acta 65, 2337–2360. doi:10.1016/S0016-7037(01)00586-5

Shotyk, W., Weiss, D.J., Appleby, P.G., Cheburkin, A.K., Frei, R., Gloor, M., Kramers, J.D., Reese, S., Van Der Knaap, W.O., 1998. History of Atmospheric Lead Deposition Since 12,370 14C yr BP from a Peat Bog, Jura Mountains, Switzerland. Science. 281, 1635–1640. doi:10.1126/science.281.5383.1635

Simmons, E.C., 1998. Strontium: Element and geochemistry, in: Encyclopedia of Geochemistry. Springer Netherlands, pp. 598–599.

Sljivar, D., Borić, D., 2014. Context is everything : comments on Radivojevic et al. Antiquity 88, 1–6.

Slotboom, R.T., van Mourik, J.M., 2015. Pollen records of mardel deposits: The effects of climatic oscillations and land management on soil erosion in Gutland, Luxembourg. CATENA 132, 72–88. doi:10.1016/j.catena.2014.12.035

Smalley, I., Marković, S.B., Svirčev, Z., 2011. Loess is [almost totally formed by] the accumulation of dust. Quat. Int. 240, 4–11. doi:10.1016/j.quaint.2010.07.011

Solecki, R.S., 1969. A Copper Mineral Pendant from Northern Iraa. Antiquity 43, 311–314. doi:10.1017/S0003598X00107525

Soto-Jiménez, M.F., Flegal, A.R., 2009. Origin of lead in the Gulf of California Ecoregion using stable isotope analysis. J. Geochemical Explor. 101, 209–217. doi:10.1016/j.gexplo.2008.07.003

Springer, G.S., Rowe, H.D., Hardt, B., Edwards, R.L., Cheng, H., 2008. Solar forcing of Holocene droughts in a stalagmite record from West Virginia in east-central North America. Geophys. Res. Lett. 35, L17703. doi:10.1029/2008GL034971

Srejović, D., 1969. Lepenski Vir – Nova praistorijska kulturau Podunavlju, CATENA. doi:10.1016/j.catena.2016.12.023

Srinavasan, S., 1994. Wootz crucible steel: a newly discovered production site in South India. Pap. from Inst. Archaeol. 5, 49–59.

Starkel, L., Soja, R., Michczyńska, D.J., 2006. Past hydrological events reflected in Holocene history of Polish rivers. CATENA 66, 24–33. doi:10.1016/j.catena.2005.07.008

Stavrianos, L.S., 1958. The Balkans since 1453. New York University Press, New York.

Stech, T., 1999. Aspects of early metallurgy in Mesopotamia and Anatolia, in: Piggott, V.C. (Ed.), The Archaeometallurgy of the Asian Old World. Museum University of Pennsylvania,

Philadelphia, pp. 59–71.

Stefan, S., Ghioca, M., Rimbu, N., Boroneant, C., 2004. Study of meteorological and hydrological drought in southern Romania from observational data. Int. J. Climatol. 24, 871–881. doi:10.1002/joc.1039

Steinhilber, F., Abreu, J.A., Beer, J., Brunner, I., Christl, M., Fischer, H., Heikkila, U., Kubik, P.W., Mann, M., McCracken, K.G., Miller, H., Miyahara, H., Oerter, H., Wilhelms, F., 2012. 9,400 Years of Cosmic Radiation and Solar Activity From Ice Cores and Tree Rings. Proc. Natl. Acad. Sci. 109, 5967–5971. doi:10.1073/pnas.1118965109

Stevenson, D., 2011. From Balkan Conflict to Global Conflict: The Spread of the First World War, 1914-1918. Foreign Policy Anal. 7, 169–182. doi:10.1111/j.1743-8594.2011.00129.x

Stock, B., Semmens, B., 2013. MixSIAR GUI user manual Version 3.1. doi:10.5281/zenodo.47719

Stockhammer, P.W., Massy, K., Knipper, C., Friedrich, R., Kromer, B., Lindauer, S., Radosavljević, J., Wittenborn, F., Krause, J., 2015. Rewriting the Central European Early Bronze Age Chronology: Evidence from Large-Scale Radiocarbon Dating. PLoS One 10, e0139705. doi:10.1371/journal.pone.0139705

Stockmarr, J., 1971. Tablets with spores used in absolute pollen analysis. Pollen et spores 13, 614–621.

Stojanović, M.M., Šmit, Ž., Glumac, M., Mutić, J., 2015. PIXE-PIGE investigation of roman imperial vessels and window glass from Mt. kosmaj, serbia (moesia superior). J. Archaeol. Sci. Reports 1, 53–63. doi:10.1016/j.jasrep.2014.11.001

Stojić, M., 2006. Ferrous metallurgy centre of the Brnjica Cultural Group (14th–13th Centuries BC) at the Hisar Site in Leskovac. Metal. – J. Metall. – MjoM 12, 105–110.

Stojkovic, M.D., 2010. Saxon Miners in Serbian Medieval laws and written texts. Min. Hist. Bull. Peak Dist. Mines Hist. Soc. 17, 49–54.

Stojković, M.D., 2013. The Influence of Saxon Mining on the Development of the Serbian Medieval State. Min. Hist. Bull. Peak Dist. Mines Hist. Soc. 18, 35–45.

Stos-Gale, Z.A., Gale, N.H., Annetts, N., Todorov, T., Lilov, P., Raduncheva, A., Panayotov, I., 1998. LEAD ISOTOPE DATA FROM THE ISOTRACE LABORATORY, OXFORD: ARCHAEOMETRY DATA BASE 5, ORES FROM BULGARIA. Archaeometry 40, 217–226. doi:10.1111/j.1475-4754.1998.tb00834.x

Stos-Gale, Z., Gale, N., Houghton, J., Speakman, R., 1995. Lead Isotope data from the Isotrace Laboratory, Oxford: Archaeometry Database 1, ores from the Western Mediterranean. Archaeometry 37, 407–415. doi:10.1111/j.1475-4754.1995.tb00753.x

Stos, Z.A., 2009. Across the wine dark seas… sailor tinkers and royal cargoes in the Late Bronze Age eastern Mediterranean, in: Shortland, A.J., Freestone, I.C., Rehren, T. (Eds.), From Mine to Microscope. Advances in the Study of Ancient Technology. Oxbow Books, Oxford, pp. 163–181. doi:10.1016/j.jas.2009.11.021

Stuut, J.B., Prins, M.A., 2014. The significance of particle size of long-range transported mineral dust. PAGES Mag. 22, 70–71. doi:10.1029/2004JD005161

Sweeney, M.R., Mason, J.A., 2013. Mechanisms of dust emission from Pleistocene loess deposits, Nebraska, USA. J. Geophys. Res. Earth Surf. 118, 1460–1471. doi:10.1002/jgrf.20101

Swierczynski, T., Lauterbach, S., Dulski, P., Delgado, J., Merz, B., Brauer, A., 2013. Mid- to late Holocene flood frequency changes in the northeastern Alps as recorded in varved sediments of Lake Mondsee (Upper Austria). Quat. Sci. Rev. 80, 78–90. doi:10.1016/j.quascirev.2013.08.018

Swindles, G.T., Patterson, R.T., Roe, H.M., Galloway, J.M., 2012. Evaluating periodicities in peat-based climate proxy records. Quat. Sci. Rev. 41, 94–103. doi:10.1016/j.quascirev.2012.03.003

Szakács, A., Seghedi, I., Pécskay, Z., Mirea, V., 2015. Eruptive history of a low-frequency and low-output rate Pleistocene volcano, Ciomadul, South Harghita Mts., Romania. Bull. Volcanol. 77, 12. doi:10.1007/s00445-014-0894-7

Tamas, C.-G., Baron, S., Cauuet, B., 2009. Mineralogy and lead isotope signature of the gold-silver ores exploited during the Roman period at Alburnus Maior (Rosia Montana, Romania). ArcheoSciences Rev. d'archaeometrie 33, 83–89.

Tămaş, T., Onac, B.P., Bojar, A.V., 2005. Lateglacial-Middle Holocene stable isotope records in two coeval stalagmites from the Bihor Mountains, NW Romania. Geol. Q. 49, 185–194.

Tanţău, I., Feurdean, A., de Beaulieu, J.L., Reille, M., Fărcaş, S., 2011. Holocene vegetation history in the upper forest belt of the Eastern Romanian Carpathians. Palaeogeogr. Palaeoclimatol. Palaeoecol. 309, 281–290. doi:10.1016/j.palaeo.2011.06.011

Tanţău, I., Feurdean, A., De Beaulieu, J.L., Reille, M., Fărcaş, S., 2014. Vegetation sensitivity to climate changes and human impact in the Harghita Mountains (Eastern Romanian Carpathians) over the past 15 000 years. J. Quat. Sci. 29, 141–152. doi:10.1002/jqs.2688

Tanțău, I., Reille, M., de Beaulieu, J.-L., Fărcaș, S., 2006. Late Glacial and Holocene vegetation history in the southern part of Transylvania (Romania): pollen analysis of two sequences from Avrig. J. Quat. Sci. 21, 49–61. doi:10.1002/jqs.937

Tantau, I., Reille, M., de Beaulieu, J.-L., Farcas, S., Brewer, S., 2009. Holocene vegetation history in Romanian Subcarpathians. Quat. Res. 72, 164–173. doi:10.1016/j.yqres.2009.05.002

Tanţău, I., Reille, M., De Beaulieu, J.L., Farcas, S., Goslar, T., Paterne, M., 2003. Vegetation history in the Eastern Romanian Carpathians: Pollen analysis of two sequences from the Mohos crater. Veg. Hist. Archaeobot. 12, 113–125. doi:10.1007/s00334-003-0015-6

Taylor, T., 1994. Thracians, Scythians, and Dacians, 800 bc–ad 300. Oxford Illus. Prehistory Eur.

Toader, T., Dumitru, I., 2004. Romanian Forests. National parks and natural parks. National Forest Administration ROMSILVA, Bucharest.

Todorova, H., 1995. The Neolithic, Eneolithic and transitional period in Bulgarian prehistory. Prehist. Bulg. 79–98.

Tomozeiu, R., Lazzeri, M., Cacciamani, C., 2002. Precipitation fluctuations during the winter season from 1960 to 1995 over Emilia-Romagna, Italy. Theor. Appl. Climatol. 72, 221–229. doi:10.1007/s00704-002-0675-7

Tomozeiu, R., Stefan, S., Busuioc, A., 2005. Winter precipitation variability and large-scale circulation patterns in Romania. Theor. Appl. Climatol. 81, 193–201. doi:10.1007/s00704-004-0082-3

Tonkov, S., Bozilova, E., Possnert, G., Velčev, A., 2008. A contribution to the postglacial vegetation history of the Rila Mountains, Bulgaria: The pollen record of Lake Trilistnika. Quat. Int. 190, 58–70. doi:10.1016/j.quaint.2007.12.007

Tornos, F., Ribera, F., Shepherd, T.J., Spiro, B., 1996. The geological and metallogenic setting of stratabound carbonate-hosted Zn-Pb mineralizations in the West Asturian Leonese Zone, NW Spain. Miner. Depos. 31, 27–40. doi:10.1007/BF00225393

Torrence, C., Compo, G.P., 1998. A Practical Guide to Wavelet Analysis. Bull. Am. Meteorol. Soc. 79, 61–78.

Tóth, M., Magyari, E.K., Brooks, S.J., Braun, M., Buczkó, K., Bálint, M., Heiri, O., 2012. A chironomid-based reconstruction of late glacial summer temperatures in the southern Carpathians (Romania). Quat. Res. 77, 122–131. doi:10.1016/j.yqres.2011.09.005

Tóth, M., Magyari, E.K., Buczkó, K., Braun, M., Panagiotopoulos, K., Heiri, O., 2015. Chironomid-inferred Holocene temperature changes in the South Carpathians (Romania). The Holocene 25, 569–582. doi:10.1177/0959683614565953

Treadgold, W., 1997. A history of the Byzantine state and society. Stanford University Press.

Treptow, K.W., 1997. A History of Romania (3rd Edition). The Centre for Romanian Studies, Iasi.

Trigo, R.M., Zêzere, J.L., Rodrigues, M.L., Trigo, I.F., Zere, J.L.Z., Rodrigues, M.L., Trigo, I.F., 2005. The Influence of the North Atlantic Oscillation on Rainfall Triggering of Landslides near Lisbon. Nat. Hazards 36, 331–354. doi:10.1007/s11069-005-1709-0

Trouet, V., Esper, J., Graham, N.E., Baker, A., Scourse, J.D., Frank, D.C., 2009. Persistent Positive North Atlantic Oscillation Mode Dominated the Medieval Climate Anomaly. Science. 324, 78–80. doi:10.1126/science.1166349

Trufas, V., 1986. Munţii Şureanu, ghid turistic. Sport-Turism Publishing House, Bucharest.

Tudya, K., Padzur, A., De Vleeschouwer, F., Lityńska-Zając, M., Chrost, L., Fagel, N., 2017. Holocene elemental, lead isotope and charcoal record from peat in southern Poland. Mires Peat 19, 1–18.

Tyler, G., 2005. Changes in the concentrations of major, minor and rare-earth elements during leaf senescence and decomposition in a Fagus sylvatica forest. For. Ecol. Manage. 206, 167–177. doi:10.1016/j.foreco.2004.10.065

Tyler, G., 2004. Ionic charge, radius, and potential control root/soil concentration ratios of fifty cationic elements in the organic horizon of a beech (Fagus sylvatica) forest podzol. Sci. Total Environ. 329, 231–9. doi:10.1016/j.scitotenv.2004.03.004

Újvári, G., Varga, A., Ramos, F.C., Kovács, J., Németh, T., Stevens, T., 2012. Evaluating the use of clay mineralogy, Sr–Nd isotopes and zircon U–Pb ages in tracking dust provenance: An example from loess of the Carpathian Basin. Chem. Geol. 304, 83–96. doi:10.1016/j.chemgeo.2012.02.007

Ujvári, G., Varga, A., Ramos, F.C., Kovács, J., Németh, T., Stevens, T., Újvári, G., Varga, A., Ramos, F.C., Kovács, J., Németh, T., Stevens, T., 2012. Evaluating the use of clay mineralogy, Sr-Nd isotopes and zircon U-Pb ages in tracking dust provenance: An example from loess of the Carpathian Basin. Chem. Geol. 304–305, 83–96. doi:10.1016/j.chemgeo.2012.02.007

Vallelonga, P., Candelone, J.P., Van de Velde, K., Curran, M. a J., Morgan, V.I., Rosman, K.J.R., 2003. Lead, Ba and Bi in Antarctic Law Dome ice corresponding to the 1815 AD Tambora eruption: An assessment of emission sources using Pb isotopes. Earth Planet. Sci. Lett. 211, 329–341. doi:10.1016/S0012-821X(03)00208-5

Vallelonga, P., Gabrielli, P., Balliana, E., Wegner, a., Delmonte, B., Turetta, C., Burton, G., Vanhaecke, F., Rosman, K.J.R., Hong, S., Boutron, C.F., Cescon, P., Barbante, C., 2010. Lead isotopic compositions in the EPICA Dome C ice core and Southern Hemisphere Potential Source Areas. Quat. Sci. Rev. 29, 247–255. doi:10.1016/j.quascirev.2009.06.019

van Andel, T.H., Runnels, C.N., 1995. The earliest farmers in Europe. Antiquity 69, 481–500. doi:10.1017/S0003598X00081886

Van de Velde, K., Vallelonga, P., Candelone, J.P., Rosman, K.J.R., Gaspari, V., Cozzi, G., Barbante, C., Udisti, R., Cescon, P., Boutron, C.F., 2005. Pb isotope record over one century

in snow from Victoria Land, Antarctica. Earth Planet. Sci. Lett. 232, 95–108. doi:10.1016/j.epsl.2005.01.007

van der Schrier, G., Briffa, K.R., Jones, P.D., Osborn, T.J., Schrier, G. van der, Briffa, K.R., Jones, P.D., Osborn, T.J., 2006. Summer Moisture Variability across Europe. J. Clim. 19, 2818–2834. doi:10.1175/JCLI3734.1

Varga, G., Cserháti, C., Kovács, J., Szalai, Z., 2016. Saharan dust deposition in the Carpathian Basin and its possible effects on interglacial soil formation. Aeolian Res. 22, 1–12. doi:10.1016/j.aeolia.2016.05.004

Varga, G., Kovács, J., Újvári, G., 2013. Analysis of Saharan dust intrusions into the Carpathian Basin (Central Europe) over the period of 1979–2011. Glob. Planet. Change 100, 333–342. doi:10.1016/j.gloplacha.2012.11.007

Vasskog, K., Nesje, a., Storen, E.N., Waldmann, N., Chapron, E., Ariztegui, D., 2011. A Holocene record of snow-avalanche and flood activity reconstructed from a lacustrine sedimentary sequence in Oldevatnet, western Norway. The Holocene 21, 597–614. doi:10.1177/0959683610391316

Vasskog, K., Paasche, Ø., Nesje, A., Boyle, J.F., Birks, H.J.B., 2012. A new approach for reconstructing glacier variability based on lake sediments recording input from more than one glacier. Quat. Res. 77, 192–204. doi:10.1016/j.yqres.2011.10.001

Velasco, F., Herrero, J.M., Yusta, I., Alonso, J.A., Seebold, I., Leach, D., 2003. Geology and Geochemistry of the Reocín Zinc-Lead Deposit, Basque-Cantabrian Basin, Northern Spain. Econ. Geol. 98.

Veres, D., Mîndrescu, M., 2013. Advancing Pleistocene and Holocene climate change research in the Carpathian–Balkan region. Quat. Int. 293, 1–4. doi:10.1016/j.quaint.2012.12.003

Verhoeven, J.D., Pendray, A.H., Dauksch, W.E., 1998. The key role of impurities in ancient damascus steel blades. JOM 50, 58–64. doi:10.1007/s11837-998-0419-y

Veron, A., Novak, M., Brizova, E., Stepanova, M., 2014. Environmental imprints of climate changes and anthropogenic activities in the Ore Mountains of Bohemia (Central Europe) since 13 cal. kyr BP. The Holocene 24, 919–931. doi:10.1177/0959683614534746

Véron, A.J., Flaux, C., Marriner, N., Poirier, A., Rigaud, S., Morhange, C., Empereur, J.-Y., 2013. A 6000-year geochemical record of human activities from Alexandria (Egypt). Quat. Sci. Rev. 81, 138–147. doi:10.1016/j.quascirev.2013.09.029

Vinichuk, M., Taylor, a. F.S., Rosén, K., Johanson, K.J., 2010. Accumulation of potassium, rubidium and caesium (133Cs and 137Cs) in various fractions of soil and fungi in a Swedish forest. Sci. Total Environ. 408, 2543–2548. doi:10.1016/j.scitotenv.2010.02.024

Vinkler, A.P., Harangi, S., Ntaflos, T., Szakács, A., 2007. A Csornád vulkán (Keleti-Kárpátok) horzsaköveinek kőzettani és geokémiai vizsgálata - petrogenetikai következtetések 137, 103–128.

Vlad, Șerban-N., Orlandea, E., 2012. Metallogeny of the Gold Quadrilateral: style and characteristics of epithermal - subvolcanic mineralized structures, South Apuseni Mts., Romania. Stud. UBB Geol. 49. doi:http://dx.doi.org/10.5038/1937-8602.49.1.2

von Quadt, A., Moritz, R., Peytcheva, I., Heinrich, C. a., 2005. 3: Geochronology and geodynamics of Late Cretaceous magmatism and Cu-Au mineralization in the Panagyurishte region of the Apuseni-Banat-Timok-Srednogorie belt, Bulgaria. Ore Geol. Rev. 27, 95–126. doi:10.1016/j.oregeorev.2005.07.024

Von Quadt, A., Peytcheva, I., Kamenov, B., Fanger, L., Heinrich, C.A., Frank, M., 2002. The Elatsite porphyry copper deposit in the Panagyurishte ore district, Srednogorie zone, Bulgaria: U-Pb zircon geochronology and isotope-geochemical investigations of magmatism and ore genesis. Geol. Soc. London, Spec. Publ. 204, 119–135. doi:10.1144/GSL.SP.2002.204.01.08

Vukmirović, Z., Unkašević, M., Lazić, L., Tošić, I., Rajšić, S., Tasić, M., 2004. Analysis of the Saharan dust regional transport. Meteorol. Atmos. Phys. 85, 265–273. doi:10.1007/s00703-003-0010-6

Vukovic, M., Weinstein, A., 2002. Kosovo Mining, Metallurgy, and Politics: Eight Centuries of Perspective. Jom 54, 21–24. doi:10.1007/BF02701690

Wagner, D.B., 1993. Iron and steel in ancient China. E.J. Brill.

Wanner, H., Solomina, O., Grosjean, M., Ritz, S.P., Jetel, M., 2011. Structure and origin of Holocene cold events. Quat. Sci. Rev. 30, 3109–3123. doi:10.1016/j.quascirev.2011.07.010

Waters, C.N., Zalasiewicz, J., Summerhayes, C., Barnosky, A.D., Poirier, C., Ga uszka, A., Cearreta, A., Edgeworth, M., Ellis, E.C., Ellis, M., Jeandel, C., Leinfelder, R., McNeill, J.R., Richter, D.D., Steffen, W., Syvitski, J., Vidas, D., Wagreich, M., Williams, M., Zhisheng, A., Grinevald, J., Odada, E., Oreskes, N., Wolfe, A.P., 2016. The Anthropocene is functionally and stratigraphically distinct from the Holocene. Science. 351, 137–148. doi:10.1126/science.aad2622

Wedepohl, K.H., 1995. The composition of the continental crust. Geochim. Cosmochim. Acta 59, 1217–1232. doi:10.1016/0016-7037(95)00038-2

Weiss, D., Shotyk, W., Appleby, P.G., Kramers, J.D., Cheburkin, A.K., 1999. Atmospheric Pb Deposition since the Industrial Revolution Recorded by Five Swiss Peat Profiles: Enrichment Factors, Fluxes, Isotopic Composition, and Sources. Environ. Sci. Technol. 33, 1340–1352. doi:10.1021/es980882q

Weiss, D., Shotyk, W., Boyle, E.A., Kramers, J.D., Appleby, P.G., Cheburkin, A.K., 2002. Comparative study of the temporal evolution of atmospheric lead deposition in Scotland and eastern Canada using blanket peat bogs. Sci. Total Environ. 292, 7–18. doi:10.1016/S0048-9697(02)00025-6

Weiss, D., Shotyk, W., Cheburkin, A.K., Gloor, M., Reese, S., 1997. Atmospheric lead deposition from 12,400 to ca. 2,000 Yrs BP in a peat bog profile, Jura Mountains, Switzerland. Water. Air. Soil Pollut. 100, 311–324. doi:10.1023/A:1018341029549

Weller, O., Dumitroaia, G., 2005. The earliest salt production in the world: an early Neolithicexploitation in Poiana Slatinei-Lunca, Romania. Antiquity 79, en ligne (http://antiquity.ac.uk/projgall/weller/).

Wells, P.., 2016. Unique objects, special deposits and elite networks in Bronze Age Europe. Oxford J. Archaeol. 35, 161–178. doi:10.1111/ojoa.12083

Wertime, T.A., 1973. The Beginnings of Metallurgy- A new look. Science. 182, 875–887.

Westner, K., 2016. Roman mining and metal production near the antique city of ULPIANA (Kosovo). Johann Wolfgang Goethe-Universitat frankfurt am Main.

Wilhelm, B., Arnaud, F., Enters, D., Allignol, F., Legaz, A., Magand, O., Revillon, S., Giguet-Covex, C., Malet, E., 2012. Does global warming favour the occurrence of extreme floods in European Alps? First evidences from a NW Alps proglacial lake sediment record. Clim. Change 113, 563–581. doi:10.1007/s10584-011-0376-2

Wilhelm, B., Arnaud, F., Sabatier, P., Magand, O., Chapron, E., Courp, T., Tachikawa, K., Fanget, B., Malet, E., Pignol, C., Bard, E., Delannoy, J.J., 2013. Palaeoflood activity and climate change over the last 1400 years recorded by lake sediments in the north-west European Alps. J. Quat. Sci. 28, 189–199. doi:10.1002/jqs.2609

Wilkes, J.J., 2005. The Roman Danube: An Archaeological Survey. J. Rom. Stud. 95, 124–225. doi:10.3815/000000005784016298

Willis, K.J., Bennett, K.D., McSweeney, K., Stewart, C., Harkness, D., Boronean, V., Bartosiewicz, L., Payton, R., Chapman, J., 1994. The Neolithic transition - fact or fiction? Palaeoecological evidence from the Balkans. The Holocene 4, 326–330. doi:10.1177/095968369400400313

Wirth, S.B., Glur, L., Gilli, A., Anselmetti, F.S., 2013. Holocene flood frequency across the Central Alps – solar forcing and evidence for variations in North Atlantic atmospheric circulation. Quat. Sci. Rev. 80, 112–128. doi:10.1016/j.quascirev.2013.09.002

Wittenberger, M., 2008. Economical Life in Noua Culture in the Transylvanian Bronze Age. Acta Mus. Napocensis 43–44, 5–46.

Wolters, S., Enters, D., Bittmann, F., 2010. Landscape history and land-use dependent soil erosion in central Bosnia from the Bronze Age to Medieval Times, in: EGU General Assembly 2010. p. 11200.

Wu, H., Guiot, J., Brewer, S., Guo, Z., 2007. Climatic changes in Eurasia and Africa at the last glacial maximum and mid-Holocene: Reconstruction from pollen data using inverse vegetation modelling. Clim. Dyn. 29, 211–229. doi:10.1007/s00382-007-0231-3

Wulf, S., Fedorowicz, S., Veres, D., Łanczont, M., Karátson, D., Gertisser, R., Bormann, M., Magyari, E., Appelt, O., Hambach, U., Gozhyk, P.F., 2016. The "Roxolany Tephra" (Ukraine) − new evidence for an origin from Ciomadul volcano, East Carpathians. J. Quat. Sci. 31, 565–576. doi:10.1002/jqs.2879

Xun, S., 2015. The Mineral Industry of Romania, in: U.S. Geological Servey Minerals Yearbook.

Yafa, C., Farmer, J.G., Graham, M.C., Bacon, J.R., Barbante, C., Cairns, W.R.L., Bindler, R., Renberg, I., Cheburkin, A., Emons, H., Handley, M.J., Norton, S. a, Krachler, M., Shotyk, W., Li, X.D., Martinez-Cortizas, A., Pulford, I.D., MacIver, V., Schweyer, J., Steinnes, E., Sjøbakk, T.E., Weiss, D., Dolgopolova, A., Kylander, M., 2004. Development of an ombrotrophic peat bog (low ash) reference material for the determination of elemental concentrations. J. Environ. Monit. 6, 493–501. doi:10.1039/b315647h

Yoshioka, M., Mahowald, N.M., Conley, A.J., Collins, W.D., Fillmore, D.W., Zender, C.S., Coleman, D.B., 2007. Impact of desert dust radiative forcing on sahel precipitation: Relative importance of dust compared to sea surface temperature variations, vegetation changes, and greenhouse gas warming. J. Clim. 20, 1445–1467. doi:10.1175/JCLI4056.1

Yu, S.-Y., 2003. Centennial-scale cycles in middle Holocene sea level along the southeastern Swedish Baltic coast. Geol. Soc. Am. Bull. 115, 1404. doi:10.1130/B25217.1

Zaruba, Q., Mencl, V., 1982. Landslides and Their Control, 2nd ed. Elsevier Science, New York.

Zhang, R., Wilson, V.L., Hou, A., Meng, G., 2015. Source of lead pollution, its influence on public health and the countermeasures. Int. J. Heal. Anim. Sci. Food Saf. 2, 18–31. doi:10.13130/2283-3927/4785

Zhang, X., Yang, L., Li, Y., Li, H., Wang, W., Ye, B., 2012. Impacts of lead/zinc mining and smelting on the environment and human health in China. Environ. Monit. Assess. 184, 2261–2273. doi:10.1007/s10661-011-2115-6